

University of Nevada, Reno

Regulation of Viruses Through Internal G-quadruplex Stabilization

A dissertation submitted in partial fulfillment of the requirements for the degree of
Doctor of Philosophy in Cellular and Molecular Biology

By

Andrew Zareie

Dr. Subhash C. Verma, Ph.D., *Dissertation Advisor*

December 2023

Copyright © 2023 Andrew Zareie

All Rights Reserved



THE GRADUATE SCHOOL

We recommend that the dissertation
prepared under our supervision by

Andrew Zareie

entitled

**“Regulation of Viruses Through Internal
G-quadruplex Stabilization”**

be accepted in partial fulfillment of the
requirements for the degree of

Doctor of Philosophy

Dr. Subhash C. Verma, Ph.D., *Advisor*

Dr. Cyprian C Rossetto, Ph.D., *Committee Member*

Dr. Paul Sumby, Ph.D., *Committee Member*

Dr. David AuCoin, Ph.D., *Committee Member*

Dr. Seungil Ro, Ph.D., *Graduate School Representative*

Dr. Markus Kemmelmeier, Ph.D., *Dean
Graduate School*

December 2023

ABSTRACT

Kaposi's sarcoma-associated herpesvirus (KSHV) is a gamma-herpesvirus implicated as the causative agent for several malignancies, including Kaposi's sarcoma, primary effusion lymphoma, and certain forms of multicentric Castleman's disease. KSHV remains latently infective in its hosts by anchoring its genome to host chromosomes and judiciously modulating viral protein expression, making it elusive to immune detection. This nuanced expression, implicated in several human malignancies, is primarily orchestrated by the Latency-associated nuclear antigen (LANA), pivotal for viral genome replication and maintenance. LANA's expression is fine-tuned at multiple strata—transcriptionally and translationally—with the mRNA's secondary structures playing a crucial role. Among these, G-quadruplexes (G4s) emerge as highly stable and evolutionarily conserved structures, influencing vital cellular processes such as replication and transcription. These G4s liaise with cellular proteins, either bolstering or disrupting these structures, thereby regulating LANA translation. Our previous work highlighted the critical role of G4s within LANA mRNA, underscoring their influence on LANA levels in infected cells. This study elucidates the role of Nucleolin (NCL) in modulating LANA expression via its affinity for the G-quadruplexes in LANA mRNA. This liaison leads to a reduction in LANA protein expression, driven by the sequestering of its mRNA in the nucleus, a phenomenon evidenced by the colocalization of G4-rich mRNA with NCL. Intriguingly, NCL's suppression, achieved through a short hairpin RNA, precipitates a surge in LANA translation, as evidenced by altered LANA mRNA levels in the cytoplasm. Collectively, our findings spotlight the regulatory capability of

G-quadruplex-mediated translational control by NCL, presenting potential avenues for therapeutically manipulating KSHV latency.

DEDICATION

This achievement would not have been possible without the unwavering love and support of my beautiful wife, Erin O'Riley Zareie. Her support has been a constant source of strength and inspiration throughout this journey. I love you, and thank you for everything you have done for me and our family.

ACKNOWLEDGMENTS

I extend my heartfelt gratitude to my advisor, Dr. Subhash Verma, for his outstanding mentorship. His unwavering support, guidance, and encouragement have been pivotal throughout my journey. Dr. Verma's remarkable tenacity and diligence in his work have left a lasting impression on me, and the lessons I have learned from him will be valued for a lifetime. I am immensely thankful for the opportunities and encouragement he has provided, which have been instrumental in shaping my path toward becoming an independent scientist and clarifying my career objectives.

I am deeply grateful to each committee member for their invaluable mentorship, astute guidance, and thorough critiques of my research and professional growth. Their willingness to mentor and guide me has been fundamental to my progress. The wealth of knowledge and expertise I have gained from each one is something I hold in high regard, and they serve as models of excellence I aim to emulate. Their dedication to nurturing and mentoring students like myself is admirable and inspiring. Witnessing the years of commitment, they have invested in their fields motivates me to achieve a similar level of influence and make a meaningful difference in the lives of students, just as they have profoundly impacted mine.

I want to thank my late mentor, Dr. Kentaro Inoue, for introducing me to laboratory work. His influence sparked my passion for research and continues to inspire me, even though he is no longer with us.

I sincerely thank my parents, Josie and Rasoul Zareie, for their unwavering love, support, and guidance. I am also profoundly grateful to the Granados, Zareie, and O'Riley families for their constant support throughout this journey. Also, thanks to my best friend,

Luis Mijo Perez, for his company during the many late nights spent in the lab. To all of you, I express my love and immense appreciation for being my pillars of strength and encouragement.

TABLE OF CONTENTS

Chapter 1: Background	
Abstract	i-ii
Dedication	iii
Acknowledgments	iv-v
Background	Pg. 1-25
References	Pg. 26-37
Chapter 2: “G-quadruplexes in regulating viral gene expressions and their impacts in controlling infection”	Pg. 38-89
Abstract	Pg. 39
Introduction	Pg. 40-73
Discussion	Pg. 73-75
References	Pg. 75-89
Chapter 3: “Nucleolin Regulates the Expression of KSHV’s LANA Through G-Quadruplexes in the mRNA”	Pg. 90-127
Abstract	Pg. 91
Introduction	Pg. 92-94
Materials and Methods Results	Pg. 94-100
Results	Pg. 101-115
Discussion	Pg. 115-121
References	Pg. 121-127
Chapter 4: “G-quadruplexes of human coronaviruses can be targeted for attenuating virus replication”	Pg. 128-177
Abstract	Pg. 129
Introduction	Pg. 130-134
Materials and Methods Results	Pg. 134-138
Results	Pg. 138-163
Discussion	Pg. 163-167
References	Pg. 168-177
Chapter 5: Conclusion and Future Work	Pg. 178-183

CHAPTER 1

INTRODUCTION

1. Background

1.1.1 G-quadruplexes

G-quadruplexes (G4s) are unique secondary structures found in guanine-rich areas of DNA and RNA. They comprise consecutive guanine blocks separated by loops, forming G-tetrads stabilized by Hoogsteen hydrogen bonds and ions like K⁺, Na⁺, or Ca²⁺¹⁻⁴. These structures, which differ from the classical Watson-Crick model, fold into multiple planar G-tetrads. Their stability, influenced by the number of tetrads and loop nucleotides, is vital in various cellular processes⁵⁻⁷. Tools like QGRS Mapper and Quadparser help identify potential G4-forming sequences (PQSs), and G4-specific antibodies have confirmed their presence in cells⁸. In DNA, G4s play roles in transcription, replication, and epigenetics, and their stabilization can impact RNA Pol II during transcription and telomere maintenance⁹⁻¹³. In RNA, G4s influence transcription, translation, RNA maturation, and non-coding RNA functions, with a higher tendency to form in RNA due to the absence of a complementary strand. They affect genome coding capacity through mechanisms like alternative splicing¹⁴. Ligands targeting G4s offer potential as antiviral therapies, often featuring polycyclic aromatic structures interacting with G4's π - π stacking¹⁵⁻¹⁸. Adjustments to these ligands have improved their selectivity and affinity. Given the widespread conservation of PQSs, G4-based antiviral therapy is a promising strategy for tackling various viral strains, marking a significant step in antiviral drug development.

The discovery of G-quadruplexes in the genomes of various organisms and their involvement in regulating biological processes linked to disease development has catalyzed the creation of drugs targeting these structures. This research has led to the

identification of G-quadruplex ligands. These small molecules exhibit a high affinity for binding to G-quadruplexes, offering greater stability than they do with double-stranded DNA. Notable examples of these ligands are BRACO-19, TMPyP4, PhenDC3, and Pyridostatin.

1.1.2 G-quadruplexes Regulating Viruses

Due to the high conservation of G4 structures and their identification in viruses, G4s present an excellent target for therapeutic intervention. G4 structures have been identified in a range of viruses, including Herpesviruses, HIV-1, and several others¹⁹⁻²⁴. HSV-1 has G4s present in the immediate early genes ICP0 and ICP4, which are crucial for viral replication. Stabilizing the G4 structures within their promoter regions impedes the binding of transcription factors and/or obstructs RNA polymerase access to these promoters, thereby inhibiting viral replication²⁵. ICP4 effectively self-regulates its promoter via a G4 interaction. BRACO-19 enhances ICP4 expression by stabilizing the same G4 site involved in ICP4's autoregulation. Additionally, quindoline derivatives have demonstrated potent anti-HSV-1 activity in the nanomolar range, effectively inhibiting the expression of ICP4²⁶.

G4s have been identified in the HIV-1 genome, particularly in the Long Terminal Repeat (LTR) regions and the Nef gene, playing a crucial role in the virus's life cycle. These G4 structures aid in RNA strand dimerization, essential for reverse transcription and integration of viral DNA into the host genome. They also contribute to genetic diversity and potential antiretroviral resistance. The Nef gene, essential in early viral replication, can evade RNA interference due to its alternative folding patterns. HIV-1

also produces miR-N367, a microRNA targeting Nef for self-regulation²⁷. Research focusing on these G4s led to the development of specific ligands like C-exNDIs, which selectively interact with viral G4s. Experiments using luciferase reporter assays demonstrated that G4-stabilizing ligands, including BRACO-19 and C-exNDIs, effectively inhibit HIV-1 activity by targeting these G4s in the LTR region. These ligands showed significant potential in reducing viral activity both before and after the integration of the HIV genome into the host¹⁶.

There are several other viruses that are regulated through internal G4 sites, however, the endeavor to target G4s faces several challenges. Firstly, despite their specificity for G4 structures, there is still a risk of off-target effects on host G4s, potentially resulting in cytotoxicity or other undesirable consequences. Secondly, the high structural diversity of G4s demands the development of specific ligands tailored for individual G4s in viruses. Lastly, achieving effective intracellular delivery of G4-binding molecules poses a challenge due to the potential for degradation or inadequate cellular uptake. Numerous small molecules have been synthesized and documented for their interaction with G4 structures, showcasing antiviral activity by stabilizing or destabilizing G4s. Research on developing G4-stabilizing ligands is continuously progressing.

1.2.1 Herpesviruses

The Herpesviridae family encompasses a diverse range of herpesviruses that infect humans and animals. Herpesviruses are large, enveloped DNA ranging from 120 to 260nm²⁸. They have a complex architecture: at their core is a linear, double-stranded

DNA genome containing 70-120 ORFs, encapsulated in an icosahedral capsid²⁹. The virus is further protected by a protein-rich tegument layer, enclosed in a lipid envelope obtained from the host cell, adorned with essential glycoproteins for viral entry and pathogenicity. Herpesviruses are obligate parasites requiring the host's intracellular machinery to replicate and produce infectious viruses. They are notorious for their ability to establish lifelong latency in host cells, typically remaining dormant and utilizing host cellular mechanisms for replication^{30,31}. They can reactivate to produce infectious progeny, leading to various pathologies. Humans commonly encounter one or more herpesviruses in their lifetime, often without severe complications unless in an immunocompromised state, where the virus can lead to severe, even life-threatening conditions³². Based on phylogenetic analysis, genome sequencing, and biological properties, Herpesviridae viruses are classified into three sub-families:

alphaherpesvirinae, *betaherpesvirinae*, and *gammaherpesvirinae*. Each subfamily is distinguished by its preferred site of latency. *Alphaherpesviruses* consist of herpes simplex 1 and 2 (HSV-1 and HSV-2) and varicella-zoster virus (VZV) and reside in neuronal cells. *Betaherpesviruses* infect epithelial cells, myeloid progenitors, or lymphocytes and consist of cytomegalovirus (HCMV), human herpesvirus 6A, 6B, and 7 (HHV-6A, HHV6B, HHV-7)²⁸. *Gammaherpesviruses* include Epstein Barr virus (EBV) and Kaposi's sarcoma-associated herpesvirus (KSHV), which infect lymphocytes and endothelial cells³³⁻³⁶.

1.2.2 KSHV Primary Infection

Most of the human population is infected with at least one type of herpesvirus,

which has the potential to cause various diseases or lead to the development of cancer. Typically, primary infection with KSHV in a healthy person is asymptomatic. The virus can remain dormant for decades; however, its clinical manifestations can be present in certain instances. These vary from lymph node inflammation to symptoms resembling a mild flu. In individuals with compromised immune systems, such as those with HIV or those undergoing immunosuppressive therapy, EBV and KSHV infection can potentially lead to various forms of cancer and may even be fatal³⁷.

1.2.3 KSHV-Associated Malignancies

In 1872, Moritz Kaposi characterized Kaposi's Sarcoma (KS) as "idiopathic multiple pigmented sarcomas of the skin" and exhibiting its highest prevalence in sub-Saharan Africa, where over 50% of the population is infected. In the Mediterranean region, the infection rate ranges between 10-25%, while in North America, Europe, and Asia, the prevalence is notably lower, falling below 10%^{38,39}. The causative agent of this condition remained unidentified until the AIDS epidemic of the 1980s, during which there was a significant surge in KS cases among patients with acquired immunodeficiency syndrome (AIDS), leading to the classification of KS as an AIDS-related cancer⁴⁰⁻⁴². Subsequently, in 1994, Patrick Moore and Yuan Chang identified KSHV in lesions of AIDS patients using a PCR-based method. This groundbreaking discovery led to the recognition of a new γ -herpesvirus⁴⁰.

Besides KS, KSHV is recognized as the causative agent of diseases such as Primary Effusion Lymphoma (PEL) and Multicentric Castleman's Disease (MCD), categorizing it as an oncogenic virus. KS is an antiproliferative tumor caused by KSHV,

predominantly affecting lymphatic-endothelial cells⁴³. It manifests in various forms, such as lesions or discolorations on the skin, oral mucosa, and internal organs⁴³⁻⁴⁵. KS is classified into four distinct subtypes: Classic, Endemic, Iatrogenic, and AIDS-associated. Classic KS typically presents as slow-developing lesions in older men, primarily affecting the lower extremities⁴⁶. Endemic KS, more aggressive and often fatal, is prevalent in Central and Eastern Africa, affecting younger populations with nodules mainly on the lower limbs⁴⁷. Iatrogenic KS, associated with immunosuppressed organ transplant patients, is characterized by rapid progression and can affect both skin and internal organs⁴⁸. Lastly, AIDS-associated KS, seen in patients with severely compromised immune systems, is the most aggressive form, with widespread lesion distribution^{49,50}. KS has many subtypes; however, AIDS-associated KS is the most aggressive form of the disease⁴². Each subtype of KS displays unique epidemiological and clinical characteristics, reflecting the diverse impact of KSHV infection.

PEL, also known as Body Cavity-Based Lymphoma (BCBL), is an uncommon and aggressive form of B cell lymphoma typically seen in individuals with compromised immune systems or the elderly. PEL is frequently diagnosed in AIDS patients, often alongside a co-infection with the EBV⁴¹. Within PEL cells, KSHV genomes are present in high numbers. Characteristically, the lymphoma manifests as fluid accumulation in body cavities like the peritoneum, pericardium, and pleura, though it's rare in lymph nodes and other regions^{51,52}. PEL tumors are aggressive, progress rapidly, and typically show high resistance to chemotherapy, with survival of 2-6 months post-diagnosis⁴².

Multicentric Castleman's Disease (MCD) is a lymphoproliferative disorder affecting B-cells. Like PEL, MCD is aggressive and results in high fatality, with patients

often succumbing within ten months of diagnosis^{42,53}. MCD manifests in two distinct forms: the unicentric type, which involves only a single lymph node, and the multicentric variant, where multiple lymph nodes are affected, with the potential to extend even to the spleen⁵⁴. In AIDS patients, KSHV is linked to the plasmablastic variant of MCD, making it the primary causative agent^{55,56}.

1.2.4 KSHV Transmission and Treatments

KSHV transmission occurs through both sexual and non-sexual means. In cases of organ transplantation, recipients can become infected if the donor is KSHV positive⁵⁷. Among those infected, saliva often contains high levels of KSHV, a result of viral shedding in the oropharynx due to lytic reactivation of the virus⁵⁸. Furthermore, the virus can also be transmitted through various forms of fluid exchange, including oral sex, blood transfusions, and the sharing of needles⁵⁹. Most treatments for KS are ineffective in targeting the KSHV virus and cannot prevent the formation of new tumors. Treatments for KS, include chemotherapy, radiation, antiviral therapy, and tumor excision. These treatments have adverse impacts and highlight the need for more effective treatment options with fewer detrimental consequences.

After initial infection, herpesviruses enter a latent phase where they remain dormant within the host cells, not producing any new infectious virions. However, under specific conditions, these viruses can switch to a lytic reactivation phase, wherein they resume replication and produce infectious virus. The lytic replication cycle of KSHV plays a crucial role in tumor development. Utilizing antiviral therapies to target and inhibit this lytic reactivation can, in some instances, effectively prevent the growth of

tumors⁶⁰. A significant challenge in developing treatments explicitly targeted at KSHV lies in the fact that in most Kaposi's Sarcoma tumors, the virus is in a latent state. The currently approved antivirals are designed to target viral components that are active only during the lytic cycle, rendering them ineffective against latent infections⁶⁰.

A combination antiviral therapy (cART) approach has decreased the incidence of AIDS-associated KS by 80% and restores immune function by eliminating replicating HIV. Additionally, cART has reduced the frequency of new KS infections and decreased the size of existing KS lesions⁶¹. Ganciclovir and valganciclovir, lytic replication inhibitors, have shown moderate effectiveness in treating MCD⁶².

1.2.5 KSHV Genome

KSHV has a genome ranging from 160 to 170kb. This includes a long unique region (LUR) of approximately 140kb, which encodes more than 90 open reading frames (ORFs)⁶³. KSHV shares 71 genes with herpesvirus saimiri (HVS), many of which are responsible for encoding structural proteins and enzymes critical for viral replication. These genes are conserved across herpesvirus subfamilies^{64,65}. The LUR is bordered by terminal repeats (TRs), each comprising 801bps with a high GC content, and these TRs do not encode any proteins. The LUR itself is known to encode homologous proteins to cellular proteins, suggesting an evolutionary acquisition during the virus-host co-evolution process⁶⁶.

1.2.6 KSHV Infection and Life Cycle

KSHV can target CD19+ peripheral blood B lymphocytes, endothelial cells,

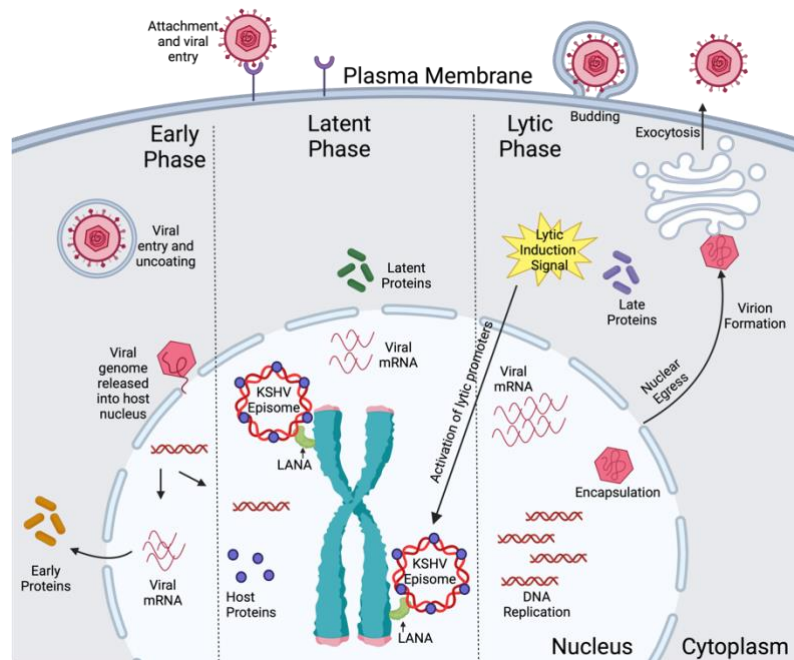
monocytes, epithelial cells, and keratinocytes. B-cells and monocytes are the primary locations the virus remains latent⁶⁷. Here transcription of ORF72 (v-Cyclin D), ORF73 (LANA), K12 (Kaposin), K13 (v-FLIP), and microRNAs occurs⁶⁸. Several cell lines, including human dermal microvascular endothelial (HMVEC-d) cells, human foreskin fibroblast (HFF) cells, human embryonic kidney 293 cells (HEK-293), human umbilical vein endothelial (HUVEC) cells, telomerase-immortalized human umbilical vein endothelial (TIVE) cells, human epithelial SLK cells, mouse fibroblasts, monkey kidney CV-1 cells, and monkey kidney epithelial VERO cells, are effective for studying viral latency. These cell lines can maintain the latent virus, making them ideal models for this type of research⁶⁹.

Herpesviruses are characterized by a biphasic lifecycle that includes both latent and lytic phases. 24 hours post-infection, KSHV established latency (Fig. 1). During latent infection, the virus expresses only a limited number of genes, and its genome exists as an episome, anchored to the host cell's chromosome. The lytic phase is transient and governed by a sequential cascade of gene expression, beginning with immediate early (IE) genes, progressing to early (E) genes, and concluding with late (L) genes. IE proteins activate the expression of E genes, which are crucial for initiating viral DNA synthesis. This is then followed by the activation of L genes, responsible for the assembly of virions^{30,31,60,69-71}.

Figure 1: KSHV Life Cycle

KSHV initiates infection by binding to specific receptors on the host cell, facilitating its entry by endocytosis or direct fusion with the cell membrane. Post-entry, the virus uncoats, allowing the viral

capsid to release its genome into the cell's nucleus. KSHV establishes latency, during which only a subset of genes are actively expressed. LANA binds to the TR sequence in KSHV to mediate replication and maintains the viral episome by tethering it to the host mitotic chromosomes. Specific triggers can prompt the virus to undergo lytic reactivation. In this active phase, KSHV replicates its genome and assembles new viral particles. The newly synthesized DNA is incorporated into the capsids within the nucleus. The viral particles are transported into the cytoplasm, where they acquire additional viral proteins (tegument proteins) and egress the cell through exocytosis and are ready to infect new cells.



1.2.7 KSHV Latency and Lytic Replication

Once infection is established, the virus utilizes the host DNA replication machinery for its own replication during latency. The virus tethers multiple copies to the host chromosome to participate in cell division⁷²⁻⁷⁴. During latency, KSHV maintains a compact chromatin structure, as limited genes are expressed: ORF72, LANA (OF73), and K33^{75,76}. The Latency-Associated Nuclear Antigen (LANA) is among the most predominantly expressed proteins during the latent phase and is widely regarded as the

“master regulator” of viral latency⁷⁷. LANA is believed to attach to LANA binding sites (LBS) located within the Terminal Repeat (TR) regions of the genome, in conjunction with histone proteins. These histones envelop the viral genome, which is crucial in anchoring it to the host chromosome. It is this mechanism of interaction that is considered pivotal in the tethering of the viral genome to the host's genetic material^{77,78}.

LANA interacts with various viral proteins, tumor suppressors, and transcription factors. It undergoes several post-translational modifications, including acetylation, phosphorylation, poly ADP-ribosylation, SUMOylation, and arginine methylation^{77,78}. For the persistence of the latent viral genome, it relies on the host's replication machinery. LANA plays a role in ensuring the inheritance of the KSHV genome by daughter cells, recruiting host cellular proteins like kinetochore proteins Bub1 and CENP-F. The viral genome features an origin of replication, ori-P, housing two LANA binding sites. These sites facilitate the recruitment of the replication complex during the cell cycle's S phase⁷⁷.

LANA also plays a critical role in regulating viral latency by inhibiting lytic reactivation. It suppresses the expression of lytic genes during primary infection by recruiting host polycomb repression complexes (PRC1 and PRC2) to promoter regions^{79,80}. Moreover, LANA interacts with the Replication and Transcriptional Activator (RTA), an immediate early gene in the lytic reactivation phase encoded by ORF50. RTA is key in determining the switch between latency and lytic reactivation and triggers the start of the lytic cycle⁸¹.

Following initial infection, the virus may re-enter the lytic cycle due to various triggers, including external stimuli, hypoxia, or signals related to cell differentiation⁸².

During this phase, all viral genes are replicated via a process known as rolling circle replication, which produces concentric viral DNA that is subsequently cleaved to facilitate viral assembly and release^{83,84}. The lytic replication phase is crucial as it enables the spread of KSHV and contributes to the progression of the disease^{73,85,86}. The switch between the latent and lytic cycles is primarily regulated by the Replication and Transcriptional Activator (RTA) and other immediate early (IE) proteins³².

1.2.8 LANA

LANA, encoded by ORF73 of KSHV, LANA, a multifunctional protein, 220-230kDa, is critical for maintaining a persistent KSHV infection⁸⁷. To ensure the virus's persistence in dividing tumor cells, KSHV's episomal DNA must replicate in tandem with the host cell's cycle and segregate effectively during mitosis. The absence of LANA disrupts the establishment and maintenance of a latent infection^{79,88}.

LANA is primarily expressed in latently infected cells and is composed of three distinct domains: the N-terminal, central, and C-terminal. The N-terminal domain features a nuclear localization signal (NLS) and a chromosome-binding site (CBS). This domain includes a 27 amino acid sequence with a bipartite NLS, rich in arginine and glycine residues, essential for facilitating LANA's nuclear translocation through interaction with importin β -1, a key nuclear cytoplasmic receptor in eukaryotic cells. Additionally, this domain is crucial for anchoring LANA to the host chromosome, thanks to its chromatin-binding site that interacts with histones^{87,89}. The central domain is characterized by multiple repeats of hydrophilic amino acids, contributing to its unique structure and function. Meanwhile, the C-terminal domain is composed of both

hydrophobic and hydrophilic residues. This domain is integral to the chromatin binding process, aids in the self-association of LANA, and is responsible for binding to the viral DNA located in the TR (Terminal Repeat) region, playing a vital role in the maintenance of the viral episome in latently infected cells^{77,90}.

As mentioned earlier, KSHV's LUR is flanked by the TR region, which facilitates the circularization of the genome. Within this TR region lies the primary LANA binding site, LBS1. Modifications in LBS1 significantly impact LANA's binding efficiency. A secondary binding site, LBS2, is also present, exhibiting a lower affinity for LANA. However, LBS1 enhances LANA's ability to bind to LBS2⁹¹. Furthermore, a third binding site, LBS3, is oriented in reverse. The dimerization of LANA leads to the stabilization of this complex, and the resulting oligomer formation enables cooperative binding to these lower affinity sites, reinforcing the viral genome's stability and persistence⁹².

The N-terminal region of LANA establishes interactions with histones H2A/H2B, effectively anchoring viral proteins to the host's chromatin. It also binds to H2AX, an H2A variant crucial in DNA break repair. This interaction enhances H2AX phosphorylation, which in turn aids the binding between LANA and the KSHV Terminal Repeat (TR) region, essential for maintaining the viral episome's persistence^{90,93}. Critical for LANA's function are its N-terminal and C-terminal regions, which bind to MeCP2, a protein involved in gene silencing and activation of euchromatin genes. This interaction is key to LANA's positioning on human chromosomes near the KSHV genome, guiding it towards heterochromatin regions⁹⁴. In addition, LANA forms complexes with kinetochore proteins such as CENP-F and Bub1, playing a significant role in mitotic

processes. It also interacts with NuMA, a protein vital to the nuclear mitotic apparatus, with this relationship evolving throughout the cell cycle⁹⁵. Furthermore, LANA's interaction with the Bromodomain and Extra-Terminal Domain (BET) family proteins, particularly BRD4, is crucial for the progression of the G1/S phase during mitosis. The co-localization of BRD4 with LANA on mitotic chromosomes indicates a potential role in LANA's mechanism for tethering the viral genome to the host chromosome⁹⁶⁻⁹⁸.

1.3.1 Coronaviruses

Coronaviruses (CoV) are from the Coronaviridae family and the Nidovirales order⁹⁹. CoV are enveloped positive-sense single-stranded RNA and are distinguished by crown-like spikes on their surface^{100,101}. These viruses exhibit a broad host range, capable of infecting various species including birds and mammals. In humans, coronaviruses are responsible for a spectrum of illnesses, ranging from respiratory to gastrointestinal and neurological disorders¹⁰².

Coronaviruses are classified into four primary sub-groups: Alpha, Beta, Gamma, and Delta coronaviruses^{100,103}. Alpha and Beta coronaviruses predominantly infect mammals, including bats, rodents, rabbits, and hedgehogs, which are considered a primary reservoir, and humans¹⁰⁴. On the other hand, Gamma and Delta coronaviruses are primarily known to infect avian species, though there have been instances of these viruses infecting mammals¹⁰⁵.

Before the year 2000, human coronaviruses were dominated by four strains: hCoV-OC43 (OC43) and hCoV-HKU1 (HKU1), which are *betacoronaviruses*, and hCoV-229E (229E) and hCoV-NL63 (NL63), classified as *alphacoronaviruses*. These

viruses typically caused mild respiratory illnesses, like the common cold, and were not known to lead to serious health issues. Their prevalence and impact on health were relatively moderate compared to the more virulent strains that would emerge later.

Prior to the turn of the millennium, the landscape of human coronaviruses was largely dominated by four types: 229E, OC43, NL63, and HKU1. These viruses were primarily associated with mild upper respiratory tract infections, akin to the common cold, and did not typically lead to severe health concerns^{106,107}. However, the early 21st century marked a dramatic shift in the perception and impact of coronaviruses due to the emergence of three highly pathogenic strains. The first of these was the Severe Acute Respiratory Syndrome Coronavirus (SARS-CoV), identified in 2002. Originating in Guangdong, China, it caused a significant outbreak, characterized by severe respiratory illness and some deaths, spreading to multiple countries before being contained in 2003¹⁰⁸. A decade later, in 2012, another deadly coronavirus emerged: the Middle East Respiratory Syndrome Coronavirus (MERS-CoV). First reported in Saudi Arabia, MERS-CoV was linked to severe respiratory illness, often accompanied by renal failure, and exhibited a high fatality rate. Unlike SARS-CoV, MERS-CoV continues to cause sporadic cases and outbreaks, primarily in the Arabian Peninsula¹⁰⁹⁻¹¹¹. The most impactful of these novel coronaviruses, however, has been Severe Acute Respiratory Syndrome Coronavirus 2 (SARS-CoV-2), which was first detected in Wuhan, China, in late 2019. This virus is the causative agent of the COVID-19 pandemic, leading to an unprecedented global health crisis with millions of infections and deaths, profound societal disruptions, and a massive international public health response¹¹²⁻¹¹⁴.

1.3.2 *Coronavirus Genomes*

Coronaviruses are among the largest RNA viruses with a single RNA strand between 26 to 32kb¹¹⁵. The positive-sense single-strand RNA can either act as a replication template or directly be translated by the host's ribosomes^{99,115}. The large genome allows for the coding of several proteins, including structural proteins: spike (S), envelope (E), membrane (M), and nucleocapsid (N) proteins, which are critical for virus assembly and infection.

Each of these proteins has a distinct role in forming the viral particle and virulence. The S protein forms a distinctive spike on the coronavirus surface and is critical for virus-host cell attachment and entry (Fig. 2). It binds to specific receptors on the host cell's surface and facilitates viral entry through direct fusion with the host cell membrane or by endocytosis¹¹⁶. The E and M proteins are involved in the viral particle formation. The M protein defines the shape of the viral envelope and is crucial for incorporating the S and E proteins into the virion¹¹⁷. The N protein binds to the coronavirus genome, packaging it into the helical ribonucleocapsid (RNP) structure. This complex is essential for protecting the viral genome and plays additional roles in the replication cycle and modulating the host cell's response to infection¹¹⁸. Following the synthesis of the structural proteins, they come together with the newly replicated genomic RNA to complete the virion particle. The assembly occurs in the endoplasmic reticulum-Golgi intermediate compartment in the host cell. After assembly, the viral particles are then released from the cell through a process known as viral egress¹¹⁹.

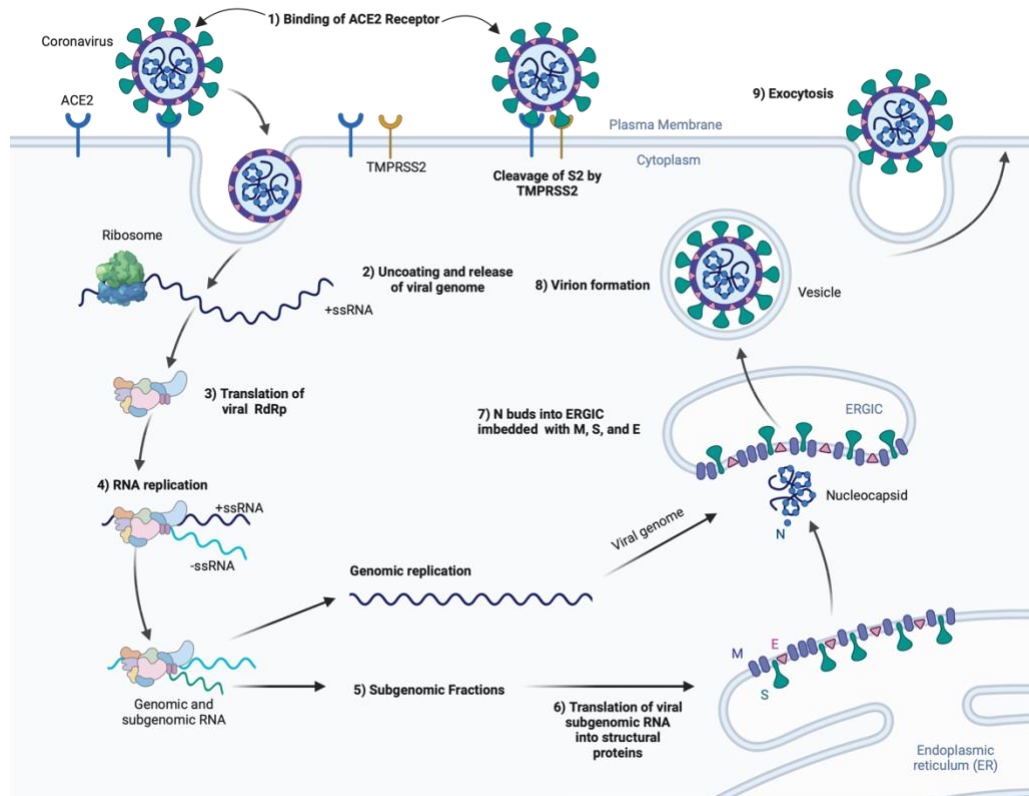


Figure 2: SARS-CoV-2 Viral Life Cycle

Spike (S) binds to the ACE2 receptor, inducing a conformation change in the S1 subunit (Step 1), exposing the S2 site for cleavage. On the right, if TMPRSS2 is present, S2 is cleaved on the cell surface. If the ACE2 complex does not encounter TMPRSS2, the ACE-2 complex is internalized. The viral genome is then released (Step 2), followed by hijacking the host's ribosomes to translate RdRp (Step 3). Using the newly synthesized RdRp, RNA replication occurs (Step 4), followed by genomic and subgenomic RNA synthesis (Step 5). Subgenomic fractions act as mRNA and are translated into structural proteins (Step 6). Following the viral genome-nucleocapsid association, the nucleocapsid buds into the ERGIC (Step 7), followed by the completion of virion formation in vesicles (Step 8). Lastly, the vesicle undergoes exocytosis, and the SARS-CoV-2 virion is ready to infect new cells (Step 9).

In addition to these structural elements, the genome encodes numerous non-structural proteins (nsps) that play roles in viral replication and modulating the host cell's

environment^{120,121}. The nsps in coronaviruses are derived from translating two large polyproteins, ORF1a and ORF1b. This translation process involves a mechanism known as ribosomal frameshifting, a unique feature in the replication strategy of coronaviruses. Once these large polyproteins are synthesized, they undergo proteolytic cleavage, which divides them into smaller, functional nsps. These nsps play critical roles in the virus's life cycle, including replication and transcription of the viral genome¹²².

1.3.3 Coronavirus Infections

Each coronavirus binds to specific receptors to initiate viral entry. NL63 recognizes the Angiotensin-Converting Enzyme 2 (ACE-2), the same receptor that SARS-CoV and SARS-CoV-2 use for viral entry^{116,123}. 229E binds to the human aminopeptidase N (hAPN) receptor to attain entry¹²⁴. HKU1 primarily utilizes 9-O-acetylated sialic acid (9-O-Ac-Sia) Sia to facilitate the initial attachment to the host cell¹²⁵. OC43 uses the N-acetyl-9-O-acetylneuraminic acid (Neu5,9Ac2) receptor, a type of sialic acid, for cell entry. MERS recognizes dipeptidyl peptidase-4 (DPP4) on the host's cell surface¹²⁶. Coronaviruses initiate infection by attaching to specific receptors on the surface of host cells, a process dictated by the viral spike (S) protein's affinity for host receptors. For instance, in the case of SARS-CoV-2, the virus binds to the angiotensin-converting enzyme 2 (ACE2) receptor¹¹⁶. Upon attachment, the virus can enter the host cell through one of two primary pathways: endocytosis or direct membrane fusion. All mentioned coronaviruses Transmembrane Protease, Serine 2 (TMPRSS2) to “prime” the S proteins for infection. TMPRSS2 cleaves the S protein, allowing for a conformation change in the S protein, exposing the fusion peptide. Without TMPRSS

facilitating the cleavage, the S protein cannot mediate the fusion of the viral and cellular membranes^{116,127-129}. Following attachment, endocytosis is the key mechanism the virus uses to enter the host cells. Following the spike protein recognizing and binding to the appropriate receptor on the host cell surface, the host cell engulfs the virus, enclosing it in an endosome. The endosome is formed from the host cell's plasma membrane allowing for internalization of the cell. After the endosome containing the virus is internalized, the acidic environment inside the endosome induces a crucial transformation in the viral E proteins. Specifically for coronaviruses, this acidic environment triggers a conformational change in the S protein. It is this alteration in the S protein structure that enables the viral envelope to effectively fuse with the endosomal membrane. Following the fusion, the viral RNA genome is released into the cytoplasm of the cell. As previously stated, the viral RNA can then undergo translation and replication^{112,116,123,125,130}.

Replication of the coronavirus genome involves the synthesis of a complementary negative-sense RNA strand, which then serves as a template to produce new positive-sense genomic RNA. This newly synthesized genomic RNA and the subgenomic RNAs are used to create additional viral components. The assembly of new viral particles occurs in the cytoplasm, typically in association with the endoplasmic reticulum and Golgi apparatus. Structural proteins, along with the genomic RNA, come together to form new virions. These newly formed viral particles are then transported to the cell surface in vesicles and released into the extracellular space through exocytosis. Alternatively, in some cases, the host cell may undergo lysis, a process where the cell breaks apart, releasing the viral particles^{99,115,120,121,131}.

1.3.4 *Human Coronavirus OC43, 229E, and NL63*

OC43 is a *betacoronavirus* that commonly infects humans¹³². OC43 infection is commonly associated with symptoms of the common cold: runny nose, cough, sore throat, and fever. Most OC43 infections are mild, that virus can cause severe respiratory illness in young children, the elderly, and those who are immune compromised. In instances, OC43 can lead to pneumonia and bronchiolitis¹³³.

OC43, 229E, and are coronaviruses known for causing mild upper respiratory illnesses like the common cold. Symptoms include runny nose, cough, sore through, fever¹³². Most infections are mild, that virus can cause severe respiratory illness in young children, the elderly, and those who are immune compromised. Occasionally these coronaviruses can lead to pneumonia and bronchiolitis¹³³. In rare cases, OC43 has been associated with neurological diseases, like encephalitis¹³⁴. NL63 can cause croup, an infection of the larynx and trachea, especially in young children¹³⁵. There are rare instances where NL63 results in acute respiratory distress syndrome (ARDS)¹³⁶. These viruses are known for their global and seasonal infections.

1.3.5 *SARS-CoV-2 Pathophysiology*

The emergence of SARS-CoV-2 is responsible for the COVID-19 pandemic and has had a multifaceted impact globally since 2019. The World Health Organization (WHO) has recorded more than 771 million confirmed cases of COVID-19 and 6.98 million deaths globally^{137,138}.

SARS-CoV-2 is transmitted through respiratory droplets and aerosols, with an average incubation period of 4-5 days before the onset of symptoms. In most cases, the

infection results in mild to moderate respiratory symptoms but can progress to a severe illness a week after symptom onset, characterized by dyspnea and hypoxemia, due to progressive respiratory failure¹³⁹. As previously mentioned, SARS-CoV-2 spike protein recognizes the host's ACE-2 receptor and TMPRSS2 cleaves the spike protein to facilitate the endocytosis of the virus^{116,140}. Most infections are cleared at this stage through the induction of type I or type III interferons and the activation of B and T cell responses. Type I and III interferons are critical components of the innate immune response. Interferons are signaling proteins released by the host cells due to pathogens. Type I includes subtypes of interferon-alpha (IFN- α) and interferon-beta (IFN- β), which are produced by infected cells. They enhance the ability of immune cells to recognize and attack infected cells, stimulate the production of antiviral proteins that inhibit viral replication, and enhance antigen presentation. Type III includes interferon-lambda (IFN- λ), which defend against infections in the mucosal surfaces, such as those in the respiratory tract where SARS-CoV-2 first establishes infection. IFN- λ works similarly to type I interferons but has a more localized effect, primarily affecting epithelial cells^{141,142}. B cells produce antibodies against the virus that ideally neutralize the virus from binding to and entering the host cells. Additionally, they mark infected cells for destruction by other cells. There are two main types of T cells involved in responding to SARS-CoV-2. CD8+ cells, also known as cytotoxic T cells, can directly kill virus-infected cells. CD4+ T cells, or helper T cells, help B cells produce antibodies and aid in activating other immune cells^{143,144}.

SARS-CoV-2 causes diffuse alveolar damage (DAD), characterized by endothelial and alveolar lining cell injury. The lung damage caused by SARS-CoV-2

infection progresses through two distinct phases: initially, an exudative phase characterized by edema, cell death, the formation of hyaline membranes, and inflammation; this is subsequently followed by a proliferative phase, wherein alveolar type 2 (AT2) cells undergo hyperplasia to repair and regenerate the damaged alveoli^{145,146}. Infected and damaged epithelial cells attract immune cells and increase monocytes and macrophage infiltration in the lungs of COVID-19 patients with aberrant activation of these cells. The immune response responds by secreting pro-inflammatory cytokines IL-1 β and IL-6, a unique feature of SARS-CoV-2 infection compared to other pneumonia infections^{147,148}. Alveolar damage and epithelium disruption cause an imbalance between coagulation and fibrinolysis, causing hyaline membrane formation. In severe cases, lung regeneration can be impeded and lead to chronic respiratory failure¹⁴⁹.

1.3.6 SARS-CoV-2 Treatments

The need to develop effective treatment for SARS-CoV-2 is essential for reducing the mortality rate associated with COVID-19, but also for mitigating the broader consequences of the pandemic on public health systems and communities worldwide. One class of treatments is antivirals, medications specifically for treating viral infections. Unlike antibiotics used to treat bacteria, they are ineffective at treating viruses. Antivirals function by inhibiting the development or proliferation of viruses. There is an array of mechanisms by which they work, such as: blocking viral entry, inhibiting viral replication, or impairing viral assembly and release. Antivirals constitute a class of medications specifically designed to treat viral infections. Contrasting with antibiotics, which combat bacterial infections, antivirals are effective against viruses. Their primary

function is to inhibit the growth and proliferation of viruses, thus playing a crucial role in the management and treatment of various viral diseases¹⁵⁰.

The antivirals and treatment strategies for SARS-CoV-2 have changed throughout the pandemic. One strategy consisted of using an RdRp inhibitor, Favipiravir, because of its promise in other RNA viruses such as Ebola and H1N1. Unfortunately, findings revealed that it is ineffective at treating COVID-19¹⁵¹. Lopinavir, in conjunction with ritonavir combination therapy, are protease inhibitors initially tested for the treatment of HIV, however, elevated triglycerides grade 3/4 and drug interactions necessitated the need for further dosage testing¹⁵². Lopinavir/ritonavir combination therapy for SARS-CoV-2 yielded no significant improvement compared to placebo groups¹⁵³. Ivermectin is effective at treating parasitic infections while having some anti-inflammatory properties. Ivermectin is effective at treating onchocerciasis, helminthiasis, and scabies, but not COVID-19. There is also the concern of misuse due to misinformation surrounding ivermectin¹⁵³⁻¹⁵⁵. Chloroquine and hydroxychloroquine have been explored due to use as an antimalarial. They increase the endosomal pH, which is necessary for virus-host membrane fusion. Despite promising initial reports, there is no conclusive data showing efficacy against SARS-CoV-2. Additionally, there is the potential of cardiovascular toxicity. Remdesivir is an antiviral developed for treating Ebola and inhibits viral RdRp. Additional antivirals that have shown to be effective are nirmatrelvir with ritonavir and Molnupiravir^{156,157}.

Vaccines have been developed that administer mRNA corresponding to the SARS-CoV-2 spike protein into patients, eliciting an immune response. mRNA vaccines like Pfizer-BioNTech's BNT162b2 and Moderna's mRNA-1273 deliver synthetic mRNA

encapsulated in lipid nanoparticles into the host cell^{158,159}. Once injected, the mRNA is used by the cell's machinery to produce the spike protein, which is then presented on the cell surface. This does not cause disease and triggers an immune response to produce antibodies against SARS-CoV-2's spike protein. Clinical trials demonstrated a high efficacy of 95% for Pfizer-BioNTech and 94.1% for Moderna, in preventing COVID-19 infections after vaccinations^{158,159}.

1.3.7 SARS-CoV-2 Variants

Late 2020, SARS-CoV-2 underwent significant mutations in its genome resulting in variants with altered transmissibility and the ability to evade immune response. These variants of concern (VOC) included Alpha, Beta, Gamma, Delta, and Omicron spread in regions or globally^{160,161}. The VOCs had mutations in their spike proteins, especially Omicron. This led to a significant antigenic shift from immune responses primed by vaccines or past infections¹⁶². The mutations that the VOC directly affected their increased fitness and dominance over previous strains. Despite mutations, many T cell responses remain effective against VOCs^{163,164}. The Furin cleavage site (FCS) is crucial for SARS-CoV-2 entry into cells, and mutations in the FCS have contributed to the enhanced transmissibility of variants like Alpha and Delta¹⁶⁵⁻¹⁶⁷. The emergence of variants is unpredictable, continuous monitoring is necessary to understand SARS-CoV-2's future trajectory.

1.4 References

1. Bochman ML, Paeschke K, Zakian VA. DNA secondary structures: stability and function of G-quadruplex structures. *Nat Rev Genet.* Nov 2012;13(11):770-80. doi:10.1038/nrg3296
2. Dhakal S, Cui Y, Koirala D, et al. Structural and mechanical properties of individual human telomeric G-quadruplexes in molecularly crowded solutions. *Nucleic Acids Res.* Apr 1 2013;41(6):3915-23. doi:10.1093/nar/gkt038
3. Biffi G, Tannahill D, McCafferty J, Balasubramanian S. Quantitative visualization of DNA G-quadruplex structures in human cells. *Nature Chemistry.* 2013/03/01 2013;5(3):182-186. doi:10.1038/nchem.1548
4. Chambers VS, Marsico G, Boutell JM, Di Antonio M, Smith GP, Balasubramanian S. High-throughput sequencing of DNA G-quadruplex structures in the human genome. *Nat Biotechnol.* Aug 2015;33(8):877-81. doi:10.1038/nbt.3295
5. Howard FB, Miles HT. Poly(inosinic acid) helices: essential chelation of alkali metal ions in the axial channel. *Biochemistry.* Dec 21 1982;21(26):6736-45. doi:10.1021/bi00269a019
6. Sundquist WI, Klug A. Telomeric DNA dimerizes by formation of guanine tetrads between hairpin loops. *Nature.* Dec 14 1989;342(6251):825-9. doi:10.1038/342825a0
7. Bouaziz S, Kettani A, Patel DJ. A K cation-induced conformational switch within a loop spanning segment of a DNA quadruplex containing G-G-G-C repeats. *Journal of molecular biology.* 1998/09// 1998;282(3):637-652. doi:10.1006/jmbi.1998.2031
8. Nazia P, Amen S, Seunghee Cho and Kyeong Kyu K. Computational Approaches to Predict the Non-canonical DNAs. *Current Bioinformatics.* 2019;14(6):470-479. doi:<http://dx.doi.org/10.2174/1574893614666190126143438>
9. Yu C-H, Teulade-Fichou M-P, Olsthoorn RCL. Stimulation of ribosomal frameshifting by RNA G-quadruplex structures. *Nucleic acids research.* 2014;42(3):1887-1892. doi:10.1093/nar/gkt1022
10. Lavezzo E, Berselli M, Frasson I, et al. G-quadruplex forming sequences in the genome of all known human viruses: a comprehensive guide. *bioRxiv.* 2018:344127. doi:10.1101/344127
11. Fay MM, Lyons SM, Ivanov P. RNA G-Quadruplexes in Biology: Principles and Molecular Mechanisms. *J Mol Biol.* Jul 7 2017;429(14):2127-2147. doi:10.1016/j.jmb.2017.05.017
12. Gellert M, Lipsett MN, Davies DR. Helix formation by guanylic acid. *Proc Natl Acad Sci U S A.* Dec 15 1962;48:2013-8. doi:10.1073/pnas.48.12.2013
13. Metifiot M, Amrane S, Litvak S, Andreola ML. G-quadruplexes in viruses: function and potential therapeutic applications. *Nucleic Acids Res.* Nov 10 2014;42(20):12352-66. doi:10.1093/nar/gku999
14. Millevoi S, Moine H, Vagner S. G-quadruplexes in RNA biology. *Wiley Interdiscip Rev RNA.* Jul-Aug 2012;3(4):495-507. doi:10.1002/wrna.1113
15. Ou TM, Lu YJ, Tan JH, Huang ZS, Wong KY, Gu LQ. G-quadruplexes: targets in anticancer drug design. *ChemMedChem.* May 2008;3(5):690-713. doi:10.1002/cmdc.200700300

16. Perrone R, Doria F, Butovskaya E, et al. Synthesis, Binding and Antiviral Properties of Potent Core-Extended Naphthalene Diimides Targeting the HIV-1 Long Terminal Repeat Promoter G-Quadruplexes. *J Med Chem*. Dec 24 2015;58(24):9639-52. doi:10.1021/acs.jmedchem.5b01283
17. Ruggiero E, Richter SN. G-quadruplexes and G-quadruplex ligands: targets and tools in antiviral therapy. *Nucleic Acids Res*. Apr 20 2018;46(7):3270-3283. doi:10.1093/nar/gky187
18. Neidle S. Human telomeric G-quadruplex: The current status of telomeric G-quadruplexes as therapeutic targets in human cancer. <https://doi.org/10.1111/j.1742-4658.2009.07463.x>. *The FEBS Journal*. 2010/03/01 2010;277(5):1118-1125. doi:<https://doi.org/10.1111/j.1742-4658.2009.07463.x>
19. Artusi S, Ruggiero E, Nadai M, et al. Antiviral Activity of the G-Quadruplex Ligand TMPyP4 against Herpes Simplex Virus-1. *Viruses*. 2021;13(2). doi:10.3390/v13020196
20. Artusi S, Nadai M, Perrone R, et al. The Herpes Simplex Virus-1 genome contains multiple clusters of repeated G-quadruplex: Implications for the antiviral activity of a G-quadruplex ligand. *Antiviral Res*. Jun 2015;118:123-31. doi:10.1016/j.antiviral.2015.03.016
21. Dabral P, Babu J, Zareie A, Verma SC. LANA and hnRNP A1 Regulate the Translation of LANA mRNA through G-Quadruplexes. *J Virol*. Jan 17 2020;94(3)doi:10.1128/JVI.01508-19
22. Daskalogianni C, Pyndiah S, Apcher S, et al. Epstein-Barr virus-encoded EBNA1 and ZEBRA: targets for therapeutic strategies against EBV-carrying cancers. *J Pathol*. Jan 2015;235(2):334-41. doi:10.1002/path.4431
23. Tomaszewska M, Szabat M, Zielińska K, Kierzek R. Identification and Structural Aspects of G-Quadruplex-Forming Sequences from the Influenza A Virus Genome. *Int J Mol Sci*. Jun 2 2021;22(11)doi:10.3390/ijms22116031
24. Molnár OR, Végh A, Somkuti J, Smeller L. Characterization of a G-quadruplex from hepatitis B virus and its stabilization by binding TMPyP4, BRACO19 and PhenDC3. *Scientific Reports*. 2021/12/01 2021;11(1):23243. doi:10.1038/s41598-021-02689-y
25. Estep KN, Butler TJ, Ding J, Brosh RM. G4-Interacting DNA Helicases and Polymerases: Potential Therapeutic Targets. *Curr Med Chem*. 2019;26(16):2881-2897. doi:10.2174/0929867324666171116123345
26. Frasson I, Soldà P, Nadai M, Lago S, Richter SN. Parallel G-quadruplexes recruit the HSV-1 transcription factor ICP4 to promote viral transcription in herpes virus-infected human cells. *Communications Biology*. 2021/04/30 2021;4(1):510. doi:10.1038/s42003-021-02035-y
27. Manzourolajdad A, Gonzalez M, Spouge JL. Changes in the Plasticity of HIV-1 Nef RNA during the Evolution of the North American Epidemic. *PLOS ONE*. 2016;11(9):e0163688. doi:10.1371/journal.pone.0163688
28. Zarrouk K, Piret J, Boivin G. Herpesvirus DNA polymerases: Structures, functions and inhibitors. *Virus Res*. Apr 15 2017;234:177-192. doi:10.1016/j.virusres.2017.01.019

29. Holzerlandt R, Orengo C, Kellam P, Albà MM. Identification of new herpesvirus gene homologs in the human genome. *Genome Res.* Nov 2002;12(11):1739-48. doi:10.1101/gr.334302
30. Renne R, Zhong W, Herndier B, et al. Lytic growth of Kaposi's sarcoma-associated herpesvirus (human herpesvirus 8) in culture. *Nature Medicine.* 1996/03/01 1996;2(3):342-346. doi:10.1038/nm0396-342
31. Decker LL, Shankar P, Khan G, et al. The Kaposi sarcoma-associated herpesvirus (KSHV) is present as an intact latent genome in KS tissue but replicates in the peripheral blood mononuclear cells of KS patients. *J Exp Med.* Jul 1 1996;184(1):283-8. doi:10.1084/jem.184.1.283
32. Purushothaman P, Uppal T, Verma SC. Molecular biology of KSHV lytic reactivation. *Viruses.* Jan 14 2015;7(1):116-53. doi:10.3390/v7010116
33. McGeoch DJ, Cook S, Dolan A, Jamieson FE, Telford EA. Molecular phylogeny and evolutionary timescale for the family of mammalian herpesviruses. *J Mol Biol.* Mar 31 1995;247(3):443-58. doi:10.1006/jmbi.1995.0152
34. McGeoch DJ, Dolan A, Ralph AC. Toward a comprehensive phylogeny for mammalian and avian herpesviruses. *J Virol.* Nov 2000;74(22):10401-6. doi:10.1128/jvi.74.22.10401-10406.2000
35. Grinde B. Herpesviruses: latency and reactivation - viral strategies and host response. *J Oral Microbiol.* Oct 25 2013;5doi:10.3402/jom.v5i0.22766
36. Whitley RJ. Herpesviruses. In: Baron S, ed. *Medical Microbiology.* University of Texas Medical Branch at Galveston
Copyright © 1996, The University of Texas Medical Branch at Galveston.; 1996.
37. Goncalves PH, Ziegelbauer J, Uldrick TS, Yarchoan R. Kaposi sarcoma herpesvirus-associated cancers and related diseases. *Curr Opin HIV AIDS.* Jan 2017;12(1):47-56. doi:10.1097/coh.0000000000000330
38. Braun M. Classics in Oncology. Idiopathic multiple pigmented sarcoma of the skin by Kaposi. *CA Cancer J Clin.* Nov-Dec 1982;32(6):340-7. doi:10.3322/canjclin.32.6.340
39. Bhutani M, Polizzotto MN, Uldrick TS, Yarchoan R. Kaposi sarcoma-associated herpesvirus-associated malignancies: epidemiology, pathogenesis, and advances in treatment. *Semin Oncol.* Apr 2015;42(2):223-46. doi:10.1053/j.seminoncol.2014.12.027
40. Chang Y, Cesarman E, Pessin MS, et al. Identification of herpesvirus-like DNA sequences in AIDS-associated Kaposi's sarcoma. *Science.* Dec 16 1994;266(5192):1865-9. doi:10.1126/science.7997879
41. Cesarman E, Chang Y, Moore PS, Said JW, Knowles DM. Kaposi's sarcoma-associated herpesvirus-like DNA sequences in AIDS-related body-cavity-based lymphomas. *N Engl J Med.* May 4 1995;332(18):1186-91. doi:10.1056/NEJM199505043321802
42. Wen KW, Damania B. Kaposi sarcoma-associated herpesvirus (KSHV): molecular biology and oncogenesis. *Cancer Lett.* Mar 28 2010;289(2):140-50. doi:10.1016/j.canlet.2009.07.004
43. Beckstead JH, Wood GS, Fletcher V. Evidence for the origin of Kaposi's sarcoma from lymphatic endothelium. *Am J Pathol.* May 1985;119(2):294-300.

44. Dupin N, Fisher C, Kellam P, et al. Distribution of human herpesvirus-8 latently infected cells in Kaposi's sarcoma, multicentric Castleman's disease, and primary effusion lymphoma. *Proc Natl Acad Sci U S A*. Apr 13 1999;96(8):4546-51. doi:10.1073/pnas.96.8.4546
45. Gessain A, Duprez R. Spindle cells and their role in Kaposi's sarcoma. *Int J Biochem Cell Biol*. Dec 2005;37(12):2457-65. doi:10.1016/j.biocel.2005.01.018
46. Iscovich J, Boffetta P, Brennan P. Classic Kaposi's sarcoma as a first primary neoplasm. *Int J Cancer*. Jan 18 1999;80(2):173-7. doi:10.1002/(sici)1097-0215(19990118)80:2<173::aid-ijc2>3.0.co;2-2
47. Dutz W, Stout AP. Kaposi's sarcoma in infants and children. *Cancer*. Jul-Aug 1960;13:684-94. doi:10.1002/1097-0142(196007/08)13:4<684::aid-cncr2820130408>3.0.co;2-g
48. Penn I. Secondary neoplasms as a consequence of transplantation and cancer therapy. *Cancer Detect Prev*. 1988;12(1-6):39-57.
49. Beral V, Peterman TA, Berkelman RL, Jaffe HW. Kaposi's sarcoma among persons with AIDS: a sexually transmitted infection? *Lancet*. Jan 20 1990;335(8682):123-8. doi:10.1016/0140-6736(90)90001-1
50. Mbulaiteye SM, Biggar RJ, Goedert JJ, Engels EA. Immune deficiency and risk for malignancy among persons with AIDS. *J Acquir Immune Defic Syndr*. Apr 15 2003;32(5):527-33. doi:10.1097/00126334-200304150-00010
51. Narkhede M, Arora S, Ujjani C. Primary effusion lymphoma: current perspectives. *Onco Targets Ther*. 2018;11:3747-3754. doi:10.2147/ott.s167392
52. Arvanitakis L, Mesri EA, Nador RG, et al. Establishment and characterization of a primary effusion (body cavity-based) lymphoma cell line (BC-3) harboring kaposi's sarcoma-associated herpesvirus (KSHV/HHV-8) in the absence of Epstein-Barr virus. *Blood*. Oct 1 1996;88(7):2648-54.
53. Oksenhendler E, Carcelain G, Aoki Y, et al. High levels of human herpesvirus 8 viral load, human interleukin-6, interleukin-10, and C reactive protein correlate with exacerbation of multicentric castleman disease in HIV-infected patients. *Blood*. Sep 15 2000;96(6):2069-73.
54. Saeed-Abdul-Rahman I, Al-Amri AM. Castleman disease. *Korean J Hematol*. Sep 2012;47(3):163-77. doi:10.5045/kjh.2012.47.3.163
55. Soulier J, Grollet L, Oksenhendler E, et al. Kaposi's sarcoma-associated herpesvirus-like DNA sequences in multicentric Castleman's disease. *Blood*. Aug 15 1995;86(4):1276-80.
56. Staudt MR, Kanan Y, Jeong JH, Papin JF, Hines-Boykin R, Dittmer DP. The tumor microenvironment controls primary effusion lymphoma growth in vivo. *Cancer Res*. Jul 15 2004;64(14):4790-9. doi:10.1158/0008-5472.can-03-3835
57. Regamey N, Tamm M, Wernli M, et al. Transmission of human herpesvirus 8 infection from renal-transplant donors to recipients. *N Engl J Med*. Nov 5 1998;339(19):1358-63. doi:10.1056/nejm199811053391903
58. Grange PA, Gressier L, Williams JF, Dyson OF, Akula SM, Dupin N. Cloning a human saliva-derived peptide for preventing KSHV transmission. *J Invest Dermatol*. 2012;1733-5. vol. 6.

59. Giffin L, Damania B. KSHV: pathways to tumorigenesis and persistent infection. *Adv Virus Res.* 2014;88:111-59. doi:10.1016/b978-0-12-800098-4.00002-7
60. Coen N, Duraffour S, Snoeck R, Andrei G. KSHV targeted therapy: an update on inhibitors of viral lytic replication. *Viruses.* Nov 24 2014;6(11):4731-59. doi:10.3390/v6114731
61. Labo N, Miley W, Benson CA, Campbell TB, Whitby D. Epidemiology of Kaposi's sarcoma-associated herpesvirus in HIV-1-infected US persons in the era of combination antiretroviral therapy. *Aids.* Jun 19 2015;29(10):1217-25. doi:10.1097/qad.0000000000000682
62. Sullivan RJ, Pantanowitz L, Casper C, Stebbing J, Dezube BJ. HIV/AIDS: epidemiology, pathophysiology, and treatment of Kaposi sarcoma-associated herpesvirus disease: Kaposi sarcoma, primary effusion lymphoma, and multicentric Castleman disease. *Clin Infect Dis.* Nov 1 2008;47(9):1209-15. doi:10.1086/592298
63. Russo JJ, Bohenzky RA, Chien MC, et al. Nucleotide sequence of the Kaposi sarcoma-associated herpesvirus (HHV8). *Proc Natl Acad Sci U S A.* Dec 10 1996;93(25):14862-7. doi:10.1073/pnas.93.25.14862
64. Searles Robert P, Bergquam Eric P, Axthelm Michael K, Wong Scott W. Sequence and Genomic Analysis of a Rhesus Macaque Rhadinovirus with Similarity to Kaposi's Sarcoma-Associated Herpesvirus/Human Herpesvirus 8. *Journal of Virology.* 1999;73(4):3040-3053. doi:10.1128/jvi.73.4.3040-3053.1999
65. Alexander L, Denekamp L, Knapp A, Auerbach MR, Damania B, Desrosiers RC. The primary sequence of rhesus monkey rhadinovirus isolate 26-95: sequence similarities to Kaposi's sarcoma-associated herpesvirus and rhesus monkey rhadinovirus isolate 17577. *J Virol.* Apr 2000;74(7):3388-98. doi:10.1128/jvi.74.7.3388-3398.2000
66. Sakakibara S, Tosato G. Contribution of viral mimics of cellular genes to KSHV infection and disease. *Viruses.* Sep 19 2014;6(9):3472-86. doi:10.3390/v6093472
67. Ganem D. KSHV-induced oncogenesis. In: Arvin A, Campadelli-Fiume G, Mocarski E, et al, eds. *Human Herpesviruses: Biology, Therapy, and Immunoprophylaxis.* Cambridge University Press Copyright © Cambridge University Press 2007.; 2007.
68. Boshoff C, Schulz TF, Kennedy MM, et al. Kaposi's sarcoma-associated herpesvirus infects endothelial and spindle cells. *Nat Med.* Dec 1995;1(12):1274-8. doi:10.1038/nm1295-1274
69. Bechtel JT, Liang Y, Hvidding J, Ganem D. Host range of Kaposi's sarcoma-associated herpesvirus in cultured cells. *J Virol.* Jun 2003;77(11):6474-81. doi:10.1128/jvi.77.11.6474-6481.2003
70. Ballestas ME, Kaye KM. The latency-associated nuclear antigen, a multifunctional protein central to Kaposi's sarcoma-associated herpesvirus latency. *Future Microbiol.* Dec 2011;6(12):1399-413. doi:10.2217/fmb.11.137
71. Atari N, Rajan KS, Chikne V, et al. Lytic Reactivation of the Kaposi's Sarcoma-Associated Herpesvirus (KSHV) Is Accompanied by Major Nucleolar Alterations. *Viruses.* Aug 4 2022;14(8)doi:10.3390/v14081720
72. Krishnan HH, Naranatt PP, Smith MS, Zeng L, Bloomer C, Chandran B. Concurrent expression of latent and a limited number of lytic genes with immune modulation and antiapoptotic function by Kaposi's sarcoma-associated herpesvirus early

during infection of primary endothelial and fibroblast cells and subsequent decline of lytic gene expression. *J Virol.* Apr 2004;78(7):3601-20. doi:10.1128/jvi.78.7.3601-3620.2004

73. Aneja KK, Yuan Y. Reactivation and Lytic Replication of Kaposi's Sarcoma-Associated Herpesvirus: An Update. *Front Microbiol.* 2017;8:613. doi:10.3389/fmicb.2017.00613

74. Toth Z, Brulois K, Jung JU. The chromatin landscape of Kaposi's sarcoma-associated herpesvirus. *Viruses.* May 23 2013;5(5):1346-73. doi:10.3390/v5051346

75. Nealon K, Newcomb WW, Pray TR, Craik CS, Brown JC, Kedes DH. Lytic replication of Kaposi's sarcoma-associated herpesvirus results in the formation of multiple capsid species: isolation and molecular characterization of A, B, and C capsids from a gammaherpesvirus. *J Virol.* Mar 2001;75(6):2866-78. doi:10.1128/jvi.75.6.2866-2878.2001

76. Verma SC, Choudhuri T, Kaul R, Robertson ES. Latency-associated nuclear antigen (LANA) of Kaposi's sarcoma-associated herpesvirus interacts with origin recognition complexes at the LANA binding sequence within the terminal repeats. *J Virol.* Mar 2006;80(5):2243-56. doi:10.1128/jvi.80.5.2243-2256.2006

77. Uppal T, Banerjee S, Sun Z, Verma SC, Robertson ES. KSHV LANA--the master regulator of KSHV latency. *Viruses.* Dec 11 2014;6(12):4961-98. doi:10.3390/v6124961

78. Purushothaman P, Dabral P, Gupta N, Sarkar R, Verma SC. KSHV Genome Replication and Maintenance. *Front Microbiol.* 2016;7:54. doi:10.3389/fmicb.2016.00054

79. Toth Z, Brulois K, Lee HR, et al. Biphasic euchromatin-to-heterochromatin transition on the KSHV genome following de novo infection. *PLoS Pathog.* 2013;9(12):e1003813. doi:10.1371/journal.ppat.1003813

80. Toth Z, Papp B, Brulois K, Choi YJ, Gao S-J, Jung JU. LANA-Mediated Recruitment of Host Polycomb Repressive Complexes onto the KSHV Genome during De Novo Infection. *PLOS Pathogens.* 2016;12(9):e1005878. doi:10.1371/journal.ppat.1005878

81. Lan K, Kuppers DA, Verma SC, Robertson ES. Kaposi's sarcoma-associated herpesvirus-encoded latency-associated nuclear antigen inhibits lytic replication by targeting Rta: a potential mechanism for virus-mediated control of latency. *J Virol.* Jun 2004;78(12):6585-94. doi:10.1128/jvi.78.12.6585-6594.2004

82. Davis DA, Rinderknecht AS, Zoetewij JP, et al. Hypoxia induces lytic replication of Kaposi sarcoma-associated herpesvirus. *Blood.* May 15 2001;97(10):3244-50. doi:10.1182/blood.v97.10.3244

83. Lin CL, Li H, Wang Y, Zhu FX, Kudchodkar S, Yuan Y. Kaposi's sarcoma-associated herpesvirus lytic origin (ori-Lyt)-dependent DNA replication: identification of the ori-Lyt and association of K8 bZip protein with the origin. *J Virol.* May 2003;77(10):5578-88. doi:10.1128/jvi.77.10.5578-5588.2003

84. Wang Y, Tang Q, Maul GG, Yuan Y. Kaposi's sarcoma-associated herpesvirus ori-Lyt-dependent DNA replication: dual role of replication and transcription activator. *J Virol.* Dec 2006;80(24):12171-86. doi:10.1128/JVI.00990-06

85. Arvanitakis L, Geras-Raaka E, Varma A, Gershengorn MC, Cesarman E. Human herpesvirus KSHV encodes a constitutively active G-protein-coupled receptor linked to cell proliferation. *Nature*. Jan 23 1997;385(6614):347-50. doi:10.1038/385347a0
86. Gao SJ, Boshoff C, Jayachandra S, Weiss RA, Chang Y, Moore PS. KSHV ORF K9 (vIRF) is an oncogene which inhibits the interferon signaling pathway. *Oncogene*. Oct 16 1997;15(16):1979-85. doi:10.1038/sj.onc.1201571
87. Verma SC, Lan K, Robertson E. Structure and function of latency-associated nuclear antigen. *Curr Top Microbiol Immunol*. 2007;312:101-36. doi:10.1007/978-3-540-34344-8_4
88. Zaldumbide A, Ossevoort M, Wiertz EJHJ, Hoeben RC. In cis inhibition of antigen processing by the latency-associated nuclear antigen I of Kaposi sarcoma Herpes virus. *Molecular Immunology*. 2007/02/01/ 2007;44(6):1352-1360. doi:<https://doi.org/10.1016/j.molimm.2006.05.012>
89. De Leo A, Deng Z, Vladimirova O, et al. LANA oligomeric architecture is essential for KSHV nuclear body formation and viral genome maintenance during latency. *PLOS Pathogens*. 2019;15(1):e1007489. doi:10.1371/journal.ppat.1007489
90. Barbera AJ, Chodaparambil JV, Kelley-Clarke B, et al. The nucleosomal surface as a docking station for Kaposi's sarcoma herpesvirus LANA. *Science*. Feb 10 2006;311(5762):856-61. doi:10.1126/science.1120541
91. Garber AC, Hu J, Renne R. Latency-associated nuclear antigen (LANA) cooperatively binds to two sites within the terminal repeat, and both sites contribute to the ability of LANA to suppress transcription and to facilitate DNA replication. *J Biol Chem*. Jul 26 2002;277(30):27401-11. doi:10.1074/jbc.M203489200
92. Hellert J, Weidner-Glunde M, Krausze J, et al. The 3D structure of Kaposi sarcoma herpesvirus LANA C-terminal domain bound to DNA. *Proc Natl Acad Sci U S A*. May 26 2015;112(21):6694-9. doi:10.1073/pnas.1421804112
93. Jha HC, Upadhyay SK, M AJP, et al. H2AX phosphorylation is important for LANA-mediated Kaposi's sarcoma-associated herpesvirus episome persistence. *J Virol*. May 2013;87(9):5255-69. doi:10.1128/jvi.03575-12
94. Krithivas A, Fujimuro M, Weidner M, Young DB, Hayward SD. Protein interactions targeting the latency-associated nuclear antigen of Kaposi's sarcoma-associated herpesvirus to cell chromosomes. *J Virol*. Nov 2002;76(22):11596-604. doi:10.1128/jvi.76.22.11596-11604.2002
95. Xiao B, Verma SC, Cai Q, et al. Bub1 and CENP-F can contribute to Kaposi's sarcoma-associated herpesvirus genome persistence by targeting LANA to kinetochores. *J Virol*. Oct 2010;84(19):9718-32. doi:10.1128/jvi.00713-10
96. Ottinger M, Christalla T, Nathan K, Brinkmann MM, Viejo-Borbolla A, Schulz TF. Kaposi's sarcoma-associated herpesvirus LANA-1 interacts with the short variant of BRD4 and releases cells from a BRD4- and BRD2/RING3-induced G1 cell cycle arrest. *J Virol*. Nov 2006;80(21):10772-86. doi:10.1128/jvi.00804-06
97. You J, Srinivasan V, Denis GV, et al. Kaposi's sarcoma-associated herpesvirus latency-associated nuclear antigen interacts with bromodomain protein Brd4 on host mitotic chromosomes. *J Virol*. Sep 2006;80(18):8909-19. doi:10.1128/jvi.00502-06

98. Taniguchi Y. The Bromodomain and Extra-Terminal Domain (BET) Family: Functional Anatomy of BET Paralogous Proteins. *International Journal of Molecular Sciences*. 2016;17(11). doi:10.3390/ijms17111849
99. Fehr AR, Perlman S. Coronaviruses: an overview of their replication and pathogenesis. *Methods Mol Biol*. 2015;1282:1-23. doi:10.1007/978-1-4939-2438-7_1
100. Gorbalenya AE, Baker SC, Baric RS, et al. The species Severe acute respiratory syndrome-related coronavirus: classifying 2019-nCoV and naming it SARS-CoV-2. *Nature Microbiology*. 2020/04/01 2020;5(4):536-544. doi:10.1038/s41564-020-0695-z
101. Corman VM, Muth D, Niemeyer D, Drosten C. Hosts and Sources of Endemic Human Coronaviruses. *Adv Virus Res*. 2018;100:163-188. doi:10.1016/bs.aivir.2018.01.001
102. Weiss SR, Leibowitz JL. Coronavirus pathogenesis. *Adv Virus Res*. 2011;81:85-164. doi:10.1016/b978-0-12-385885-6.00009-2
103. Liu DX, Liang JQ, Fung TS. Human Coronavirus-229E, -OC43, -NL63, and -HKU1 (Coronaviridae). *Encyclopedia of Virology*. Copyright © 2021 Elsevier Ltd. All rights reserved.; 2021:428-40.
104. Monchatre-Leroy E, Boué F, Boucher JM, et al. Identification of Alpha and Beta Coronavirus in Wildlife Species in France: Bats, Rodents, Rabbits, and Hedgehogs. *Viruses*. Nov 29 2017;9(12)doi:10.3390/v9120364
105. Domańska-Blicharz K, Miłek-Krupa J, Piłkuła A. Gulls as a host for both gamma and deltacoronaviruses. *Scientific Reports*. 2023/09/13 2023;13(1):15104. doi:10.1038/s41598-023-42241-8
106. van der Hoek L, Pyrc K, Jebbink MF, et al. Identification of a new human coronavirus. *Nat Med*. Apr 2004;10(4):368-73. doi:10.1038/nm1024
107. Woo PC, Lau SK, Chu CM, et al. Characterization and complete genome sequence of a novel coronavirus, coronavirus HKU1, from patients with pneumonia. *J Virol*. Jan 2005;79(2):884-95. doi:10.1128/jvi.79.2.884-895.2005
108. Peiris JS, Lai ST, Poon LL, et al. Coronavirus as a possible cause of severe acute respiratory syndrome. *Lancet*. Apr 19 2003;361(9366):1319-25. doi:10.1016/s0140-6736(03)13077-2
109. Zaki AM, van Boheemen S, Bestebroer TM, Osterhaus AD, Fouchier RA. Isolation of a novel coronavirus from a man with pneumonia in Saudi Arabia. *N Engl J Med*. Nov 8 2012;367(19):1814-20. doi:10.1056/NEJMoa1211721
110. Assiri A, Al-Tawfiq JA, Al-Rabeeh AA, et al. Epidemiological, demographic, and clinical characteristics of 47 cases of Middle East respiratory syndrome coronavirus disease from Saudi Arabia: a descriptive study. *Lancet Infect Dis*. Sep 2013;13(9):752-61. doi:10.1016/s1473-3099(13)70204-4
111. Assiri A, McGeer A, Perl TM, et al. Hospital outbreak of Middle East respiratory syndrome coronavirus. *N Engl J Med*. Aug 1 2013;369(5):407-16. doi:10.1056/NEJMoa1306742
112. Ou X, Liu Y, Lei X, et al. Characterization of spike glycoprotein of SARS-CoV-2 on virus entry and its immune cross-reactivity with SARS-CoV. *Nat Commun*. Mar 27 2020;11(1):1620. doi:10.1038/s41467-020-15562-9

113. Zhu N, Zhang D, Wang W, et al. A Novel Coronavirus from Patients with Pneumonia in China, 2019. *N Engl J Med*. Feb 20 2020;382(8):727-733. doi:10.1056/NEJMoa2001017
114. Huang C, Wang Y, Li X, et al. Clinical features of patients infected with 2019 novel coronavirus in Wuhan, China. *Lancet*. Feb 15 2020;395(10223):497-506. doi:10.1016/s0140-6736(20)30183-5
115. Sola I, Almazán F, Zúñiga S, Enjuanes L. Continuous and Discontinuous RNA Synthesis in Coronaviruses. *Annu Rev Virol*. Nov 2015;2(1):265-88. doi:10.1146/annurev-virology-100114-055218
116. Hoffmann M, Kleine-Weber H, Schroeder S, et al. SARS-CoV-2 Cell Entry Depends on ACE2 and TMPRSS2 and Is Blocked by a Clinically Proven Protease Inhibitor. *Cell*. Apr 16 2020;181(2):271-280.e8. doi:10.1016/j.cell.2020.02.052
117. Schoeman D, Fielding BC. Coronavirus envelope protein: current knowledge. *Virol J*. May 27 2019;16(1):69. doi:10.1186/s12985-019-1182-0
118. Cong Y, Kriegenburg F, de Haan CAM, Reggiori F. Coronavirus nucleocapsid proteins assemble constitutively in high molecular oligomers. *Scientific Reports*. 2017/07/18 2017;7(1):5740. doi:10.1038/s41598-017-06062-w
119. Ghosh S, Dellibovi-Ragheb TA, Kerviel A, et al. β -Coronaviruses Use Lysosomes for Egress Instead of the Biosynthetic Secretory Pathway. *Cell*. Dec 10 2020;183(6):1520-1535.e14. doi:10.1016/j.cell.2020.10.039
120. Denison MR, Graham RL, Donaldson EF, Eckerle LD, Baric RS. Coronaviruses: an RNA proofreading machine regulates replication fidelity and diversity. *RNA Biol*. Mar-Apr 2011;8(2):270-9. doi:10.4161/rna.8.2.15013
121. Wang Y, Grunewald M, Perlman S. Coronaviruses: An Updated Overview of Their Replication and Pathogenesis. *Methods Mol Biol*. 2020;2203:1-29. doi:10.1007/978-1-0716-0900-2_1
122. Snijder EJ, Decroly E, Ziebuhr J. The Nonstructural Proteins Directing Coronavirus RNA Synthesis and Processing. *Adv Virus Res*. 2016;96:59-126. doi:10.1016/bs.aivir.2016.08.008
123. Hofmann H, Pyrc K, van der Hoek L, Geier M, Berkhout B, Pöhlmann S. Human coronavirus NL63 employs the severe acute respiratory syndrome coronavirus receptor for cellular entry. *Proc Natl Acad Sci U S A*. May 31 2005;102(22):7988-93. doi:10.1073/pnas.0409465102
124. Yeager CL, Ashmun RA, Williams RK, et al. Human aminopeptidase N is a receptor for human coronavirus 229E. *Nature*. 1992/06/01 1992;357(6377):420-422. doi:10.1038/357420a0
125. Huang X, Dong W, Milewska A, et al. Human Coronavirus HKU1 Spike Protein Uses O-Acetylated Sialic Acid as an Attachment Receptor Determinant and Employs Hemagglutinin-Esterase Protein as a Receptor-Destroying Enzyme. *J Virol*. Jul 2015;89(14):7202-13. doi:10.1128/jvi.00854-15
126. Du L, Yang Y, Zhou Y, Lu L, Li F, Jiang S. MERS-CoV spike protein: a key target for antivirals. *Expert Opin Ther Targets*. Feb 2017;21(2):131-143. doi:10.1080/14728222.2017.1271415

127. Castillo G, Mora-Díaz JC, Breuer M, Singh P, Nelli RK, Giménez-Lirola LG. Molecular mechanisms of human coronavirus NL63 infection and replication. *Virus Res.* Apr 2 2023;327:199078. doi:10.1016/j.virusres.2023.199078
128. Bertram S, Dijkman R, Habjan M, et al. TMPRSS2 activates the human coronavirus 229E for cathepsin-independent host cell entry and is expressed in viral target cells in the respiratory epithelium. *J Virol.* Jun 2013;87(11):6150-60. doi:10.1128/jvi.03372-12
129. Saunders N, Fernandez I, Planchais C, et al. TMPRSS2 is a functional receptor for human coronavirus HKU1. *Nature.* 2023/10/25 2023;doi:10.1038/s41586-023-06761-7
130. Choi CH, Hao L, Narayan SP, Auyeung E, Mirkin CA. Mechanism for the endocytosis of spherical nucleic acid nanoparticle conjugates. *Proc Natl Acad Sci U S A.* May 7 2013;110(19):7625-30. doi:10.1073/pnas.1305804110
131. Li W, Moore MJ, Vasilieva N, et al. Angiotensin-converting enzyme 2 is a functional receptor for the SARS coronavirus. *Nature.* Nov 27 2003;426(6965):450-4. doi:10.1038/nature02145
132. Masters PS. The molecular biology of coronaviruses. *Adv Virus Res.* 2006;66:193-292. doi:10.1016/s0065-3527(06)66005-3
133. Gaunt ER, Hardie A, Claas EC, Simmonds P, Templeton KE. Epidemiology and clinical presentations of the four human coronaviruses 229E, HKU1, NL63, and OC43 detected over 3 years using a novel multiplex real-time PCR method. *J Clin Microbiol.* Aug 2010;48(8):2940-7. doi:10.1128/jcm.00636-10
134. Kasereka MC, Hawkes MT. Neuroinvasive potential of human coronavirus OC43: case report of fatal encephalitis in an immunocompromised host. *J Neurovirol.* Apr 2021;27(2):340-344. doi:10.1007/s13365-020-00926-0
135. van der Hoek L, Sure K, Ihorst G, et al. Croup is associated with the novel coronavirus NL63. *PLoS Med.* Aug 2005;2(8):e240. doi:10.1371/journal.pmed.0020240
136. Mayer K, Nellessen C, Hahn-Ast C, et al. Fatal outcome of human coronavirus NL63 infection despite successful viral elimination by IFN-alpha in a patient with newly diagnosed ALL. *Eur J Haematol.* © 2016 John Wiley & Sons A/S. Published by John Wiley & Sons Ltd.; 2016:208-210. vol. 2.
137. Irkham I, Ibrahim AU, Nwekwo CW, Al-Turjman F, Hartati YW. Current Technologies for Detection of COVID-19: Biosensors, Artificial Intelligence and Internet of Medical Things (IoMT): Review. *Sensors.* 2023;23(1). doi:10.3390/s23010426
138. Organization GWH. WHO Coronavirus (COVID-19) Dashboard. <https://covid19.who.int/?mapFilter=deaths>
139. Yang X, Yu Y, Xu J, et al. Clinical course and outcomes of critically ill patients with SARS-CoV-2 pneumonia in Wuhan, China: a single-centered, retrospective, observational study. *The Lancet Respiratory Medicine.* 2020/05/01/ 2020;8(5):475-481. doi:[https://doi.org/10.1016/S2213-2600\(20\)30079-5](https://doi.org/10.1016/S2213-2600(20)30079-5)
140. Liu G, Du W, Sang X, et al. RNA G-quadruplex in TMPRSS2 reduces SARS-CoV-2 infection. *Nature Communications.* 2022/03/17 2022;13(1):1444. doi:10.1038/s41467-022-29135-5
141. Lamers MM, Haagmans BL. SARS-CoV-2 pathogenesis. *Nature Reviews Microbiology.* 2022/05/01 2022;20(5):270-284. doi:10.1038/s41579-022-00713-0

142. Vallamkonda J, John A, Wani WY, et al. SARS-CoV-2 pathophysiology and assessment of coronaviruses in CNS diseases with a focus on therapeutic targets. *Biochim Biophys Acta Mol Basis Dis*. Oct 1 2020;1866(10):165889. doi:10.1016/j.bbadis.2020.165889
143. Tarke A, Sidney J, Methot N, et al. Impact of SARS-CoV-2 variants on the total CD4(+) and CD8(+) T cell reactivity in infected or vaccinated individuals. *Cell Rep Med*. Jul 20 2021;2(7):100355. doi:10.1016/j.xcrm.2021.100355
144. Sette A, Crotty S. Adaptive immunity to SARS-CoV-2 and COVID-19. *Cell*. Feb 18 2021;184(4):861-880. doi:10.1016/j.cell.2021.01.007
145. Falcón-Cama V, Montero-González T, Acosta-Medina EF, et al. Evidence of SARS-CoV-2 infection in postmortem lung, kidney, and liver samples, revealing cellular targets involved in COVID-19 pathogenesis. *Arch Virol*. Feb 26 2023;168(3):96. doi:10.1007/s00705-023-05711-y
146. Erjefält JS, de Souza Xavier Costa N, Jönsson J, et al. Diffuse alveolar damage patterns reflect the immunological and molecular heterogeneity in fatal COVID-19. *EBioMedicine*. Sep 2022;83:104229. doi:10.1016/j.ebiom.2022.104229
147. Esakandari H, Nabi-Afjadi M, Fakkari-Afjadi J, Farahmandian N, Miresmaeili SM, Bahreini E. A comprehensive review of COVID-19 characteristics. *Biol Proced Online*. 2020;22:19. doi:10.1186/s12575-020-00128-2
148. Conti P, Ronconi G, Caraffa A, et al. Induction of pro-inflammatory cytokines (IL-1 and IL-6) and lung inflammation by Coronavirus-19 (COVI-19 or SARS-CoV-2): anti-inflammatory strategies. *J Biol Regul Homeost Agents*. March-April 2020;34(2):327-331. doi:10.23812/conti-e
149. Zaim S, Chong JH, Sankaranarayanan V, Harky A. COVID-19 and Multiorgan Response. *Current problems in cardiology*. 2020;45(8):100618-100618. doi:10.1016/j.cpcardiol.2020.100618
150. Bezzi G, Piga EJ, Binolfi A, Armas P. CNBP Binds and Unfolds In Vitro G-Quadruplexes Formed in the SARS-CoV-2 Positive and Negative Genome Strands. *Int J Mol Sci*. Mar 5 2021;22(5)doi:10.3390/ijms22052614
151. McMahon JH, Lau JSY, Coldham A, et al. Favipiravir in early symptomatic COVID-19, a randomised placebo-controlled trial. *EClinicalMedicine*. Dec 2022;54:101703. doi:10.1016/j.eclinm.2022.101703
152. Cvetkovic RS, Goa KL. Lopinavir/ritonavir: a review of its use in the management of HIV infection. *Drugs*. 2003;63(8):769-802. doi:10.2165/00003495-200363080-00004
153. Patel TK, Patel PB, Barvaliya M, Saurabh MK, Bhalla HL, Khosla PP. Efficacy and safety of lopinavir-ritonavir in COVID-19: A systematic review of randomized controlled trials. *J Infect Public Health*. Jun 2021;14(6):740-748. doi:10.1016/j.jiph.2021.03.015
154. Vallejos J, Zoni R, Bangher M, et al. Ivermectin to prevent hospitalizations in patients with COVID-19 (IVERCOR-COVID19) a randomized, double-blind, placebo-controlled trial. *BMC Infect Dis*. Jul 2 2021;21(1):635. doi:10.1186/s12879-021-06348-5
155. López-Medina E, López P, Hurtado IC, et al. Effect of Ivermectin on Time to Resolution of Symptoms Among Adults With Mild COVID-19: A Randomized Clinical Trial. *Jama*. Apr 13 2021;325(14):1426-1435. doi:10.1001/jama.2021.3071

156. Ganatra S, Dani SS, Ahmad J, et al. Oral Nirmatrelvir and Ritonavir in Nonhospitalized Vaccinated Patients With Coronavirus Disease 2019. *Clin Infect Dis*. Feb 18 2023;76(4):563-572. doi:10.1093/cid/ciac673
157. Jayk Bernal A, Gomes da Silva MM, Musungaie DB, et al. Molnupiravir for Oral Treatment of Covid-19 in Nonhospitalized Patients. *New England Journal of Medicine*. 2022/02/10 2021;386(6):509-520. doi:10.1056/NEJMoa2116044
158. Polack FP, Thomas SJ, Kitchin N, et al. Safety and Efficacy of the BNT162b2 mRNA Covid-19 Vaccine. *New England Journal of Medicine*. 2020/12/31 2020;383(27):2603-2615. doi:10.1056/NEJMoa2034577
159. Baden LR, El Sahly HM, Essink B, et al. Efficacy and Safety of the mRNA-1273 SARS-CoV-2 Vaccine. *New England Journal of Medicine*. 2021/02/04 2020;384(5):403-416. doi:10.1056/NEJMoa2035389
160. Thomson EC, Rosen LE, Shepherd JG, et al. Circulating SARS-CoV-2 spike N439K variants maintain fitness while evading antibody-mediated immunity. *Cell*. Mar 4 2021;184(5):1171-1187.e20. doi:10.1016/j.cell.2021.01.037
161. Carabelli AM, Peacock TP, Thorne LG, et al. SARS-CoV-2 variant biology: immune escape, transmission and fitness. *Nature Reviews Microbiology*. 2023/03/01 2023;21(3):162-177. doi:10.1038/s41579-022-00841-7
162. Meng B, Kemp SA, Papa G, et al. Recurrent emergence of SARS-CoV-2 spike deletion H69/V70 and its role in the Alpha variant B.1.1.7. *Cell Rep*. Jun 29 2021;35(13):109292. doi:10.1016/j.celrep.2021.109292
163. Motozono C, Toyoda M, Zahradnik J, et al. SARS-CoV-2 spike L452R variant evades cellular immunity and increases infectivity. *Cell Host Microbe*. Jul 14 2021;29(7):1124-1136.e11. doi:10.1016/j.chom.2021.06.006
164. Dolton G, Rius C, Hasan MS, et al. Emergence of immune escape at dominant SARS-CoV-2 killer T cell epitope. *Cell*. Aug 4 2022;185(16):2936-2951.e19. doi:10.1016/j.cell.2022.07.002
165. Campbell F, Archer B, Laurenson-Schafer H, et al. Increased transmissibility and global spread of SARS-CoV-2 variants of concern as at June 2021. *Euro Surveill*. Jun 2021;26(24)doi:10.2807/1560-7917.es.2021.26.24.2100509
166. Davies NG, Abbott S, Barnard RC, et al. Estimated transmissibility and impact of SARS-CoV-2 lineage B.1.1.7 in England. *Science*. Apr 9 2021;372(6538)doi:10.1126/science.abg3055
167. Liu Y, Liu J, Johnson BA, et al. Delta spike P681R mutation enhances SARS-CoV-2 fitness over Alpha variant. *Cell Rep*. May 17 2022;39(7):110829. doi:10.1016/j.celrep.2022.110829

CHAPTER 2

2. G-QUADRUPLEXES IN REGULATING VIRAL GENE EXPRESSIONS AND THEIR IMPACTS IN CONTROLLING INFECTION.

Zarerie A. R. et al. *Pathogens* (In Review) (2023)

2.1 Abstract

G-quadruplexes (G4s) are non-canonical nucleic acid structures that play significant roles in regulating various biological processes, including replication, transcription, translation, and recombination. Recent studies have identified G4s in the genomes of several viruses, such as herpes viruses, hepatitis viruses, and human coronaviruses. These structures are implicated in regulating viral transcription, replication, and virion production, influencing viral infectivity and pathogenesis. G4-stabilizing ligands, like TMPyP4, PhenDC3, and BRACO-19, show potential antiviral properties by targeting and stabilizing G4 structures, inhibiting essential viral life cycle processes. This review delves into the existing literature on G-quadruplexes' involvement in viral regulation, emphasizing specific G-quadruplex-stabilizing ligands. While progress has been made in understanding how these ligands regulate viruses, further research is needed to elucidate the mechanisms through which G-quadruplexes impact viral processes. More research is necessary to develop G-quadruplex-stabilizing ligands as novel antiviral agents. The increasing body of literature underscores the importance of G-quadruplexes in viral biology and the development of innovative therapeutic strategies against viral infections. Despite some ligands' known regulatory effects on viruses, a deeper comprehension of the multifaceted impact of G-quadruplexes on viral processes is essential. This review advocates for intensified research to unravel the intricate relationship between G-quadruplexes and viral processes, paving the way for novel antiviral treatments.

Keywords: G-quadruplex; G4; Secondary Structure; Virus Regulation; G4-Stabilizers; DNA; RNA

2.2 Introduction

G-quadruplex (G4) are non-canonical secondary structures in guanine-rich DNA and RNA sequences. These structures form two or more consecutive guanine blocks separated by single-stranded loop regions. Four successive runs of guanine blocks result in G-tetrads held together by Hoogsteen hydrogen bonding¹⁻⁴. The hydrogen bonding in G4s differs from the classical Watson-Crick model by the N7 group of guanines interacting with an exocyclic amino group from a neighboring base. A monovalent or divalent cation, such as K^+ , Na^+ , or Ca^{2+} , stabilizes the tetrad⁵⁻⁷. Potassium is the prevalent stabilizer due to its favorable ionic radius and Gibbs free energy of solvation¹⁶⁸. These structures fold into two or more planar G-tetrads, held together by Hoogsteen hydrogen bonding between the guanines and π - π stacking between the quartets. The stability of G4s is proportional to the number of stacked quartets, resulting in higher strength and lower numbers of nucleotides comprising the loop regions, increasing stability¹⁶⁹. Computational tools are available for in silico determination of potential G4-forming sequences (PQSs), such as QGRS Mapper, Quadparser, and PQSFinder⁸. The formation of G-quadruplexes in cells has been demonstrated by G4-specific antibodies^{3,170}.

G4 structures serve different regulatory roles in both DNA and RNA. G4s have been identified in transcriptional, replicative, and epigenetic regulation in DNA. Stabilizing G4s in DNA through ligands can cause stalling of the RNA Pol II during transcription due to the bulky secondary structure of G4s⁹. Furthermore, there is extensive research on the stabilizing properties G4s play in telomere maintenance¹⁰⁻¹³. This review discusses various G-quadruplex stabilizing agents and their roles in

modulating the G4s present in viruses. G4s serve as regulatory elements in transcription, translation, RNA maturation, and regulating non-coding RNA¹⁴. PQSs are prone to adopt a secondary structure in RNA rather than DNA, given RNA's absence of a complementary strand. This folding propensity contributes to the enhanced stability of the RNA molecule¹⁷¹. PQSs are present in functional domains 5'-U2TR, ORF, and 3'-UTR. G4s have been shown to affect the coding capacity of a genome through alternative polyadenylation, alternative splicing, and induced frame shifts¹⁴.

Several ligands can target the G-quadruplexes to modulate their stability. These ligands show the establishment of a potential therapeutic avenue as antivirals. G4 stabilizing ligands share many characteristics, including polycyclic aromatic scaffolding¹⁵⁻¹⁷. The ligands interact with the G4's $\pi - \pi$ stacking, with the terminal tetrad, and the lateral positive charged moieties interact with the phosphate groups within the loops¹⁸. Modifications to G4 stabilizing ligands have enhanced their selectivity and binding affinity to G4 structures. Given the high conservation of PQSs., the feasibility of a G4-based antiviral therapy is heightened, providing a promising avenue for combating diverse viral strains. Consequently, targeting G4 structures in viruses presents a strategic approach for effective antiviral interventions.

2.3 G-quadruplexes as antiviral targets

The prospect of utilizing G-quadruplexes as targets for antiviral therapy stems from their involvement in multiple stages of the viral life cycle, their evolutionary conservation, and their distinct structural characteristics compared to canonical nucleic acid structures. These attributes provide a foundation for developing broad-spectrum

antiviral agents with minimal off-target effects on host cells. However, the endeavor to target G4s faces several challenges. Firstly, despite their specificity for G4 structures, there is still a risk of off-target effects on host G4s, potentially resulting in cytotoxicity or other undesirable consequences. Secondly, the high structural diversity of G4s demands the development of specific ligands tailored for individual G4s in viruses. Lastly, achieving effective intracellular delivery of G4-binding molecules poses a challenge due to the potential for degradation or inadequate cellular uptake. Numerous small molecules have been synthesized and documented for their interaction with G4 structures, showcasing antiviral activity by stabilizing or destabilizing G4s. Some notable examples include:

2.3.1 Porphyrins

Porphyrins are a class of heterocyclic macrocycle compounds that interact and stabilize G4s. This class of molecules has a central metal ion surrounded by four pyrrole subunits connected through methine bridges, forming a planar ring¹⁷². Porphyrins, owing to their strong affinity for G-quadruplex structures and their capability to modulate G-quadruplex-mediated processes, hold promise as potential antiviral agents within this class¹⁷³. One well-studied porphyrin is TMPyP4 (5,10,15,20-Tetrakis-(N-methyl-4-pyridyl)porphine), which is a small molecule shown to interact with and stabilize G4s¹⁷⁴. TMPyP4's positively charged porphyrin ring system binds to G4 tetrads and intercalates between the stacked guanine planes, forming electrostatic interactions with the negatively charged phosphate backbone of DNA/RNA^{175,176}. This stabilization can inhibit the activity of enzymes that would otherwise disrupt or unwind the structure. Studies have

shown that the TMPyP4 can selectively bind to and stabilize G4s over other DNA/RNA structures and can inhibit the activity of telomerase, an enzyme that adds telomeric DNA repeats to the end of chromosomes and is highly active in cancer cells. TMPyP4 has been proposed as a potential anticancer agent that can selectively target cancer cells by inhibiting telomerase activity and inducing telomere shortening, leading to apoptosis or senescence^{177,178}. TMPyP2 is a structural isomer of TMPyP4 with the N-methyl groups in the 2-position, causing steric hindrance and preventing binding to the G4, making it an ideal negative control¹⁷⁹.

N-methyl mesoporphyrin IX (NMM) is a porphyrin derivative that contains a positively charged porphyrin ring with an N-methyl. The ring can interact with the negatively charged phosphate backbone of DNA/RNA through electrostatic interactions, while the methyl group can intercalate between the stacked guanine planes of the G4 structure, allowing for further stabilization. Specifically for parallel G4s, the N-methyl can fit into the center of the G4 core and align with the stabilizing cation, allowing for efficient $\pi - \pi$ stacking¹⁸⁰. NMM preferentially binds to G4s over duplexed DNA and binds to both parallel and antiparallel G4s¹⁸¹. NMM induces the folding of guanine-rich sequences into G4 structures. This has been exploited to develop NMM to detect G4 structures in cells and tissues. NMM is a fluorescent molecule (excitation at $\lambda=393\text{nm}$ and emission at $\lambda=610\text{nm}$) when bound selectively to parallel G4s, resulting in up to a 60-fold amplified signal. Since NMM preferentially binds to parallel G4 topology, it can discriminate between different strand orientations based on fluorescent fold enhancement¹⁸².

NMM has been shown to inhibit telomerase activity, just like the previously mentioned G4 stabilizers¹⁸³. NMM has been shown to inhibit the expression of oncogenes and induce the expression of tumor suppressor genes by stabilizing G4s in the promoter regions of these genes. This stabilization can prevent transcription factors and RNA polymerase binding to the promoter regions, thereby inhibiting the oncogenes' expression and inducing the tumor suppressor genes¹¹. While porphyrins exhibit significant promise as G4-mediated antiviral agents, particular challenges warrant attention. Their relatively non-specific binding to diverse G4 structures may induce off-target effects on host G4 structures. Additionally, porphyrins' bioavailability and cellular uptake require optimization to achieve sufficient intracellular concentrations for effective antiviral activity. Nevertheless, porphyrins are a promising class of G4-targeting compounds with potential applications in antiviral therapies. Ongoing research to refine their selectivity, potency, and pharmacokinetic properties is essential in developing safe and efficacious antiviral treatments.

2.3.2 Bisquinolinium compounds

Bisquinolinium compounds are small molecules containing bisquinoline moiety, having high affinity and selectivity for G4 structures. PhenDC3 is a well-studied bisquinolinium-derivatized phenanthroline-dicarboxamide that interacts with G4s through extensive $\pi - \pi$ bonding between the external tetrads¹⁸⁴. PhenDC3 has a higher affinity for nuclear G4 DNA than predominant duplexed DNA. This compound can organize its internal hydrogen bonds into syn-syn conformation; this is critical for G4 binding¹⁸⁵. PhenDC3 binds to G4s through its planar, aromatic perylene ring system, which can

intercalate between the stacked guanine planes of the G4 structure. This interaction increases thermal stability, making it more resistant to thermal denaturation or degradation by the nucleases¹⁸⁶. Like TMPyP4, PhenDC3 has been proposed as a potential anticancer agent, as it selectively targets cancer cells by inhibiting telomerase activity and inducing telomere shortening, leading to apoptosis or senescence^{185,187,188}. PhenDC3 has been shown to have other biological activities, including the inhibition of topoisomerase II, a DNA enzyme involved in DNA replication and transcription^{187,189}. Much like porphyrins, bisquinolium compounds carry the potential for off-target effects. Nevertheless, through ongoing refinement efforts, bisquinolium compounds exhibit promising potential as G4-mediated antiviral agents.

3.3.3 *Naphthalene Diimides*

Naphthalene Diimides (NDIs) are a class of organic molecules that exhibit high affinity for and stabilize G4s. NDIs have a flat, planar structure that allows them to stack into the planar guanine bases of G-quadruplex structures¹⁹⁰. The π - π stacking interaction between the planar naphthalene core of NDIs and the G-tetrads of the G-quadruplex and the imide groups interacting with the loops and grooves of the G4 structure enhances the overall polarity of the G-quadruplex. The increased polarity consequently results in heightened structural instability. The interaction between NDIs and G-quadruplexes is further stabilized by hydrogen bonding and Van der Waals forces¹⁹⁰. With remarkable stability, the G4-NDI complex is valuable for diagnostic and therapeutic applications. Developing derivatives with heightened G4 affinity and selectivity further enhances their potential. Specifically, these compounds demonstrate a strong binding capacity to G4s in

telomeres and oncogene promoters, rendering them particularly advantageous for anticancer research^{191,15-17}. NDI derivatives have been developed to improve G4 binding affinity, selectivity, and pharmacokinetic properties.

2.3.4 BRACO-19 and Derivatives

The N,N'-9((4(dimethylamino)phenyl)amino)acridine-3-6-diyl)bis(3-(pyrrolidine-1-yl)propenamide), commonly known as BRACO-19, is a 3,6,9-trisubstituted acridine compound that stabilizes G4 structures. 3,6,9-trisubstituted acridine compounds have high selectivity for G4s over duplexed DNA, lower cytotoxicity, and inhibit telomerase activity¹⁹²⁻¹⁹⁴. This interaction is based on a central planar pharmacophore that facilitates binding to G-quartets via π - π interactions. Meanwhile, the two side chains containing a tertiary amine moiety allow recognition of the grooves in G4 structures¹⁹².

2.3.5 Pyridostatin/Derivatives

Pyridostatin (PDS) is an electron-rich, flat, aromatic G4 stabilizing ligand able to participate in hydrogen bonding. Through G4 stabilization, PDS inhibits telomeric elongation and triggers a DNA damage response to the telomeres¹⁹⁵. Utilizing the PDS scaffold has come many derivatives capable of inhibiting cancer cell replication through G4-mediation¹⁹⁶.

2.4 Therapeutic Strategies Exploiting G-quadruplexes

Strategic therapeutic approaches harnessing the unique structural attributes of G4s seek to pioneer innovative strategies for combating viral infections. By intricately targeting and manipulating the distinct features of G4s, researchers aim to develop novel antiviral agents that selectively interact with these specialized nucleic acid arrangements. This tailored interaction is anticipated to modulate critical viral processes, including replication, transcription, and translation, ultimately leading to the suppression or eradication of the virus. However, a critical consideration in these strategies is the potential for off-target effects, such as inadvertent binding to host G4s, possibly resulting in cytotoxicity or other unintended adverse effects. Furthermore, the delivery of many of these strategies into target cells presents a formidable challenge, as they may be susceptible to degradation or insufficient uptake by cells, potentially limiting their efficacy¹⁹⁷.

2.4.1 Antisense oligonucleotides (ASOs)

Antisense oligonucleotides (ASOs) have risen as a promising therapeutic avenue for G-quadruplex (G4) targeting within viral genomes, owing to their exceptional specificity and capacity to regulate gene expression. These succinct, synthetic DNA/RNA molecules are meticulously designed to bind with high precision to complementary target RNA sequences, specifically those within PQSs in the viral genome. This targeted binding enables the meticulous manipulation of viral gene expression, presenting a distinctive opportunity for developing groundbreaking antiviral therapies¹⁹⁸. Upon hybridization with the target RNA, ASOs disrupt G4 structures, interfering with RNA folding and preventing the formation of stable, functional G4s. This disruption affects

various aspects of viral gene expression, including transcription, translation, and post-transcriptional modifications, ultimately impacting viral replication and pathogenesis¹⁹⁸.

ASOs offer several advantages over traditional antiviral therapies, including high specificity for viral target sequences, the ability to target multiple G4 structures simultaneously, and a reduced likelihood of developing resistance due to their unique mode of action¹⁹⁹. Additionally, ASOs can be chemically modified to improve stability, binding affinity, and pharmacokinetic properties, further enhancing their therapeutic p

2.4.2 CRISPR/Cas9-mediated G-quadruplex stabilization

The CRISPR/Cas9 system has emerged as a potent genome-editing tool with the potential to be repurposed for targeting and stabilizing G4s within viral genomes²⁰⁰. Utilizing guide RNAs (gRNAs) specifically designed to recognize PQS regions, CRISPR/Cas9 can introduce targeted mutations or insertions that facilitate G4 stabilization. Targeting G4s with CRISPR/Cas9 can offer multiple advantages, such as high specificity and efficiency, along with the potential to target multiple G4 structures simultaneously by employing an array of guide RNAs (gRNAs) designed to recognize distinct PQS regions within the viral genome²⁰¹. The versatility of the CRISPR/Cas9 system also enables the investigation of various G4-mediated regulatory mechanisms, such as replication, transcription, and translation, by generating targeted modifications within the viral genome. This could ultimately lead to identifying new therapeutic targets and strategies for combating viral infections. Further research into optimizing gRNA design, delivery methods, and potential off-target effects will be essential in harnessing the potential of the CRISPR/Cas9 system for G4-based antiviral therapy.

2.4.3 RNA interference (RNAi) and small interfering RNA (siRNA)

RNA interference (RNAi) is a highly conserved mechanism within cells that has a critical function in regulating gene expression using small RNA molecules, such as microRNAs and small interfering RNAs²⁰². The process involves introducing small RNA molecules into the RNA-induced silencing complex (RISC), which then binds to the target mRNA sequences causing either cleavage or translational repression, ultimately resulting in post-transcriptional gene silencing²⁰³. RNAi-based therapies offer several advantages over traditional antiviral treatments, including high specificity for target sequences, reduced likelihood of developing resistance due to the unique mode of action, and the ability to target multiple G4 structures simultaneously²⁰⁴. Additionally, RNAi can be tailored to target highly conserved regions within viral genomes, potentially enabling the development of broad-spectrum antiviral agents²⁰⁵. As an effective therapeutic approach, RNAi targets G4s in viral genomes by degrading complementary messenger RNAs selectively and efficiently to reduce the replication of viruses^{206,207}. Targeting PQSs responsible for forming G-quadruplexes decreases gene expression levels, ultimately leading to post-transcriptional silencing of genes via mRNA cleavage or translational repression through incorporation into the RISC complex^{208,209}.

2.4.4 Aptamers

Aptamers are oligonucleotides composed of short, single-stranded DNA or RNA with unique three-dimensional configurations capable of specifically and tightly binding to target molecules. These nucleic acid-based agents, also known as "chemical

antibodies," can recognize a broad range of targets, including proteins, small molecules, and nucleic acids²¹⁰. Leveraging this versatility, aptamers emerge as a promising strategy for antiviral interventions, showcasing the potential to disrupt viral propagation by specifically targeting G-quadruplex structures within the viral genome²¹¹. By attaching themselves to G4 structures within viral genomes or interfering with those interactions between viral proteins and G4s, aptamers can disrupt vital processes during the virus life cycle, such as replication, transcriptional activities, and protein-nucleic acid associations. Consequently, reducing expression rates of genes belonging to viruses or even impairing critical functions played by proteins can ultimately suppress virus propagation.

Aptamers are promising antiviral agents due to their remarkable specificity and high affinity for targets, minimizing off-target effects on host cells. Their synthesis and modification are relatively straightforward, facilitating rapid development and optimization. The Systematic Evolution of Ligands by Exponential Enrichment (SELEX) process allows for the selection of aptamers with optimal binding characteristics for a given target^{211,212}. However, challenges accompany aptamer-based antiviral therapies, including the imperative to ensure stability and effective delivery to target cells.

Aptamers are susceptible to degradation by nucleases or may experience inadequate uptake by cells. Additionally, the potential for resistance build-up to aptamer-based therapies poses a concern, either through viral mutations or alterations in G-quadruplex structures.

2.4.5 G4-based drug delivery systems

The distinctive secondary structures of G4s present a unique opportunity to target gene regulatory regions, specifically in various cancer-associated genes. By serving as

molecular switches, G4s can modulate gene expression, opening novel avenues for drug targeting. When used in conjunction with nanoparticles, G4s enhance anti-cancer drugs' loading capacity and amplify their biological effects. A notable example is AS1411, an aptamer designed to recognize Nucleolin (NCL), a multifunctional DNA/RNA binding protein overexpressed on the surface of diverse cancer cell types, including B-cell chronic lymphocytic leukemia, breast cancer, cervical cancer, gastric cancer etc.²¹³⁻²¹⁷. TMPyP4 is crucial in photodynamic therapy, demonstrating efficacy in treating malignant and premalignant tissues. Upon excitation by optimal light, TMPyP4 generates singlet oxygen in cancer cells, inducing cell death²¹⁸. When combined with AS1411, TMPyP4 exhibits a notable 3.8-fold increased accumulation in breast cancer cells compared to normal fibroblasts and epithelial cells²¹⁹. AS1411 has been used as a transporter for various compounds, including acridines, phthalocyanines, and porphyrin derivatives²¹⁹⁻²²¹. An array of AS1411 derivatives have been synthesized, and ongoing research has been conducted to increase their delivery specificity/uptake, anti-cancer properties, and greater nuclease resistance^{222,215,223}. While several AS1411 derivatives show promise, further testing is required, and the development of additional G-quadruplex aptamers is also underway. This concerted effort underscores the potential for advancing targeted therapies in cancer treatment^{224,225}.

Liposomes are nanoparticles that are a form of drug delivery system. Liposomes are desired for their pharmacokinetics, biocompatibility, and potential immunogenicity²²⁶. In a successful application, liposomes encapsulating cis-diamminedichloroplatinum(II) (cisplatin), a chemotherapeutic agent, were modified with AS1411 anchored to their surface, ensuring precise delivery to target cells. The endocytosis of the liposome proved

to be NCL-dependent, with NCL-negative or non-cancerous cells exhibiting minimal uptake of the drug²²⁷. This strategic utilization of liposomes, guided by AS1411, highlights the potential for targeted drug delivery systems in cancer therapy.

Micelles, characterized by a small amphiphilic structure with a hydrophobic core and hydrophilic shell, uniquely accumulate in tumor environments²²⁸. An innovative mixed micellar system was devised, combining AS1411 with D- α -tocopheryl polyethylene glycol 1000 (TPGS) polymer and pH-sensitive D- α -tocopheryl polyethylene glycol 1000-block-poly-(β -amino ester) (TPGS-b-PBAE, TP) copolymer, providing a targeted approach for cancer cell intervention. This system enables the selective cytoplasmic release of paclitaxel in ovarian cancer cells, substantially increasing cytotoxicity and cellular arrest²²⁹. Moreover, this method of drug delivery proves effective in reducing multidrug resistance²³⁰. Another ingenious approach involves using the amphiphilic polymer F127, integrated with beta-cyclodextrin-linked poly (ethylene glycol)-b-poly lactide (β -CD-PELA) block copolymers. Coated with AS1411 and employed for doxorubicin delivery, this system exhibits efficient drug release, specifically at a pH of 5.0, achieving nearly 80% efficiency in drug liberation²³¹. These advancements highlight the potential of micellar-based drug delivery systems in achieving targeted and efficient cancer therapy.

Dendrimers are hyper-branched polymers that have repetitive units extending outward from the core. They have been used as drug delivery systems due to their controllable molecular weight and their precise and high geometric symmetry²³²⁻²³⁴. An additional desired quality is that these aptamer-functionalized dendrimers have a high transfection efficiency while maintaining low cytotoxicity and bxl-xL selective inhibition

of cancer cells²³³. AS1411-conjugated polyamidation dendrimers successfully target NCL positive cells and knock down Bcl-xL protein expression, leading to apoptosis of cancer cells²³³. These findings underscore the potential of dendrimer-AS1411 nanoparticles as a promising strategy for precisely targeting NCL-expressing cancer cells, offering prospects for innovative and targeted therapeutic interventions.

Gold nanoparticles (AuNPs) modified with oligos have high cellular internalization^{130,235}; however, AuNPs alone are inefficient at drug delivery, as they can be recognized and sequestered by macrophages²³⁶. AuNPs conjugated with AS1411 improve cellular uptake and cytotoxic effects. In an animal model of breast cancer, this conjugation demonstrated notable antitumor efficiency²³⁷. This conjugation and a porphyrin derivative can be used for targeted imaging and efficient photodynamic therapy (PDT)²³⁸.

Compared to heavy metal-based inorganic nanoparticles, graphene oxide (GO), a carbon-based nanoparticle, has greater biocompatibility²³⁹. GO can be modified with biopolymers on their surface, allowing degradation by peroxidases, ideally after the drug delivery²⁴⁰. Conjugation of GO with G4 sequence/aptamer is a promising therapeutic option in targeted drug delivery. Silica nanoparticles, an alternative to GO, can incorporate a photosensitizer (TMPyP4). When irradiated, these G-quadruplex DNA-capped silica nanoparticles generate reactive oxygen species, cleaving the G-quadruplex DNA cap and facilitating drug release²⁴¹. Folate receptors are upregulated in certain cancer cells; therefore, adding folic acid to the silica nanoparticles can increase targeting efficiency^{241,242}.

5-fluorouracil (5-FU) is a fluoropyrimidine and chemotherapy agent for treating colorectal cancer²⁴³. Exploiting two G4 delivery systems with four and six G-tetrads (TG₄T) and (TG₆T) connected to FdU showed transport of the FdU pentamer and increased cytotoxic effects of the FU drug in FU-resistant colorectal cancer cells. Due to these results and the fact that parallel G4 structures are not being affected by incorporating the FdU pentamer at the 5'-end, parallel G4s are shown to be a promising strategy in delivering fluoropyrimidines to cancer cells²⁴⁴.

2.5 DNA Viruses

DNA viruses are a diverse group of viruses with either a single or double-stranded DNA genome. DNA viruses can have circular or linear DNA and vary in size. Unlike RNA viruses, DNA viruses replicate their genome within the host cell's nucleus, allowing for more complex replication strategies. Replication of DNA viruses starts with the delivery of the viral genome to the host cells' nucleus²⁴⁵. The viral DNA is then transcribed by the host's transcription machinery, producing viral mRNA that is translated into viral proteins. These proteins then replicate the viral genome and assemble new virus particles. The replication of DNA viruses within the host cell's nucleus additionally allows for the establishment of latent infections, where the viral genome is maintained in a silent state within the host cell²⁴⁶. This is seen in herpesviruses, which can establish lifelong infections in the host and reactivate to cause disease later in life²⁴⁷.

DNA viruses exhibit diverse replication mechanisms based on their virus family. For instance, herpesviruses employ a rolling circle mechanism, replicating viral DNA as a long, single-stranded molecule that cleaves into unit-length genomes. In contrast,

adenoviruses utilize a strand displacement mechanism, replicating viral DNA as a double-stranded molecule with a displaced strand serving as a template for further replication. Additionally, DNA viruses possess protein capsids that encapsulate the genome, with variations in capsid shape, including icosahedral or helical forms. Some of these viruses are enveloped, featuring a lipid membrane surrounding the capsid, as observed in the case of herpesvirus²⁴⁸.

2.5.1 Herpesviridae

Human herpesviruses (HHVs) cause life-long infections that can lead to many diseases. All HHVs have large dsDNA genomes enriched in GCs and PQSs²⁴⁹. Herpesviruses are divided into three subfamilies: alpha, beta, and gamma herpesviruses. Alpha herpesviruses include herpes simplex virus 1 (HSV-1), responsible for oral infections leading to sores, fever, or blisters; herpes simplex virus 2 (HSV-2), responsible for genital herpes infections; and varicella-zoster virus (VZV), causes chickenpox (varicella) in the initial infection and shingles (zoster) upon reactivation²⁵⁰.

HSV-1 contains the most abundant PQS in the repeat region of the viral genome. Specifically, G4s have been found in the promoters of several HSV-1 genes, including the immediate early genes ICP0 and ICP4. ICP0 and ICP4 are essential for HSV-1 replication, resulting in high regulation. Regulation of ICP0 and ICP4 are essential for HSV-1 replication, and their expression is tightly regulated. Studies have shown that the formation of G4s in the promoter regions of these genes can regulate their transcription by inhibiting the binding of transcription factors or blocking the access of RNA polymerase to the promoter region²⁵. For example, ICP4 positively autoregulates its

promoter through a G4 interaction. Additionally, BRACO-19 stabilizes the expression of ICP4 by stabilizing the same G4-site that ICP4 uses to autoregulate²⁶. Quindoline derivatives displayed a nanomolar-range anti-HSV-1 activity, inhibiting ICP4 expression. This is done through the stabilization of the G4s in the ICP4 promoter.

TMPyP4 interacts and stabilizes the most abundant HSV-1 PQS within the repeat regions of the viral genome. Interestingly, TMPyP4 does not affect either HSV-1 viral entry or replication; however, it does trap fully infectious virions in vesicles, which is independent of the autophagy process¹⁹. Furthermore, TMPyP4 interacts with HSV-1 G4 structures, inhibiting polymerase progression *in vitro*, and exhibits substantial antiviral activity in infected cells, despite being independent of virus DNA replication or entry inhibition¹⁹. Examination of HSV-1 immediate early (IE) genes reveals that adding BRACO-19 increases the melting temperature, confirming G4 stabilization through CD thermal unfolding analysis. Utilizing the luciferase firefly gene cloned downstream of the promoter of two HSV-1 IE genes, treatment with BRACO-19 affected the activity of both promoters in a dose-dependent manner. Stabilizing the HSV-1's G4 sites results in the inhibition of IE transcription²⁵¹. Additionally, the gp054 gene, responsible for encoding UL36, a critical component of the tegument protein, contains a PQS that can be stabilized by BRACO-19, resulting in transcriptional regulation of UL36. Lastly, BRACO-19 impedes the processing of Taq polymerase at sequences that form G4 structures in the HSV-1 genome, reducing intracellular viral DNA levels within infected cells¹⁹.

The investigation of the VZV revealed an abundance of G4 motifs in the internal repeat short and terminal repeat short regions adjacent to the unique short region and certain reiteration (R) sequence regions. A notably high concentration of G4 motifs was

detected on the template strand within ORF14, responsible for encoding glycoprotein C (gC), a virulent agent essential for viral growth in skin cells, specifically located in the R2 region. G4 formation through the reiteration sequence results in suppressed gC expression during VZV infection and results in the regulation of viral cell-to-cell transmission²⁵².

Beta herpesviruses include human cytomegalovirus (HCMV), which can lead to severe infections in immunocompromised individuals and is the leading cause of congenital abnormalities; human herpesvirus 6A and 6B (HHV-6A and HHV-6B), associated with roseola infantum, a common childhood illness characterized by a high fever and rash; human herpesvirus 7 (HHV-7), linked to febrile illnesses that primarily affect young children²⁵³⁻²⁵⁵.

Analyzing 36 PQSs within 20 genes of HCMV showed that in the presence of G4-stabilizing ligands, nine genes were affected by the G4 formation/stabilization by NMM in HCMV gene promoters¹⁸⁶. The application of NMM on cells caused a significant inhibition in the expression of the UL76 gene, likely due to its impact on GQ18 located within the promoter region. This observation is noteworthy as previous research has demonstrated that double-stranded DNA favors parallel conformation regardless of sequence, thus indicating that G4 structures may transform within cell environments. NMM stabilized parallel G4s in HCMV but did no effects on antiparallel G4s¹⁸⁶.

Additionally, these PQSs were stabilized by TMPyP4, increasing their stability while not affecting their conformations¹⁸⁶. HCMV has a PQS motif upstream of the microRNA cluster miR-US33 promoter. Viral miRNAs are essential for maintaining viral latency and are heavily dependent on the presence of viral miRNAs, which exert their inhibitory

effects on host genes and viral modulators²⁵⁶. TMPyP4 destabilizes miRNA G4s for HCMV, inhibiting miR-US33 promoter activity, while PDS has the opposite effect by stabilizing miRNA G4s in HCMV²⁵⁷.

Gamma herpesviruses include Epstein-Barr virus (EBV), which causes infectious mononucleosis and is associated with different cancers including Burkitt's lymphoma, nasopharyngeal carcinoma, and Hodgkin's lymphoma; Kaposi's sarcoma-associated herpesvirus (KSHV), associated with Kaposi's sarcomas, primary effusion lymphoma, and multicentric Castleman's disease²⁵⁸. Epstein-Barr virus-encoded nuclear antigen 1 (EBNA1) is essential for viral gene regulation, extrachromosomal replication, and maintenance of the EBV episome^{259,260}. The G4s in EBNA1 mRNA modulate viral translation. Destabilizing the G4s in EBNA1 using antisense oligos complementary to EBNA1's glycine-alanine repeat domain (GAR) mRNA results in enhanced translation and antigen presentation on the cell surface. However, the opposite is also true; stabilizing EBNA1's GAR results in decreased translation and antigen presentation²⁶¹. NCL binds with the GAR region of EBV's EBNA1 mRNA, leading to a consequential downregulation of EBNA1 expression. Intriguingly, PhenDC3 exhibits a higher affinity for these G-quadruplex structures than NCL, thereby promoting the increased translation of EBNA1 and enhancing antigen presentation²⁶². Compared to PhenDC3, PyDH2, and PhenDH2 demonstrated an improved capacity to enhance EBNA1 expression with reduced toxicity. These ligands exhibited the ability to disrupt the NCL-EBNA1 mRNA interaction, ultimately facilitating enhanced antigen presentation²⁶³.

It is important to note that the precise positioning of G-quadruplexes in RNA is crucial for their activity. As Lista et al. (2017) proposed, the interaction between NCL and

G-quadruplexes within EBNA1 mRNA is sufficient to impede the synthesis of both antigenic peptides and complete proteins²⁶². A recent study by Zheng et al. (2022) elucidated that the positioning of EBNA1 GAr mRNA at either the 5' or 3' end of the chicken ovalbumin (Ova) open reading frame (ORF), leading to the formation of N or C terminus GAr-OVA and OVA-GAr fusion proteins, resulted in distinct expression levels. Notably, NCL exhibited nearly double the binding affinity to GAr-Ova compared to Ova-GAr. This emphasizes that the precise location of GAr G-quadruplexes within the mRNA coding sequence is a crucial modulator of NCL binding and translation inhibition²⁶⁴.

In Kaposi's sarcoma-associated herpesvirus (KSHV), PQSs were identified upstream of the miRNA cluster miR-K12p1-9-11 promoter. Treatment with TMPyP4 destabilized miRNA G-quadruplexes, enhancing the activity of the KSHV miR-K12 cluster promoter activity²⁶⁵. Furthermore, PDS also stabilizes miR-K12p1-9-11 promoter similarly to TMPyP4. Additionally, TMPyP4 stabilized G4 structures identified in the latency-associated nuclear antigen (LANA)²¹¹²², the protein most expressed during latency and fundamental for viral transmission and host immune surveillance evasion^{70,266-268}. The addition of TMPyP4 resulted in a decrease in the levels of LANA within cells infected with KSHV. This observation provides corroboration for the hypothesis that enhancing G4 stability within LANA mRNA prompts inhibition of translation processes. Fortifying G-quadruplex structures in LANA mRNA led to diminished surface expression and presentation of the corresponding antigen amongst KSHV-positive cells, thereby aiding in maintaining viral infection²¹. Conversely, heterogeneous nuclear ribonucleoprotein A1 (hnRNP A1) has been demonstrated to modulate various biological processes by interacting with G-quadruplex structures²⁶⁹.

This interaction involves the selective binding of hnRNP A1 to the guanine-rich region of mRNA, consequently leading to the unfolding of G-quadruplex structures^{89,269}. hnRNP A1 functions as a helicase, destabilizing the G4 secondary structure, leading to increased LANA translation and enhanced antigen presentation²¹. G-quadruplexes in KS-Bcl-2 and BHRF1 significantly enhanced vBcl-2 expression, with PDS stabilizing the G-quadruplexes in their promoters, resulting in increased promoter activity²⁷⁰. In the terminal repeat (TR) regions of KSHV, PhenDC3 stabilized G-quadruplexes, causing replication fork stalling and reducing viral DNA replication. Additionally, PhenDC3 decreased overall genome copies, leading to the eventual loss of the viral episome in infected cells²⁷¹. These findings underscore the intricate regulatory roles of G-quadruplexes in KSHV, offering potential targets for therapeutic interventions.

2.5.2 Human Papillomavirus

Human papillomaviruses (HPVs), a double-stranded DNA virus, is a prevalent sexually transmitted infection that can result in the onset of skin, head, and neck, as well as anogenital cancer. Among these cancers is cervical cancer, which poses one of the most crucial global health issues. Only 8 out of 120 known HPVs contain G4s, and there are only 7 PQS located in the long control region (LCR), structural protein L2, early region E1 and E4 regions of the HPV genome^{272,273}. Incubation of TMPyP4 with the PQSs identified in the 7 HPV strains reported high G4 stabilization, assessed by FRET and CD melting experiments²⁷⁴. PhenDC effectively stabilizes HPVs' G4s in vitro, confirmed through CD, FRET, and TO displacement. Despite encouraging in vitro studies, the compound was unsuccessful in reducing viral replication and protein

expression when tested on organotypic raft cultures²⁷⁴. However, BRACO-19, along with C8, an acridine derivative, was found with a high affinity to HPV G4s with high affinity by fluorescent intercalator displacement assay (G4-FID).

The antiviral activity of C8 was assessed in organotypic epithelial cultures infected with HPV16 or HPV18. Results showed that administering C8 for a period of 20 days effectively decreased viral replication. As current treatments cannot eliminate HPV due to latent reservoirs, targeting G4s within the viral genome presents a potential approach for addressing both active and latent viruses²⁷⁴.

2.5.3 *Polyomavirus*

Polyomaviruses are non-enveloped, double-stranded DNA viruses that belong to the Polyomaviridae family. These viruses have been associated with various diseases in humans and animals, including tumors, nephropathy, and progressive multifocal leukoencephalopathy (PML)^{275,276}s. Some well-known members of the Polyomaviridae family include the JC virus (JCV), BK virus (BKV), and simian virus 40 (SV40). Polyomaviruses possess a circular, double-stranded DNA genome comprising about 5,000 base pairs. This genetic material is partitioned into three sections: the early, late, and noncoding control regions (NCCR). The early section encodes vital viral regulatory proteins such as large T-antigen and small t-antigen, indispensable for viral replication and transformation. Meanwhile, structural proteins like viral capsid proteins VP1, VP2, and VP3 are encoded in the late section of the genome²⁷⁷. Additionally, NCCR holds within it both the origin of replication and regulatory elements that monitor viral transcriptional activity alongside its overall duplication process²⁷⁸.

NCRR in SV40 is a crucial element that not only contains the ORI and encapsulation sequence but also regulates transcription direction. The presence of six GC boxes with repeated GGGCGG sequences forms an unusual quadruplex structure, which NMR has determined to contain a C-tetrad stacked between two G-tetrads²⁷⁹. These GC-rich motifs act as binding sites for SP1 and significantly involve early transcription. However, replication of the SV40 genome necessitates TAg, a multifunctional protein that interacts with p53 and Rb besides binding to ORI and possessing adenosine triphosphate-dependent helicase activity²⁸⁰. Notably, TAg can unravel G4 DNA structures, thereby playing an imperative role in controlling both early/late transcription along with replication regulation²⁸¹. Inhibiting both the duplex DNA helicase activities of TAg alongside destabilizing G4 structures is feasible using Perylene di-imide derivatives (PDI). Notably, TE111, TE101, and PIPER effectively stabilize the G4 structure, inhibiting Tag helicase activity. NMM and coralyne interact with the loops and grooves of the G4, resulting in adequate G4 protection. On the other hand, end-stackers such as TMPyP4 are ineffective at inhibiting TAg helicase activity²⁸².

2.5.4 Hepatitis B (HBV)

Hepatitis B virus (HBV) is a small, partially double-stranded DNA virus from the Hepadnaviridae family. HBV is responsible for acute and chronic hepatitis infections that can lead to liver disease, including cirrhosis and hepatocellular carcinoma²⁸³. A G4 motif, which is highly conserved, was identified in the promoters of the preS2/S gene. This motif forms a hybrid intramolecular G4 structure, which regulates transcription and virion secretion in HBV genotype B²⁸⁴. More recently, a G4 structure in the pre-core

promoter of the HBV genome is conserved among nearly all HBV genotypes. This is essential for generating pre-genomic RNA, synthesis of core and polymerase proteins, and genome encapsidation²⁸⁵. TMPyP4, BRACO-19, and PhenDC3 have been shown to bind to G4s in HBV²⁴; however, research is still ongoing to see if these interactions result in regulating HBV infectivity.









Virus	Compound	Biological Effects
 HSV-1	Braco19	Immediate early genes promoters are downregulated
	TMPyP4	Traps fully infectious virions in vesicles
 VZV	Not Tested	Regulation of viral cell-to-cell transmission
 HCMV	NMM	Downregulation of viral genes
	TMPyP4	Destabilizes miRNA, inhibiting miR-US33 promoter
	PDS	Stabilizes miRNA, promoter activity down regulated
 EBV	NCL	Upregulates viral protein expression
	PhenDC3 PhenDH2 PyDH2	Displaces NCL and increases viral protein expression
	TMPyP4	Destabilizes miRNA increasing miR-K12 cluster promoter activity
 KSHV	PDS	Stabilizes miRNA increasing miR-K12 cluster promoter activity
	hnRNP A1	Destabilizes G4 in LANA mRNA, increasing translation and antigen presentation
	TMPyP4	Undetermined
 HPV	PhenDC3	Undetermined
	Braco19 + C8	Increased G4 stabilization, decreases viral replication
	PDI	Destabilizes G4, inhibiting helicase activity
 Polyomavirus	NMM	Stabilizes G4, inhibiting helicase activity
	TMPyP4 Braco19 PhenDC3	Binds to G4s but effects are undetermined
 HBV		

Figure 1: Summary of DNA viruses and the modulatory effects of the G4 stabilizing compounds that regulate them.

2.6 RNA Viruses

RNA viruses comprise a major class of pathogens with substantial implications for human health and disease. Their genomes are composed of single-stranded RNA compared to double-stranded DNA. DNA viruses replicate within the host cell's nucleus, exploiting the host's DNA replication machinery. In the case of RNA viruses, their replication occurs within the host cell's cytoplasm, facilitated by a virus-encoded RNA-dependent RNA polymerase (RdRp) responsible for copying their RNA genome²⁸⁶. Another significant difference between RNA and DNA viruses is that RNA viruses tend to mutate faster than DNA viruses due to the lack of proofreading activity in their RNA polymerase, leading to higher rates of mutations²⁸⁷. This rapid evolution is a factor that allows RNA viruses to adapt to new hosts and environments, contributing to their ability to cause emerging infectious diseases, as seen with the SARS-CoV-2 virus. RNA viruses can be categorized based on whether they are positive-sense or negative-sense RNA. Positive-sense viruses have RNA that functions like mRNA and can be immediately translated into proteins by the host cell's machinery. Contrastingly, negative-sense RNA viruses have RNA complementary to mRNA and must first be transcribed into positive-sense RNA before translation can occur¹²⁰.

2.6.1 HIV

Human immunodeficiency virus (HIV) was first recorded in 1983²⁸⁸⁻²⁹⁰. HIV can maintain latency for over a decade before reactivation, resulting in acquired immunodeficiency syndrome (AIDS). As of 2018, the CDC reports 1.7 million new cases

of HIV, resulting in a total of 37.9 million infected worldwide. Since 1981, over 35 million people have died, and approximately 750,000 die annually²⁹¹. HIV surfaced through the multi-independent zoonotic transmission of the simian immunodeficiency virus, changing host from primates to humans^{292,293}. It is a lentivirus, part of the Retroviridae family, and utilizes reverse transcription (RT) and integrates its viral genome into the host's. This allows for a persistent and lifelong infection²⁹⁴.

G4 structures were identified and confirmed using circular dichroism (CD) in Long Terminal Repeat (LTR) 1 and 3 and the Nef gene^{295,296}. LTRs serve as viral promoters and have regulatory enhancer/suppressor regions^{297,298}. G-quadruplexes in HIV promote dimerization of the two viral RNA strands when encapsulated by the nucleocapsid. This allows RT to strand-hop if there are breaks in the template. This facilitates the successful completion of reverse transcription, subsequently allowing the integration of viral DNA into the host's genome^{299,300}. In addition, strand hopping promotes genetic diversity between strains, which can lead to resistance to different antiretrovirals³⁰¹. Nef is essential for viral replication and pathogenesis in early infection³⁰². Nef RNA can evade interfering RNA with alternative folding and prevent downregulation. HIV encodes its own miRNA (miR-N367) that targets Nef for self-transcriptional regulation²⁷.

C-exNDIs were designed and selective of viral G4s¹⁶. Luciferase reporter assays using HIV LTR and mutated LTR, without G4 secondary structures, were cloned upstream of the firefly luciferase plasmid. Indirect transcriptional repression was measured by the translational output of luciferase intensity between G4 stabilizing ligands BRACO-19 and c-exNDIs. TMPyP2, a non-G4 stabilizing porphyrin, was used as

a control to ensure the presence of a bulky G4 ligand, but it did not result in G4 stabilization. Previous results have shown that G4 stabilizing ligands can induce G4 assembly²⁹⁶. Both inhibited HIV-1 viral activity by interacting with the G4s in the LTR region. Looking at their respective data, BRACO-19 has up to 50% HIV inhibition pre-host integration and 80% post-integration, whereas c-exNDIs have up to a 65% reduction post-genome integration¹⁶.

2.6.2 Hepatitis C (HCV)

The Flaviviridae family includes the small, enveloped, and single-stranded RNA virus known as Hepatitis C (HCV), which has a global impact on public health. HCV predominantly targets the liver, causing chronic hepatitis, hepatocellular carcinoma, and cirrhosis³⁰³. While direct-acting antiviral drugs have transformed treatment options for HCV patients, drug resistance remains problematic, along with inadequate accessibility to therapy and lack of an efficacious vaccine. The genome of HCV spans approximately 9.6 kilobases and is composed of a solitary ORF flanked by untranslated regions at the 5' and 3' ends³⁰⁴. The ORF encodes for a polyprotein that undergoes co- and post-translational processing to produce no less than ten viral proteins, comprising structural proteins such as core, E1, E2, and non-structural ones like p7, NS2, and NS5B. Within the 5' UTR lies an internal ribosome entry site (IRES), responsible for facilitating cap-independent translation of the viral polyprotein, while the essential replication components lie in the contiguous 3' UTR region necessary for assembling virions³⁰⁵. A recent study showed that PhenDC3 could hinder HCV's RdRp and inhibit viral replication in cells³⁰⁶.

PQSs have been identified in the HCV genome, particularly in the 5' UTR, the core-coding region, and the 3' UTR³⁰⁷. The formation of G4s in these regions has been implicated in the regulation of HCV replication, translation, and virion assembly. In RNA viruses, RdRp is responsible for viral replication³⁰⁵. Performing an RNA stop assay with an RdRp-based primer-dependent mechanism showed that PDP, a PDS variant, successfully binds and stabilizes a G4 structure, preventing RdRp from completing replication. Additionally, both PDP and TMPyP4 reduced HCV RNA levels in living cells in a dose-dependent manner³⁰⁸. To investigate NCL and viral RNA G4 interaction, PDP competed for G4 binding. Colocalization results showed reduced NCL levels when incubated with PDP³⁰⁹. Nonstructural protein 3 (NS3) of HCV contains helicase activity that is essential for viral replication. Utilizing Fluorescence anisotropy binding and G4 reporter assays, it has been determined that NS3 can unfold the conserved G4 structures within HCV's genome and the negative strand. These new findings imply that NS3 could hold an important novel role in regulating HCV³¹⁰.

2.6.3 Zika Virus (ZIKV) and other Flaviviruses

Zika virus (ZIKV) is a flavivirus transmitted by mosquitoes and shares similarities with other medically significant flaviviruses such as dengue, West Nile, Japanese encephalitis, and yellow fever viruses. While ZIKV infections are often asymptomatic or result in mild illness, recent outbreaks have shown severe neurological complications, including microcephaly in newborns and Guillain-Barré syndrome in adults³¹¹. Flaviviruses possess a positive-sense RNA genome of about 11 kb with an open reading frame flanked by untranslated regions at the 5' and 3' ends. The polyprotein

encoded by this ORF is cleaved into three structural proteins (capsid, pre-membrane/membrane, envelope) and seven non-structural proteins (NS1, NS2A, NS2B, NS3, NS4A, NS4B, and NS5). PQSs have been discovered within the genomes of various flaviviruses, including ZIKV, DENV, and WNV. It has been suggested that these G4s play a role in regulating viral replication, translation, and virion³¹². ZIKV's genome contains several PQSs throughout its genes and untranslated regions³¹². In vivo, experiments show that TMPyP4 and BRACO-19 act as G4-stabilizers in ZIKV, resulting in inhibited viral growth, genome replication, and protein expression. The effects of these stabilizing ligands are seen in a dose-dependent manner³¹³.

2.6.4 Influenza

The Orthomyxoviridae family comprises segmented, negative-sense RNA viruses, also called influenza viruses that cause seasonal flu and result in significant morbidity and mortality worldwide. Influenza A (IAV) and B are responsible for most human infections among the four types of influenza viruses classified based on their structure³¹⁴. Although vaccines and antiviral drugs exist to combat the virus's spread, they remain a substantial public health concern due to their rapid antigenic drift, leading to drug-resistant strains. The genome of these viruses consists of eight or seven single-stranded segments encoding ten to fourteen proteins depending on the type, with each segment encircled by viral nucleoprotein alongside an RNA-dependent RNA polymerase composed of PA subunit with PB1 & PB2 units assigned for replication activities³¹⁵.

The Transmembrane protease serine 2 (TMPRSS2) protein is an essential element in the life cycle of many respiratory viruses, including influenza and coronaviruses.

TMPRSS2 is a membrane-spanning protein that belongs to the type II transmembrane serine proteases (TTSPs) family and is implicated in many physiological and pathological processes³¹⁶. TMPRSS2 cleaves the hemagglutinin component of numerous influenza virus subtypes, a pivotal surface protein for viral entry into host cells^{317,318}. The promoter region of TMPRSS2 contains a guanine-rich sequence that forms a G-quadruplex (G4) structure. Seven benzoselenoxanthene analogs were tested against the Influenza A Virus (IAV) in in vitro experiments, demonstrating four analogs to have significant G4-stabilizing effects. These benzoselenoxanthenes effectively stabilized the G4 structure within TMPRSS2's promoter, resulting in a dose-dependent reduction in TMPRSS2 expression observed in Calu3 cells³¹⁹. Additional PQSs have been recognized within the IAV, including regions encoding polymerase complex proteins²³. Nevertheless, further investigation is imperative to ascertain whether these regions exert a regulatory function on this viral pathogen.

2.6.5 Enterovirus

Enteroviruses belong to the Picornaviridae family and are positive-sense, single-stranded RNA viruses that cause various human diseases such as myocarditis, meningitis, poliomyelitis, and hand-foot-and-mouth disease³²⁰. Despite being a significant public health concern, effective antiviral treatments for enteroviruses remain limited. Recent research has identified PQSs sequences in enterovirus genomes that regulate viral processes. Targeting these G4s with stabilizing ligands is a promising new approach for combating enterovirus infections. G4 sequences have been detected in the genomes of various enteroviruses, comprising coxsackievirus, poliovirus, and enterovirus 71

(EV71)¹⁰. Typically located in the 5'UTR, G4 motifs may regulate various viral processes, including replication, transcription, and translation. Creating G4 structures can potentially influence secondary RNA structures, leading to changes in interactions between viral proteins or host/viral proteins. This, in turn, can impact protein synthesis and the overall process of viral replication³²¹.

EV71, with its 21 PQSs, exhibited effective inhibition of viral replication using G-quadruplex-stabilizing ligands such as BRACO-19, PDS, and TMPyP4. This inhibition was demonstrated without compromising cell viability, as evidenced by quantitative PCR data showing a significant decrease in viral RNA levels upon treatment with these ligands. The inhibitory impact of BRACO-19 was further validated by plaque assay results, showcasing a substantial reduction in infectivity exceeding an order of magnitude. Beyond replication, BRACO-19 has an additional effect on viral translation, specifically reducing the synthesis of the nonstructural protein 2C. In contrast, PDS treatment shows a more modest reduction in the synthesis of this protein³²¹.

2.6.6 SARS-CoV-2

The COVID-19 pandemic, caused by the novel coronavirus SARS-CoV-2, has significantly impacted global public health, and highlights an urgent need for effective antiviral therapies. This positive-sense, single-stranded RNA virus is responsible for high morbidity and mortality rates worldwide. Despite the rapid development of vaccines, there is a critical need for potent antiviral treatments. Bioinformatic analyses have identified PQSs in specific regions of the SARS-CoV-2 genome, including those encoding proteins and untranslated sections like 5' and 3' UTRs, which may influence the

secondary structures of viral RNA and impact host/viral protein interactions, similar to other viruses^{150,322,323}. Moreover, G-quadruplexes are located in critical regions such as ORF1ab, 3a, nucleocapsid, and membrane, suggesting their potential involvement in regulating viral replication, assembly, and immune-response modulation³²⁴. A primer extension assay, utilizing plasmids with inserted SARS-CoV-2 G4 sequences into the GFP gene, demonstrated that G4-stabilizing ligands BRACO-19 and TMPyP4 successfully stabilized the G4 structure, preventing primer extension. Transfecting these plasmids into cells, with or without BRACO-19 and TMPyP4 treatment, revealed a decrease in GFP expression, highlighting the impact of G4-stabilizing ligands on gene expression³²⁵.

The SARS-Unique Domain (SUD) has been proposed to be crucial for viral transcription and replication^{326,327}. There is high homology between the SARS-CoV and SARS-CoV-2 NSP3 SUD proteins¹⁰⁶. PhenDC3, PDC, phenanthroline derivatives, and metalated porphyrins were subjected to testing to assess their potential interaction with the SARS-CoV-2 SUD. Employing the cellular RNA G4 sequence (TRF2) and employing Homogenous Time-Resolved Fluorescence (HTRF), the study revealed that all the mentioned G4-stabilizing ligands effectively inhibited the interaction between SUD and G4. These findings imply a preferential interaction with the host cell DNA or RNA rather than viral RNA³²⁸.

TMPRSS2 is a highly expressed serine protease in human tissues and is involved in the entry of coronaviruses into host cells¹¹⁶. Specifically, SARS-CoV-2 utilizes its spike (S) protein to bind to the angiotensin-converting enzyme 2 (ACE2) host cell receptor. Following binding, the S protein is primed by TMPRSS2 to enable membrane

fusion and viral entry into the host cell¹¹⁶. Interestingly, PDS, carboxypyridostatin (cPDS), and TMPyP4 bind to a G4 in TMPRSS2, reducing protein levels. Using a pseudovirus system, where vesicular stomatitis virus was pseudotyped with SARS-CoV-2 S glycoprotein (SARS-CoV-2-S-Luc) to determine if stabilizing the G4 in TMPRSS2 affected viral entry. Luciferase activity indicates that PDS, cPDS, and TMPyP4 all reduced pseudovirus entry into cells. Furthermore, utilizing mice that heterogeneously expressed hACE2 via adeno-associated virus (AAV) treated with PDS showed a decrease in VSV-SARS-2-luc infection¹⁴⁰. In their study, Qin et al. demonstrated the targeting of SARS-CoV-2 G4s by TMPyP4 through experiments conducted on Syrian hamsters and transgenic mouse models. The results indicated that non-toxic levels of TMPyP4 effectively suppressed SARS-CoV-2 infection, leading to reduced viral loads and lung lesions. Moreover, in experimental assessments, TMPyP4 exhibited greater efficacy than remdesivir, a compound that has demonstrated clinical benefits for patient outcomes in trials³²⁹, in both in vitro and in vivo experiments³³⁰.

Within the coding region of SARS-CoV-2, a stable RNA G4 structure (RG1) is formed in the nucleocapsid phosphoprotein (N). The G4 in the N sequence has been confirmed to be stabilized by PDP, leading to a substantial reduction in SARS-CoV-2 N protein levels. This occurs through the inhibition of N translation in both in vitro and in vivo settings³³¹. Oliva et al. showed that berberine, an isoquinoline alkaloid, is also able to bind to and stabilize RG1 in SARS-CoV-2³³². However, further investigation in infected cells is required to assess whether berberine effectively reduces SARS-CoV-2 infectivity. Methylene blue (M-Blue), a tricyclic phenothiazine compound, has been shown to have G4-stabilizing properties³³³. M-Blue has been previously approved by the FDA for the

treatment of methemoglobinemia and other medical applications³³⁴. M-Blue has been shown to inhibit the entry of SARS-CoV-2 spike-bearing pseudovirus into ACE2-expressing cells³³⁵.





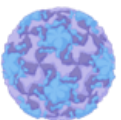
Virus	Compound	Biological Effects
 HIV	BRACO-19	Inhibits transcription and viral replication
	c-exNDIs	Inhibits transcription
 HCV	PhenDC3	Inhibits viral replication
	TMPyP4	Inhibits viral expression
	PDP (PDS)	Stabilizes G4, reduces viral replication
 ZIKA	TMPyP4	Decreased viral replication and translation
	BRACO-19	Decreased viral replication and translation
 Influenza	Benzoseleno-xanthenes	Stabilizes G4, reducing TMPRSS2 expression
 Enterovirus	PDS	Reduce viral replication
	PhenDC3	Reduce viral replication
	TMPyP4	Reduce viral replication

Figure 2: Summary of RNA viruses and the modulatory effects of the G4 stabilizing compounds that regulate them

2.7 Discussion

The recent exploration of viral G-quadruplexes and utilizing G4-stabilizing ligands as potential targeting agents present a promising avenue for developing a novel antiviral strategy. The regulatory role of G4s in viral processes such as replication,

transcription, and virion secretion has garnered increasing attention. These non-canonical nucleic acid structures, formed in guanine-rich sequences, have been identified in the genomes of various viruses, including human papillomavirus, HCV, SARS-CoV-2, and polyomaviruses like JCV and BKV. The modulation of viral processes occurs by forming G4 structures in the viral genome, influencing interactions with host and viral proteins. G4-stabilizing ligands, including TMPyP4, PhenDC3, and BRACO-19, have exhibited the ability to inhibit viral replication by stabilizing G-quadruplex structures in viral genomes. This underscores the potential of G-quadruplex stabilizing ligands as novel therapeutic strategies against viral infections, particularly those lacking effective treatments. Notably, research has been directed towards combatting SARS-CoV-2, poliovirus, and EV71, showcasing the broad applicability of this approach.

Beyond impacting actively replicating viruses, antiviral G-quadruplex ligands offer the potential to target latent viruses that remain dormant within the host and can reactivate under favorable conditions. Current treatments for infections caused by HHVs, HPV, and HIV-1 necessitate long-term maintenance to prevent disease resurgence upon viral reactivation. A strategy targeting G-quadruplexes could influence replicating and latent viruses, potentially leading to virus eradication and developing innovative therapeutic approaches for treating fatal human diseases.

However, challenges persist in translating these findings into clinical applications. Developing antiviral G-quadruplex binders faces hurdles in achieving selectivity for viral G4s over cellular counterparts. The typical chemical features shared by many G4 ligands hinder their selectivity, limiting their druggability. Structural characterization of G-quadruplex moieties, particularly in the loop and groove regions, is essential for

designing more selective ligands, although research in this direction remains limited. Strengthening the potency of G4-stabilizing ligands is imperative to maximize their antiviral potential. Moreover, as our understanding of the regulatory role of G-quadruplexes in viral processes expands, identifying additional G4 structures in viral genomes becomes crucial for identifying viable therapeutic targets. Simultaneously, continued investigation into G-quadruplex's role in other viral genotypes and their potential impact on pathogenesis will contribute to an enhanced understanding of viral biology.

2.9 References

1. Bochman ML, Paeschke K, Zakian VA. DNA secondary structures: stability and function of G-quadruplex structures. *Nat Rev Genet.* Nov 2012;13(11):770-80. doi:10.1038/nrg3296
2. Dhakal S, Cui Y, Koirala D, et al. Structural and mechanical properties of individual human telomeric G-quadruplexes in molecularly crowded solutions. *Nucleic Acids Res.* Apr 1 2013;41(6):3915-23. doi:10.1093/nar/gkt038
3. Biffi G, Tannahill D, McCafferty J, Balasubramanian S. Quantitative visualization of DNA G-quadruplex structures in human cells. *Nature Chemistry.* 2013/03/01 2013;5(3):182-186. doi:10.1038/nchem.1548
4. Chambers VS, Marsico G, Boutell JM, Di Antonio M, Smith GP, Balasubramanian S. High-throughput sequencing of DNA G-quadruplex structures in the human genome. *Nat Biotechnol.* Aug 2015;33(8):877-81. doi:10.1038/nbt.3295
5. Howard FB, Miles HT. Poly(inosinic acid) helices: essential chelation of alkali metal ions in the axial channel. *Biochemistry.* Dec 21 1982;21(26):6736-45. doi:10.1021/bi00269a019
6. Sundquist WI, Klug A. Telomeric DNA dimerizes by formation of guanine tetrads between hairpin loops. *Nature.* Dec 14 1989;342(6251):825-9. doi:10.1038/342825a0
7. Bouaziz S, Kettani A, Patel DJ. A K cation-induced conformational switch within a loop spanning segment of a DNA quadruplex containing G-G-G-C repeats. *Journal of molecular biology.* 1998/09// 1998;282(3):637-652. doi:10.1006/jmbi.1998.2031
8. Zaccaria F, Paragi G, Fonseca Guerra C. The role of alkali metal cations in the stabilization of guanine quadruplexes: why K(+) is the best. *Phys Chem Chem Phys.* Aug 21 2016;18(31):20895-904. doi:10.1039/c6cp01030j

9. Pandey S, Agarwala P, Maiti S. Effect of Loops and G-Quartets on the Stability of RNA G-Quadruplexes. *The Journal of Physical Chemistry B*. 2013/06/13 2013;117(23):6896-6905. doi:10.1021/jp401739m
10. Nazia P, Amen S, Seunghee Cho and Kyeong Kyu K. Computational Approaches to Predict the Non-canonical DNAs. *Current Bioinformatics*. 2019;14(6):470-479. doi:<http://dx.doi.org/10.2174/1574893614666190126143438>
11. Henderson A, Wu Y, Huang YC, et al. Detection of G-quadruplex DNA in mammalian cells. *Nucleic acids research*. 2014;42(2):860-869. doi:10.1093/nar/gkt957
12. Yu C-H, Teulade-Fichou M-P, Olsthoorn RCL. Stimulation of ribosomal frameshifting by RNA G-quadruplex structures. *Nucleic acids research*. 2014;42(3):1887-1892. doi:10.1093/nar/gkt1022
13. Lavezzo E, Berselli M, Frasson I, et al. G-quadruplex forming sequences in the genome of all known human viruses: a comprehensive guide. *bioRxiv*. 2018:344127. doi:10.1101/344127
14. Fay MM, Lyons SM, Ivanov P. RNA G-Quadruplexes in Biology: Principles and Molecular Mechanisms. *Journal of molecular biology*. Jul 7 2017;429(14):2127-2147. doi:10.1016/j.jmb.2017.05.017
15. Gellert M, Lipsett MN, Davies DR. Helix formation by guanylic acid. *Proc Natl Acad Sci U S A*. Dec 15 1962;48:2013-8. doi:10.1073/pnas.48.12.2013
16. Metifiot M, Amrane S, Litvak S, Andreola ML. G-quadruplexes in viruses: function and potential therapeutic applications. *Nucleic Acids Res*. Nov 10 2014;42(20):12352-66. doi:10.1093/nar/gku999
17. Millevoi S, Moine H, Vagner S. G-quadruplexes in RNA biology. *Wiley Interdiscip Rev RNA*. Jul-Aug 2012;3(4):495-507. doi:10.1002/wrna.1113
18. Bhattacharyya D, Mirihana Arachchilage G, Basu S. Metal Cations in G-Quadruplex Folding and Stability. *Frontiers in chemistry*. 2016;4:38-38. doi:10.3389/fchem.2016.00038
19. Ou TM, Lu YJ, Tan JH, Huang ZS, Wong KY, Gu LQ. G-quadruplexes: targets in anticancer drug design. *ChemMedChem*. May 2008;3(5):690-713. doi:10.1002/cmdc.200700300
20. Perrone R, Doria F, Butovskaya E, et al. Synthesis, Binding and Antiviral Properties of Potent Core-Extended Naphthalene Diimides Targeting the HIV-1 Long Terminal Repeat Promoter G-Quadruplexes. *J Med Chem*. Dec 24 2015;58(24):9639-52. doi:10.1021/acs.jmedchem.5b01283
21. Ruggiero E, Richter SN. G-quadruplexes and G-quadruplex ligands: targets and tools in antiviral therapy. *Nucleic Acids Res*. Apr 20 2018;46(7):3270-3283. doi:10.1093/nar/gky187
22. Neidle S. Human telomeric G-quadruplex: The current status of telomeric G-quadruplexes as therapeutic targets in human cancer. <https://doi.org/10.1111/j.1742-4658.2009.07463.x>. *The FEBS Journal*. 2010/03/01 2010;277(5):1118-1125. doi:<https://doi.org/10.1111/j.1742-4658.2009.07463.x>
23. Kingsbury CJ, Senge MO. The shape of porphyrins. *Coordination Chemistry Reviews*. 2021/03/15/ 2021;431:213760. doi:<https://doi.org/10.1016/j.ccr.2020.213760>

24. Cavallari M, Garbesi A, Di Felice R. Porphyrin Intercalation in G4-DNA Quadruplexes by Molecular Dynamics Simulations. *The Journal of Physical Chemistry B*. 2009/10/08 2009;113(40):13152-13160. doi:10.1021/jp9039226
25. Fujiwara N, Mazzola M, Cai E, Wang M, Cave JW. TMPyP4, a Stabilizer of Nucleic Acid Secondary Structure, Is a Novel Acetylcholinesterase Inhibitor. *PLOS ONE*. 2015;10(9):e0139167. doi:10.1371/journal.pone.0139167
26. Le VH, Nagesh N, Lewis EA. Bcl-2 promoter sequence G-quadruplex interactions with three planar and non-planar cationic porphyrins: TMPyP4, TMPyP3, and TMPyP2. *PLoS One*. 2013;8(8):e72462. doi:10.1371/journal.pone.0072462
27. Haq I, Trent JO, Chowdhry BZ, Jenkins TC. Intercalative G-Tetraplex Stabilization of Telomeric DNA by a Cationic Porphyrin1. *Journal of the American Chemical Society*. 1999/03/01 1999;121(9):1768-1779. doi:10.1021/ja981554t
28. Grand CL, Han H, Muñoz RM, et al. The cationic porphyrin TMPyP4 down-regulates c-MYC and human telomerase reverse transcriptase expression and inhibits tumor growth in vivo. *Mol Cancer Ther*. Jun 2002;1(8):565-73.
29. Izbicka E, Wheelhouse RT, Raymond E, et al. Effects of Cationic Porphyrins as G-Quadruplex Interactive Agents in Human Tumor Cells1. *Cancer Research*. 1999;59(3):639-644.
30. Han FX, Wheelhouse RT, Hurley LH. Interactions of TMPyP4 and TMPyP2 with Quadruplex DNA. Structural Basis for the Differential Effects on Telomerase Inhibition. *Journal of the American Chemical Society*. 1999/04/01 1999;121(15):3561-3570. doi:10.1021/ja984153m
31. Nicoludis JM, Miller ST, Jeffrey PD, et al. Optimized End-Stacking Provides Specificity of N-Methyl Mesoporphyrin IX for Human Telomeric G-Quadruplex DNA. *Journal of the American Chemical Society*. 2012/12/19 2012;134(50):20446-20456. doi:10.1021/ja3088746
32. Nicoludis JM, Barrett SP, Mergny J-L, Yatsunyk LA. Interaction of human telomeric DNA with N- methyl mesoporphyrin IX. *Nucleic Acids Research*. 2012;40(12):5432-5447. doi:10.1093/nar/gks152
33. Sabharwal NC, Savikhin V, Turek-Herman JR, Nicoludis JM, Szalai VA, Yatsunyk LA. N-methylmesoporphyrin IX fluorescence as a reporter of strand orientation in guanine quadruplexes. <https://doi.org/10.1111/febs.12734>. *The FEBS Journal*. 2014/04/01 2014;281(7):1726-1737. doi:<https://doi.org/10.1111/febs.12734>
34. Zhang QS, Manche L, Xu RM, Krainer AR. hnRNP A1 associates with telomere ends and stimulates telomerase activity. *Rna*. Jun 2006;12(6):1116-28. doi:10.1261/rna.58806
35. Chung WJ, Heddi B, Hamon F, Teulade-Fichou M-P, Phan AT. Solution Structure of a G-quadruplex Bound to the Bisquinolinium Compound Phen-DC3. <https://doi.org/10.1002/anie.201308063>. *Angewandte Chemie International Edition*. 2014/01/20 2014;53(4):999-1002. doi:<https://doi.org/10.1002/anie.201308063>
36. De Cian A, DeLemos E, Mergny J-L, Teulade-Fichou M-P, Monchaud D. Highly Efficient G-Quadruplex Recognition by Bisquinolinium Compounds. *Journal of the American Chemical Society*. 2007/02/01 2007;129(7):1856-1857. doi:10.1021/ja067352b

37. Ravichandran S, Kim YE, Bansal V, et al. Genome-wide analysis of regulatory G-quadruplexes affecting gene expression in human cytomegalovirus. *PLoS Pathog.* Sep 2018;14(9):e1007334. doi:10.1371/journal.ppat.1007334
38. Piazza A, Boulé JB, Lopes J, et al. Genetic instability triggered by G-quadruplex interacting Phen-DC compounds in *Saccharomyces cerevisiae*. *Nucleic Acids Res.* Jul 2010;38(13):4337-48. doi:10.1093/nar/gkq136
39. De Cian A, Cristofari G, Reichenbach P, et al. Reevaluation of telomerase inhibition by quadruplex ligands and their mechanisms of action. *Proceedings of the National Academy of Sciences.* 2007/10/30 2007;104(44):17347-17352. doi:10.1073/pnas.0707365104
40. Keller JG, Hymøller KM, Thorsager ME, et al. Topoisomerase 1 inhibits MYC promoter activity by inducing G-quadruplex formation. *Nucleic Acids Research.* 2022;50(11):6332-6342. doi:10.1093/nar/gkac482
41. Al Kobaisi M, Bhosale SV, Latham K, Raynor AM, Bhosale SV. Functional Naphthalene Diimides: Synthesis, Properties, and Applications. *Chemical Reviews.* 2016/10/12 2016;116(19):11685-11796. doi:10.1021/acs.chemrev.6b00160
42. Pirolta V, Nadai M, Doria F, Richter SN. Naphthalene Diimides as Multimodal G-Quadruplex-Selective Ligands. *Molecules.* 2019;24(3). doi:10.3390/molecules24030426
43. Read M, Harrison RJ, Romagnoli B, et al. Structure-based design of selective and potent G quadruplex-mediated telomerase inhibitors. *Proc Natl Acad Sci U S A.* Apr 24 2001;98(9):4844-9. doi:10.1073/pnas.081560598
44. White EW, Tanious F, Ismail MA, et al. Structure-specific recognition of quadruplex DNA by organic cations: influence of shape, substituents and charge. *Biophys Chem.* Mar 2007;126(1-3):140-53. doi:10.1016/j.bpc.2006.06.006
45. Harrison RJ, Cuesta J, Chessari G, et al. Trisubstituted acridine derivatives as potent and selective telomerase inhibitors. *J Med Chem.* Oct 9 2003;46(21):4463-76. doi:10.1021/jm0308693
46. Moruno-Manchon JF, Koellhoffer EC, Gopakumar J, et al. The G-quadruplex DNA stabilizing drug pyridostatin promotes DNA damage and downregulates transcription of *Brc1* in neurons. *Aging (Albany NY).* Sep 12 2017;9(9):1957-1970. doi:10.18632/aging.101282
47. Rodriguez R, Müller S, Yeoman JA, Trentesaux C, Riou J-F, Balasubramanian S. A Novel Small Molecule That Alters Shelterin Integrity and Triggers a DNA-Damage Response at Telomeres. *Journal of the American Chemical Society.* 2008/11/26 2008;130(47):15758-15759. doi:10.1021/ja805615w
48. Balasubramanian S, Neidle S. G-quadruplex nucleic acids as therapeutic targets. *Curr Opin Chem Biol.* Jun 2009;13(3):345-53. doi:10.1016/j.cbpa.2009.04.637
49. Rouleau SG, Beaudoin JD, Bisailon M, Perreault JP. Small antisense oligonucleotides against G-quadruplexes: specific mRNA translational switches. *Nucleic Acids Res.* Jan 2015;43(1):595-606. doi:10.1093/nar/gku1311
50. Cadoni E, De Paepé L, Manicardi A, Madder A. Beyond small molecules: targeting G-quadruplex structures with oligonucleotides and their analogues. *Nucleic Acids Res.* Jul 9 2021;49(12):6638-6659. doi:10.1093/nar/gkab334

51. Balci H, Globyte V, Joo C. Targeting G-quadruplex Forming Sequences with Cas9. *ACS Chemical Biology*. 2021/04/16 2021;16(4):596-603. doi:10.1021/acscchembio.0c00687
52. Hoque ME, Mustafa G, Basu S, Balci H. Encounters between Cas9/dCas9 and G-Quadruplexes: Implications for Transcription Regulation and Cas9-Mediated DNA Cleavage. *ACS Synthetic Biology*. 2021/05/21 2021;10(5):972-978. doi:10.1021/acssynbio.1c00067
53. Fire A, Xu S, Montgomery MK, Kostas SA, Driver SE, Mello CC. Potent and specific genetic interference by double-stranded RNA in *Caenorhabditis elegans*. *Nature*. 1998/02/01 1998;391(6669):806-811. doi:10.1038/35888
54. Hutvagner G, Zamore PD. RNAi: nature abhors a double-strand. *Curr Opin Genet Dev*. Apr 2002;12(2):225-32. doi:10.1016/s0959-437x(02)00290-3
55. Chery J. RNA therapeutics: RNAi and antisense mechanisms and clinical applications. *Postdoc J*. Jul 2016;4(7):35-50. doi:10.14304/surya.jpr.v4n7.5
56. Gitlin L, Karelsky S, Andino R. Short interfering RNA confers intracellular antiviral immunity in human cells. *Nature*. Jul 25 2002;418(6896):430-4. doi:10.1038/nature00873
57. Liu Z, Wang J, Cheng H, et al. Cryo-EM Structure of Human Dicer and Its Complexes with a Pre-miRNA Substrate. *Cell*. May 17 2018;173(5):1191-1203.e12. doi:10.1016/j.cell.2018.03.080
58. Heale BSE, Soifer HS, Bowers C, Rossi JJ. siRNA target site secondary structure predictions using local stable substructures. *Nucleic Acids Research*. 2005;33(3):e30-e30. doi:10.1093/nar/gni026
59. Meister G, Tuschl T. Mechanisms of gene silencing by double-stranded RNA. *Nature*. 2004/09/01 2004;431(7006):343-349. doi:10.1038/nature02873
60. Dumas L, Herviou P, Dassi E, Cammas A, Millevoi S. G-Quadruplexes in RNA Biology: Recent Advances and Future Directions. *Trends in Biochemical Sciences*. 2021/04/01/ 2021;46(4):270-283. doi:<https://doi.org/10.1016/j.tibs.2020.11.001>
61. Rader C. Chemically programmed antibodies. *Trends Biotechnol*. Apr 2014;32(4):186-97. doi:10.1016/j.tibtech.2014.02.003
62. Platella C, Riccardi C, Montesarchio D, Roviello GN, Musumeci D. G-quadruplex-based aptamers against protein targets in therapy and diagnostics. *Biochim Biophys Acta Gen Subj*. May 2017;1861(5 Pt B):1429-1447. doi:10.1016/j.bbagen.2016.11.027
63. Roxo C, Kotkowiak W, Pasternak A. G-Quadruplex-Forming Aptamers-Characteristics, Applications, and Perspectives. *Molecules*. Oct 21 2019;24(20)doi:10.3390/molecules24203781
64. Ramos IVC, Almeida PS, Lourenço MOL, et al. Multicharged Phthalocyanines as Selective Ligands for G-Quadruplex DNA Structures. *Molecules*. 2019;24(4)doi:10.3390/molecules24040733
65. Soundararajan S, Chen W, Spicer EK, Courtenay-Luck N, Fernandes DJ. The nucleolin targeting aptamer AS1411 destabilizes Bcl-2 messenger RNA in human breast cancer cells. *Cancer Res*. Apr 1 2008;68(7):2358-65. doi:10.1158/0008-5472.can-07-5723

66. Bates PJ, Reyes-Reyes EM, Malik MT, Murphy EM, O'Toole MG, Trent JO. G-quadruplex oligonucleotide AS1411 as a cancer-targeting agent: Uses and mechanisms. *Biochim Biophys Acta Gen Subj*. May 2017;1861(5 Pt B):1414-1428. doi:10.1016/j.bbagen.2016.12.015
67. Qiu W, Zhou F, Zhang Q, et al. Overexpression of nucleolin and different expression sites both related to the prognosis of gastric cancer. *Apmis*. Oct 2013;121(10):919-25. doi:10.1111/apm.12131
68. Otake Y, Soundararajan S, Sengupta TK, et al. Overexpression of nucleolin in chronic lymphocytic leukemia cells induces stabilization of bcl2 mRNA. *Blood*. Apr 1 2007;109(7):3069-75. doi:10.1182/blood-2006-08-043257
69. Oleinick NL, Morris RL, Belichenko I. The role of apoptosis in response to photodynamic therapy: what, where, why, and how. *Photochem Photobiol Sci*. Jan 2002;1(1):1-21. doi:10.1039/b108586g
70. Shieh YA, Yang SJ, Wei MF, Shieh MJ. Aptamer-based tumor-targeted drug delivery for photodynamic therapy. *ACS Nano*. Mar 23 2010;4(3):1433-42. doi:10.1021/nn901374b
71. Carvalho J, Lopes-Nunes J, Lopes AC, et al. Aptamer-guided acridine derivatives for cervical cancer. *Org Biomol Chem*. Mar 13 2019;17(11):2992-3002. doi:10.1039/c9ob00318e
72. Lopes-Nunes J, Carvalho J, Figueiredo J, et al. Phthalocyanines for G-quadruplex aptamers binding. *Bioorg Chem*. Jul 2020;100:103920. doi:10.1016/j.bioorg.2020.103920
73. Do NQ, Chung WJ, Truong THA, Heddi B, Phan AT. G-quadruplex structure of an anti-proliferative DNA sequence. *Nucleic Acids Res*. Jul 7 2017;45(12):7487-7493. doi:10.1093/nar/gkx274
74. Park JY, Cho YL, Chae JR, et al. Gemcitabine-Incorporated G-Quadruplex Aptamer for Targeted Drug Delivery into Pancreas Cancer. *Mol Ther Nucleic Acids*. Sep 7 2018;12:543-553. doi:10.1016/j.omtn.2018.06.003
75. García-Recio EM, Pinto-Díez C, Pérez-Morgado MI, et al. Characterization of MNK1b DNA Aptamers That Inhibit Proliferation in MDA-MB231 Breast Cancer Cells. *Mol Ther Nucleic Acids*. Jan 5 2016;5(1):e275. doi:10.1038/mtna.2015.50
76. Esposito V, Russo A, Vellecco V, et al. Thrombin binding aptamer analogues containing inversion of polarity sites endowed with antiproliferative and anti-motility properties against Calu-6 cells. *Biochim Biophys Acta Gen Subj*. Dec 2018;1862(12):2645-2650. doi:10.1016/j.bbagen.2018.07.031
77. Crommelin DJA, van Hoogevest P, Storm G. The role of liposomes in clinical nanomedicine development. What now? Now what? *J Control Release*. Feb 2020;318:256-263. doi:10.1016/j.jconrel.2019.12.023
78. Xing H, Tang L, Yang X, et al. Selective Delivery of an Anticancer Drug with Aptamer-Functionalized Liposomes to Breast Cancer Cells in Vitro and in Vivo. *J Mater Chem B*. Oct 21 2013;1(39):5288-5297. doi:10.1039/c3tb20412j
79. Wakaskar RR. General overview of lipid-polymer hybrid nanoparticles, dendrimers, micelles, liposomes, spongosomes and cubosomes. *J Drug Target*. Apr 2018;26(4):311-318. doi:10.1080/1061186x.2017.1367006
80. Zhang J, Chen R, Fang X, Chen F, Wang Y, Chen M. Nucleolin targeting AS1411 aptamer modified pH-sensitive micelles for enhanced delivery and antitumor efficacy of

- paclitaxel. *Nano Research*. 2015/01/01 2015;8(1):201-218. doi:10.1007/s12274-014-0619-4
81. Zhao S, Tan S, Guo Y, et al. pH-sensitive docetaxel-loaded D- α -tocopheryl polyethylene glycol succinate-poly(β -amino ester) copolymer nanoparticles for overcoming multidrug resistance. *Biomacromolecules*. Aug 12 2013;14(8):2636-46. doi:10.1021/bm4005113
82. Li X, Yu Y, Ji Q, Qiu L. Targeted delivery of anticancer drugs by aptamer AS1411 mediated Pluronic F127/cyclodextrin-linked polymer composite micelles. *Nanomedicine*. Jan 2015;11(1):175-84. doi:10.1016/j.nano.2014.08.013
83. Zhang HJ, Zhao X, Chen LJ, Yang CX, Yan XP. Dendrimer grafted persistent luminescent nanoplatforam for aptamer guided tumor imaging and acid-responsive drug delivery. *Talanta*. Nov 1 2020;219:121209. doi:10.1016/j.talanta.2020.121209
84. Ayatollahi S, Salmasi Z, Hashemi M, et al. Aptamer-targeted delivery of Bcl-xL shRNA using alkyl modified PAMAM dendrimers into lung cancer cells. *Int J Biochem Cell Biol*. Nov 2017;92:210-217. doi:10.1016/j.biocel.2017.10.005
85. Alibolandi M, Taghdisi SM, Ramezani P, et al. Smart AS1411-aptamer conjugated pegylated PAMAM dendrimer for the superior delivery of camptothecin to colon adenocarcinoma in vitro and in vivo. *Int J Pharm*. Mar 15 2017;519(1-2):352-364. doi:10.1016/j.ijpharm.2017.01.044
86. Choi CH, Hao L, Narayan SP, Auyeung E, Mirkin CA. Mechanism for the endocytosis of spherical nucleic acid nanoparticle conjugates. *Proc Natl Acad Sci U S A*. May 7 2013;110(19):7625-30. doi:10.1073/pnas.1305804110
87. Seferos DS, Prigodich AE, Giljohann DA, Patel PC, Mirkin CA. Polyvalent DNA nanoparticle conjugates stabilize nucleic acids. *Nano Lett*. Jan 2009;9(1):308-11. doi:10.1021/nl802958f
88. Chinen AB, Guan CM, Mirkin CA. Spherical nucleic acid nanoparticle conjugates enhance G-quadruplex formation and increase serum protein interactions. *Angew Chem Int Ed Engl*. Jan 7 2015;54(2):527-31. doi:10.1002/anie.201409211
89. Malik MT, O'Toole MG, Casson LK, et al. AS1411-conjugated gold nanospheres and their potential for breast cancer therapy. *Oncotarget*. Sep 8 2015;6(26):22270-81. doi:10.18632/oncotarget.4207
90. Ai J, Xu Y, Lou B, Li D, Wang E. Multifunctional AS1411-functionalized fluorescent gold nanoparticles for targeted cancer cell imaging and efficient photodynamic therapy. *Talanta*. Jan 2014;118:54-60. doi:10.1016/j.talanta.2013.09.062
91. Lee H, Kim J, Lee J, et al. In vivo self-degradable graphene nanomedicine operated by DNase and photo-switch for controlled anticancer therapy. *Biomaterials*. Dec 2020;263:120402. doi:10.1016/j.biomaterials.2020.120402
92. Goenka S, Sant V, Sant S. Graphene-based nanomaterials for drug delivery and tissue engineering. *J Control Release*. Jan 10 2014;173:75-88. doi:10.1016/j.jconrel.2013.10.017
93. Chen C, Zhou L, Geng J, Ren J, Qu X. Photosensitizer-incorporated quadruplex DNA-gated nanovehicles for light-triggered, targeted dual drug delivery to cancer cells. *Small*. Aug 26 2013;9(16):2793-800, 2653. doi:10.1002/sml.201201916

94. Fernández M, Javaid F, Chudasama V. Advances in targeting the folate receptor in the treatment/imaging of cancers. *Chem Sci*. Jan 28 2018;9(4):790-810. doi:10.1039/c7sc04004k
95. Wohlhueter RM, McIvor RS, Plagemann PG. Facilitated transport of uracil and 5-fluorouracil, and permeation of orotic acid into cultured mammalian cells. *J Cell Physiol*. Sep 1980;104(3):309-19. doi:10.1002/jcp.1041040305
96. Clua A, Fàbrega C, García-Chica J, Grijalvo S, Eritja R. Parallel G-quadruplex Structures Increase Cellular Uptake and Cytotoxicity of 5-Fluoro-2'-deoxyuridine Oligomers in 5-Fluorouracil Resistant Cells. *Molecules*. Mar 20 2021;26(6)doi:10.3390/molecules26061741
97. Louten J. Virus Replication. *Essential Human Virology*. © 2016 Jennifer Louten.; 2016:49-70.
98. Speck SH, Ganem D. Viral latency and its regulation: lessons from the gamma-herpesviruses. *Cell Host Microbe*. Jul 22 2010;8(1):100-15. doi:10.1016/j.chom.2010.06.014
99. Cohen JI. Herpesvirus latency. *J Clin Invest*. Jul 1 2020;130(7):3361-3369. doi:10.1172/JCI136225
100. Sevana M, Klose T, Rossmann MG. Principles of Virus Structure. *Encyclopedia of Virology*. Copyright © 2021 Elsevier Ltd. All rights reserved.; 2021:257-77.
101. Biswas B, Kandpal M, Jauhari UK, Vivekanandan P. Genome-wide analysis of G-quadruplexes in herpesvirus genomes. *BMC Genomics*. 2016/11/21 2016;17(1):949. doi:10.1186/s12864-016-3282-1
102. Norberg P. Divergence and genotyping of human α -herpesviruses: An overview. *Infection, Genetics and Evolution*. 2010/01/01/ 2010;10(1):14-25. doi:<https://doi.org/10.1016/j.meegid.2009.09.004>
103. Estep KN, Butler TJ, Ding J, Brosh RM. G4-Interacting DNA Helicases and Polymerases: Potential Therapeutic Targets. *Curr Med Chem*. 2019;26(16):2881-2897. doi:10.2174/0929867324666171116123345
104. Frasson I, Soldà P, Nadai M, Lago S, Richter SN. Parallel G-quadruplexes recruit the HSV-1 transcription factor ICP4 to promote viral transcription in herpes virus-infected human cells. *Communications Biology*. 2021/04/30 2021;4(1):510. doi:10.1038/s42003-021-02035-y
105. Artusi S, Ruggiero E, Nadai M, et al. Antiviral Activity of the G-Quadruplex Ligand TMPyP4 against Herpes Simplex Virus-1. *Viruses*. 2021;13(2). doi:10.3390/v13020196
106. Frasson I, Nadai M, Richter SN. Conserved G-Quadruplexes Regulate the Immediate Early Promoters of Human Alphaherpesviruses. *Molecules*. 2019;24(13). doi:10.3390/molecules24132375
107. Chung W-C, Ravichandran S, Park D, et al. G-quadruplexes formed by Varicella-Zoster virus reiteration sequences suppress expression of glycoprotein C and regulate viral cell-to-cell spread. *PLoS Pathogens*. 2023;19(1):e1011095. doi:10.1371/journal.ppat.1011095
108. Nogalski MT, Collins-McMillen D, Yurochko AD. Overview of human cytomegalovirus pathogenesis. *Methods Mol Biol*. 2014;1119:15-28. doi:10.1007/978-1-62703-788-4_2

109. De Bolle L, Naesens L, De Clercq E. Update on Human Herpesvirus 6 Biology, Clinical Features, and Therapy. *Clinical Microbiology Reviews*. 2005/01/01 2005;18(1):217-245. doi:10.1128/CMR.18.1.217-245.2005
110. Agut H, Bonnafous P, Gautheret-Dejean A. Human Herpesviruses 6A, 6B, and 7. *Microbiol Spectr*. Jun 2016;4(3)doi:10.1128/microbiolspec.DMIH2-0007-2015
111. Gottwein E. Kaposi's Sarcoma-Associated Herpesvirus microRNAs. *Front Microbiol*. 2012;3:165. doi:10.3389/fmicb.2012.00165
112. Singhal N, Kumar M, Kanaujia PK, Virdi JS. MALDI-TOF mass spectrometry: an emerging technology for microbial identification and diagnosis. *Frontiers in microbiology*. 2015;6:791-791. doi:10.3389/fmicb.2015.00791
113. Weed DJ, Damania B. Pathogenesis of Human Gammaherpesviruses: Recent Advances. *Curr Clin Microbiol Rep*. 2019;6(3):166-174. doi:10.1007/s40588-019-00127-2
114. Duellman SJ, Thompson KL, Coon JJ, Burgess RR. Phosphorylation sites of Epstein-Barr virus EBNA1 regulate its function. *J Gen Virol*. Sep 2009;90(Pt 9):2251-9. doi:10.1099/vir.0.012260-0
115. Kennedy G, Sugden B. EBNA-1, a bifunctional transcriptional activator. *Mol Cell Biol*. Oct 2003;23(19):6901-8. doi:10.1128/mcb.23.19.6901-6908.2003
116. Murat P, Zhong J, Lekieffre L, et al. G-quadruplexes regulate Epstein-Barr virus–encoded nuclear antigen 1 mRNA translation. *Nature Chemical Biology*. 2014/05/01 2014;10(5):358-364. doi:10.1038/nchembio.1479
117. Lista MJ, Martins RP, Billant O, et al. Nucleolin directly mediates Epstein-Barr virus immune evasion through binding to G-quadruplexes of EBNA1 mRNA. *Nat Commun*. Jul 7 2017;8:16043. doi:10.1038/ncomms16043
118. Reznichenko O, Quillévéré A, Martins RP, et al. Novel cationic bis(acylhydrazones) as modulators of Epstein–Barr virus immune evasion acting through disruption of interaction between nucleolin and G-quadruplexes of EBNA1 mRNA. *European Journal of Medicinal Chemistry*. 2019/09/15/ 2019;178:13-29. doi:<https://doi.org/10.1016/j.ejmech.2019.05.042>
119. Zheng AJ, Thermou A, Guixens Gallardo P, et al. The different activities of RNA G-quadruplex structures are controlled by flanking sequences. *Life Sci Alliance*. Feb 2022;5(2)doi:10.26508/lsa.202101232
120. Kumar S, Choudhary D, Patra A, Bhavesh NS, Vivekanandan P. Analysis of G-quadruplexes upstream of herpesvirus miRNAs: evidence of G-quadruplex mediated regulation of KSHV miR-K12–1-9,11 cluster and HCMV miR-US33. *BMC Molecular and Cell Biology*. 2020/09/24 2020;21(1):67. doi:10.1186/s12860-020-00306-w
121. Dabral P, Babu J, Zareie A, Verma SC. LANA and hnRNP A1 Regulate the Translation of LANA mRNA through G-Quadruplexes. *J Virol*. Jan 17 2020;94(3)doi:10.1128/JVI.01508-19
122. Kwun Hyun J, da Silva Suzane R, Shah Ishita M, Blake N, Moore Patrick S, Chang Y. Kaposi's Sarcoma-Associated Herpesvirus Latency-Associated Nuclear Antigen 1 Mimics Epstein-Barr Virus EBNA1 Immune Evasion through Central Repeat Domain Effects on Protein Processing. *Journal of Virology*. 2007/08/01 2007;81(15):8225-8235. doi:10.1128/JVI.00411-07

123. Kwun HJ, da Silva SR, Qin H, et al. The central repeat domain 1 of Kaposi's sarcoma-associated herpesvirus (KSHV) latency associated-nuclear antigen 1 (LANA1) prevents cis MHC class I peptide presentation. *Virology*. Apr 10 2011;412(2):357-65. doi:10.1016/j.virol.2011.01.026
124. Ballestas ME, Kaye KM. The latency-associated nuclear antigen, a multifunctional protein central to Kaposi's sarcoma-associated herpesvirus latency. *Future Microbiol*. Dec 2011;6(12):1399-413. doi:10.2217/fmb.11.137
125. Lee HR, Lee S, Chaudhary PM, Gill P, Jung JU. Immune evasion by Kaposi's sarcoma-associated herpesvirus. *Future Microbiol*. Sep 2010;5(9):1349-65. doi:10.2217/fmb.10.105
126. Krüger AC, Raarup MK, Nielsen MM, et al. Interaction of hnRNP A1 with telomere DNA G-quadruplex structures studied at the single molecule level. *Eur Biophys J*. Aug 2010;39(9):1343-50. doi:10.1007/s00249-010-0587-x
127. De Leo A, Deng Z, Vladimirova O, et al. LANA oligomeric architecture is essential for KSHV nuclear body formation and viral genome maintenance during latency. *PLoS Pathogens*. 2019;15(1):e1007489. doi:10.1371/journal.ppat.1007489
128. Kumar S, Ramamurthy C, Choudhary D, et al. Contrasting roles for G-quadruplexes in regulating human Bcl-2 and virus homologues KSHV KS-Bcl-2 and EBV BHRF1. *Sci Rep*. Mar 23 2022;12(1):5019. doi:10.1038/s41598-022-08161-9
129. Madireddy A, Purushothaman P, Loosbroock CP, Robertson ES, Schildkraut CL, Verma SC. G-quadruplex-interacting compounds alter latent DNA replication and episomal persistence of KSHV. *Nucleic Acids Res*. May 5 2016;44(8):3675-94. doi:10.1093/nar/gkw038
130. Tlučková K, Marušič M, Tóthová P, et al. Human Papillomavirus G-Quadruplexes. *Biochemistry*. 2013/10/15 2013;52(41):7207-7216. doi:10.1021/bi400897g
131. Marušič M, Hošnjak L, Krafčikova P, Poljak M, Viglasky V, Plavec J. The effect of single nucleotide polymorphisms in G-rich regions of high-risk human papillomaviruses on structural diversity of DNA. *Biochim Biophys Acta Gen Subj*. May 2017;1861(5 Pt B):1229-1236. doi:10.1016/j.bbagen.2016.11.007
132. Carvalho J, Lopes-Nunes J, Campello MPC, et al. Human Papillomavirus G-Rich Regions as Potential Antiviral Drug Targets. *Nucleic Acid Ther*. Feb 2021;31(1):68-81. doi:10.1089/nat.2020.0869
133. Ahsan N, Shah KV. Polyomaviruses and human diseases. *Adv Exp Med Biol*. 2006;577:1-18. doi:10.1007/0-387-32957-9_1
134. Jiang M, Abend JR, Johnson SF, Imperiale MJ. The role of polyomaviruses in human disease. *Virology*. Feb 20 2009;384(2):266-73. doi:10.1016/j.virol.2008.09.027
135. Saribas AS, Coric P, Bouaziz S, Safak M. Expression of novel proteins by polyomaviruses and recent advances in the structural and functional features of agnoprotein of JC virus, BK virus, and simian virus 40. *J Cell Physiol*. Jun 2019;234(6):8295-8315. doi:10.1002/jcp.27715
136. Yang JF, You J. Regulation of Polyomavirus Transcription by Viral and Cellular Factors. *Viruses*. Sep 24 2020;12(10)doi:10.3390/v12101072

137. Patel PK, Bhavesh NS, Hosur RV. NMR observation of a novel C-tetrad in the structure of the SV40 repeat sequence GGGCGG. *Biochem Biophys Res Commun*. Apr 21 2000;270(3):967-71. doi:10.1006/bbrc.2000.2479
138. Topalis D, Andrei G, Snoeck R. The large tumor antigen: a "Swiss Army knife" protein possessing the functions required for the polyomavirus life cycle. *Antiviral Res*. Feb 2013;97(2):122-36. doi:10.1016/j.antiviral.2012.11.007
139. Plyler J, Jasheway K, Tuesuwan B, et al. Real-time investigation of SV40 large T-antigen helicase activity using surface plasmon resonance. *Cell Biochem Biophys*. 2009;53(1):43-52. doi:10.1007/s12013-008-9038-z
140. Tuesuwan B, Kern JT, Thomas PW, et al. Simian Virus 40 Large T-Antigen G-Quadruplex DNA Helicase Inhibition by G-Quadruplex DNA-Interactive Agents. *Biochemistry*. 2008/02/01 2008;47(7):1896-1909. doi:10.1021/bi701747d
141. Sunbul M. Hepatitis B virus genotypes: global distribution and clinical importance. *World J Gastroenterol*. May 14 2014;20(18):5427-34. doi:10.3748/wjg.v20.i18.5427
142. Biswas B, Kandpal M, Vivekanandan P. A G-quadruplex motif in an envelope gene promoter regulates transcription and virion secretion in HBV genotype B. *Nucleic Acids Res*. Nov 2 2017;45(19):11268-11280. doi:10.1093/nar/gkx823
143. Meier-Stephenson V, Badmalia MD, Mrozowich T, et al. Identification and characterization of a G-quadruplex structure in the pre-core promoter region of hepatitis B virus covalently closed circular DNA. *J Biol Chem*. Jan-Jun 2021;296:100589. doi:10.1016/j.jbc.2021.100589
144. Molnár OR, Végh A, Somkuti J, Smeller L. Characterization of a G-quadruplex from hepatitis B virus and its stabilization by binding TMPyP4, BRACO19 and PhenDC3. *Scientific Reports*. 2021/12/01 2021;11(1):23243. doi:10.1038/s41598-021-02689-y
145. Nagy PD, Pogany J. The dependence of viral RNA replication on co-opted host factors. *Nature Reviews Microbiology*. 2012/02/01 2012;10(2):137-149. doi:10.1038/nrmicro2692
146. Lauring AS, Andino R. Quasispecies theory and the behavior of RNA viruses. *PLoS Pathog*. Jul 22 2010;6(7):e1001005. doi:10.1371/journal.ppat.1001005
147. Denison MR, Graham RL, Donaldson EF, Eckerle LD, Baric RS. Coronaviruses: an RNA proofreading machine regulates replication fidelity and diversity. *RNA Biol*. Mar-Apr 2011;8(2):270-9. doi:10.4161/rna.8.2.15013
148. Gallo RC, Sarin PS, Gelmann E, et al. Isolation of Human T-Cell Leukemia Virus in Acquired Immune Deficiency Syndrome (AIDS). *Science (New York, NY)*. 06/01 1983;220:865-7. doi:10.1126/science.6601823
149. What to call the AIDS virus? *Nature*. 1986/05/01 1986;321(6065):10-10. doi:10.1038/321010a0
150. Barré-Sinoussi F, Chermann JC, Rey F, et al. Isolation of a T-lymphotropic retrovirus from a patient at risk for acquired immune deficiency syndrome (AIDS). *Revista de investigación clínica; organo del Hospital de Enfermedades de la Nutrición*. 01/01 1983;56:126-9.
151. Prevention CfDca. HIV Surveillance Report, 2018 (Preliminary). 30. <http://www.cdc.gov/hiv/library/reports/hiv-surveillance.html>

152. Gao F, Bailes E, Robertson DL, et al. Origin of HIV-1 in the chimpanzee Pan troglodytes troglodytes. *Nature*. 1999/02/01 1999;397(6718):436-441. doi:10.1038/17130
153. Korber B, Muldoon M, Theiler J, et al. Timing the Ancestor of the HIV-1 Pandemic Strains. *Science*. 2000;288(5472):1789. doi:10.1126/science.288.5472.1789
154. Deeks SG, Overbaugh J, Phillips A, Buchbinder S. HIV infection. *Nat Rev Dis Primers*. Oct 1 2015;1:15035. doi:10.1038/nrdp.2015.35
155. Perrone R, Nadai M, Frasson I, et al. A dynamic G-quadruplex region regulates the HIV-1 long terminal repeat promoter. *J Med Chem*. Aug 22 2013;56(16):6521-30. doi:10.1021/jm400914r
156. Perrone R, Nadai M, Poe JA, et al. Formation of a unique cluster of G-quadruplex structures in the HIV-1 Nef coding region: implications for antiviral activity. *PLoS one*. 2013;8(8):e73121-e73121. doi:10.1371/journal.pone.0073121
157. Quinones-Mateu ME, Mas A, Lain de Lera T, et al. LTR and tat variability of HIV-1 isolates from patients with divergent rates of disease progression. *Virus Res*. Sep 1998;57(1):11-20. doi:10.1016/s0168-1702(98)00082-3
158. Nonnemacher MR, Irish BP, Liu Y, Mauger D, Wigdahl B. Specific sequence configurations of HIV-1 LTR G/C box array result in altered recruitment of Sp isoforms and correlate with disease progression. *J Neuroimmunol*. Dec 2004;157(1-2):39-47. doi:10.1016/j.jneuroim.2004.08.021
159. Sundquist WI, Heaphy S. Evidence for interstrand quadruplex formation in the dimerization of human immunodeficiency virus 1 genomic RNA. *Proc Natl Acad Sci U S A*. Apr 15 1993;90(8):3393-7. doi:10.1073/pnas.90.8.3393
160. Piekna-Przybylska D, Sharma G, Bambara RA. Mechanism of HIV-1 RNA dimerization in the central region of the genome and significance for viral evolution. *The Journal of biological chemistry*. 2013;288(33):24140-24150. doi:10.1074/jbc.M113.477265
161. Shen W, Gao L, Balakrishnan M, Bambara RA. A recombination hot spot in HIV-1 contains guanosine runs that can form a G-quartet structure and promote strand transfer in vitro. *The Journal of biological chemistry*. 2009;284(49):33883-33893. doi:10.1074/jbc.M109.055368
162. Miller MD, Warmerdam MT, Gaston I, Greene WC, Feinberg MB. The human immunodeficiency virus-1 nef gene product: a positive factor for viral infection and replication in primary lymphocytes and macrophages. *J Exp Med*. Jan 1 1994;179(1):101-13. doi:10.1084/jem.179.1.101
163. Manzouralajdad A, Gonzalez M, Spouge JL. Changes in the Plasticity of HIV-1 Nef RNA during the Evolution of the North American Epidemic. *PLOS ONE*. 2016;11(9):e0163688. doi:10.1371/journal.pone.0163688
164. Khullar V, Firpi RJ. Hepatitis C cirrhosis: New perspectives for diagnosis and treatment. *World J Hepatol*. Jul 18 2015;7(14):1843-55. doi:10.4254/wjh.v7.i14.1843
165. Vassilaki N, Friebe P, Meuleman P, et al. Role of the hepatitis C virus core+1 open reading frame and core cis-acting RNA elements in viral RNA translation and replication. *J Virol*. Dec 2008;82(23):11503-15. doi:10.1128/jvi.01640-08
166. Moradpour D, Penin F, Rice CM. Replication of hepatitis C virus. *Nat Rev Microbiol*. Jun 2007;5(6):453-63. doi:10.1038/nrmicro1645

167. Jaubert C, Bedrat A, Bartolucci L, et al. RNA synthesis is modulated by G-quadruplex formation in Hepatitis C virus negative RNA strand. *Sci Rep*. May 25 2018;8(1):8120. doi:10.1038/s41598-018-26582-3
168. Pirakitikulr N, Kohlway A, Lindenbach BD, Pyle AM. The Coding Region of the HCV Genome Contains a Network of Regulatory RNA Structures. *Mol Cell*. Apr 7 2016;62(1):111-20. doi:10.1016/j.molcel.2016.01.024
169. Wang SR, Min YQ, Wang JQ, et al. A highly conserved G-rich consensus sequence in hepatitis C virus core gene represents a new anti-hepatitis C target. *Sci Adv*. Apr 2016;2(4):e1501535. doi:10.1126/sciadv.1501535
170. Bian W-X, Xie Y, Wang X-N, et al. Binding of cellular nucleolin with the viral core RNA G-quadruplex structure suppresses HCV replication. *Nucleic acids research*. 2019;47(1):56-68. doi:10.1093/nar/gky1177
171. Belachew B, Gao J, Byrd AK, Raney KD. Hepatitis C virus nonstructural protein NS3 unfolds viral G-quadruplex RNA structures. *Journal of Biological Chemistry*. 2022/11/01/ 2022;298(11):102486. doi:<https://doi.org/10.1016/j.jbc.2022.102486>
172. Noorbakhsh F, Abdolmohammadi K, Fatahi Y, et al. Zika Virus Infection, Basic and Clinical Aspects: A Review Article. *Iran J Public Health*. Jan 2019;48(1):20-31.
173. Fleming AM, Ding Y, Alenko A, Burrows CJ. Zika Virus Genomic RNA Possesses Conserved G-Quadruplexes Characteristic of the Flaviviridae Family. *ACS Infectious Diseases*. 2016/10/14 2016;2(10):674-681. doi:10.1021/acsinfectdis.6b00109
174. Majee P, Pattnaik A, Sahoo BR, et al. Inhibition of Zika virus replication by G-quadruplex-binding ligands. *Molecular Therapy - Nucleic Acids*. 2021/03/05/ 2021;23:691-701. doi:<https://doi.org/10.1016/j.omtn.2020.12.030>
175. Krammer F. The human antibody response to influenza A virus infection and vaccination. *Nat Rev Immunol*. Jun 2019;19(6):383-397. doi:10.1038/s41577-019-0143-6
176. Te Velthuis AJ, Fodor E. Influenza virus RNA polymerase: insights into the mechanisms of viral RNA synthesis. *Nat Rev Microbiol*. Aug 2016;14(8):479-93. doi:10.1038/nrmicro.2016.87
177. Szabo R, Bugge TH. Type II transmembrane serine proteases in development and disease. *Int J Biochem Cell Biol*. 2008;40(6-7):1297-316. doi:10.1016/j.biocel.2007.11.013
178. Böttcher-Friebertshäuser E, Klenk HD, Garten W. Activation of influenza viruses by proteases from host cells and bacteria in the human airway epithelium. *Pathog Dis*. Nov 2013;69(2):87-100. doi:10.1111/2049-632x.12053
179. Shen LW, Mao HJ, Wu YL, Tanaka Y, Zhang W. TMPRSS2: A potential target for treatment of influenza virus and coronavirus infections. *Biochimie*. Nov 2017;142:1-10. doi:10.1016/j.biochi.2017.07.016
180. Shen L-W, Qian M-Q, Yu K, et al. Inhibition of Influenza A virus propagation by benzoselenoxanthenes stabilizing TMPRSS2 Gene G-quadruplex and hence down-regulating TMPRSS2 expression. *Scientific Reports*. 2020/05/06 2020;10(1):7635. doi:10.1038/s41598-020-64368-8
181. Tomaszewska M, Szabat M, Zielińska K, Kierzek R. Identification and Structural Aspects of G-Quadruplex-Forming Sequences from the Influenza A Virus Genome. *Int J Mol Sci*. Jun 2 2021;22(11)doi:10.3390/ijms22116031

182. Lugo D, Krogstad P. Enteroviruses in the early 21st century: new manifestations and challenges. *Curr Opin Pediatr*. Feb 2016;28(1):107-13. doi:10.1097/mop.0000000000000303
183. Lv L, Zhang L. Characterization of G-Quadruplexes in Enterovirus A71 Genome and Their Interaction with G-Quadruplex Ligands. *Microbiol Spectr*. Jun 29 2022;10(3):e0046022. doi:10.1128/spectrum.00460-22
184. Bezzi G, Piga EJ, Binolfi A, Armas P. CNBP Binds and Unfolds In Vitro G-Quadruplexes Formed in the SARS-CoV-2 Positive and Negative Genome Strands. *Int J Mol Sci*. Mar 5 2021;22(5)doi:10.3390/ijms22052614
185. Gu H, Chen Q, Yang G, et al. Adaptation of SARS-CoV-2 in BALB/c mice for testing vaccine efficacy. *Science*. 2020;369(6511):1603. doi:10.1126/science.abc4730
186. Zhang R, Xiao K, Gu Y, Liu H, Sun X. Whole Genome Identification of Potential G-Quadruplexes and Analysis of the G-Quadruplex Binding Domain for SARS-CoV-2. *Front Genet*. 2020;11:587829. doi:10.3389/fgene.2020.587829
187. Ji D, Juhas M, Tsang CM, Kwok CK, Li Y, Zhang Y. Discovery of G-quadruplex-forming sequences in SARS-CoV-2. *Briefings in Bioinformatics*. 2021;22(2):1150-1160. doi:10.1093/bib/bbaa114
188. Cui H, Zhang L. G-Quadruplexes Are Present in Human Coronaviruses Including SARS-CoV-2. *Front Microbiol*. 2020;11:567317. doi:10.3389/fmicb.2020.567317
189. Kusov Y, Tan J, Alvarez E, Enjuanes L, Hilgenfeld R. A G-quadruplex-binding macrodomain within the “SARS-unique domain” is essential for the activity of the SARS-coronavirus replication–transcription complex. *Virology*. 2015/10/01/ 2015;484:313-322. doi:<https://doi.org/10.1016/j.virol.2015.06.016>
190. Lei J, Ma-Lauer Y, Han Y, et al. The SARS-unique domain (SUD) of SARS-CoV and SARS-CoV-2 interacts with human Paip1 to enhance viral RNA translation. *Embo j*. Jun 1 2021;40(11):e102277. doi:10.15252/embj.2019102277
191. Lavigne M, Helynck O, Rigolet P, et al. SARS-CoV-2 Nsp3 unique domain SUD interacts with guanine quadruplexes and G4-ligands inhibit this interaction. *Nucleic Acids Research*. 2021;49(13):7695-7712. doi:10.1093/nar/gkab571
192. Hoffmann M, Kleine-Weber H, Schroeder S, et al. SARS-CoV-2 Cell Entry Depends on ACE2 and TMPRSS2 and Is Blocked by a Clinically Proven Protease Inhibitor. *Cell*. Apr 16 2020;181(2):271-280.e8. doi:10.1016/j.cell.2020.02.052
193. Liu G, Du W, Sang X, et al. RNA G-quadruplex in TMPRSS2 reduces SARS-CoV-2 infection. *Nature Communications*. 2022/03/17 2022;13(1):1444. doi:10.1038/s41467-022-29135-5
194. Beigel JH, Tomashek KM, Dodd LE, et al. Remdesivir for the Treatment of Covid-19 - Final Report. *N Engl J Med*. Nov 5 2020;383(19):1813-1826. doi:10.1056/NEJMoa2007764
195. Qin G, Zhao C, Liu Y, et al. RNA G-quadruplex formed in SARS-CoV-2 used for COVID-19 treatment in animal models. *Cell Discovery*. 2022/09/06 2022;8(1):86. doi:10.1038/s41421-022-00450-x
196. Zhao C, Qin G, Niu J, et al. Targeting RNA G-Quadruplex in SARS-CoV-2: A Promising Therapeutic Target for COVID-19? <https://doi.org/10.1002/anie.202011419>. *Angewandte Chemie International Edition*. 2021/01/04 2021;60(1):432-438. doi:<https://doi.org/10.1002/anie.202011419>

197. Oliva R, Mukherjee S, Manisegaran M, et al. Binding Properties of RNA Quadruplex of SARS-CoV-2 to Berberine Compared to Telomeric DNA Quadruplex. *International Journal of Molecular Sciences*. 2022;23(10). doi:10.3390/ijms23105690
198. Ting Cao and Fang-Ting Zhang and Liangyuan Cai and Yinglin Zhou and Niklaas JBaXZ. Investigation of the interactions between methylene blue and intramolecular G-quadruplexes: an explicit distinction in electrochemical behavior. *The Analyst*. 2017;142 6:987-993.
199. do Nascimento TS, Pereira RO, de Mello HL, Costa J. Methemoglobinemia: from diagnosis to treatment. *Rev Bras Anesthesiol*. Nov-Dec 2008;58(6):651-64. doi:10.1590/s0034-70942008000600011
200. Bojadzic D, Alcazar O, Buchwald P. Methylene Blue Inhibits the SARS-CoV-2 Spike–ACE2 Protein-Protein Interaction—a Mechanism that can Contribute to its Antiviral Activity Against COVID-19. Brief Research Report. *Frontiers in Pharmacology*. 2021-January-13 2021;11doi:10.3389/fphar.2020.600372

CHAPTER 3

3. NUCLEOLIN REGULATES THE EXPRESSION OF KSHV'S LANA THROUGH G-QUADRUPLEXES IN THE MRNA.

Zarerie A. R. et al. *Viruses* (In Review) (2023).

3.1 Abstract

Kaposi's sarcoma-associated herpesvirus (KSHV) establishes life-long latent infection and is linked to several human malignancies. Latency-associated nuclear antigen (LANA) is highly expressed during latency and responsible for the replication and maintenance of the viral genome. The expression of LANA is regulated at transcriptional/translational levels through multiple mechanisms, including the secondary structures in the mRNA sequence. LANA mRNA has multiple G-quadruplexes (G4s) bound by multiple proteins to stabilize/destabilize these secondary structures for regulating LANA. In this manuscript, we demonstrate the role of Nucleolin (NCL) in regulating LANA expression through its interaction with G-quadruplexes of LANA mRNA. This interaction reduced LANA's protein expression through the sequestration of mRNA into the nucleus, demonstrated by the colocalization of G4-carrying mRNA with NCL. Furthermore, the downregulation of NCL, by way of a short hairpin, showed an increase in LANA translation following an alteration in the levels of LANA mRNA in the cytoplasm. Overall, the data presented in this manuscript showed that G-quadruplex-mediated translational control could be regulated by NCL, which can be exploited for controlling KSHV latency.

Keywords: G-quadruplex; LANA; KSHV; Nucleolin (NCL)

3.2 Introduction

Kaposi's sarcoma-associated herpesvirus (KSHV) is a DNA virus linked to several human malignancies, including Kaposi's sarcomas (KS), multicentric Castleman's disease, and primary effusion lymphoma (PEL)¹⁻⁴. KSHV establishes a life-long infection with two distinct phases, a prevalent latent phase and a short lytic phase^{5,6}. ORF73 encoded latency-associated nuclear antigen (LANA) is predominantly expressed during the latent phase^{7,8}. LANA is essential for replication and the maintenance of the viral episome⁹. The virus evades the host's immune surveillance while maintaining the viral genome by expressing the LANA protein at a level sufficient for maintaining its genome. LANA evades CD8⁺ T-cells by controlling its expression through downregulation of its promoter to suppress LANA expression. CD8⁺ T-cell evasion is also achieved by inhibiting the translocation of LANA peptide to the endoplasmic reticulum and its presentation through MHC-I¹⁰⁻¹². We previously showed that LANA also inhibits CD4⁺ T-cell response by downregulating the MHC-II gene by blocking CIITA transcription through its interaction with the regulatory factor X (RFX) complex¹³.

This study focuses on G-quadruplexes (G4s), non-canonical secondary structures in guanine-rich DNA and RNA sequences. G4s are formed when two or more consecutive guanine blocks are separated by a single-stranded loop region¹⁴. Four consecutive runs of guanine blocks result in G-tetrads held together by Hoogsteen hydrogen bonding between the guanines (Fig. 1A). These structures fold into two or more stacked planar G-tetrads, and stability is increased by way of π - π stacking between the quartets, and further stabilized by a cation, such as potassium¹⁵. The stability of G4s is increased with more quartets stacked and lower numbers of nucleotides comprising the loop regions. G4s are

energetically favorable, with a negative ΔG , and form spontaneously^{14,16-19}. The G4s serve as regulatory elements in transcription, translation, RNA maturation, and regulation of non-coding RNA²⁰. Potential G4 sequences are more likely to fold into a secondary structure in RNA due to the lack of a complementary strand compared to DNA. Notably, the folding of potential G4-forming sequences results in more stable RNA molecules¹⁵.

G4 sequences are present in functional domains of mRNA, including 5'-UTR, ORFs, and 3'-UTR²¹⁻²³. G4s can affect the genome's coding capacity through alternative polyadenylation, alternative splicing, and induced frameshifts²⁰. G4s can be regulated by either stabilizing or unwinding the secondary structure²¹. Recently, G4s gained interest as potential therapeutic targets against pathogenic viruses. For instance, the Hepatitis B virus contains a G4 that positively regulates its transcription, and disruption of this G4 reduces virion production²⁴. Human immunodeficiency virus (HIV-1) has a G4 that reduces the transcriptional activation of HIV²⁵. Stabilization of a G4 in Herpes Simplex Virus 1 resulted in reduced virion production²⁶. The G4 in Epstein-Barr virus (EBV) nuclear antigen (EBNA1) can regulate translation and antigen presentation²⁷. Previously, our lab reported the formation of a G4 in the terminal repeat of KSHV and its impact on latent viral replication²⁸. We also showed that the mRNA of LANA has multiple G4 sites (Fig.1B), and the disruption of these sites led to increased LANA translation and antigen presentation²⁹. Notably, the expression of EBV's latent antigen, EBNA1, a homolog of LANA, is maintained at optimal levels for viral episome replication/maintenance^{27,30,31}. Interestingly, EBNA1 has a glycine-alanine repeat (GAR) region, which forms G-quadruplex structures to regulate its expression through interaction with Nucleolin (NCL)²⁷. NCL is a multifunction DNA/RNA-binding protein

that is conserved among eukaryotes. NCL binds to the mRNAs of many cancer-related genes to regulate their translation³². For example, NCL binds to G-quadruplexes formed in the LTR promoter of HIV, resulting in the downregulation of viral transcription³³. Additionally, NCL binds and stabilizes a G-quadruplex within the c-MYC promoter, affecting HIV transcription³⁴.

Several open-source programs based on G-quadruplex prediction algorithms are available for detecting putative G4-forming sequences (PQSs). Noteworthy examples include G4Hunter, Quadparser, and QGRS Mapper. G4Hunter and Quadparser identify a relatively smaller number of G4s and require programming skills for their usage. On the other hand, QGRS Mapper can identify a greater number of potential G4s and operates as a standalone web-based program³⁵. The potential G-quadruplex sites can be determined *in silico* using QGRS Mapper, which led to the identification of multiple G-quadruplex forming sites in LANA^{20,29,35-45}. Furthermore, the role of these G-quadruplexes in regulating LANA expression through the helicase activity of hnRNP A1 in unwinding these G4s was demonstrated earlier²⁹. In this paper, we set out to determine whether NCL plays a role in regulating the expression of LANA, and the data presented here convincingly show that NCL controls LANA expression through G quadruplexes.

3.3 Materials and Methods

3.3.1 Cells

Human kidney (HEK 293L) cells maintained using Dulbecco's Modified Eagle's Medium (DMEM) supplemented with 8% BGS (Hyclone Laboratories, UT), 2mM L-glutamine (GE Healthcare Life Sciences, South Logan, Utah), 25 U/mL penicillin (GE

Healthcare, South Logan, Utah), and 25 ug/mL streptomycin (GE Healthcare, South Logan, UT, USA). HEK293KbC2 cells were a generous gift from Johnathan Yewdell (NIH) and maintained in DMEM with 8% BGS, 2mM L-glutamine, 25 U/mL, 25U/mL penicillin, and 25 ug/mL streptomycin. T cell hybridoma line (B3Z), a kind gift from Nilabh Shastri (John Hopkins University) and Charles L. Stentman (Dartmouth University), were grown in RPMI with 10% FBS, 2mM glutamine, 1mM pyruvate, 25 U/mL penicillin, and 25 ug/mL streptomycin. Human epithelial (HELA) cells were grown in DMEM supplemented with 10% FBS, 2mM L-glutamine, 25 U/mL penicillin, and 25 ug/mL streptomycin. pA3F-LANA, LANA-luciferase, pA3F-G4WT, pA3F-G4Dis, pA3F-LANA-OVA, pA3F-G4WT-OVA, pA3F-G4Dis-OVA have been described previously in (Verma 2013, Purushothaman 2012, Dabral 2021)^{29,46,47}.

Cell transfections were carried out either by polyethylamine (PEI) or Lipofectamine 3000. For a 6-well plate containing 1 million cells/well, 3µg of the desired plasmid was mixed with 180 of 150mM NaCl (Fisher Scientific, NJ), and 15µL (1mg/mL) PEI was incubated for 15 minutes before adding the solution to the well. After 4hr of incubation, media was aspirated off, and new media was added to the cells. 24hr post-transfection, the cells were used for the indicated experiments. Scaling of components was done according to well size: 10cm TC dish (900µL 150mM NaCl with 75µL 1mg/mL PEI), 12-well plate (90µL 150mM NaCl with 7.5µL 1mg/mL PEI), 24-well plate (45µL 150mM NaCl with 3.75µL 1mg/mL PEI). Transfection using Lipofectamine 3000 (Thermofisher, CA) was done as per the manufacturer's protocol.

3.3.2. Dual Luciferase Assay

The Dual-Luciferase Reporter Assay System (Promega Inc., Madison, WI, USA) was used for the luciferase assays. Cells were lysed with 100 μ L of 1x passive lysis buffer for 15 min, with gentle rocking. 20 μ L of the lysate was collected and transferred into a 96-well plate. 20 μ L of LAR reagent was added to the lysate to detect Firefly luciferase activity. Renilla luciferase activity was measured by adding 20 μ L of Stop&Glo reagent. The data were analyzed and presented as the ratio of Firefly/Renilla.

3.3.3 *Fluorescent in situ Hybridization (FISH)*

Fluorescent in situ Hybridization was performed as described previously (Kochan et al. 2015)⁴⁸. Briefly, the cell monolayers were fixed directly to the coverslip using 4% paraformaldehyde (Sigma-Aldrich, St. Louis, MO, USA) for 15min at room temp (RT). Following 3x wash with PBS (Life Technologies, NY) with 5min of gentle rocking, cells were permeabilized for 10min while shaking with 1% BSA (Sigma, MO), 0.3% Triton X-100 (Fisher Scientific, NJ), 2mM Vanadyl ribonucleoside complexes (Sigma, MO), 1x PBS, and DEPC-treated water (Sigma, MO). These cells were washed 3x with PBS for 5 min while rocking gently. 200nM of biotinylated OVA-oligonucleotide (5'-UCCAUCAUCAAUUUCGAGAAACUC-biotin-3'), WT LANA RNA oligonucleotide (WT-LANA-Oligo) (5'-UGGAAGAGCAGGAAGA GCAGGAGUUAGAGGA-biotin-3') or Dis-LANA RNA oligonucleotide (Dis-LANA-Oligo) (5'-UAACCGAUGAUAUGAGUC AGAUAUAUAAGCA-biotin-3') (IDT, IA) was added in 2x SSC (diluted from 20x SSC: NaCl 3M and trisodium citrate dihydrate 300nM), 10% formamide (Fisher Scientific, NJ), 10% dextran sulfate (Sigma, MO) DEPC-treated water for hybridization. Following an overnight Incubation at 37⁰C, cells were washed 3x

with gentle rocking in PBS for 5min. 5 μ L of NCL antibody (Invitrogen, MA, Cat#PA3-16875) was added into 1mL of permeabilization solution for immune localization by using 200 μ L of the mixture to each coverslip. Following overnight incubation at 37 $^{\circ}$ C, coverslips were washed 3x with PBS for 5min/each with gentle rocking. Alexa Fluor streptavidin-594 (Invitrogen, MA) and Alexa Fluor 488 (Invitrogen, MA) added to the permeabilization buffer were used for the localization of the biotin-labeled probe and NCL, respectively. Streptavidin Alexafluor-594 and Alexa Fluor 488 mix were added onto the coverslips and incubated for 1hr at 37 $^{\circ}$ C, followed by 3x PBS washes for 5min/each with gentle rocking. The nuclei were stained with DAPI (Invitrogen, MA) or ToPro3 (Thermofisher, CA) for 1 min at RT and washed 3x with PBS for 5min before mounting with antifade (Invitrogen, MA) onto a slide. These slides were dried overnight before imaging on a Zeiss Imager M2. BCBL-1 cells are subjected to the same protocol, except that they are fixed to the coverslips using 10% formaldehyde for 10 minutes, following a 30-minute incubation in PBS on the coverslips.

3.3.4 Antigen Presentation Assay

HEK293Kbc2 cells were transfected with LANA-OVA, G4WT-OVA, or G4Dis-OVA plasmids. 24hrs post transfection, the cells were incubated with B3Z cells for 18 hours at a ratio of 1:2, 1:1, and 1:0.5. Cells were incubated with buffer containing 0.124% NP-40, 9mM MgCl₂, and 5mM ONPG for 4 hours at 37 $^{\circ}$ C with 5% CO₂. Absorbance was measured at 450nm GloMax Explorer microplate reader (Promega, WI). For the MTT Assay, the same ratio of cells as the antigen presentation is used and pipetted into a 96-well plate. After incubating for 18 hours, cells were incubated with 150 μ L of MTT

(Invitrogen, MA) for four hours. The absorbance was measured at 560nm using a Hidex Chameleon (Hidex, Finland) microplate reader at 570nm.

3.3.5 RNA Cross-linking Immunoprecipitation Assay (RNA-CLIP)

RNA-CLIP was modified as described previously⁴⁹. Briefly, 5 million cells were transfected in 10cm TC dish with LANA-OVA, G4WT-OVA, or G4Dis-OVA plasmids. 24hrs post-transfection, the cells were fixed with 4% formaldehyde and quenched with the addition of 125mM glycine. Cells were then washed and pelleted. Following resuspension in DNA/RNA Shield (Zymo Research, CA). The nuclei were isolated by sonicating cells at 30W, 20 sec on, 30 sec off, for a total runtime of 7min and 30 sec. Chromatin was sheared between 200-400bp using QSonica CL-334 Sonicator (Fisher Scientific, NJ), following which the cell debris was pelleted. The chromatin was incubated with specific antibodies overnight, followed by a 1 hr protein A/G magnetic Sepharose bead incubation to capture the protein-RNA complex. The beads were washed once with low-salt buffer (0.1% SDS, 1% Triton X-100, 2 mM EDTA, 20 mM Tris [pH 8.0], 150 mM NaCl) and once with high-salt buffer (0.1% SDS, 1% Triton X-100, 2 mM EDTA, 20 mM Tris [pH 8.0], 500 mM NaCl). Beads were washed with 1mL TE, and a 10% aliquot was set aside for Western Blotting. Beads were resuspended in 150 μ L of elution buffer (1% SDS, 100 mM NaHCO₃), with gentle vortexing for 15 min to elute the complex. Elutions were reverse cross-linked overnight at 65°C using 0.3 M NaCl. The following day, RNA was extracted using Direct-zol RNA Miniprep Plus (Zymo Research, CA) per the manufacturer's instructions.

3.3.6. *In Vitro* RNA Pulldown Assay

WT LANA RNA oligonucleotide (5'-UGGAAGAGCAGGAAGA GCAGGAGUUAGAGGA-biotin-3') (IDT, IA) and Dis-LANA-Oligo RNA oligonucleotide (5'-UAACCGAUGAUAUGAGUC AGAUAUAUAAGCA-biotin-3'). 20 million HEK293L cells were lysed in 1% NP-40 lysis buffer (50mM Tris-HCl pH7.5, 150mM NaCl, 1% NP-40, 1mM EDTA pH 8.0) with protease inhibitors and RNaseOut. Prior to incubation, oligos were heated to 95⁰C for 5 min to allow G4 formation, then cooled at 1⁰C per minute until 25⁰C. A second set of oligos were snap-cooled after the 95⁰C incubation to prevent G4 formation. Cells were sonicated and centrifuged to remove cellular debris. RNA oligos were incubated with the cellular lysate overnight while rotating at 4⁰C. Pierce streptavidin-agarose beads (ThermoFisher Scientific, CA) were added to the samples for 2 hours to pulldown proteins bound to the RNA oligos. Beads were washed thrice with 1%NP-40 lysis buffer, loaded onto a 9% SDS gel, and then transferred onto a nitrocellulose membrane. The membrane was incubated with anti-NCL antibodies, followed by the secondary antibodies labeled with IR dye. The membrane was scanned using LI-COR Odyssey Imaging System.

3.3.7 *Fractionation and qRT-PCR*

HEK293L cells are transfected with shNCL (Horizon Discovery, United Kingdom) plasmid and incubated with and without 1 μ g/mL [final concentration] doxycycline for 24 hours prior to transfection. Cells are then transfected with G4WT-OVA or G4Dis-OVA and allowed to incubate overnight. 24hr post-transfection, cells were washed with PBS then lysed in 300 μ L Nuclear Extraction Buffer (NEB: 20mM

HEPES pH 7.2, 50mM NaCl, 3mM MgCl₂, 300mM sucrose, and 0.5% NP-40) by incubating for 15min on ice after resuspending the cells. The nuclei were pelleted at 800 x g, 10min, 4⁰C, followed by collecting the cytoplasmic fraction in a separate tube. The nuclei were washed twice with PBS and resuspended in 300μL NEB to sonicate for 10 sec on and 10 sec off twice. The debris was removed by centrifuging at 800 x g, 10 min, 4⁰C. RNA was extracted using Trizol-LS (Life Technologies, CA) and Direct-zol RNA Miniprep Plus (Zymo Research, CA), as per the manufacturer's instructions. cDNA synthesis was performed using a High-Capacity RNA-to-cDNA Kit (Applied Biosystems, Lithuania) and quantified using specific primers with SsoAdvanced Universal SYBR Green Supermix (Biorad, CA) on a Quant Studio 5 (Thermo Scientific, Inc. CA).

3.3.8 Statistical analysis

P values were calculated by a two-tailed t-test using GraphPad Inc. (Prism 8) software for statistical significance. In the figures, asterisks represent P values as follows: *, P value < 0.05; **, P value < 0.01; ***, P value < 0.001; and ****, P value < 0.0001. All experiments were performed at least three times with three biological replicates where applicable.

3.3.9 Figure Generation

Figures were generated using Prism 8, ImageJ, Adobe Illustrator, Adobe Photoshop, SnapGene software (www.snapgene.com), and Biorender.com.

3.4 Results

3.4.1. Nucleolin binds to the G-quadruplex of LANA mRNA

G-quadruplexes are essential regulatory elements that can modulate a variety of biological processes. The expression of Epstein-Barr Virus Nuclear Antigen 1 (EBNA1), a functional homolog of LANA, has been shown to be regulated by G-quadruplexes in its mRNA⁵⁰. In silico mapping of LANA mRNA through QGRS Mapper identified multiple G-quadruplex in the QE domain of LANA (supplementary information), which can be bound by a cellular RNA helicase, hnRNP A1, to modulate the expression of LANA protein²⁹. Crucially, EBNA1 expression was shown to be regulated by Nucleolin, a multifunctional DNA/RNA binding protein that stabilizes the G4 structure through direct binding²⁷. Here, we sought to determine whether NCL plays a role in regulating the expression of LANA through the G-quadruplexes in its mRNA. To this end, we first tested the interaction of NCL with LANA mRNA by performing an RNA-cross-linking immunoprecipitation assay (RNA-CLIP). We used RNA oligonucleotides of a portion of the LANA mRNA with G4 sites as wild-type (WT) oligonucleotide along with an oligonucleotide of the same length with disrupted G4 sites as a control (Dis) oligonucleotide (Fig. 1C). The WT LANA oligonucleotide forms a stable G-quadruplex, but not the control (Dis) oligonucleotide²⁹. Cell lysate from the HEK293L was incubated with biotinylated WT or Dis-LANA-Oligo oligonucleotides for 24 hours, followed by precipitation of the oligonucleotide-bound proteins with Streptavidin Sepharose beads. A set of oligonucleotides were snap-cooled to prevent the formation of G4s and used in the pulldown assay as another control. Samples were subjected to immunoblot to detect any NCL bound to the G-quadruplexes (Fig. 1D). Our data showed that NCL binds to the WT

LANA oligonucleotide more efficiently than the Dis or snap-cooled oligos demonstrated by an efficient pulldown of NCL with G4 forming oligo. This suggested that NCL can interact with the G4s of LANA mRNA. The fainter band of NCL in the Dis oligonucleotide lane could be because NCL is a multifunctional DNA/RNA binding protein, and the Dis-LANA-Oligo oligonucleotide may have some necessary characteristics for its binding to NCL. However, it is essential to emphasize that the WT-LANA-Oligo consistently showed higher affinity to dNCL than the Dis-LANA-Oligo.

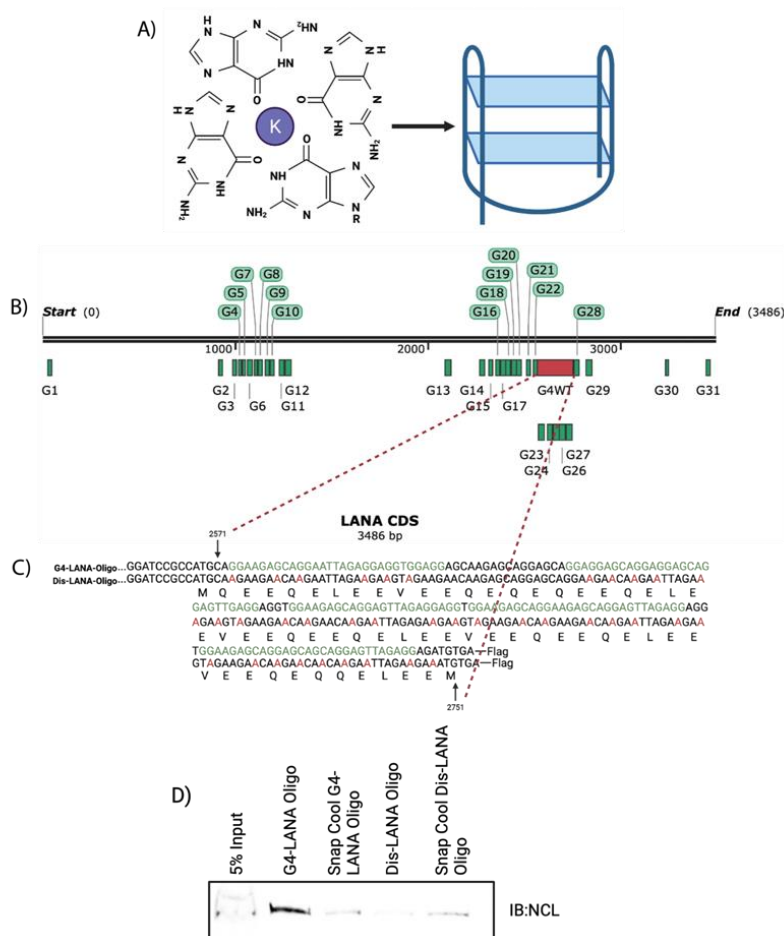


Figure 1. G-quadruplexes in LANA mRNA

A) Four guanines stabilized by non-canonical hydrogen bonding and a potassium ion form a G-tetrad. On

the right, three G-tetrads stacked upon one another, further stabilized by $\pi - \pi$ bonding, forming a G-quadruplex. B) LANA mRNA showing the locations of all the potential non-overlapping G-quadruplexes identified through QGRS Mapper. G4 sites are represented by “G” and then the number indicating the order of the G4s in LANA mRNA. The red region indicates the G4WT region encompassing G4 sites, G23-G27. C) Sequences of G4WT and G4Dis constructs. In the G4WT sequence, potential G4 sites are in green. In the G4Dis sequence, critical Gs have been changed to As to eliminate the G4 formation while maintaining the amino acid sequence. D) Immunoblot blot (IB) showing Nucleolin from affinity pulldown assay with wild-type (WT) LANA oligo. Biotinylated WT-LANA or Dis-LANA oligonucleotides were heated to 95°C and allowed to slowly cool by 1°C per minute until room temperature was reached to enable the formation of G4 or snap cooled on ice post-heating to prevent G4 formation. Oligos were incubated with cellular lysate from HEK293L cells for 24h, then incubated with streptavidin beads to pulldown the RNA-bound proteins. Samples were resolved on an SDS-PAGE and immunoblotted with NCL antibody.

Furthermore, we wanted to see if NCL binds to LANA mRNA in vivo, which we investigated by using our previously designed constructs with a 250-nucleotide long QE region of LANA encompassing the G-quadruplex forming region (G4WT) (Figure 1B and C)²⁹. We used a codon-optimized construct with a disrupted G4 (G4Dis) site as a control while maintaining the amino acid sequence identical to the G4 WT²⁹. The constructs with the ovalbumin epitope (SIINFEKL) downstream of the full-length LANA (FL-LANA-ova), G4WT (G4WT-ova), and G4Dis (G4Dis-ova) were transfected in HEK293L cells, and 24hrs post-transfection, the NCL-bound complexes were immunoprecipitated followed by cross-linking, using an anti-NCL and a control, IgG antibodies. RNA-protein complex was sheared to approximately 300 bp, followed by immunoprecipitation with magnetic protein A/G beads. A fraction (10%) of the immunoprecipitated complex was subjected to SDS-PAGE/immunoblot to confirm the

immunoprecipitation of NCL protein (Fig 2A).

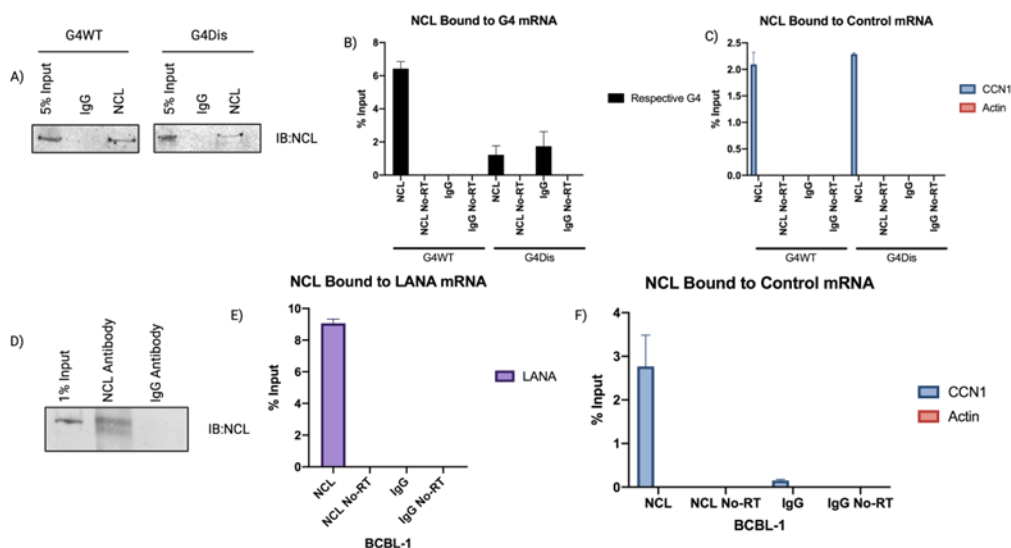
Results indicated that the NCL antibody efficiently pulldown comparable levels of NCL protein from cells transfected with G4WT and G4-Dis constructs, as expected. Control, IgG antibody did not precipitate any detectable levels of NCL from either set, confirming specific precipitation of NCL with anti-NCL antibodies. To determine the levels of NCL-bound RNA, the immunoprecipitated complexes were subjected to RNA extraction and cDNA synthesis for the quantification of G4-WT or G4-Dis mRNA using gene-specific primers. The relative levels of NCL-bound G4WT mRNA were calculated in reference to respective inputs (Fig. 2B). Our data showed a significant binding of G4WT mRNA to NCL, presented as percent input as compared to the G4-Dis mRNA. G4Dis mRNA and IgG control showed significantly lower binding levels, confirming the specific association of NCL with G4-containing mRNA. RNA without Reverse-Transcriptase (No RT) did not show specific amplification confirming the binding of NCL with the mRNA. To substantiate the interaction between NCL and the G4 sequences, we evaluated the levels of Cyclin I (CCNI) mRNA binding to NCL in our assay, given its already documented association of NCL (Fig. 2C)³². We found specific binding of CCNI with NCL precipitated from both, G4WT and G4Dis samples, confirming the specificity of NCL's binding to the G-quadruplexes. Additionally, we checked the binding of a control mRNA, actin, which has not been shown to interact with NCL, showed no binding (Fig. 2C). We further sought to determine whether this interaction occurred in KSHV-infected PEL (primary effusion lymphoma) cells, which we did by utilizing the BCBL-1 cell line. Latently infected BCBL-1 cells were cross-linked and subjected to RNA-CLIP as above. Immunoprecipitation of NCL was

confirmed by anti-NCL immunoblot (Fig. 2D), followed by the extraction of RNA bound to NCL for quantification of LANA mRNA using specific primers. Relative quantitation compared to the input showed a significant binding of LANA mRNA with NCL as compared to the control antibody, IgG (Fig. 2E). RNA with Reverse-Transcriptase (No-RT) did not show any amplification, confirming the specificity. Importantly, we found comparable levels of CCN1 mRNA binding to NCL in KSHV-infected as well as transfected (G4WT and G4Dis) cells. Similarly, a comparable level of NCL binding to G4WT mRNA and LANA mRNA binding was detected in both systems. Similar to the transfection system, actin mRNA did not show any binding in BCBL-1 cells (Fig. 2F). These results confirmed that NCL specifically binds to the G-quadruplex region present in LANA mRNA.

We wanted to demonstrate the importance of G4 sites of full-length LANA mRNA by ablating all the G4 sites, without affecting the amino acid sequence, but failed to generate such construct because of the presence of highly repetitive GC-rich region in LANA, which led to the re-introduction of G4 sites following codon optimization after scrambling G4 sequences.

Figure 2. Nucleolin binds to the G-quadruplexes in LANA mRNA. RNA-CLIP assay confirming the direct interaction between LANA mRNA and NCL. HEK293L cells were transfected with G4WT-ova and G4Dis-ova plasmids and harvested 24h post transfection. Cells were cross-linked, lysed, and incubated with anti-NCL antibodies and magnetic protein A/G beads. RNA bound to the beads was purified and quantified in two steps using a High-Capacity RNA-to-cDNA Kit followed by SsoAdvanced Universal SYBR Green Supermix with G4WT and G4Dis clone-specific primers. A) Immunoblot showing a specific pulldown of NCL with anti-NCL antibody compared to the control antibody, IgG. B) qRT-PCR data

showing relative binding of G4-WT or G4-Dis RNA in the RNA-CLIP assay. C) qRT-PCR data showing relative binding of CCN1 to NCL, used as a positive control and Actin as a negative control. D) RNA-CLIP from KSHV-infected cells, BCBL-1. NCL was specifically immunoprecipitated with anti-NCL antibodies but not control IgG, as expected. E) Relative binding of LANA mRNA bound to NCL compared to the control IgG. F) qRT-PCR data of relative CCN1 and Actin mRNA bound to NCL in BCBL-1 cells. All qPCR rxns were run with “no reverse transcriptase” (No RT) as a control.



3.4.2. Increasing expression of NCL inhibited LANA translation

NCL can bind to the G-quadruplexes to reduce the availability of mRNA for translation; therefore, we sought to determine whether NCL overexpression altered the expression of LANA protein. Using a full-length LANA construct with Luciferase fused downstream in-frame (Fig. 3A), HEK293L cells were cotransfected with increasing amounts of NCL. 24hrs post-transfection, cells were lysed for the quantification of luminescence, which showed a gradual decrease in luminescence with increasing NCL levels (Fig. 3B). Reduction in luminescence, an indirect measure of LANA expressions, was further validated by detecting the LANA protein levels through immunoblotting (Fig.

3C). Band intensities of LANA with increasing levels of NCL were quantified via pixel density of these bands using ImageJ (Fig. 3D). Band intensities of LANA, normalized to respective GAPDH band intensities, showed a dose-dependent reduction in LANA expression, supporting our hypothesis that NCL can reduce LANA translation by restricting the translocation of LANA mRNA.

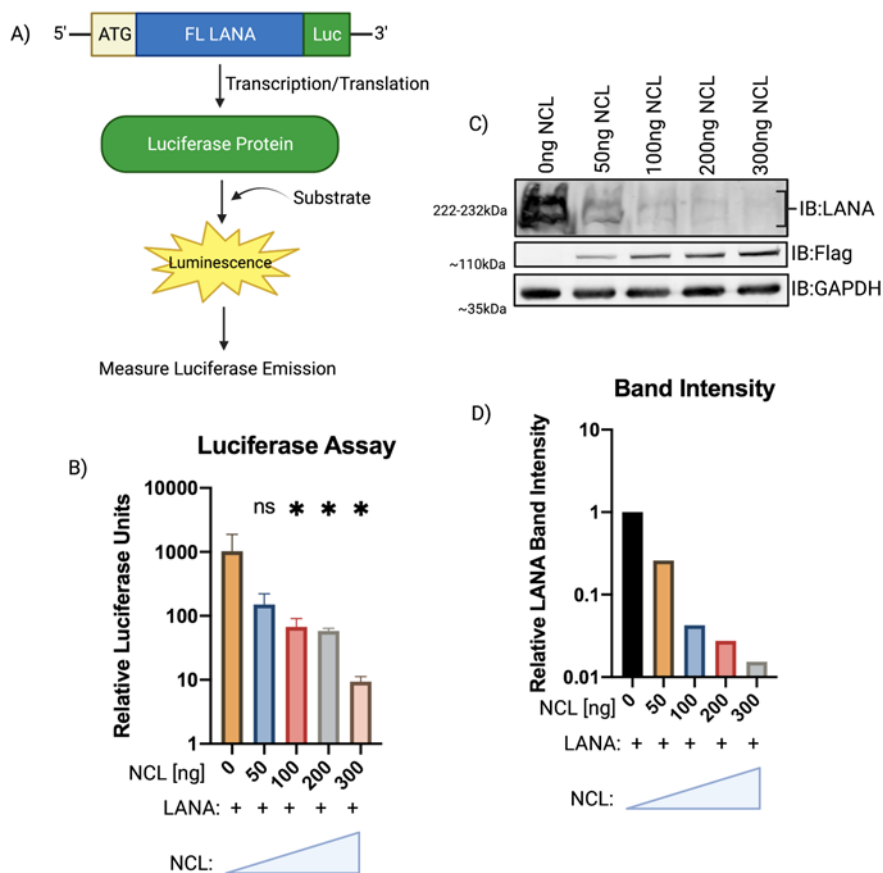


Figure 3. Nucleolin regulates LANA translation. A) A flowchart of luciferase assay along with LANA construct. The coding sequence of LANA was subcloned into a pGL3 vector upstream of the luciferase gene in-frame to produce a LANA-luciferase fusion protein. B) HEK293L cells were transfected with a constant amount of LANA-luciferase and increasing amounts of NCL-expressing plasmid. 24h post-transfection, determination of relative luciferase units showed a decrease in luciferase levels with

increasing amounts of NCL. C) Immunoblot showing an increasing level of NCL (Flag tagged) with constant levels of LANA cotransfected. LANA presents as a “ladder,” detected as two bands. GAPDH immunoblot was used as a control. D) Graphical depiction of LANA band intensities. Levels of LANA were normalized to 0ng NCL sample. The asterisk (*) represents the significance level of the relative band intensity below 0ng NCL sample.

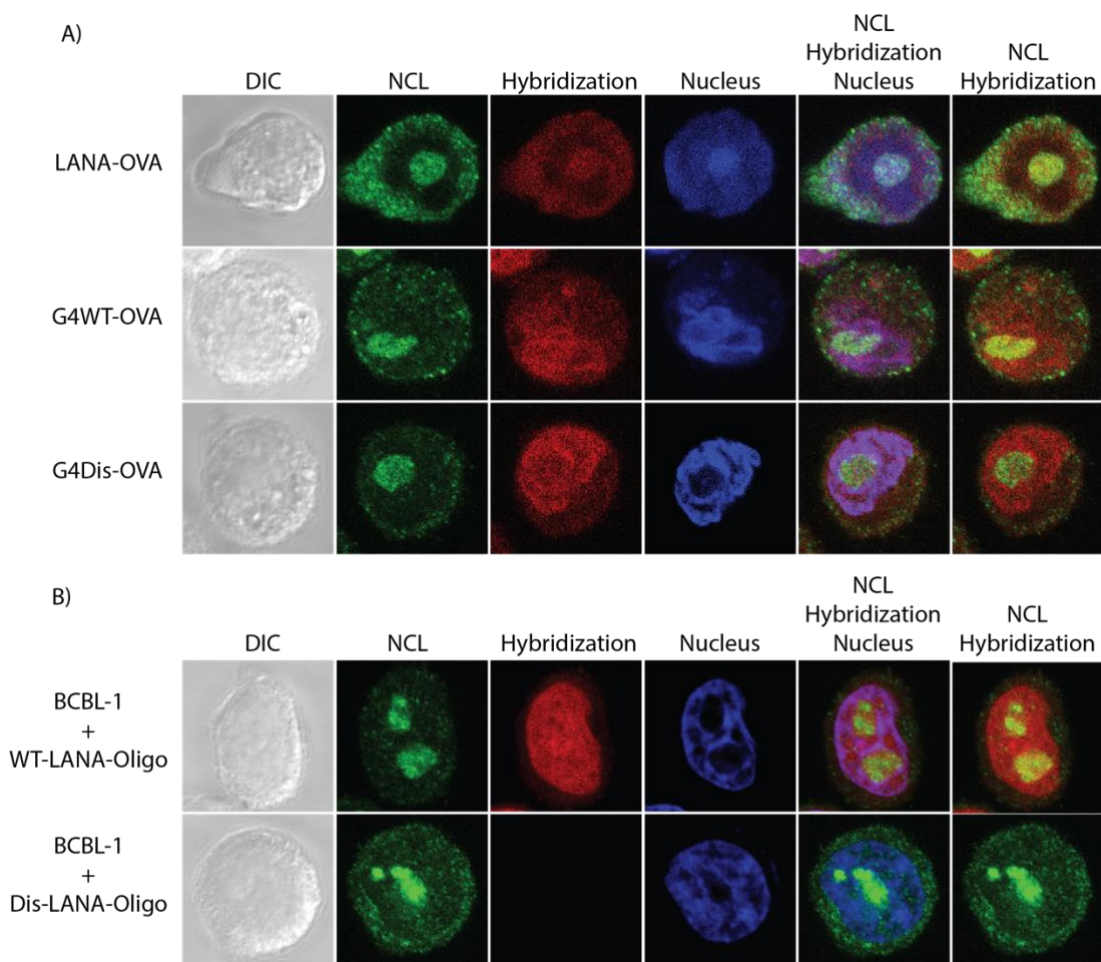
3.4.3 *LANA mRNA colocalizes with NCL*

We further wanted to determine whether LANA expression decreased due to the binding of LANA mRNA with NCL. To address this, we performed RNA fluorescent in situ hybridization (FISH)⁴⁸ of mRNA with G4 sites using constructs with the ovalbumin epitope (SIINFEKL) downstream of the full-length LANA (FL-LANA-ova) and the previously discussed G4WT-ova and G4Dis-ova. These plasmids were transfected in a monolayer of HeLa cells cultured onto coverslips. Cells were fixed with 4% formaldehyde, permeabilized, and incubated with a blocking buffer 24 hours post-transfection. Following, cells were hybridized with biotinylated ovalbumin oligonucleotide sequence overnight. Cells were subsequently incubated with anti-NCL antibodies overnight, followed by detection with Alexa Fluor 488. Biotin-labeled probes were detected by Streptavidin Alexa Fluor 594 and the nuclei with TOPRO-3. We also used latently infected KSHV-positive BCBL-1 cells alongside these samples to determine the colocalization of LANA mRNA with NCL. Our results showed that NCL colocalizes with a subset of LANA mRNA as well as the full-length LANA mRNA (Fig. 4A).

Hybridization signals showing LANA mRNA were seen throughout the cells with defined puncta within the nucleus. The merge panels of NCL and the hybridization signals for mRNA showed a colocalization demonstrated by the yellow signals (Fig. 4,

lane title “NCL” and “Hybridization”). We also calculated the colocalization coefficients using FIJI software in conjunction with the "Just Another Colocalization Plugin" (JACoP). These coefficients ranged from 0 for no colocalization to 1 for complete colocalization^{51,52}. Our results showed FL-LANA-ova to have a score of 0.401, G4WT-ova with 0.455, and G4Dis-ova 0.272. This suggested colocalization of LANA mRNA with NCL in the nucleus. The BCBL-1 cells were subjected to the FISH assay but were hybridized with either WT-LANA or Dis-LANA oligonucleotides cells showed a greater degree of colocalization of 0.78, based on 10 optical fields, with the WT-LANA-Oligo and 0.08 for the Dis- Oligo (Fig. 4B). In the case for FL-LANA and G4WT transfected cells, and BCBL-1 cells, there is a higher colocalization index compared to G4Dis, suggesting the presence LANA mRNA and NCL in the same cellular compartment.

Figure 4. RNA Fluorescent in situ Hybridization. A) HeLa cells were transfected with a plasmid expressing G4WT or FL-LANA. 24h posttransfection, cells were fixed, permeabilized, and incubated with biotinylated ovalbumin oligonucleotide sequence. Cells were further incubated with anti-NCL antibodies to localize NCL using goat anti-rabbit Alexa Four 488 antibody (green). Biotinlated hybridized oligos were detected using Streptavidin Alexa Fluor 594 (red). Nuclei were stained with TOPRO-3 (blue). B) BCBL-1 cells hybridized with G4-specific oligos (WT-LANA-Oligo) or the control (Dis-LANA-Oligo). Images were taken with a Zeiss confocal microscope at 100x magnification. Exposure settings were constant between WT-LANA-Oligo and Dis-LANA-Oligo.



3.4.4. Interaction of LANA mRNA with NCL decreases antigen presentation

LANA can evade the host's immune surveillance system by inhibiting various components of the MHC class I & II antigen presentation pathways. Previously, we showed that LANA regulates its expression by recruiting hnRNP A1 to the G-quadruplex sites for controlled expression of LANA and its presentation on the cell surface. Since NCL could bind to the G-quadruplex in LANA, we aimed to determine the presentation of LANA peptide through antigen presentation assay in the presence of NCL. Previously described ovalbumin constructs were cotransfected with either pA3F-NCL or pA3F-vector into HEK293Kbc2 antigen-presenting cells. 24hrs post-transfection, cells were

incubated with T-cell receptor cells (B3Z) for 18hrs and then incubated with an ONPG substrate for 4hrs. The β -galactosidase activity was then quantified by measuring the optical density (OD) at 450 nm (Fig. 5A). Our data showed that expression of NCL decreased antigen presentation of FL-LANA-ova and G4WT-ova transfected cells compared to cells with endogenous levels of NCL (Fig. 5B). Cells transfected with the disrupted G-quadruplexes (G4Dis-ova) did not show any alteration in the levels of antigen presentation. A metabolic assay of the cells transfected with the above construct was performed to ensure that there weren't any adverse effects of these proteins in the cell's metabolism, which may have affected the assay. Our assay (MTT) data showed no statistically significant differences among these samples (Fig. 5C). This confirmed that NCL plays a regulatory role in antigen presentation for KSHV's LANA.

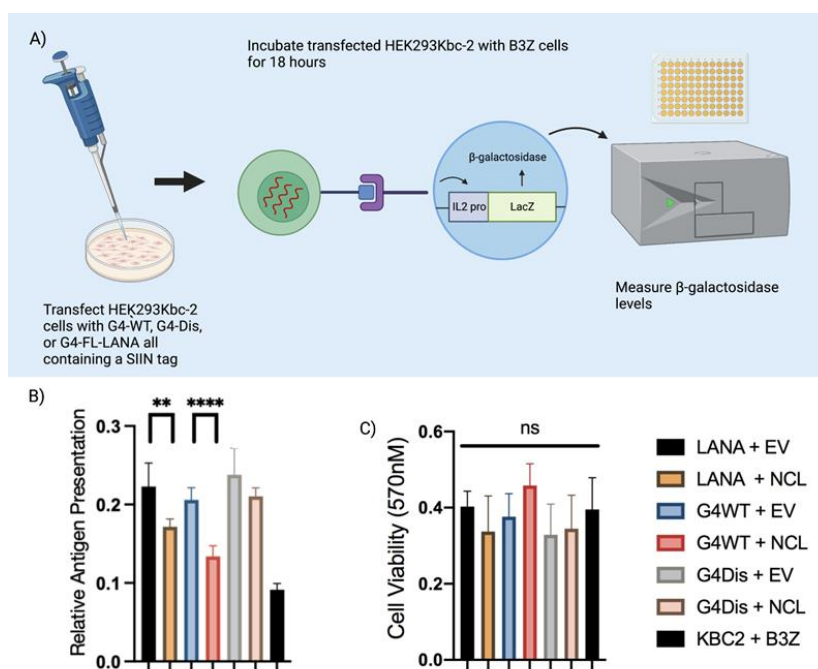


Figure 5. Nucleolin stabilizing G-quadruplex in LANA mRNA decreases antigen presentation. A) A

schematic of the antigen presentation assay. Transfected antigen-presenting HEK293Kbc2 cells with a construct encoding sequence-specific ovalbumin epitope, SIINFEKL, with effector T cell hybridoma B3Z cells capable of recognizing the ovalbumin epitope. This interaction results in β -galactosidase activity, which is measured to determine the T cell activation quantitatively. B) T-cell activation from cells transiently expressing FL-LANA, G4WT, and G4Dis. HEK293Kbc2 cells were transfected with pA3F-FL-LANA-ova, pA3F-G4WT-ova, and pA3F-G4Dis-ova (all ovalbumin tagged). 24h posttransfection, cells were incubated with B3Z cells for 18h, then ONPG was added to the cells, followed by measuring β -galactosidase activity at 450nm. C) MTT assay to measure the metabolic activity of these cells.

3.4.5. Downregulation of Nucleolin resulted in an altered LANA mRNA localization and increased LANA expression

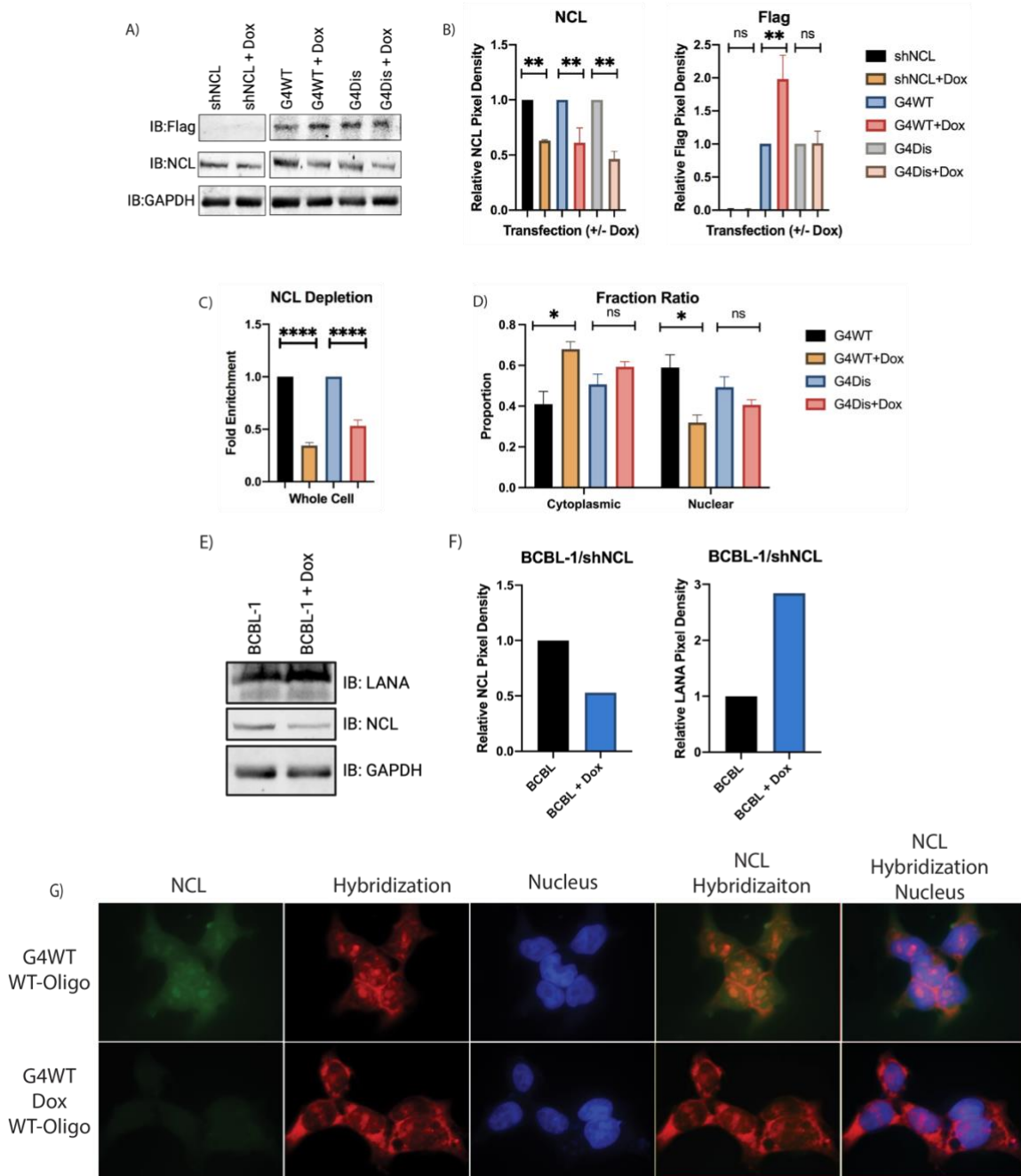
RNA interference (RNAi) is a post-transcriptional mechanism for regulating gene expression and has been extensively used for altering protein levels through the introduction of short hairpin RNA (shRNA)⁵³⁻⁵⁵. shRNA are RNA molecules with a hairpin, which are cleaved to generate siRNA for downregulating protein expression⁵⁶. Since increasing NCL resulted in a reduced LANA translation, we sought to determine the effects of NCL downregulation on LANA expression through transfection of HEK293L cells with short hairpin NCL (shNCL) plasmid. Treatment with 1 μ g/mL of Dox to induce shRNA expression, we saw an increase in G4WT protein levels (Fig. 6A). Contrastingly, G4Dis treated and untreated cells showed no significant difference in protein levels. Reduction in NCL levels was confirmed through immunoblot. Using ImageJ to quantify the pixel density, we see approximately a 50% reduction in NCL protein for all treated samples (Fig. 6B). Looking at the relative pixel densities and normalizing to their respective GAPDHs, G4WT-shNCL treated with Dox results in

approximately 2-fold increase. In the G4Dis groups, there is no statistical difference between the treated and untreated.

NCL is predominantly found in the nucleolus, and by utilizing the shRNA, we looked at any difference in the distribution of mRNA containing G4 sites. HEK293L cells cotransfected with shNCL and the pA3F-G4WT/Dis clones, we fractionated the nuclear and cytoplasmic fractions, followed by the extraction of RNA from the respective fractions. Firstly, we confirmed that there was an expected downregulation of NCL through quantitative PCR (Fig. 6C). The levels of G4WT and G4Dis mRNA were determined using sequence-specific primers (Fig. 6D). In Dox-treated G4WT transfected cells, there was a greater proportion of mRNA exported to the cytoplasm and reduced nuclear retention compared to non-Dox treated cells. There wasn't any statistically significant difference in G4Dis mRNA localization between Dox-treated and untreated cells. An increase in G4WT mRNA export to the cytoplasm under reduced NCL conditions may allow higher protein translation. Additionally, the altered localization of G4WT mRNA was confirmed through fluorescent in situ hybridization (Fig 6G). The hybridization signal in the Dox-treated group was lower in the nucleolus. As expected, the nucleolus showed the highest levels of NCL, and interestingly, it appears that when NCL was downregulated, the hybridization signal increased in the cytoplasm. This may mean that when NCL was reduced, LANA G4 mRNA was exported into the cytoplasm. This corroborated the qPCR data presented in Fig. 6D.

Using latently infected KSHV-positive BCBL-1 cells, we aimed to determine the effect of NCL on LANA levels in vitro. Transfecting shNCL in BCBL-1 cells and treating with Dox resulted in increased LANA levels (Fig. 6E). Calculating the relative LANA

pixel density, in the Dox-treated BCBL-1 cells, there is approximately a 2-fold increase in LANA protein levels (Fig. 6F). This indicates that NCL plays a regulatory role in the



expression of G4 sites containing LANAmRNA.

Figure 6. Nucleolin depletion enhanced the expression of LANA mRNA containing G-quadruplexes.

A) Immunoblot showing the levels of NCL (IB: NCL) and LANA regions (IB: Flag) in doxycycline and untreated cells transfected with G4 WT or G4 Dis plasmids. Untransfected cells were used as control. GAPDH was used as the loading control. B) Graphical representation of the pixel density of the western blot in panel “A.” C) NCL mRNA levels in shNCL transfected cells treated with and without doxycycline (Dox). Samples normalized to GAPDH. D) The ratio of G4WT/G4Dis mRNA copies in the cytoplasmic and nuclear fraction in cells with depleted NCL. The ratio of G4WT mRNA in the cytoplasm of NCL-depleted (Dox) cells was increased compared to those without Dox. Samples were normalized to GAPDH. A proportionate reduction of G4WT mRNA in the nuclear fraction was seen in NCL-depleted cells. The distribution of G4Dis mRNA in the cytoplasmic and nuclear fractions was largely unaffected. E) Immunoblot showing LANA (IB: LANA) levels in BCBL-1 transfected with shNCL and treated with and without doxycycline. F) The left graph shows the relative pixel density of NCL normalized to their respective GAPDHs and then to untreated BCBL-1 cells. The graph on the right shows the relative pixel density of NCL normalized to their respective GAPDHs and then to the untreated BCBL-1 cells. G) Localization of NCL and G4WT mRNA through FISH. shNCL-HEK293L cells cotransfected with shNCL and G4WT plasmid; then treated with and without Dox were fixed, permeabilized, and incubated with biotinylated WT-LANA oligonucleotides. These cells were further incubated with anti-NCL antibodies followed by Alexa Fluor secondary antibodies 488nm (goat anti-rabbit) and Alexa Fluor 594 (streptavidin). Images were taken with a fluorescent microscope at 100x magnification. The green color represents the localization of NCL, red for oligonucleotide hybridizing with LANA plasmids, and blue for the nucleus.

3.5 Discussion

KSHV establishes a life-long latent infection and can avoid detection from the host's immune system. During the latent phase, KSHV limits its gene expression with abundant expression of LANA, which is essential for viral replication, distribution of viral genome to daughter cells, and avoiding the host's immune detection⁵⁷. LANA autoregulates its expression by regulating its promoter and inhibiting peptide synthesis

and proteasomal degradation through two central region domains (CR2 and CR3)^{10,58-61}. Here, we build on our previous findings and explore how Nucleolin regulates the expression of LANA. We previously identified regions in LANA mRNA that form G-quadruplexes. Additionally, we showed that hnRNP A1 acts as a helicase, disrupting the G4 secondary structure and resulting in an upregulation of LANA translation and antigen presentation²⁹.

G-quadruplexes have gained popularity as potential therapeutic targets for regulating viral genome replication and transcription^{40,62,63}. G4s act as immunomodulatory structures in gamma herpesviruses. For example, in EBV and KSHV, G4s alter protein synthesis and antigen presentation and thus affect host immune detection^{29,61}. Due to the homology of EBV's EBNA1 being downregulated by NCL, we sought to see if KSHV's LANA expression is regulated by NCL. Utilizing RNA oligonucleotides containing LANA's mRNA region that forms a G4 structure, we showed that NCL interacts with LANA mRNA. To determine if this interaction occurred in cells, we transfected pA3F-G4WT and pA3F-G4Dis plasmids in HEK293L cells and performed RNA-CLIP to quantify the amounts of these mRNAs bound to NCL. Our data showed a specific association of LANA's guanine-rich mRNA capable of forming a G-quadruplex to NCL. Basal but detectable binding of G4Dis mRNA with NCL could be due to some secondary structure in G4Dis mRNA that facilitated the interaction. Additionally, LANA mRNA in KSHV-infected cells, BCBL-1, showed a selective binding to NCL. Our LANA-Luciferase fusion protein confirmed that the NCL-LANA mRNA interaction decreases LANA translation. This is likely due to the ability of NCL to bind to the G-quadruplex in the mRNA and restrict them from being available for translation. Detection

of protein levels through immunoblot confirmed a reduction in translation. Importantly, the localization of G4-containing mRNA through FISH confirmed that this interaction occurs within the nucleus. These results support that NCL binding to a G4 in LANA mRNA resulting in translational regulation through sequestration of mRNA in the nucleus.

LANA has been shown to regulate antigen presentation^{10,13}. We previously found that stabilization/destabilization of the G-quadruplex in LANA regulates protein synthesis and antigen presentation. The nuclear LANA protein binds to the G-quadruplex in its mRNA, inhibiting the export of those bound mRNA molecules to the cytoplasm. This, in turn, reduces LANA protein translation, which is regulated by the levels of LANA in the cells. In cells with lower levels of LANA, hnRNP A1 binds to LANA mRNA, acts as a helicase, and disrupts the G-quadruplex within the mRNA. This leads to an export of LANA mRNA into the cytoplasm for its translation to maintain the viral genome. Cells having a threshold level of LANA in the nucleus, required for viral persistence, a relatively higher level of LANA than hnRNP A1 may become available to bind and retain the LANA mRNA in the nucleus²⁹. This inhibits mRNA export into the cytoplasm, allowing the cycle to continue when LANA protein levels drop in the nucleus. In this paper, we showed that NCL can bind to LANA mRNA and localize in the nucleus, with a subset of NCL colocalizing with LANA mRNA. We further tested whether this interaction reduced antigen presentation of these peptides to the cell surface in the presence of NCL. For this, cells expressing G4WT-ova or G4Dis-ova in the presence of NCL were utilized. Reduction in the presentation of G4WT-ova but not G4Dis-ova in the presence of NCL confirmed the role of NCL in regulating expression. These results

confirmed that stabilization of G-quadruplex in LANA mRNA can reduce expression and antigen presentation similar to what we reported previously²⁹. Reduction in the expression of LANA is due to its mRNA being sequestered by NCL and reducing in LANA mRNA exported to the cytoplasm (Fig. 7). Nucleolin is abundantly expressed in cells and is involved in rRNA maturation³². NCL binds to guanine-rich regions in coding and non-coding regions of various mRNAs⁶⁴. Additionally, NCL binds to G-quadruplexes in both RNA and DNA, such as at the G4 in the LTR of HIV-1, to silence transcription³³. Additionally, NCL binds to a G4 in the promoter of c-MYC, affecting its transcription^{34,65}. As NCL has a myriad of roles in the cell, we studied the function of NCL in LANA expression by depleting its level by way of shRNA, which showed a reduction in the sequestration of LANA mRNA in the nucleus. This led to an increase in the expression levels of LANA. Sequestration of mRNA was determined by the fraction of cytoplasmic/nuclear fraction, and the FISH assay confirmed that NCL can regulate LANA mRNA translocation and expression.

The specificity of NCL and LANA interactions within the nucleus may be attributed to the presence of nucleolar organizing regions (NORs), where NCL is notably abundant and actively participates in ribosomal biogenesis^{66,67}. NCL, recognized for its RNA affinity and its significant role in organizing chromatin structure, could facilitate the localization of LANA RNA to these NORs, thereby promoting their interaction. Furthermore, the nucleolus is integral to the interplay between KSHV and the host cell's ribosomal biogenesis, a crucial aspect of the virus's strategy to manipulate host cellular machinery for its replication. In the nucleolus, the synthesis and initial assembly of ribosomal RNA (rRNA) and ribosomal proteins into ribosomal subunits take place.

KSHV actively modifies this ribosomal assembly process in the nucleolus, leveraging it to support its replication needs^{68,69}. During the lytic replication phase of KSHV, there is a significant alteration in the normal process of ribosome biogenesis within the nucleolus. During its lytic phase, KSHV disrupts normal ribosome biogenesis in the nucleolus. This leads to the creation of specialized ribosomes, uniquely modified for efficient translation of viral mRNAs, especially those crucial for the virus's late lytic cycle. This modification is hypothesized to result from KSHV-induced methylation patterns, tailoring ribosomes for viral protein synthesis. Thus, KSHV manipulates nucleolar activity, particularly rRNA modification, to produce ribosomes optimized for its replication, highlighting its sophisticated strategy to control host translation machinery⁶⁸.

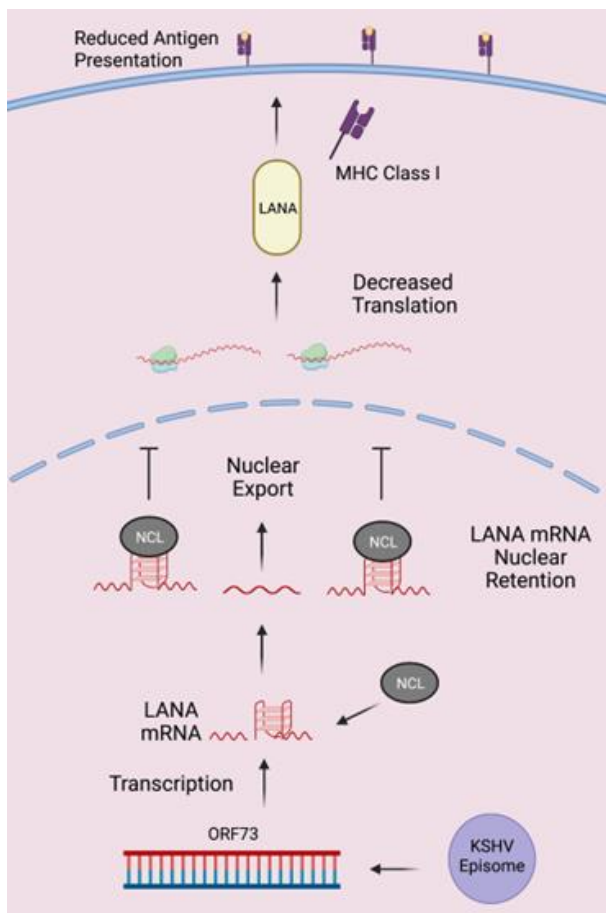
During KSHV infection, angiogenin is produced as a result and translocates to the nucleolus of the cell. It then attaches to the regulatory region of the 45S rDNA. The attachment increases the production of rRNA and enhances the survival of the infected endothelial cell⁷⁰. LANA and angiogenin have been found to form a complex with the p53 protein in the nucleus. It is suspected that angiogenin and LANA hold p53 in the nucleus in a deactivated state^{71,72}. Therefore, angiogenin could play a role in preserving the survival of cells infected with KSHV and in maintaining the virus in a dormant or latent state, potentially by influencing pathways that involve p53. Therefore, it is expected that a subset of KSHV's LANA would colocalize with NCL in the nucleolus.

G-quadruplexes have become increasingly popular as therapeutic agents^{40,62,63}. Regulating LANA expression through G-quadruplexes may offer a therapeutic target to control KSHV latency and remove latent virus from the infected cells. Our findings shed light on the intricate cellular functions NCL plays in regulating LANA mRNA. As

mentioned, previously, we showed that hnRNP A1 acts as a helicase and unwinds a G4 structure in LANA mRNA²⁹. Our study opens up the possibility to study the potential interplay between NCL and hnRNP A1. Given the established functions of hnRNP A1 in mRNA metabolism and the novel insights provided by our findings, it is tempting to speculate on the existence of a regulatory axis involving NCL and hnRNP A1 that could impact the life cycle of KSHV. For example, NCL may influence the expression of hnRNP A1 through various post-transcriptional mechanisms or by affecting its protein stability. Alternatively, NCL could modulate the binding affinity of hnRNP A1 for LANA, thereby influencing the viral latency and reactivation process. Such interactions may not only be limited to the direct control of gene expression but could also encompass the broader epigenetic landscape, thus impacting viral replication and cell fate. This could offer insights into how viruses harness host cell machinery for their replication and survival, as well as reveal novel targets for antiviral therapy. The exploration of this regulatory interplay is, therefore, not only of basic scientific interest but also of potential therapeutic relevance. Further studies, employing a combination of biochemical, molecular, and systems biology approaches, are warranted to dissect the layers of this complex interaction network. Through such multidimensional studies, we can hope to illuminate the full scope of NCL's and hnRNP A1's roles in viral latency and reactivation, thereby enhancing our understanding of viral pathogenesis and informing the development of novel therapeutic strategies.

Figure 7. Proposed model of the regulation of LANA expression through NCL. NCL binds to the G-quadruplex of LANA mRNA, resulting in reduced levels of nuclear export of LANA mRNA into the

cytoplasm. A lower transcript level for translation results in a reduced expression and, subsequently, lower antigen presentation on the cell surface.



3.8 References

1. Chang Y, Cesarman E, Pessin MS, et al. Identification of herpesvirus-like DNA sequences in AIDS-associated Kaposi's sarcoma. *Science*. Dec 16 1994;266(5192):1865-9. doi:10.1126/science.7997879
2. Cesarman E, Chang Y, Moore PS, Said JW, Knowles DM. Kaposi's sarcoma-associated herpesvirus-like DNA sequences in AIDS-related body-cavity-based lymphomas. *N Engl J Med*. May 4 1995;332(18):1186-91. doi:10.1056/NEJM199505043321802
3. Soulier J, Grollet L, Oksenhendler E, et al. Kaposi's sarcoma-associated herpesvirus-like DNA sequences in multicentric Castleman's disease. *Blood*. Aug 15 1995;86(4):1276-80.
4. Nador RG, Cesarman E, Chadburn A, et al. Primary effusion lymphoma: a distinct clinicopathologic entity associated with the Kaposi's sarcoma-associated herpes virus. *Blood*. Jul 15 1996;88(2):645-56.

5. Renne R, Zhong W, Herndier B, et al. Lytic growth of Kaposi's sarcoma-associated herpesvirus (human herpesvirus 8) in culture. *Nat Med.* Mar 1996;2(3):342-6. doi:10.1038/nm0396-342
6. Decker LL, Shankar P, Khan G, et al. The Kaposi sarcoma-associated herpesvirus (KSHV) is present as an intact latent genome in KS tissue but replicates in the peripheral blood mononuclear cells of KS patients. *J Exp Med.* Jul 1 1996;184(1):283-8. doi:10.1084/jem.184.1.283
7. Ballestas ME, Kaye KM. The latency-associated nuclear antigen, a multifunctional protein central to Kaposi's sarcoma-associated herpesvirus latency. *Future Microbiol.* Dec 2011;6(12):1399-413. doi:10.2217/fmb.11.137
8. Kedes DH, Lagunoff M, Renne R, Ganem D. Identification of the gene encoding the major latency-associated nuclear antigen of the Kaposi's sarcoma-associated herpesvirus. *J Clin Invest.* Nov 15 1997;100(10):2606-10. doi:10.1172/JCI119804
9. Rezaee SAR, Cunningham C, Davison AJ, Blackbourn DJ. Kaposi's sarcoma-associated herpesvirus immune modulation: an overview. *J Gen Virol.* Jul 2006;87(Pt 7):1781-1804. doi:10.1099/vir.0.81919-0
10. Kwun HJ, da Silva SR, Qin H, et al. The central repeat domain 1 of Kaposi's sarcoma-associated herpesvirus (KSHV) latency associated-nuclear antigen 1 (LANA1) prevents cis MHC class I peptide presentation. *Virology.* Apr 10 2011;412(2):357-65. doi:10.1016/j.virol.2011.01.026
11. Zaldumbide A, Ossevoort M, Wiertz EJ, Hoeben RC. In cis inhibition of antigen processing by the latency-associated nuclear antigen I of Kaposi sarcoma herpes virus. *Mol Immunol.* Feb 2007;44(6):1352-60. doi:10.1016/j.molimm.2006.05.012
12. Sorel O, Chen T, Myster F, Javaux J, Vanderplasschen A, Dewals BG. Macavirus latency-associated protein evades immune detection through regulation of protein synthesis in cis depending upon its glycin/glutamate-rich domain. *PLoS Pathog.* Oct 2017;13(10):e1006691. doi:10.1371/journal.ppat.1006691
13. Thakker S, Purushothaman P, Gupta N, Challa S, Cai Q, Verma SC. Kaposi's Sarcoma-Associated Herpesvirus Latency-Associated Nuclear Antigen Inhibits Major Histocompatibility Complex Class II Expression by Disrupting Enhanceosome Assembly through Binding with the Regulatory Factor X Complex. *J Virol.* May 2015;89(10):5536-56. doi:10.1128/JVI.03713-14
14. Bochman ML, Paeschke K, Zakian VA. DNA secondary structures: stability and function of G-quadruplex structures. *Nat Rev Genet.* Nov 2012;13(11):770-80. doi:10.1038/nrg3296
15. Bhattacharyya D, Mirihana Arachchilage G, Basu S. Metal Cations in G-Quadruplex Folding and Stability. *Front Chem.* 2016;4:38. doi:10.3389/fchem.2016.00038
16. Dhakal S, Cui Y, Koirala D, et al. Structural and mechanical properties of individual human telomeric G-quadruplexes in molecularly crowded solutions. *Nucleic Acids Res.* Apr 1 2013;41(6):3915-23. doi:10.1093/nar/gkt038
17. Biffi G, Tannahill D, McCafferty J, Balasubramanian S. Quantitative visualization of DNA G-quadruplex structures in human cells. *Nat Chem.* Mar 2013;5(3):182-6. doi:10.1038/nchem.1548

18. Chambers VS, Marsico G, Boutell JM, Di Antonio M, Smith GP, Balasubramanian S. High-throughput sequencing of DNA G-quadruplex structures in the human genome. *Nat Biotechnol.* Aug 2015;33(8):877-81. doi:10.1038/nbt.3295
19. Pandey S, Agarwala P, Maiti S. Effect of loops and G-quartets on the stability of RNA G-quadruplexes. *J Phys Chem B.* Jun 13 2013;117(23):6896-905. doi:10.1021/jp401739m
20. Millevoi S, Moine H, Vagner S. G-quadruplexes in RNA biology. *Wiley Interdiscip Rev RNA.* Jul-Aug 2012;3(4):495-507. doi:10.1002/wrna.1113
21. Rhodes D, Lipps HJ. G-quadruplexes and their regulatory roles in biology. *Nucleic Acids Res.* Oct 15 2015;43(18):8627-37. doi:10.1093/nar/gkv862
22. Huppert JL, Bugaut A, Kumari S, Balasubramanian S. G-quadruplexes: the beginning and end of UTRs. *Nucleic Acids Res.* Nov 2008;36(19):6260-8. doi:10.1093/nar/gkn511
23. Song J, Perreault JP, Topisirovic I, Richard S. RNA G-quadruplexes and their potential regulatory roles in translation. *Translation (Austin).* 2016;4(2):e1244031. doi:10.1080/21690731.2016.1244031
24. Biswas B, Kandpal M, Jauhari UK, Vivekanandan P. Genome-wide analysis of G-quadruplexes in herpesvirus genomes. *BMC Genomics.* Nov 21 2016;17(1):949. doi:10.1186/s12864-016-3282-1
25. Perrone R, Nadai M, Frasson I, et al. A dynamic G-quadruplex region regulates the HIV-1 long terminal repeat promoter. *J Med Chem.* Aug 22 2013;56(16):6521-30. doi:10.1021/jm400914r
26. Artusi S, Nadai M, Perrone R, et al. The Herpes Simplex Virus-1 genome contains multiple clusters of repeated G-quadruplex: Implications for the antiviral activity of a G-quadruplex ligand. *Antiviral Res.* Jun 2015;118:123-31. doi:10.1016/j.antiviral.2015.03.016
27. Lista MJ, Martins RP, Billant O, et al. Nucleolin directly mediates Epstein-Barr virus immune evasion through binding to G-quadruplexes of EBNA1 mRNA. *Nat Commun.* Jul 7 2017;8:16043. doi:10.1038/ncomms16043
28. Madireddy A, Purushothaman P, Loosbroock CP, Robertson ES, Schildkraut CL, Verma SC. G-quadruplex-interacting compounds alter latent DNA replication and episomal persistence of KSHV. *Nucleic Acids Res.* May 5 2016;44(8):3675-94. doi:10.1093/nar/gkw038
29. Dabral P, Babu J, Zareie A, Verma SC. LANA and hnRNP A1 Regulate the Translation of LANA mRNA through G-Quadruplexes. *J Virol.* Jan 17 2020;94(3)doi:10.1128/jvi.01508-19
30. Blake N. Immune evasion by gammaherpesvirus genome maintenance proteins. *J Gen Virol.* Apr 2010;91(Pt 4):829-46. doi:10.1099/vir.0.018242-0
31. Daskalogianni C, Pyndiah S, Apcher S, et al. Epstein-Barr virus-encoded EBNA1 and ZEBRA: targets for therapeutic strategies against EBV-carrying cancers. *J Pathol.* Jan 2015;235(2):334-41. doi:10.1002/path.4431
32. Abdelmohsen K, Gorospe M. RNA-binding protein nucleolin in disease. *RNA Biol.* Jun 2012;9(6):799-808. doi:10.4161/rna.19718

33. Tosoni E, Frasson I, Scalabrin M, et al. Nucleolin stabilizes G-quadruplex structures folded by the LTR promoter and silences HIV-1 viral transcription. *Nucleic Acids Res.* Oct 15 2015;43(18):8884-97. doi:10.1093/nar/gkv897
34. Gonzalez V, Guo K, Hurley L, Sun D. Identification and characterization of nucleolin as a c-myc G-quadruplex-binding protein. *J Biol Chem.* Aug 28 2009;284(35):23622-35. doi:10.1074/jbc.M109.018028
35. Puig Lombardi E, Londono-Vallejo A. A guide to computational methods for G-quadruplex prediction. *Nucleic Acids Res.* Jan 10 2020;48(1):1-15. doi:10.1093/nar/gkz1097
36. Kharel P, Balaratnam S, Beals N, Basu S. The role of RNA G-quadruplexes in human diseases and therapeutic strategies. *Wiley Interdiscip Rev RNA.* Jan 2020;11(1):e1568. doi:10.1002/wrna.1568
37. Novoseltseva AA, Ivanov NM, Novikov RA, et al. Structural and Functional Aspects of G-Quadruplex Aptamers Which Bind a Broad Range of Influenza A Viruses. *Biomolecules.* Jan 10 2020;10(1):119. doi:10.3390/biom10010119
38. Panera N, Tozzi AE, Alisi A. The G-Quadruplex/Helicase World as a Potential Antiviral Approach Against COVID-19. *Drugs.* Jul 2020;80(10):941-946. doi:10.1007/s40265-020-01321-z
39. Parveen N, Shamim A, Cho S, Kim KK. Computational Approaches to Predict the Non-canonical DNAs. *Current Bioinformatics.* 2019;14(6):470-479. doi:10.2174/1574893614666190126143438
40. Ruggiero E, Richter SN. G-quadruplexes and G-quadruplex ligands: targets and tools in antiviral therapy. *Nucleic Acids Res.* Apr 20 2018;46(7):3270-3283. doi:10.1093/nar/gky187
41. Fay MM, Lyons SM, Ivanov P. RNA G-Quadruplexes in Biology: Principles and Molecular Mechanisms. *Journal of molecular biology.* Jul 7 2017;429(14):2127-2147. doi:10.1016/j.jmb.2017.05.017
42. Maizels N. G4-associated human diseases. *EMBO Rep.* Aug 2015;16(8):910-22. doi:10.15252/embr.201540607
43. Ou TM, Lu YJ, Tan JH, Huang ZS, Wong KY, Gu LQ. G-quadruplexes: targets in anticancer drug design. *ChemMedChem.* May 2008;3(5):690-713. doi:10.1002/cmde.200700300
44. White EW, Tanious F, Ismail MA, et al. Structure-specific recognition of quadruplex DNA by organic cations: influence of shape, substituents and charge. *Biophys Chem.* Mar 2007;126(1-3):140-53. doi:10.1016/j.bpc.2006.06.006
45. Kikin O, D'Antonio L, Bagga PS. QGRS Mapper: a web-based server for predicting G-quadruplexes in nucleotide sequences. *Nucleic Acids Res.* Jul 1 2006;34(Web Server issue):W676-82. doi:10.1093/nar/gkl253
46. Verma SC, Cai Q, Kreider E, Lu J, Robertson ES. Comprehensive analysis of LANA interacting proteins essential for viral genome tethering and persistence. *PLoS One.* 2013;8(9):e74662. doi:10.1371/journal.pone.0074662
47. Purushothaman P, McDowell ME, McGuinness J, Salas R, Rumjahn SM, Verma SC. Kaposi's sarcoma-associated herpesvirus-encoded LANA recruits topoisomerase IIbeta for latent DNA replication of the terminal repeats. *J Virol.* Sep 2012;86(18):9983-94. doi:10.1128/JVI.00839-12

48. Kochan J, Wawro M, Kasza A. Simultaneous detection of mRNA and protein in single cells using immunofluorescence-combined single-molecule RNA FISH. *Biotechniques*. Oct 2015;59(4):209-12, 214, 216 passim. doi:10.2144/000114340
49. Rossetto CC, Pari G. KSHV PAN RNA associates with demethylases UTX and JMJD3 to activate lytic replication through a physical interaction with the virus genome. *PLoS Pathog*. 2012;8(5):e1002680. doi:10.1371/journal.ppat.1002680
50. Murat P, Zhong J, Lekieffre L, et al. G-quadruplexes regulate Epstein-Barr virus-encoded nuclear antigen 1 mRNA translation. *Nat Chem Biol*. May 2014;10(5):358-64. doi:10.1038/nchembio.1479
51. Bolte S, Cordelieres FP. A guided tour into subcellular colocalization analysis in light microscopy. *J Microsc*. Dec 2006;224(Pt 3):213-32. doi:10.1111/j.1365-2818.2006.01706.x
52. Dunn KW, Kamocka MM, McDonald JH. A practical guide to evaluating colocalization in biological microscopy. *Am J Physiol Cell Physiol*. Apr 2011;300(4):C723-42. doi:10.1152/ajpcell.00462.2010
53. Carthew RW, Sontheimer EJ. Origins and Mechanisms of miRNAs and siRNAs. *Cell*. Feb 20 2009;136(4):642-55. doi:10.1016/j.cell.2009.01.035
54. Bobbin ML, Rossi JJ. RNA Interference (RNAi)-Based Therapeutics: Delivering on the Promise? *Annu Rev Pharmacol Toxicol*. 2016;56:103-22. doi:10.1146/annurev-pharmtox-010715-103633
55. Lama L, Seidl CI, Ryan K. New insights into the promoterless transcription of DNA coligo templates by RNA polymerase III. *Transcription*. 2014;5(2):e27913. doi:10.4161/trns.27913
56. Paddison PJ, Caudy AA, Bernstein E, Hannon GJ, Conklin DS. Short hairpin RNAs (shRNAs) induce sequence-specific silencing in mammalian cells. *Genes Dev*. Apr 15 2002;16(8):948-58. doi:10.1101/gad.981002
57. Purushothaman P, Dabral P, Gupta N, Sarkar R, Verma SC. KSHV Genome Replication and Maintenance. *Front Microbiol*. 2016;7:54. doi:10.3389/fmicb.2016.00054
58. De Leo A, Deng Z, Vladimirova O, et al. LANA oligomeric architecture is essential for KSHV nuclear body formation and viral genome maintenance during latency. *PLOS Pathogens*. 2019;15(1):e1007489. doi:10.1371/journal.ppat.1007489
59. Renne R, Barry C, Dittmer D, Compitello N, Brown Patrick O, Ganem D. Modulation of Cellular and Viral Gene Expression by the Latency-Associated Nuclear Antigen of Kaposi's Sarcoma-Associated Herpesvirus. *Journal of Virology*. 2001/01/01 2001;75(1):458-468. doi:10.1128/JVI.75.1.458-468.2001
60. Jeong JH, Orvis J, Kim JW, McMurtrey CP, Renne R, Dittmer DP. Regulation and autoregulation of the promoter for the latency-associated nuclear antigen of Kaposi's sarcoma-associated herpesvirus. *J Biol Chem*. Apr 16 2004;279(16):16822-31. doi:10.1074/jbc.M312801200
61. Kwun Hyun J, da Silva Suzane R, Shah Ishita M, Blake N, Moore Patrick S, Chang Y. Kaposi's Sarcoma-Associated Herpesvirus Latency-Associated Nuclear Antigen 1 Mimics Epstein-Barr Virus EBNA1 Immune Evasion through Central Repeat Domain Effects on Protein Processing. *Journal of Virology*. 2007/08/01 2007;81(15):8225-8235. doi:10.1128/JVI.00411-07

62. Kwun HJ, da Silva SR, Qin H, et al. The central repeat domain 1 of Kaposi's sarcoma-associated herpesvirus (KSHV) latency associated-nuclear antigen 1 (LANA1) prevents cis MHC class I peptide presentation. *Virology*. 2011/04/10/ 2011;412(2):357-365. doi:<https://doi.org/10.1016/j.virol.2011.01.026>
63. Balasubramanian S, Neidle S. G-quadruplex nucleic acids as therapeutic targets. *Curr Opin Chem Biol*. Jun 2009;13(3):345-53. doi:10.1016/j.cbpa.2009.04.637
64. Neidle S, Read MA. G-quadruplexes as therapeutic targets. *Biopolymers*. 2000;56(3):195-208. doi:10.1002/1097-0282(2000)56:3<195::aid-bip10009>3.0.co;2-5
65. Thakker S, Purushothaman P, Gupta N, Challa S, Cai Q, Verma Subhash C. Kaposi's Sarcoma-Associated Herpesvirus Latency-Associated Nuclear Antigen Inhibits Major Histocompatibility Complex Class II Expression by Disrupting Enhanceosome Assembly through Binding with the Regulatory Factor X Complex. *Journal of Virology*. 2015;89(10):5536-5556. doi:10.1128/JVI.03713-14
66. Abdelmohsen K, Gorospe M. RNA-binding protein nucleolin in disease. *RNA biology*. 2012;9(6):799-808. doi:10.4161/rna.19718
67. Abdelmohsen K, Tominaga K, Lee EK, et al. Enhanced translation by Nucleolin via G-rich elements in coding and non-coding regions of target mRNAs. *Nucleic Acids Res*. Oct 2011;39(19):8513-30. doi:10.1093/nar/gkr488
68. Siddiqui-Jain A, Grand CL, Bearss DJ, Hurley LH. Direct evidence for a G-quadruplex in a promoter region and its targeting with a small molecule to repress c-MYC transcription. *Proc Natl Acad Sci U S A*. Sep 3 2002;99(18):11593-8. doi:10.1073/pnas.182256799
69. González V, Guo K, Hurley L, Sun D. Identification and characterization of nucleolin as a c-myc G-quadruplex-binding protein. *J Biol Chem*. Aug 28 2009;284(35):23622-35. doi:10.1074/jbc.M109.018028
70. McStay B. Nucleolar organizer regions: genomic 'dark matter' requiring illumination. *Genes Dev*. Jul 15 2016;30(14):1598-610. doi:10.1101/gad.283838.116
71. Azman MS, Alard EL, Dodel M, et al. An ERK1/2-driven RNA-binding switch in nucleolin drives ribosome biogenesis and pancreatic tumorigenesis downstream of RAS oncogene. *Embo j*. Jun 1 2023;42(11):e110902. doi:10.15252/embj.2022110902
72. Murphy JC, Harrington EM, Schumann S, et al. Kaposi's sarcoma-associated herpesvirus induces specialised ribosomes to efficiently translate viral lytic mRNAs. *Nature Communications*. 2023/01/18 2023;14(1):300. doi:10.1038/s41467-023-35914-5
73. Atari N, Rajan KS, Chikne V, et al. Lytic Reactivation of the Kaposi's Sarcoma-Associated Herpesvirus (KSHV) Is Accompanied by Major Nucleolar Alterations. *Viruses*. Aug 4 2022;14(8)doi:10.3390/v14081720
74. Sadagopan S, Sharma-Walia N, Veetil Mohanan V, et al. Kaposi's Sarcoma-Associated Herpesvirus Upregulates Angiogenin during Infection of Human Dermal Microvascular Endothelial Cells, Which Induces 45S rRNA Synthesis, Antiapoptosis, Cell Proliferation, Migration, and Angiogenesis. *Journal of Virology*. 2009;83(7):3342-3364. doi:10.1128/jvi.02052-08
75. Paudel N, Sadagopan S, Balasubramanian S, Chandran B. Kaposi's Sarcoma-Associated Herpesvirus Latency-Associated Nuclear Antigen and Angiogenin Interact with Common Host Proteins, Including Annexin A2, Which Is Essential for Survival of

Latently Infected Cells. *Journal of Virology*. 2012;86(3):1589-1607.
doi:10.1128/jvi.05754-11

76. Paudel N, Sadagopan S, Chakraborty S, Sarek G, Ojala Päivi M, Chandran B. Kaposi's Sarcoma-Associated Herpesvirus Latency-Associated Nuclear Antigen Interacts with Multifunctional Angiogenin To Utilize Its Antiapoptotic Functions. *Journal of Virology*. 2012;86(11):5974-5991. doi:10.1128/jvi.00070-12

CHAPTER 4

4. G-QUADRUPLEXES OF HUMAN CORONAVIRUSES CAN BE TARGETED FOR ATTENUATING VIRUS REPLICATION

4.1 Abstract

Severe Acute Respiratory Syndrome Coronavirus 2 (SARS-CoV-2), identified as the causative agent of the Coronavirus Disease 2019 (COVID-19) pandemic that emerged in late 2019, has spurred global efforts to identify effective therapeutic strategies. Among the various approaches investigated, G-quadruplexes (G4s). G4s, are non-canonical secondary structures in guanine-rich DNA and RNA sequences. They regulate critical cellular functions such as replication and transcription. Targeting viral G4s for stabilization has revealed promising avenues for inhibiting essential processes related to viral replication and virulence. Several coronaviruses, including the beta-coronavirus hCoV-OC43 (OC43), possess guanine-rich sites with the potential to form G4-structures. Specifically, the potential G4 structure within OC43's RNA-dependent RNA-polymerase (RdRp) has been confirmed to form through an electromobility shift assay (EMSA). Previous *in vitro* studies demonstrated that Methylene blue (M-Blue), an FDA-approved drug, exhibits anti-SARS-CoV-2 activity. *In vivo* experiments indicated that treatment with M-blue not only inhibits viral entry during infection for OC43 and but also reduces post-infection viral replication for OC43 and the alpha-coronaviruses hCoV-NL63 (NL63) hCoV-229E (229E). Furthermore, *in vivo* analysis shows that M-blue was found to suppress SARS-CoV-2 replication post-infection. Additionally, PABPC4 and Rab4A may serve a regulatory role in coronavirus replication. Cumulatively, our findings strongly suggest that M-blue represents a promising therapeutic candidate for treating and preventing coronavirus infections, underlining its potential as a significant addition to our arsenal against COVID-19.

Keywords: Methylene Blue, SARS-CoV-2, G-quadruplex, G4, OC43, NL63, 229E

4.2 Introduction

Severe Acute Respiratory Syndrome Coronavirus 2 (SARS-CoV-2), a novel coronavirus strain, emerged as causing the outbreak of Coronavirus Disease 2019 (COVID-19) in Wuhan, China, in late 2019¹⁻³. The World Health Organization (WHO) declared the rapidly spreading infection a pandemic on March 11th, 2020⁴⁻⁶. The clinical manifestations of COVID-19 vary from asymptomatic and mild respiratory symptoms to severe pneumonia leading to respiratory failure and death⁷⁻⁹. Although there are currently vaccines to aid in combating COVID-19, there is still the need to continue searching for alternative therapeutic options.

Coronaviruses (CoVs) are enveloped positive-sense RNA viruses. They are in the *Coronaviridae* family and further divided into four genera: *alphacoronavirus*, *betacoronavirus*, *gammacoronavirus*, and *deltacoronavirus*. *Alpha* and *betacoronaviruses* solely infect mammalian species, whereas *gamma* and *deltacoronavirus* have a broader host range^{10,11}. Historically, *alphacoronaviruses* hCoV-229E (229E) and hCoV-NL63 (NL63), as well as *betacoronaviruses* hCoV-OC43 (OC43) and hCoV-HKU1 (HKU1), have been linked to seasonal, mild respiratory infections akin to the common cold^{12,13}. Betacoronaviruses, a subset of the *Coronaviridae* family, have been responsible for multiple significant epidemic and pandemic diseases. The Severe Acute Respiratory Syndrome (SARS) outbreak of 2002-2003, caused by the SARS-CoV virus, was the first such global health crisis, resulting in over 8,000 cases and 774 deaths, with a fatality rate of 9.6%. It emerged in Guangdong, China, and rapidly spread to over 26 countries before containment in July 2003¹⁴. Following SARS, the Middle East Respiratory Syndrome (MERS), emerged in 2012 in Saudi Arabia and was caused by MERS-CoV. MERS has

been linked to dromedary camels as a reservoir and has a significantly higher fatality rate of around 34.4%, with 2,494 confirmed cases and 858 deaths as of 2019¹⁵. Most recently, the COVID-19 pandemic has become the most impactful of these outbreaks. Although SARS-CoV-2 only has a 2.13% fatality rate, there have been millions of infections globally, compared to the thousands of SARS and MERS^{15,16}. COVID-19's ongoing impact, driven by the emergence of various strains, continues to pose significant challenges to global health and highlights the critical need to study these viruses to manage future outbreaks of similar viruses.

SARS-CoV-2 enters the target cells by binding their spike (S) protein to the angiotensin-converting enzyme 2 (ACE2)¹⁷⁻²¹. After binding, transmembrane protease serine 2 (TMPRSS2) cleaves the S protein, causing a conformation change. This activates membrane fusion and post-fusion; the viral RNA is released into the host cell and hijacks the cell's replication machinery to produce new viral particles. New virions are assembled and released to infect more cells^{19,22}.

It has been suggested that targeting G-quadruplex (G4) regions in SARS-CoV-2 could be a viable therapeutic approach for treating COVID-19²³. G4 are non-canonical secondary structures found in guanine-rich DNA and RNA sequences²⁴. G4s are formed from two or more consecutive guanine blocks separated by a single-stranded loop region. Four consecutive sequences of guanine blocks resulting in G-tetrads held together by Hoogsteen hydrogen bonding (Fig. 1)²⁵⁻²⁸. G4s are formed from stacking two or more G-tetrads and further stabilized through π - π stacking between the quartets and adding a cation such as potassium²⁹⁻³¹. The stability of G4s is proportional to the number of stacked quartets, resulting in greater stability and lower numbers of nucleotides

comprising the loop regions^{25-28,32}. G4s serve as regulatory elements in translation, RNA maturation, and regulating non-coding RNA³³. There is a higher potential for G4 formation in RNA sequence due to the lack of a complementary strand resulting in a more stable RNA molecule³⁴. Sequences with a potential of G4 formation can be found in functional domains, 5'-UTR, ORF, and 3'-UTR. G4 could affect the coding capacity of a genome through alternative polyadenylation, alternative splicing, and induce frame shifts³³.

In silico analysis identified 25 putative G4-forming sequences (PQSs) in SARS-CoV-2 (Fig. 1). Each site with G-scores corresponding to the likelihood that sequence will form G4 structure^{23,24,33,35-43}. There are several open-source software that can predict PQRSs, with notable examples being G4Hunter, Quadsparser, and QGRSMapper. G4Hunter and Quadsparser identify a relatively smaller number of G4s and require programming expertise. In contrast, QGRSMapper discerns a broader array of potential G4s and functions as an independent web-based program^{37,44}. From the 25 G4 sites identified in SARS-CoV-2, 9 have a G-score equal to or greater than 15, indicating a high probability of G4 formation. These sites were found in ORF1a/b (NSP2, NSP3, and NSP10), nucleocapsid phosphoprotein (N) and the spike (S) coding region of SARS-CoV-2. It should be noted that N and S proteins are essential for virus replication and binding to a target cells⁴⁵. Therefore, the G4 structures in N and S can be a potential therapeutic target in combating SARS-CoV-2.

G4 can cause up or downregulation of genes through their stabilization and unwinding⁴⁶⁻⁴⁸. Agents with stabilizing G4 properties, identified in the Federal Drug Administration (FDA) approved drug list,

(<https://www.accessdata.fda.gov/scripts/cder/daf/>), including methylene blue (M-Blue)⁴⁹. M-Blue is also an FDA approved therapeutic used to treat methemoglobinemia^{50,51}. M-Blue has antimicrobial, anti-inflammatory capacity⁵². It also has low toxicity, stable at room temperature, and affordable drug for treating the disease^{50,52,53}. Additionally, *in vitro* analysis indicates that M-Blue has anti-SARS-CoV-2 activity⁵⁴. Several mechanisms were proposed to explain the antiviral efficacy of M-Blue. M-Blue can affect viral ingress in cells⁵⁵. M-Blue can undergo redox reactions to form leuco-methylene blue (MBH₂) and can transfer electrons to acids, disrupting viral DNA/RNA integrity. In the presence of oxygen, M-Blue makes singlet oxygen, a reactive agent that can induce guanine oxidation leading to damaged DNA/RNA⁵⁶. Photoactivated M-Blue can cause single strand breaks in RNA and interfere with the formation of RNA-protein cross-linkage⁵⁷.

To demonstrate the feasibility of targeting G4 regions to control *coronavirus* replication, preliminary experiments were completed using OC43. OC43 was discovered during the 1960s, is responsible for mild upper respiratory tract, and is one of the primary culprits behind common cold cases⁵⁸. However, individuals with compromised immunity or young children and older adults can suffer severe lower respiratory tract infections caused by OC43^{59,60}. Additionally, OC43 has caused encephalitis in immunocompromised humans⁶¹. We have found 30 potential G4 sites in OC43, with 18 having at least 15 as a G-score, indicating a high likelihood of G4 formation. These sites are in ORF 1a/b, S, and N proteins. Next, we completed a similar analysis using coronaviruses 229E and NL63. We have found that 229E contains 36 potential G4 sites with 18 out having a G-score of 15 or greater. There were 22 potential G4 sites in NL63,

with 12 having a G-score of 15 or greater. Our paper aims to show that M-Blue is a viable therapeutic option for preventing and treating coronavirus infections.

4.3 Materials and Methods

4.3.1 Cells

NCI-H441 Lung Adenocarcinoma Human (H441) were obtained from American Tissue Cell Collection (ATCC, Manassas, VA, USA) and maintained using Roswell Park Memorial Institute (RPMI) 1640 medium supplemented with 10% FBS (Atlanta Biologicals, Fort Collins, CO), 2mM L-glutamine (GE Healthcare Life Sciences, South Logan, Utah), 25 U/mL penicillin (GE Healthcare, South Logan, Utah), and 25 ug/mL streptomycin (GE Healthcare, South Logan, UT). Kidney epithelial cells of the African green monkey (Vero E6) were obtained from (ATCC, Manassas, VA, USA) and maintained using Dulbecco's Modified Eagle Medium (DMEM) (Corning, Glendale, Arizona), with 10% FBS (Atlanta Biologicals, Fort Collins, CO), 2mM L-glutamine (GE Healthcare Life Sciences, South Logan, Utah), 25 U/mL penicillin (GE Healthcare, South Logan, Utah), and 25 ug/mL streptomycin (GE Healthcare, South Logan, UT). LLC-MK2 Kidney Rhesus Monkey were obtained from (ATCC, Manassas, VA, USA) and maintained using Minimum Essential Medium (MEM) (Gibco, Dun Laoghaire, Co Dublin, Ireland) with 1% MEM Non-Essential Amino Acids) (Gibco, Dun Laoghaire, Co Dublin, Ireland), 10% FBS (Atlanta Biologicals, Fort Collins, CO), 2mM L-glutamine (GE Healthcare Life Sciences, South Logan, Utah), 25 U/mL penicillin (GE Healthcare, South Logan, Utah), and 25 ug/mL streptomycin (GE Healthcare, South Logan, UT). The Vero E6 cell line has been modified to constitutively express the serine protease

TMPRSS2 (TMPRSS2) were obtained from (ATCC, Manassas, VA, USA) and maintained using Dulbecco's Modified Eagle Medium (DMEM) (Corning, Glendale, Arizona), with 10% FBS (Atlanta Biologicals, Fort Collins, CO), 2mM L-glutamine (GE Healthcare Life Sciences, South Logan, Utah), 25 U/mL penicillin (GE Healthcare, South Logan, Utah), and 25 ug/mL streptomycin (GE Healthcare, South Logan, UT).

4.3.2 In Vitro RNA Pulldown Procedure

G26 (sequence: 5'-GGUAAUCUGGGGAGUAAUGGUAAACCCGG- -biotin-3') and Disrupted-LANA (Dis-LANA) Oligo Sc26 (sequence: 5'-AUACGGACGGAAGUGUCGACGGUGUUGAA-biotin-3') were used. For this, 20 million HEK293L cells underwent lysis using a 1% NP-40 buffer (containing 50mM Tris-HCl pH7.5, 150mM NaCl, 1% NP-40, 1mM EDTA pH 8.0, protease inhibitors, and RNaseOut). The oligonucleotides were heated to 95°C for 5 minutes to facilitate G4 structure formation, followed by gradual cooling to 25°C at a rate of 10°C per minute. A separate batch of oligos was rapidly cooled post-heating to inhibit G4 formation. Post sonication and centrifugation to discard cell debris, the RNA oligos were mixed with the cell lysate and incubated overnight at 4°C with rotation. Then, Pierce streptavidin-agarose beads (ThermoFisher Scientific, Waltham, MA, USA) were added for 2 hours to isolate proteins attached to the RNA oligos. After washing the beads three times with the 1% NP-40 lysis buffer, they were applied to a 9% SDS gel, transferred to a nitrocellulose membrane, which was then incubated with anti-NCL antibodies and IR dye-labeled secondary antibodies. The final step involved scanning the membrane using the LI-COR Odyssey Imaging System.

4.3.3 *Human Coronaviruses*

The HCoV-NL63 was obtained through BEI Resources, NIAID, NIH: Human Coronavirus, NL63, NR-470.” The HCoV-229E was obtained through BEI Resources, NIAID, NIH: Human Coronavirus, 229E, NR-52726. The HCoV-OC43 was obtained through BEI Resources, NIAID, NIH: Human Coronavirus, OC43, NR-52725. ARS-CoV-2 (USA-WA1/2020) was deposited by the Centers for Disease Control and Prevention and obtained through BEI Resources, NIAID, NIH: SARS-Related Coronavirus 2, Isolate hCoV-19/USA-WA1/2020, NR-52281. OC43 was propagated using H441 and Vero E6 cells, NL63 in LLC-MK2, 229E, and SARS-CoV-2 in TMPRSS2 expressing cells. Cell monolayers were inoculated with 8.9×10^3 Tissue Culture Infectious Dose 50 (TCID₅₀) for 2 hours (34⁰C, 5% CO₅). The unattached virus was removed, and a fresh culture medium was added. Infected monolayers were maintained for five days (34⁰C, 5% CO₅) before the virus was harvested, and aliquots were stored at -80⁰C.

4.3.4 *Immunofluorescence Assay (IFA)*

Cell monolayers were fixed using 4% paraformaldehyde (Sigma-Aldrich, St. Louis, MO, USA) 20min at room temp (RT). Following 3x wash with PBS, monolayers were permeabilized with 0.2% Triton x-100 (Fisher Scientific, NJ, USA), in PBS for 10min at RT, washed 3x again (PBS), and blocked (0.4% fish skin gelatin (FSG), 0.05% TX-100 in PBS) for 40min at RT. Following 3 washes, cell monolayers were incubated with anti-OC43-nucleocapsid antibodies (1:1000; EMD Millipore Corporation, Darmstadt, Germany) in 0.25 FSG and 0.05% TX-100 overnight at RT. Following day

cell monolayers were washed (3x, PBS) and incubated with Alexa Fluor 594 chicken anti-mouse IgG (H+L) antibody (1:1000; Invitrogen, Waltham, MA, USA) in 0.2% FSG and 0.05% TX-100 for 1h at RT. Nuclei were stained with DAPI for 1 min at RT (1:5000 dilution). Slides were mounted with Prolong Gold Antifade (Invitrogen, Eugene, OR, USA) and examined using Carl Zeiss LSM 780 confocal laser-scanning microscope.

4.3.5 RNA extraction and qPCR analysis

Total RNA was extracted using Trizol reagent (Invitrogen, Carlsbad, CA, USA) by directly adding the reagent onto the cells for lysis according to the manufacturer's recommendation. An aliquot of RNA (1 μ g) was used for synthesizing the cDNA (Superscript kit; Invitrogen, Carlsbad, CA, USA). cDNA (2 μ L) was used for determining subgenomic RNA. Taqpath reagent (ThermoFisher Scientific, Waltham, MA, USA) and TaqMan Gene Expression Assay Probes for OC43, NL63, 229E, SARS-CoV-2, and GAPDH (ThermoFisher Scientific, Waltham, MA, USA) for determining relative genome copies.

4.3.6 Western blot

Total proteins were extracted using Sodium dodecyl sulfate (SDS) reducing buffer (Bio-Rad Laboratories, Hercules, CA, USA), separated on 8-12% gradient SDS polyacrylamide gels, and transferred on Polyvinylidene difluoride (PVDF) membranes (Bio-Rad Laboratories, Hercules, CA, USA). Membranes were blocked (Tris-buffered saline (TBS), 0.1% Tween 20, 5% low-fat milk) for 1 hr followed by overnight incubation with the HCoV-OC43 Nucleocapsid Polyclonal Antibody (1:1000, Invitrogen,

Waltham, MA, USA) antibody at 4°C. Membranes were washed (TBS, 0.1% Tween 20) and incubated for 1 hour at room temperature with IRDye800CW (LI-COR Biosciences, Lincoln, NE, USA)) Proteins were revealed using ChemiDoc MP Imaging system (Bio-Rad Laboratories, Hercules, CA, USA).

4.3.7 siRNA Transfection

Vero E6 or TMPRSS2 cells were transfected with siRNA control, siRNA-PABPC4, and siRNA-Rab4A (IDT Integrated DNA technologies, Newark, NJ, USA) using Lipofectamine RNAiMAX Transfection Reagent (ThermoFisher Scientific, Waltham, MA, USA). After 48hr incubation, cells were infected with either OC43 or SARS-CoV-2. 24hr post-infection, cells were harvested for analysis.

4.3.8 Statistical Analysis

Statistical significance was assessed using the standard t-test and one-way ANOVA with GraphPad Prism version 8 software. In the graphical representations, asterisks denote the levels of significance corresponding to the P values: * for $P \leq 0.05$,

4.4 Results

4.4.1 Coronavirus mRNA form G-quadruplexes

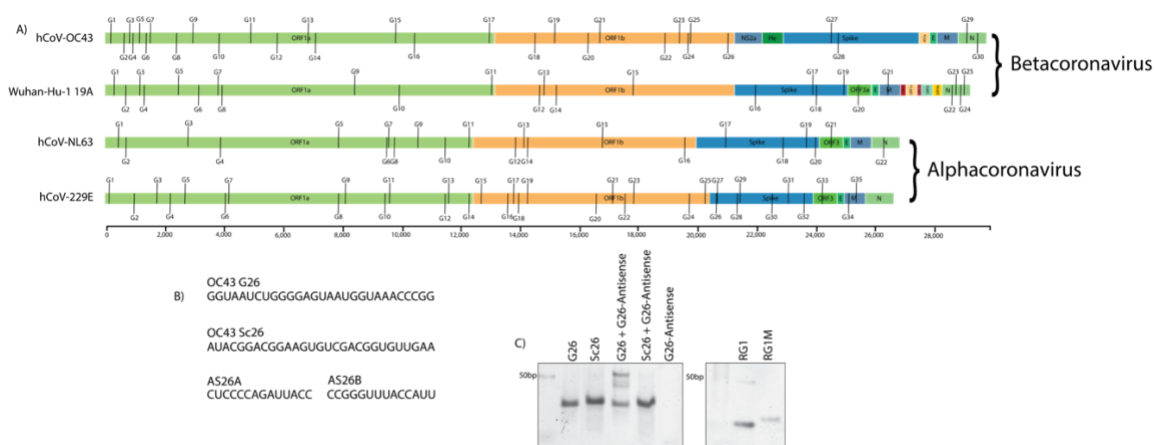
Sequences of hCoV-OC43, hCoV-NL63, hCoV-229E, as well as SARS-CoV-2 variants were obtained from the NCBI nucleotide database. Using the online G4 prediction software, QGRS Mapper, we identified 30, 22, 35, and 25 potential G4 sites in OC43, NL63, and SARS2 viruses, respectively (Fig. 1A)⁴³. We synthesized 3'

biotinylated RNA oligonucleotide (oligo) representing 26th potential G4 site in OC43 as well as the scrambled version (Sc26), which was used as a control (Fig. 1B). This G4 was selected due to having the highest G-score within the viral genome and its location in the RdRp. Through an electromobility shift assay (EMSA), we determined that G26 forms a G4 structure indicated by its faster migration through the native gel, compared to the Sc26 (Fig. 1C, left blot). As an additional control, we tested RG1, previously confirmed to form G4 structure in SARS-CoV-2's nucleocapsid phosphoprotein⁶². The EMSA assay showed a similar migration pattern for the RG1 and mutated RG1 (RG1M) oligos (Fig. 1C, right blot). Next, we confirm the faster mobility of G26 RNA oligo was due to the forming of a G4 secondary structure. For that, we disrupted the formation of the G4 structure by incubating the G26 oligo with two antisense oligos complementary to each arm of the G26 Oligo (AS1, CUCCCCAGUAUUACC, and AS2, CCGGGUUUACCAUU). After incubation with complementary oligos, G26 moved slower (Fig. 1C, lane 3). The antisense oligos binding to the arms of G26 prevents the formation of the compact G4 structure, which results in a slower migration. These results validate the formation of a G4 in OC43's RdRp.

Figure 1: G4s in coronaviruses

A) Schematic of G4 sites in OC43, SARS-CoV-2, NL63 and 229E. G4 sites are represented by “G” and then the number indicating the order of the G4s in the coronavirus' mRNA. B) Oligonucleotides: G26 is a PQS in OC43, Sc26 is a scrambled iteration of G26 to prevent G4 formation. Antisense (AS26A and AS26B) are complementary to the G26 oligonucleotide. C) Electrophoretic mobility shift assay (EMSA) performed with G26 and Sc26 oligonucleotides, resolved on a native polyacrylamide gel. Antisense oligonucleotides were used in molar excess and used in the indicated lanes to confirm the specificity of the

mobility shift by the PQS. RG1 is a PQS in SARS-CoV-2 confirmed to form a G4 structure. RG1M is the scrambled version of RG1.



4.4.2 Methylene blue inhibits coronavirus expression in vivo

Targeting viral G4s has been shown to exhibit antiviral activity⁶³. For example, when human cytomegalovirus (HCMV) is treated with N-methyl mesoporphyrin IX (NMM), a porphyrin derivative, there is a downregulation of viral genes⁶⁴. Braco19 along with C8, an acridine derivative, stabilizes a G4 structure in human papillomavirus (HPV), resulting in decreased viral replication⁶⁵. TMPyP4, a porphyrin, inhibits the viral expression of Hepatitis C (HCV), Zika, and Enterovirus⁶⁶⁻⁶⁸. Bioinformatic analysis shows that SARS-CoV-2 contains several PQSs in ORF1ab, 3a, nucleocapsid, and the membrane^{69,70}. PQSs in these regions indicate possible G4 involvement in regulating viral replication, immune-response modulation, and assembly⁴⁵. *In vitro* experiments show that Braco19 and TMPyP4 successfully stabilize a G4 structure in SARS-CoV-2, showing reduced expression⁷¹. TMPRSS2, a serine protease expressed in human tissue, is involved in the entry of coronaviruses into host cells. SARS-CoV-2 utilizes its spike (S) protein to bind to the angiotensin-converting enzyme 2 (ACE2) cell receptor. This

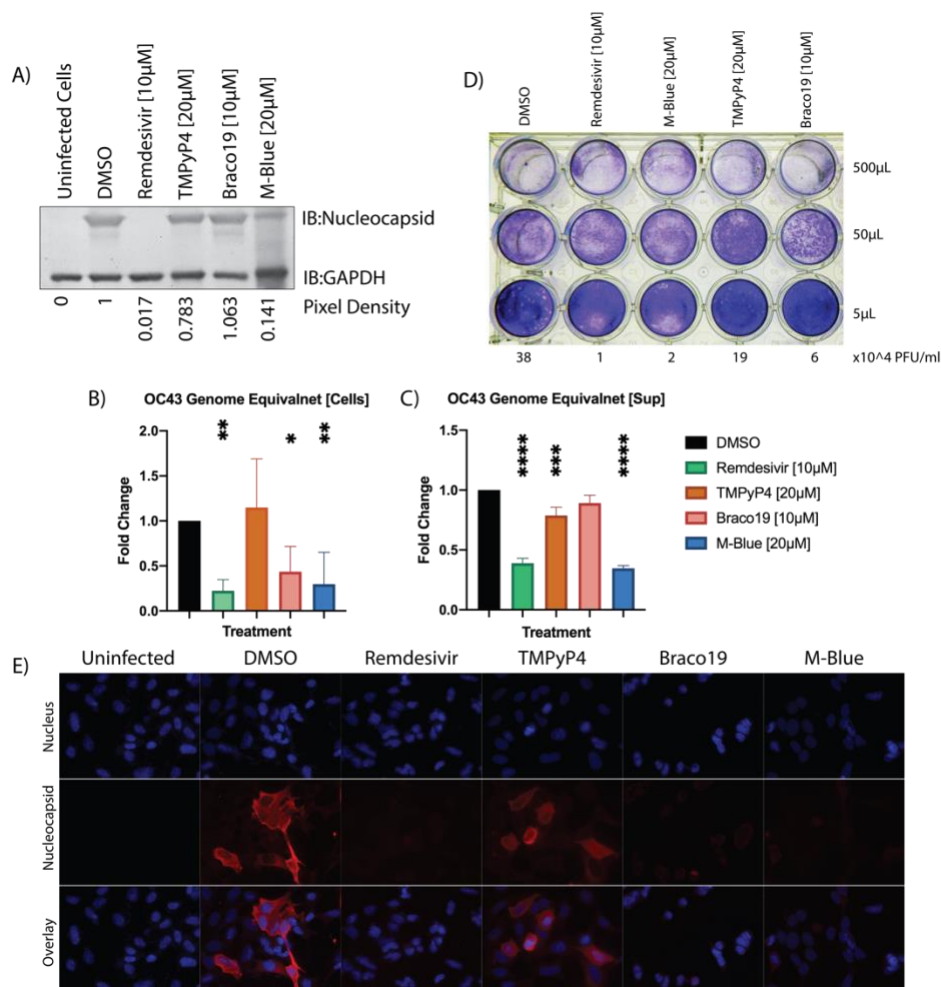
interaction enables membrane fusion and viral entry¹⁹. Pyridostatin (PDS), a G4 stabilizing ligand, and TMPyP4 bind to a G4 structure in TMPRSS2, reducing pseudotyped SARS-CoV-2 S glycoprotein viral entry²². In transgenic mouse models of SARS-CoV-2 infection, TMPyP4 suppressed SARS-CoV-2 infection and reduced viral loads and lung lesions⁷².

Causing the formation or stabilization of G4s comes with a potential caveat. G4 stabilizing ligands can lead to unintended biological consequences, including toxicity, due to lacking G4 specificity. This may disrupt normal cellular processes, such as replication and transcription. This disruption can induce cell cycle arrest, trigger apoptosis, or lead to off-target effects where the ligands bind to non-G4 structures⁷³⁻⁷⁵. For these reasons, it is crucial to have a G4 stabilizing ligand with low toxicity and minimal off-target effects. As mentioned, M-Blue has low toxicity and is already FDA-approved to treat methemoglobinemia⁵¹. Additionally, M-Blue has also been used to treat malaria, refractory hypotension in septic endocarditis, vasoplegia, ifosfamide neurotoxicity⁷⁶⁻⁷⁹. M-Blue has been shown to inhibit the entry of SARS-CoV-2 spike-bearing pseudovirus into ACE2 expressing cells⁸⁰. This led us to test M-Blue as a viable therapeutic agent in combating coronaviruses.

Figure 2: Effects of G4 stabilizing ligands on Coronavirus Expression.

A) Western blot of OC43 infected Vero E6 cells treated with G4 stabilizing ligands. Relative nucleocapsid pixel density is presented below the blot. Pixel density was normalized to respective samples' GAPDH. B) qRT-PCR of OC43 infected cells treated with G4 stabilizing ligands. Performed using OC43-specific “Taqman Gene Expression Assay” probes. C) qRT-PCR using sequence specific primers of the supernatant from samples in B. D) Plaque assay from supernatant of treated OC43 infected Vero E6 cells. E) H441

cells infected with OC43 virus for 2hrs, followed by compound treatments. 24hrs post-treatment, cells were incubated with OC43 nucleocapsid antibody overnight, followed by incubating with DAPI. Red fluorescence corresponds to OC43 nucleocapsid protein and blue for the cell nucleus.



Initial experimentation was completed using OC43. Vero E6 cells were infected with OC43 virus, followed by treatment with DMSO (mock treatment), 10 μ M remdesivir, 20 μ M TMPyP4, 10 μ M Braco19, and 20 μ M M-Blue. 24hrs post-treatment, samples were analyzed using western blot and probed for OC43 N protein (Fig. 2A). We have found that compared to DMSO, remdesivir completely abrogates expression of

OC43 N protein. In contrast, TMPyP4 slightly reduces, while Braco19 demonstrated no significant change in N protein expression. Interestingly, M-Blue shows a significant decrease in OC43 N protein expression. Given that M-blue reduced N protein expression, we were keen to examine the effects of the treatments on relative genome copies.

Performing the same post-infection treatment, samples were subjected to RNA extraction followed by 1-step quantitative reverse transcription PCR (qRT-PCR). We have found a statistically significant decrease in viral mRNA when cells were treated with remdesivir, Braco19, and M-Blue (Fig. 2B). There was no statistical difference between TMPyP4 and the mock treatment. Analysis of the supernatant reveals that remdesivir and M-Blue display a similar trend, characterized by an overall decrease in virus genome copies (Fig. 2C). In contrast, TMPyP4 decreased, while Braco19 had no statistical difference in viral genome load in the supernatant of infected cells. TMPyP4 could be preventing the egress of the virus, and that is why although there is no change in relative OC43 genome copies in the cell, there is less detected in the supernatant. Braco19 may reduce detectable OC43 genome copies in the cells, however, both the western blot (Fig. 2A) and the qPCR results for the supernatant (Fig. 2C), indicate that protein levels do not decrease. The results show that remdesivir and M-Blue reduce both viral RNA and protein detected. This suggests that M-Blue holds the potential for inhibiting OC43 replication.

Next, we sought to analyze the virus titer in the supernatant using a plaque assay to calculate the plaque forming units (PFU) (Fig. 2D). The PFU data indicate that remdesivir, M-Blue, and Braco19 significantly reduced plaques formed, compared to DMSO mock treatment. TMPyP4 had almost a 50% reduction in PFU. The plaque assay cannot conclusively show the relative live virus in the supernatant. Neither TMPyP4 nor

Braco19 has been evaluated for their impact on viral entry. This might account for Braco19 displaying a significant reduction in PFU, even when qRT-PCR results indicate no significant difference in relative genome copies in the supernatant. Aside from this, G4-stabilizing ligands appear to reduce PFU.

Utilizing an antibody specific for OC43's nucleocapsid, we performed an immunofluorescence assay (IFA) to qualitatively see how the treatments reduced viral infection (Fig. 2E). The IFA intensity appears to match the qRT-PCR results from Fig. 2B. DMSO mock treatment showed the highest number and intensity of signal, whereas remdesivir, Braco19, and M-Blue showed significantly diminished signal. TMPyP4 showed only a slight reduction in signal, compared to DMSO. These results match the qPCR data in Fig. 2B and indicate that G4-stabilizing ligands show the potential to diminish viruses within the cells.

4.4.3 G4-stabilizing compounds reduce available translational capability in OC43

Coronaviruses are positive-strand RNA viruses and utilize the synthesis of subgenomic (SG) messenger RNA⁸¹. SG RNAs allow for differential expression of viral genes in infected cells^{81,82}. These sequences are shorter than genomic viral RNAs and predominately co-terminal with the 3' genomic sequence (Fig. 3A)⁸³⁻⁸⁵. The majority of SG RNAs produced by positive-strand RNA viruses act as messenger RNA⁸⁶. We utilize the SG RNA to determine if the G4-stabilizing ligands regulate viral replication/virion production. SG RNA levels were determined using a 5' UTR forward primer instead of random primers during cDNA synthesis, followed by qPCR. OC43-infected cells, treated with remdesivir, Braco19, and M-blue, showed a significant decrease in subgenomic S mRNA (Fig. 3B). Interestingly, only remdesivir and M-Blue significantly reduced

mRNA coding for N protein. It is important to note that the N and S regions contain PQSs with relatively high G-scores. We believe that M-Blue stabilizes the G4 sites in the positive RNA strand at these gene sites, which interferes with transcription, translation, and replication. However, Braco19 is likely unable to bind/stabilize the G4 PQS in the N region sequence. Similarly, TMPyP4 does not appear to cause a reduction in SG RNA but may even enhance N SG RNA synthesis. Therefore, we suggest that M-Blue can reduce OC43 subgenomic RNA synthesis, which reduces structural proteins from being synthesized. In turn, M-Blue reduces the capacity for OC43 viral assembly.

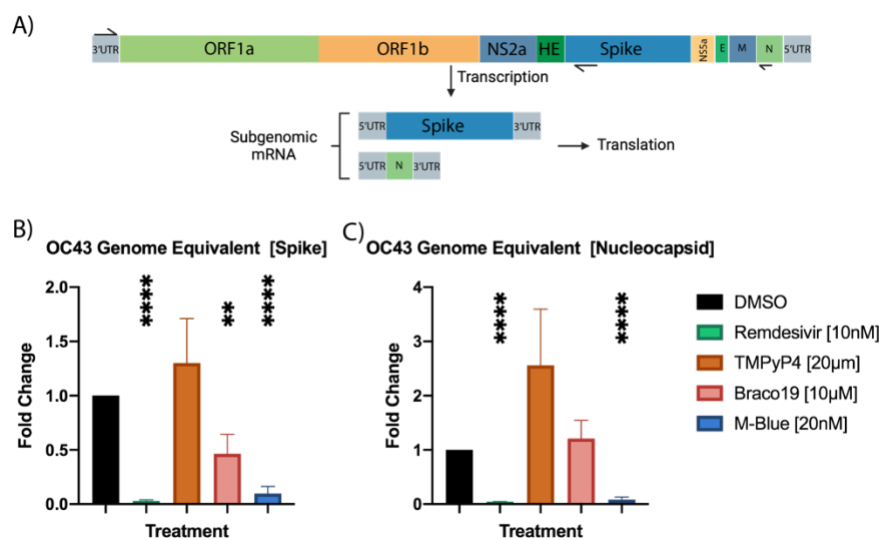


Figure 3: OC43 Subgenomic Fractions. A) Schematic of subgenomic (SG) RNA synthesis. B) qPCR showing SG levels of OC43's spike RNA. C) qPCR showing SG levels of OC43's nucleocapsid RNA.

4.4.4 Methylene Blue inhibits both viral entry and attenuates subsequent viral replication

M-blue has been shown to inhibit the entry of a pseudovirus containing the SARS-CoV-2 spike protein into HEK293T cells expressing ACE2⁸⁰. Therefore, we

aimed to demonstrate whether the same mechanism is used to Inhibit OC43 replication *in vivo*. Treatment consisted of three groups: 1st group (Entry) had compounds added immediately before infection and then harvested after the 2hr infection period; 2nd group (Entry/Continued) was the same as the first however, continued treatment 24hrs post-infection then harvested 24hr later; the 3rd group (Post-Infection) was treated post-infection and harvested 24hrs later. RNA was extracted and used for qRT-PCR. In Group 1, the pre-treatment with M-Blue significantly reduced, whereas remdesivir showed no effect on viral RNA load (Fig. 4A). The effects of Remdesivir could be explained by its stalling RdRp, which would have a limited effect on viral ingress⁸⁷. In both, the 2nd and 3rd groups, remdesivir and M-Blue significantly reduced OC43 RNA. Remdesivir demonstrated a comparable reduction between these two groups, however, M-Blue had a greater degree of reduction in group 2 over group 3. This is likely due to M-Blue reducing the viral entry. The results using the supernatant from cells from each group follow the same pattern as what was found using the cells (Fig. 4B). Overall, these findings suggest that M-Blue exerts its antiviral effects via several mechanisms, by acting both at the initial stage of viral entry into the host cell and subsequent post-entry phases. During the entry stage, M-Blue appears to interfere with the virus's ability to penetrate the cell membrane or to bind with its entry receptors, thereby hindering its capacity to establish an infection. After the virus has entered the cell, M-Blue continues to exhibit antiviral activity by disrupting subsequent stages of the viral life cycle, such as genome replication, protein synthesis, or assembly of new virions, ultimately attenuating the virus's ability to propagate within the host.

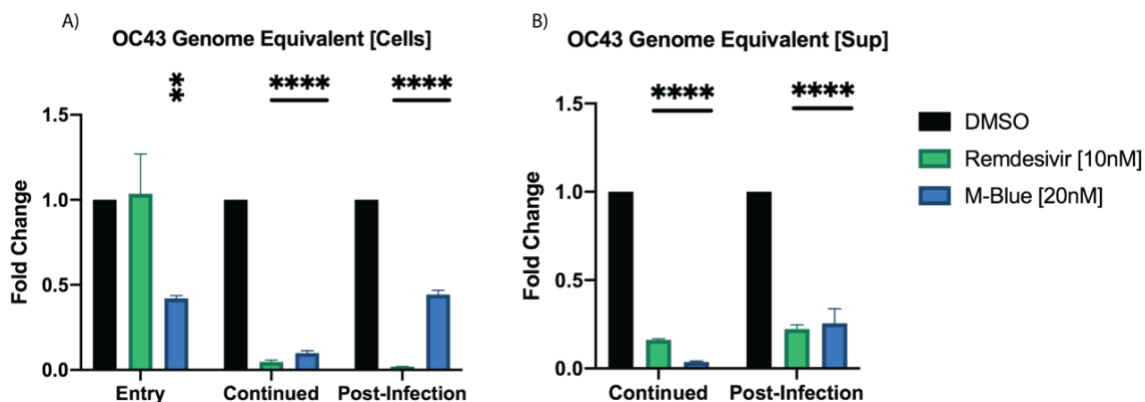


Figure 4: Time point treatment. Vero E6 cells underwent treatments at distinct stages of infection. The "Entry" groups refer to cells exposed to the compounds immediately before the infection process. These cells were then harvested after 2 hours. Conversely, the "Continued" groups were treated identically to the "Entry" groups but were allowed to incubate for 24 hours post-infection before harvesting. For the "Post-Infection" groups, cells were first infected for 2 hours, after which the compounds were applied; harvesting occurred 24 hours post-infection. For both "Continued" and "Post-Infection" groups, the supernatant was also collected. A) The qRT-PCR analysis employed OC43-specific TaqMan Gene Expression Assays to quantify viral RNA in cell extracts. B) Using the same TaqMan probes, viral RNA in the supernatant was measured.

4.4.5 M-Blue inhibits viral replication in alphacoronaviruses

Next, we extended our investigation to explore 4G regulatory effects on *alphacoronaviruses* NL63 and 229E. We used LLC-MK2 cells and Vero E6 cells expressing the full-length human TMPRSS2 to infect with NL63 and 229E viruses, respectively. After infection, cells were treated with the 4G stabilizing compounds to assess their antiviral activity against these *alphacoronaviruses*. Employing a TaqMan method, we quantified relative genome copies in cells. Remdesivir reduced the viral RNA copies to approximately 6% of what was found in DMSO treated cells. Similarly,

Braco19 and M-Blue decreased viral RNA copies to about 50% and 40%, respectively, of that in DMSO-treated cells (Fig. 5A). TMPyP4, however, had a limited effect on viral RNA copy levels. A similar trend was found when we assessed the virus release (Fig. 5B). By using primer targeting the 5' UTR of NL63, we conducted qPCR analysis to determine the levels of SG RNA. We found that the levels of both S and N SG RNAs mirrored the trends for overall genome copies, as depicted in Figures 5B and C (Figures 5D and E).

TMPrSS2 cells infected with 229E were analyzed via qRT-PCR. TaqMan probe designed specifically to target 229E, we found significantly decreased intracellular levels of 229E genome copies, like that in NL63 Infected cells (Fig. 5G). The 4G -stabilizing ligands Braco19 and M-Blue also decreased viral RNA levels. In contrast, TMPyP4 had a limited effect on viral RNA levels. The pattern of viral release for 229E mirrored the trends observed for intracellular RNA levels (Fig. 5H). Intriguingly, when assessing SG RNA levels, M-Blue had an effect like that of remdesivir, reducing the levels of S and N mRNAs to around 10% of what was found in treated cells (Fig. 5I and J). Braco19 had an approximately ~50% reduction, whereas, TMPyP4-had limited effect on viral SG RNA level.

Both *alphacoronaviruses*, NL63 and 229E, show similar patterns in viral genome copies and SG RNA accumulation, as OC43 infected/treated cells, in cells treated with remdesivir and G4-stabilizing compounds: Braco19, M-Blue, and TMPyP4. The data shows that both Braco19 and M-Blue show the potential to regulate *alphacoronaviruses*. However, only M-Blue can inhibit viral entry and inhibit virion production post-infection. There is likely sufficient overlap in the G4 sequences present in the

alphacoronaviruses that both Braco19 and M-Blue can stabilize the structure and inhibit the replication machinery.

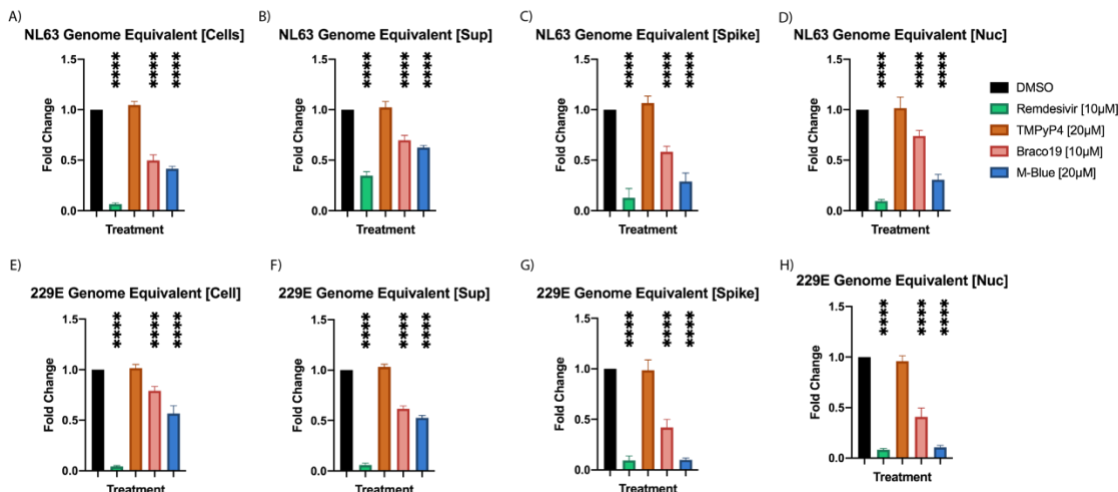


Figure 5: NL63 and 229E G4-stabilization. Cells infected with either NL63 (A-D) or 229E (E-H) and treated identically to OC43. A) NL63 genome equivalent from RNA extracted from cells using TaqMan probes. B) NL63 genome equivalent from RNA extracted from the supernatant from “A” using TaqMan probes. C&D) cDNA synthesized using NL63 5’UTR primer and using primer specific for spike SG RNA “C” and Nuc SG RNA “D”. E) 229E genome equivalent from RNA extracted from cells using TaqMan probes. F) 229E genome equivalent from RNA extracted from the supernatant from “A” using TaqMan probes. G&H) cDNA synthesized using 229E 5’UTR primer and using primer specific for spike SG RNA “G” and Nuc SG RNA “H”.

4.4.6 PABPC4 and RAB4A bind to OC43 G4 mRNA

We sought to determine whether there are cellular proteins that interacted with OC43’s G26 oligonucleotide. Vero E6 cells were infected with OC43 virus and used to prepare the lysate. G26 and Sc26 oligos were incubated with the cell lysate for 24hrs and washed prior to the mass spectrometry analysis. Multiple proteins were found interacting

with 4G sites. In this study, we focused on poly(A) binding protein cytoplasmic 4 (PABPC4) and Ras-related protein Rab-4A (RAB4A). Poly(A)-binding proteins (PABP) are a class of nucleocytoplasmic shuttling proteins that promote gene expression through enhancing mRNA stability and translation^{88,89}. PABP can bind to the 3' end of mRNA via the polyA tail and the 5' end cap and form a closed loop^{90,91}. This unique complex formed between PABP, and mRNA has the potential to boost the assembly of ribosome subunits, thereby aiding the commencement of translation. Additionally, it shields mRNAs from being broken down by exonucleases^{92,93}. PABP can bind to the nucleocapsid protein of bovine coronavirus (BCoV) and downregulate translation of viral RNA^{94,95}. PABP was first discovered as a protein whose production increases when human T-cells are activated. Poly(A)-binding protein cytoplasmic 4 (PABPC4), is a homolog of PABP and is the least studied isoform⁹⁶. It has been proposed that downregulating PABPC4 may be an adaptive event necessary to induce mitochondrial activity during metabolic stress in skeletal muscle⁹⁷.

Ras-associated binding (Rab) proteins are small GTPase and serve to continuously cycle between the cytosol and various membranes. More than 60 Rab proteins have been identified and 20 have been identified as prenylated proteins localized to membrane-bound compartments^{98,99}. Rab proteins regulate vesicle trafficking, including vesicle formation, and Rab4A is involved in fast cargo recycling to the cell surface¹⁰⁰⁻¹⁰². Rab4A is known to directly influence the process of autophagy, as well as in response to the stretching of cell membranes. It also plays a part in the secretion process of phagosomes, which are cellular structures that engulf and aim to destroy pathogenic bacteria¹⁰³⁻¹⁰⁵. Rab4A is a key regulator of cargo segregation for sorting

endosomes, Rab4A knockdown causes a rise in the number of vacuole-like endosomes and disrupts the distribution of their contents. This disorganization results in melanosome-related proteins being erroneously sent to lysosomes, the cell surface, and exosomes instead of their correct destinations.

To assess the impact of PABPC4 and Rab4A on coronavirus replication, we knocked down these proteins in Vero E6 cells using respective siRNAs. After 48 hours, cells were infected with OC43 and used for the analysis of protein expression. We have found that the depletion of PABPC4 and Rab4A quantitative real-time PCR (qRT-PCR) using TaqMan probes demonstrated an increase in viral genome copies for reduced PABPC4 and a decrease Rab4A knock down samples (Fig. 6). These results collectively suggest that PABPC4 and Rab4A may play a facilitating role in the life cycle of coronaviruses within host cells.

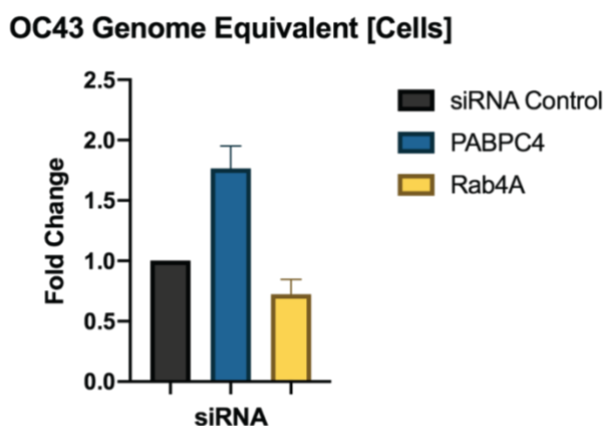


Figure 6: PABPC4 and Rab4A knockdown reduces OC43 transcription

qRT-PCR results TaqMan OC43 probe for vero E6 cells transfected with either siRNA control, PABPC4, or Rab4A.

4.4.7 G4-stabilizing regulate SARS-CoV-2

SARS-CoV-2, the etiological agent of COVID-19, a novel member of the *Coronaviridae* family, rapidly captured global attention due to its rapid transmission between humans, leading to an unprecedented international public health emergency¹⁰⁶. The virus's rapid spread and significant mortality rate triggered intense scientific research to understand its pathology, transmission mechanisms, and potential therapeutic targets, as well as a worldwide effort to develop effective vaccines. To combat SARS-CoV-2, mRNA vaccines were developed. These vaccines contained a piece of the virus' genetic code, allowing the cells to produce a portion of the SARS-CoV-2 spike protein and stimulate an immune response without causing the disease^{107,108}. While these vaccines have been instrumental in mitigating the transmission of the virus, continuous research is essential to uncover further strategies to combat the virus effectively.

Next, we sought to determine whether G4-stabilizing ligands could modulate SARS-CoV-2 infection. Cells were infected with OC43, NL63, and 229E viruses and treated with DMSO mock treatment, 10 μ M remdesivir, TMPyP4 20 μ M, 10 μ M Braco19, and 20 μ M M-Blue. SARS-CoV-2 RNA was analyzed using qPCR. We have found that remdesivir inhibited virus replication in all coronaviruses tested. Also, SARS-CoV-2 virus RNA accumulation was reduced in cells treated with Braco19 and M-Blue like that found in cells infected with OC43 virus (Fig. 7A). M-Blue reduced virus RNA to about 20% of that in DMSO mock controls. TMPyP4 substantially decreased viral RNA quantity, compared to Braco19, which may be attributed to a specific PQS that TMPyP4 can effectively bind and stabilize. We also analyzed the virus in the supernatant of the infected cells. M-Blue reduced virus load in supernatant like that of remdesivir.

After quantifying the viral genome copies within the cells, we evaluated the amount of live virus present in the supernatant. M-Blue substantially reduced virus load in the supernatant like that of remdesivir (Fig. 7B). TMPyP4 and Braco19 reduced SARS-CoV-2 virus, however, the effect was lower compared to M-Blue and remdesivir. We also completed the plaque assay to determine the PFU to demonstrate the infectious virus particles (Fig. 7C). In the DMSO mock controls, the PFU count was high, reaching 600×10^5 PFU/ml. In contrast, treatment with remdesivir led to a drastic reduction in viral infectivity, with only 0.18% of the PFU found compared to that in DMSO control. Remarkably, M-Blue completely abolished the release of infectious units, demonstrating a 100% reduction in PFU count. Meanwhile, TMPyP4 cuts down the PFU to half of the control levels, indicating a 50% reduction. Braco19, although the least effective among the treatments, still significantly decreased viral infectivity to 70% of that in DMSO control. These results highlight the various degrees of efficacy of these compounds in reducing live SARS-CoV-2 virus replication, with M-Blue standing out for its potent antiviral activity. The level of attenuation efficiency M-Blue has in SARS-CoV-2 is comparable to its regulation in OC43. Referring back to Fig 1A, there are significant overlaps in the location of G4 PQSs between the two viruses. The conserved locations could

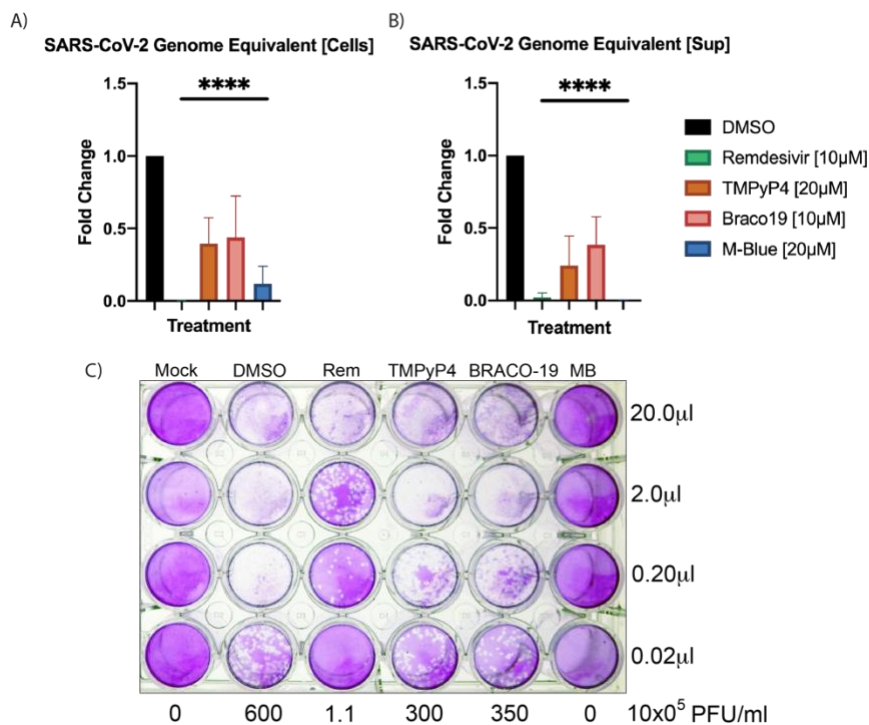


Figure 7: Inhibition of SARS-CoV-2 replication by G4-stabilizing compounds

TMPRSS2-expressing cells were transfected with the SARS-CoV-2 virus and subsequently treated using a protocol analogous to the one employed for the previously tested coronaviruses. Quantitative reverse transcription PCR (qRT-PCR) was conducted utilizing TaqMan probes targeting SARS-CoV-2 and the housekeeping gene GAPDH as an internal standard for normalization. The analysis yielded results for viral RNA in both cellular extracts (A) and corresponding cell culture supernatants (B). C) The supernatant from “A”, the same sample analyzed in “B”, for conducting plaque assays to quantify infectious viral particles.

4.4.8 G4-stabilizing compounds reduce available translational capability in SARS-CoV-2

We assess the effect of G4-stabilizing ligands on virus replication and virion production by quantifying SG RNA. A forward primer specific to the 5' UTR in SARS-CoV-2 was used for cDNA synthesis, rather than using random primers. The amplicons were then used for a qPCR analysis using primers selectively targeting the SARS-CoV-2 S and N (Fig. 8A and B). The results revealed a congruent trend across all treatment

groups, with each exhibiting a reduction in subgenomic (SG) RNA levels by more than 70%. Notably, TMPyP4 and M-Blue demonstrated efficacy like that of remdesivir in diminishing SG RNA quantities. These findings suggest that G4-stabilizing ligands represent a promising strategy for decreasing the levels of SARS-CoV-2 mRNA availability for protein synthesis.

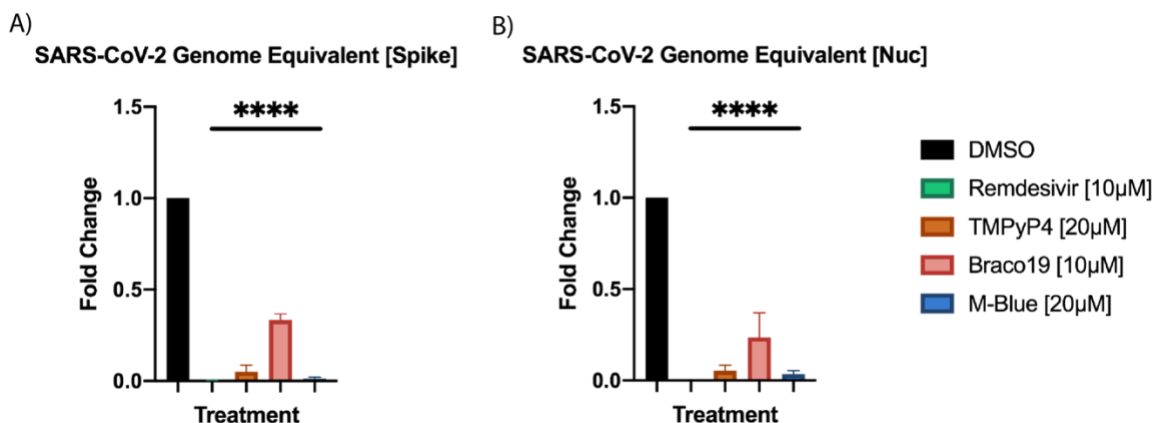


Figure 8: SARS-CoV-2 subgenomic fractions. cDNA was synthesized from the RNA samples depicted in Figure 7 using a primer specific to the 5'UTR of SARS-CoV-2. A) The qPCR results, obtained with primers targeting the SARS-CoV-2 spike protein, are shown. B) The qPCR results, using primers specific for the SARS-CoV-2 nucleocapsid protein.

4.4.9 M-Blue exerts multimodal regulatory effects on SARS-CoV-2

Our data demonstrated that M-blue effectively prevented the entry of OC43 virus into cells. Additionally, others have shown that M-Blue prevents the entry of a pseudovirus, equipped with the SARS-CoV-2 spike protein, into HEK293T cells that express the ACE2 receptor⁸⁰. Therefore, we sought to investigate whether M-Blue could effectively reduce the entry of SARS-CoV-2 into TMPRSS2-expressing cells. The

treatment was divided into three distinct groups: the first group, labeled “Entry,” received compounds just before infection and was harvested following a 2-hour infection period; the second group, “Entry/Continued,” was treated identically to the first but with continued treatment for 24 hours post-infection, followed by harvesting after 24 hours; the third group, “Post-Infection,” was treated only after infection and harvested 24 hours later. Subsequently, RNA was extracted and analyzed using qRT-PCR, with OC43-specific probes. qRT-PCR results indicated that M-Blue does inhibit SARS-CoV-2 viral entry, but not to the extent of our previously tested coronaviruses (Fig. 9A). There is approximately a 30% reduction in SARS-CoV-2 detected, whereas M-Blue reduced OC43 detected by approximately 60%. We included TMPyP4 and Braco19 alongside remdesivir and M-Blue to assess their potential to inhibit viral entry. Like remdesivir, both TMPyP4 and Braco19 were ineffective in preventing viral entry. As anticipated, the treatments labeled “Continued” and “Post-Infection” demonstrated a significant decrease in relative viral load (Fig. 9B). When analyzing viral copies in the supernatant, a reduction was found across all treatment conditions in both groups. Notably, M-Blue reduced viral copies comparable to remdesivir in both the “Continued” and “Post-Infection” treatments, affecting both the cells and the supernatant. These findings suggest that M-Blue employs multiple mechanisms to mitigate SARS-CoV infection, including the inhibition of viral entry and subsequent post-entry suppression.

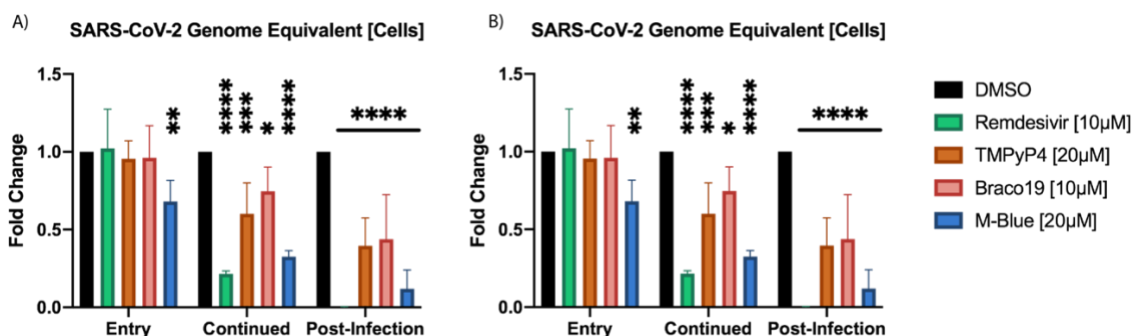


Figure 9: Multi-timepoint SARS-CoV-2 treatment. TMPRSS2 cells underwent treatments at distinct stages of infection. The "Entry" groups refer to cells that were exposed to the compounds immediately before the infection process. These cells were then harvested after 2 hours. Conversely, the "Continued" groups were treated identically to the "Entry" groups but were allowed to incubate for 24 hours post-infection before harvesting. For the "Post-Infection" groups, cells were first infected for 2 hours, after which the compounds were applied; harvesting occurred 24 hours post-infection. For both "Continued" and "Post-Infection" groups, the supernatant was also collected. A) The qRT-PCR analysis employed SARS-CoV-2-specific TaqMan Gene Expression Assays to quantify viral RNA in cell extracts. B) Using the same TaqMan probes, viral RNA in the supernatant was measured.

4.4.10 PABPC4 and Rab4A play a role in SARS-CoV-2 viral life cycle

Our research has established that the transcriptional regulation of OC43 is influenced by the downregulation of PABPC4 and Rab4A. Translating our work from OC43, we set to investigate whether these proteins interact with G4 structure(s) in SARS-CoV-2 and subsequently regulate it. We transfected TMPRSS2 cells with either siRNA-Control, siRNA-PABPC4, or siRNA-Rab4A, followed by SARS-CoV-2 infection 48 hours post-transfection. At 24 hours post-infection, the cells were collected and subjected to qRT-PCR using TaqMan specific probes. The results indicated that suppressing PABPC4 did not significantly alter the levels of SARS-CoV-2 detected. However, in

contrast, the reduction of Rab4A led to a noticeable decrease of approximately 45% in viral copies detected. Drawing on the parallels from our OC43 mass spectrometry results, we hypothesize that Rab4A interacts with SARS-CoV-2 and plays a crucial role in its replication cycle. This insight could be pivotal in understanding the mechanisms of viral replication and potentially in developing targeted antiviral therapies.

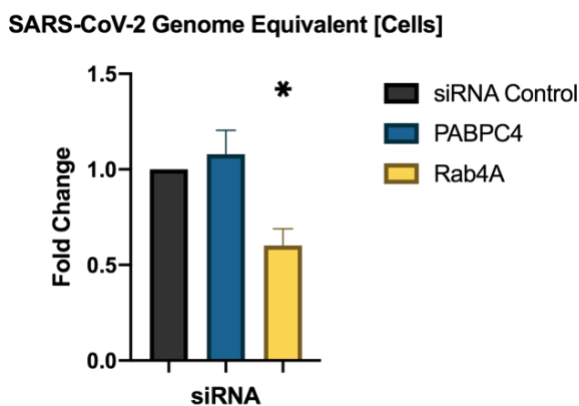


Figure 10: PABPC4 and Rab4A knockdown in SARS-CoV-2. TMRSS2 cells were transfected with either siRNA control, PABPC4, or Rab4A. Corresponding qRT-PCR using TaqMan OC43 probe.

4.4.11 G4 homology between SARS-CoV-2 variants

The understanding of G4 in SARS-CoV-2 and its variants holds significant importance in virology, particularly in the context of therapeutic development and viral evolution. G4s are highly conserved structures, present in SARS-CoV-2 and can serve as potential targets for antiviral therapy. Drugs or small molecules designed to bind and stabilize these structures could disrupt the normal lifecycle of the virus, leading to a reduction in its replication and spread. The homology of these structures across different variants can inform the development of broad-spectrum antivirals that are effective

against multiple strains of the virus. Studying the homology of G4ses among various SARS-CoV-2 variants can provide insights into the evolutionary trajectory of the virus. Variants with changes in these structures might exhibit different characteristics regarding infectivity, immune evasion, or drug resistance. Monitoring these changes can aid in predicting future trends in the virus's evolution and prepare more effective public health responses. G4ses in SARS-CoV-2 might interact with host cellular machinery. Deciphering these interactions can reveal how the virus exploits host cell processes for its benefit and how these interactions vary across different variants. This could lead to identifying novel strategies to disrupt these interactions and curb the infection.

There is a high homology of PQSs between all the SARS-CoV-2 variants compared to Wuhan-WA1 (Fig. 11 and Table 1). The Beta 20H, is characterized by a PQS deletion within the S RNA sequence. The S protein is a key component of the SARS-CoV-2 virus, as it plays a crucial role in the virus's ability to enter and infect human cells. It does so by binding to the ACE2 receptor on the surface of human cells^{20,80,109,110}. Mutations in the S protein, including deletions, can potentially alter the virus's infectiousness, its ability to evade the immune response, and even affect the efficacy of vaccines^{111,112}. Deletion in the S protein, along with other mutations, has been associated with increased transmissibility and a potential for immune escape¹¹³⁻¹¹⁶. This could suggest that the variant might be able to partly evade the immune protection granted by previous infection with other strains, or by vaccines designed based on the original strain of the virus.

The Delta 21A variant is characterized by several mutations that distinguish it from the original Wuhan-1 strain of SARS-CoV-2. One such mutation includes a deletion

in the RdRp, a key enzyme responsible for viral RNA replication. This deletion in the RdRp region could potentially contribute to the higher transmissibility observed in the Delta variant. The RdRp enzyme is crucial for the replication of the viral genome, and alterations in its structure or function can significantly impact the virus's replication efficiency. A deletion in this enzyme could lead to changes in the replication fidelity or speed, potentially enabling the virus to replicate more rapidly or efficiently. This, in turn, could facilitate faster spread of the virus from person to person, contributing to the heightened transmissibility seen with the Delta variant. It is important to note that viral transmissibility is influenced by a combination of genetic factors, and not solely by mutations in the RdRp^{117,118}. Other mutations in the spike protein and elsewhere in the Delta variant's genome also play significant roles in its ability to spread more easily compared to earlier strains like Wuhan-WA1. The N protein plays a crucial role in viral replication, genome packaging, and immune response modulation. Any modification, such as the addition of a potential PQS, could influence the nucleocapsid protein's structure and function. This could have downstream effects on the virus's ability to replicate efficiently, package its RNA, and evade the host immune system. Such changes in the nucleocapsid may also affect the virus's interaction with host cells and its overall pathogenicity.

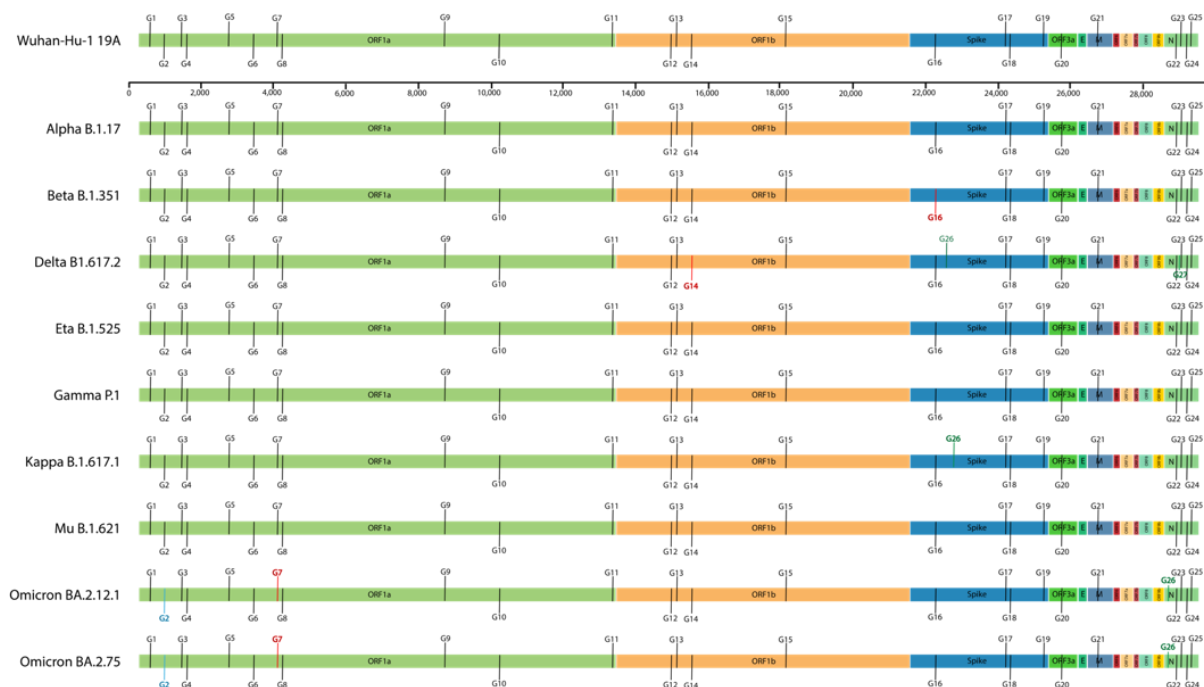


Figure 11: SARS-CoV-2 Variants. The schematic provides a detailed comparison of various SARS-CoV-2 variants against the original Wuhan-WA1 strain, focusing on the sequence positioning and alterations of PQS. Each PQS is labeled with a "G" followed by a number, representing its sequential order in the genome. PQS labels after G25 are marked in green text, denoting their addition in the variants compared to the Wuhan-WA1 strain. Deletions of PQS in the variants relative to Wuhan-WA1 are highlighted with red text, while an increase in the G-score of a particular PQS is indicated in blue. This schematic format allows for a clear and concise visual representation of the PQS variations and their implications across different SARS-CoV-2 variants.

Kappa 21B has an additional PQS the S region. The G4 alterations observed in the Omicron variants 22C and 22D, including a deletion in the Nsp3 region, an increase in the G-score of a G4 within the leader protein, and the addition of a potential PQS in the N sequence. Nsp3 is a key component of the virus's replication and immune evasion mechanisms, and changes in its structure due to G4 alterations could substantially impact

the virus's lifecycle¹¹⁹. The N protein plays a crucial role in viral replication, genome packaging, and immune response modulation. Any modification, such as the addition of a potential PQS, could influence the N protein's structure and function^{62,114}. This specific alteration might affect the virus's ability to replicate its RNA, potentially altering its infectivity and virulence. Furthermore, the G4 changes within the leader protein and the addition of a potential PQS in the N sequence could influence the synthesis of these critical viral components, affecting the virus's assembly, immune system interactions, and host cell entry.

G4 alterations are critical for understanding the virus's adaptive mechanisms, potentially providing insights into how SARS-CoV-2 is evolving in response to external pressures such as host immunity or therapeutic interventions. Furthermore, these variations could impact the development of targeted therapies, as they offer new potential drug targets. Additionally, understanding these changes is essential for assessing the continued efficacy of current vaccines and for guiding the development of future vaccines, underlining the need for ongoing genetic surveillance of SARS-CoV-2 variants.

Pango Lineage	Column1	B.1.1.7	B.1.351	B.1.617.2	B.1.525	P.1	B.1.617.1	B.1.621	BA.2.12.1	BA.2.75	Column2	Column3	Column4	Column5
WHO Label	Wuhan-WA1	Alpha 20I	Beta 20H	Delta 21A	Eta 21D	Gamma 20J	Kappa 21B	Mu	Omicron 22C	Omicron 22D	G4 #	G-Quadruplex Sequence [Wuhan-WA1]	G-Score	Location
	✓	✓	✓	✓	✓	✓	✓	✓	✓	✓	G1	GGCTTTGGAGACTCCGTGGAGGAGG	16	Leader Protein
	✓	✓	✓	✓	✓	✓	✓	✓	✓	✓	G2	GGTAATAAGGAGCTGGTGG	15	Leader Protein
	✓	✓	✓	✓	✓	✓	✓	✓	✓	✓	G3	GGTGGTCGCACATTTGCTTTGGAGG	6	Nsp2
	✓	✓	✓	✓	✓	✓	✓	✓	✓	✓	G4	GGTGTGTTGGAGAGGTTCCGAAGG	18	Nsp2
	✓	✓	✓	✓	✓	✓	✓	✓	✓	✓	G5	GGCGGTGCACCAACAAGGTTACTTTTGG	10	Nsp2-Nsp3
	✓	✓	✓	✓	✓	✓	✓	✓	✓	✓	G6	GGAGGAGGTGTTGCAGG	15	Nsp3
	✓	✓	✓	✓	✓	✓	✓	✓	✓	✓	G7	GGTTAACCCTACTAAAAGCTGGTGG	6	Nsp3
	✓	✓	✓	✓	✓	✓	✓	✓	✓	✓	G8	GGTTTAATGGTTACACTGTAGAGGAGG	10	Nsp3
	✓	✓	✓	✓	✓	✓	✓	✓	✓	✓	G9	GGATACAAGGCTATTGATGGTGG	14	Nsp4
	✓	✓	✓	✓	✓	✓	✓	✓	✓	✓	G10	GGCTGGTAATGTTCAACTCAGGGTATTGG	9	C3-Like Proteinase
	✓	✓	✓	✓	✓	✓	✓	✓	✓	✓	G11	GGTATGSGAAGGTTATGG	19	Nsp10
	✓	✓	✓	✓	✓	✓	✓	✓	✓	✓	G12	GGTTTTCCATTAAATAAGGGGTAAGG	4	RdRp
	✓	✓	✓	✓	✓	✓	✓	✓	✓	✓	G13	GGAAACAAGCAATTCTATGGTGTGG	6	RdRp
	✓	✓	✓	✓	✓	✓	✓	✓	✓	✓	G14	GGCGTTTCACTATATGTTAAACAGGTGG	3	RdRp
	✓	✓	✓	✓	✓	✓	✓	✓	✓	✓	G15	GGATTGGCTTCGATGTCAGGCGG	9	Exonuclease
	✓	✓	✓	✓	✓	✓	✓	✓	✓	✓	G16	GGTGATTCTTCTCAGGTTGGACAGCTGG	10	Spike
	✓	✓	✓	✓	✓	✓	✓	✓	✓	✓	G17	GGTTGGTGGTAATTATAATTACCGG	8	Spike
	✓	✓	✓	✓	✓	✓	✓	✓	✓	✓	G18	GGTTGGACCTTTGGTGACGG	17	Spike
	✓	✓	✓	✓	✓	✓	✓	✓	✓	✓	G19	GGCTATAGGTTTAATGGTATTGG	19	Spike
	✓	✓	✓	✓	✓	✓	✓	✓	✓	✓	G20	GGCCATGTACATTTGGCTAGG	17	ORF3a
	✓	✓	✓	✓	✓	✓	✓	✓	✓	✓	G21	GGTGGTTACTGAAAAATGGAACTCTGG	8	Membrane
	✓	✓	✓	✓	✓	✓	✓	✓	✓	✓	G22	GGATCACCGGTGGAAATGCTATCGCAATGG	7	Nucleocapsid
	✓	✓	✓	✓	✓	✓	✓	✓	✓	✓	G23	GGCTTACGCGAAGGGAGCAGAGGCGG	9	Nucleocapsid
	✓	✓	✓	✓	✓	✓	✓	✓	✓	✓	G24	GGCTGGCAATGGCGG	18	Nucleocapsid
	✓	✓	✓	✓	✓	✓	✓	✓	✓	✓	G25	GGAAATTTGGGGACCAGG	14	Nucleocapsid
				Spike			Spike		Nuc	Nuc	G26	Variable	Variable	Variable
				Nuc							G27	Variable	Variable	Variable

Table 1: PQSs within SARS-CoV-2 Variants

The table provides a comparative analysis between the Wuhan-WA1 strain and various SARS-CoV-2 variants, focusing on the conservation and variation of PQS. A check mark signifies a conserved PQS between the strains. A blue box containing a number indicates that the corresponding PQS in the variant has an increased G-score, with the number denoting the magnitude of this increase. A red “X” marks the deletion of a PQS in a variant compared to the Wuhan-WA1 strain. Conversely, a green box highlights the addition of a new PQS in a variant. This comparison is based on the analysis of 10 sequences from each variant, from which a consensus sequence for each variant was derived. This approach ensures a comprehensive and representative overview of the PQS variations among the SARS-CoV-2 variants.

4.5 Discussion

The regulation of coronaviruses through G4 represents a fascinating and increasingly relevant area of virological research, particularly considering the ongoing SARS-CoV-2 pandemic. G4s are unique nucleic acid structures formed by guanine-rich sequences in DNA and RNA^{38,120,121}. They have been identified in various regions of the coronavirus genome, including those coding for critical proteins and regulatory elements⁴⁵. The presence and alteration of these structures can have significant implications for virus replication, pathogenicity, and host interaction¹²². The identification and development of compounds that can target and stabilize G4 structures is of great importance in antiviral research. Consequently, we selected M-Blue, an FDA-approved drug known for its efficacy in treating methemoglobinemia and its low toxicity profile, for our investigations⁵¹. We focused on testing this compound's effects on OC43, a less severe member of the *betacoronavirus* family. This approach allows us to explore the potential of M-Blue as a G4-targeting agent in a relatively safe and controlled context,

setting the groundwork for its possible application against more pathogenic coronaviruses, including *SARS-CoV-2*.

M-Blue has been widely recognized for its role as an electron transporter, particularly evident in its ability to accelerate the reduction rate of cytochrome c in isolated mitochondria¹²³⁻¹²⁶. This process effectively enhances cellular oxygen uptake while concurrently reducing anaerobic glycolysis, both in laboratory settings and living organisms. Moreover, prolonged exposure to MB has been found to boost both the activity and expression of mitochondrial complex IV, further highlighting its impact on cellular bioenergetics^{127,128}. In its oxidized state, M-Blue (M-Blue-ox), as a phenothiazinium molecule, absorbs light in the 600-700nm wavelength range while transmitting light from 350-600nm¹²⁹. Conversely, when reduced to leucomethylene blue (leucoMB), it becomes colorless and ceases to absorb visible light. This reduced form of M-Blue is uncharged and lipophilic, diffusing effortlessly across cellular plasma membranes. Once inside the cell, leucoMB undergoes re-oxidation and becomes sequestered intracellularly¹³⁰. Coronavirus envelopes are comprised of a lipid bilayer embedded with structural proteins, which are derived from the membranes of the endoplasmic reticulum-Golgi intermediate compartment in the host cell¹³¹. A plausible mechanism for how M-Blue might inhibit viral entry is that when in solution and upon adding the virus, M-Blue penetrates the coronavirus membrane. Subsequently, it undergoes a redox reaction within this environment. M-Blue embeds itself between nucleic acid strands, and upon exposure to light, it becomes excited, leading to the generation of highly reactive singlet oxygen. This reactive oxygen species specifically targets and oxidizes guanosine bases, resulting in the cleavage of nucleic acid strands¹³².

Alternatively, there is the possibility that M-Blue can disrupt the protein-protein interaction and disrupt viral entry, as we see for OC43 in Figure 4A and SARS-CoV-2 in Figure 9. Interestingly, it was found that the binding of M-Blue to the receptor binding domain (RBD) affects the interaction of the S protein with the ACE2 receptor and, in turn, reduces viral infectivity. Our results indicate that M-blue can reduce viral entry for *betacoronaviruses* OC43 and SARS-CoV-2.

During the infection, coronaviruses instigate an imbalance by simultaneously amplifying the production of reactive oxygen species (ROS) and diminishing the host's antioxidant responses. This imbalance escalates redox stress within the cells. The production of mitochondrial reactive oxygen species (mito-ROS) is stimulated during coronavirus infections, alongside suppression of antiapoptotic pathways like Nrf2¹³³. This excessive generation of ROS can compromise mitochondrial function, leading to the apoptosis of lung epithelial cells¹³⁴. The heightened levels of mito-ROS are also directly linked to acute lung tissue damage in mouse models of viral infections¹³⁵. The heightened redox stress, in turn, undermines the host's antiviral defenses, exacerbating virus-induced inflammation and triggering increased rates of apoptosis¹³³. This intricate interplay between virus-triggered redox imbalances and the subsequent weakening of host immune responses is a key factor in the progression and severity of the infection¹³³. As previously mentioned, leucoMB is reduced and can act as an antioxidant. LeucoMB antioxidative properties have been shown to improve mitochondrial function and stop the ROS-mitochondrial damage cycle^{136,137}. This could explain why when treated with M-Blue, there is a drastic drop in viral genome copies detected across all coronaviruses tested, as seen in our previous figures. Alternatively, M-Blue has been shown to bind to G4

structures and there are several PQSs in the tested coronaviruses, illustrated in Figure 1^{49,138}. qPCR results also revealed a reduction in both, the level of viral genome copies and SG fractions, indicating lower virus replication and decreased translational capacity, respectively. Nevertheless, we found that TMPyP4 and Braco19, s G4-stabilizers, have some capacity to attenuate coronavirus replication. OC43 has the highest homology, 68.93%, to SARS-CoV-2 and this can account for the similar pattern in virus reduction¹³⁹.

Mass spectrophotometry results identified PABPC4 and Rab4A interacting with a G4 in OC43 RNA. PABPC4 has been suggested to induce mitochondrial activity during metabolic stress⁹⁷. Given that coronaviruses produce mito-ROS, the downregulation of PABPC4 could lead to a further decrease in mitochondrial activity. This may create an ideal environment for coronavirus replication. Rab4A is known to directly influence the process of autophagy, as well as in response to the stretching of cell membranes¹⁰⁵. Therefore, knocking down Rab4A can lead to the prevention of viral egress. Rab4A plays a critical role in regulating autophagy, a cellular process that involves the degradation and recycling of cellular components, as well as responding to mechanical stimuli such as the stretching of cell membranes^{104,140}. This protein is involved in various intracellular trafficking processes, including transporting materials to and from the cell membrane and autophagosomes, which are key structures in autophagy. The direct involvement of Rab4A in autophagy suggests that it may influence how cells respond to and manage stress, including stress induced by viral infections¹⁰⁵. Additionally, its role in response to membrane stretching could be significant in viral infection, as many viruses rely on alterations in cellular membranes for their replication and egress¹⁴¹. Consequently, the knockdown of Rab4A can have important implications for viral life cycles, particularly in

the stages of virus assembly, maturation, and release (egress) from the host cell. By reducing Rab4A levels, the cellular pathways, and mechanisms essential for the efficient egress of viruses from infected cells could potentially be disrupted¹⁴². This disruption could lead to the retention of viral particles within the cells, effectively impeding the spread of the virus to neighboring cells and potentially limiting the overall progression of the viral infection.

The highly conserved nature of G4 across various organisms renders them an intriguing and unique target for therapeutic intervention. This conservation is particularly relevant in viral pathogens like SARS-CoV-2, where multiple variants share nearly identical PQSs (Fig. 11). Such uniformity across different strains suggests that a single G4-stabilizing compound could effectively target and regulate various coronavirus variants. G4-stabilizers bind to these unique nucleic acid structures, thereby influencing the virus's ability to replicate and express its genes^{47,143}. The stabilization of G4 can lead to changes in the viral genome's structure and function, potentially interfering with critical processes such as the transcription and replication of viral RNA. Conversely, destabilizing these structures can also have significant impacts, potentially exposing previously inaccessible regions of the viral genome to the cellular machinery, leading to altered gene expression patterns. G4-stabilizers could, therefore, provide a novel means of controlling viral activity, offering a broad-spectrum approach against different coronavirus strains. This strategy could be particularly valuable in managing the emergence of new variants, as the conserved nature of PQSs may allow for continued efficacy despite other genetic changes in the virus.

4.8 References

1. Organization WH. Novel Coronavirus – China. 2020.
2. Wu F, Zhao S, Yu B, et al. A new coronavirus associated with human respiratory disease in China. *Nature*. 2020/03/01 2020;579(7798):265-269. doi:10.1038/s41586-020-2008-3
3. About COVID-19. <https://www.cdc.gov/coronavirus/2019-ncov/cdcresponse/about-COVID-19.html>
4. Medicine JHUo. COVID-19 MAP. <https://coronavirus.jhu.edu/map.html>
5. Organization WH. WHO Director-General's remarks at the media briefing on 2019-nCoV on 11 February 2020. 2020.
6. Organization WH. WHO Director-General's opening remarks at the media briefing on COVID-19 - 11 March 2020. <https://www.who.int/director-general/speeches/detail/who-director-general-s-opening-remarks-at-the-media-briefing-on-covid-19---11-march-2020>
7. Andrew T. Chan MD, M.P.H., and John S. Brownstein, Ph.D. Putting the Public Back in Public Health — Surveying Symptoms of Covid-19. Massachusetts Medical Society; 2020.
8. Lovato A, de Filippis C. Clinical Presentation of COVID-19: A Systematic Review Focusing on Upper Airway Symptoms. *Ear Nose Throat J*. Nov 2020;99(9):569-576. doi:10.1177/0145561320920762
9. Zaim S, Chong JH, Sankaranarayanan V, Harky A. COVID-19 and Multiorgan Response. *Current problems in cardiology*. 2020;45(8):100618-100618. doi:10.1016/j.cpcardiol.2020.100618
10. Gorbalenya AE, Baker SC, Baric RS, et al. The species Severe acute respiratory syndrome-related coronavirus: classifying 2019-nCoV and naming it SARS-CoV-2. *Nature Microbiology*. 2020/04/01 2020;5(4):536-544. doi:10.1038/s41564-020-0695-z
11. Corman VM, Muth D, Niemeyer D, Drosten C. Hosts and Sources of Endemic Human Coronaviruses. *Adv Virus Res*. 2018;100:163-188. doi:10.1016/bs.aivir.2018.01.001
12. Mesel-Lemoine M, Millet J, Vidalain PO, et al. A human coronavirus responsible for the common cold massively kills dendritic cells but not monocytes. *J Virol*. Jul 2012;86(14):7577-87. doi:10.1128/jvi.00269-12
13. Gagneur A, Sizun J, Vallet S, Legr MC, Picard B, Talbot PJ. Coronavirus-related nosocomial viral respiratory infections in a neonatal and paediatric intensive care unit: a prospective study. *J Hosp Infect*. May 2002;51(1):59-64. doi:10.1053/jhin.2002.1179
14. Peeri NC, Shrestha N, Rahman MS, et al. The SARS, MERS and novel coronavirus (COVID-19) epidemics, the newest and biggest global health threats: what lessons have we learned? *Int J Epidemiol*. Jun 1 2020;49(3):717-726. doi:10.1093/ije/dyaa033
15. Pustake M, Tambolkar I, Giri P, Gandhi C. SARS, MERS and CoVID-19: An overview and comparison of clinical, laboratory and radiological features. *J Family Med Prim Care*. Jan 2022;11(1):10-17. doi:10.4103/jfmprc.jfmprc_839_21

16. Huang C, Wang Y, Li X, et al. Clinical features of patients infected with 2019 novel coronavirus in Wuhan, China. *Lancet*. Feb 15 2020;395(10223):497-506. doi:10.1016/s0140-6736(20)30183-5
17. Collins AR. HLA class I antigen serves as a receptor for human coronavirus OC43. *Immunol Invest*. Mar 1993;22(2):95-103. doi:10.3109/08820139309063393
18. Krempl C, Schultze B, Herrler G. Analysis of cellular receptors for human coronavirus OC43. *Adv Exp Med Biol*. 1995;380:371-4. doi:10.1007/978-1-4615-1899-0_60
19. Hoffmann M, Kleine-Weber H, Schroeder S, et al. SARS-CoV-2 Cell Entry Depends on ACE2 and TMPRSS2 and Is Blocked by a Clinically Proven Protease Inhibitor. *Cell*. Apr 16 2020;181(2):271-280.e8. doi:10.1016/j.cell.2020.02.052
20. Li W, Moore MJ, Vasilieva N, et al. Angiotensin-converting enzyme 2 is a functional receptor for the SARS coronavirus. *Nature*. Nov 27 2003;426(6965):450-4. doi:10.1038/nature02145
21. Liu DX, Liang JQ, Fung TS. Human Coronavirus-229E, -OC43, -NL63, and -HKU1 (Coronaviridae). *Encyclopedia of Virology*. Copyright © 2021 Elsevier Ltd. All rights reserved.; 2021:428-40.
22. Liu G, Du W, Sang X, et al. RNA G-quadruplex in TMPRSS2 reduces SARS-CoV-2 infection. *Nature Communications*. 2022/03/17 2022;13(1):1444. doi:10.1038/s41467-022-29135-5
23. Panera N, Tozzi AE, Alisi A. The G-Quadruplex/Helicase World as a Potential Antiviral Approach Against COVID-19. *Drugs*. 2020/07/01 2020;80(10):941-946. doi:10.1007/s40265-020-01321-z
24. Nazia P, Amen S, Seunghye Cho and Kyeong Kyu K. Computational Approaches to Predict the Non-canonical DNAs. *Current Bioinformatics*. 2019;14(6):470-479. doi:<http://dx.doi.org/10.2174/1574893614666190126143438>
25. Bochman ML, Paeschke K, Zakian VA. DNA secondary structures: stability and function of G-quadruplex structures. *Nat Rev Genet*. Nov 2012;13(11):770-80. doi:10.1038/nrg3296
26. Dhakal S, Cui Y, Koirala D, et al. Structural and mechanical properties of individual human telomeric G-quadruplexes in molecularly crowded solutions. *Nucleic Acids Res*. Apr 1 2013;41(6):3915-23. doi:10.1093/nar/gkt038
27. Biffi G, Tannahill D, McCafferty J, Balasubramanian S. Quantitative visualization of DNA G-quadruplex structures in human cells. *Nature Chemistry*. 2013/03/01 2013;5(3):182-186. doi:10.1038/nchem.1548
28. Chambers VS, Marsico G, Boutell JM, Di Antonio M, Smith GP, Balasubramanian S. High-throughput sequencing of DNA G-quadruplex structures in the human genome. *Nat Biotechnol*. Aug 2015;33(8):877-81. doi:10.1038/nbt.3295
29. Howard FB, Miles HT. Poly(inosinic acid) helices: essential chelation of alkali metal ions in the axial channel. *Biochemistry*. Dec 21 1982;21(26):6736-45. doi:10.1021/bi00269a019
30. Sundquist WI, Klug A. Telomeric DNA dimerizes by formation of guanine tetrads between hairpin loops. *Nature*. Dec 14 1989;342(6251):825-9. doi:10.1038/342825a0

31. Bouaziz S, Kettani A, Patel DJ. A K cation-induced conformational switch within a loop spanning segment of a DNA quadruplex containing G-G-G-C repeats. *Journal of molecular biology*. 1998/09// 1998;282(3):637-652. doi:10.1006/jmbi.1998.2031
32. Pandey S, Agarwala P, Maiti S. Effect of Loops and G-Quartets on the Stability of RNA G-Quadruplexes. *The Journal of Physical Chemistry B*. 2013/06/13 2013;117(23):6896-6905. doi:10.1021/jp401739m
33. Millevoi S, Moine H, Vagner S. G-quadruplexes in RNA biology. *Wiley Interdiscip Rev RNA*. Jul-Aug 2012;3(4):495-507. doi:10.1002/wrna.1113
34. Bhattacharyya D, Mirihana Arachchilage G, Basu S. Metal Cations in G-Quadruplex Folding and Stability. *Frontiers in chemistry*. 2016;4:38-38. doi:10.3389/fchem.2016.00038
35. Kharel P, Balaratnam S, Beals N, Basu S. The role of RNA G-quadruplexes in human diseases and therapeutic strategies. *Wiley Interdiscip Rev RNA*. Jan 2020;11(1):e1568. doi:10.1002/wrna.1568
36. Novoseltseva AA, Ivanov NM, Novikov RA, et al. Structural and Functional Aspects of G-Quadruplex Aptamers Which Bind a Broad Range of Influenza A Viruses. *Biomolecules*. 2020;10(1):119. doi:10.3390/biom10010119
37. Puig Lombardi E, Londoño-Vallejo A. A guide to computational methods for G-quadruplex prediction. *Nucleic Acids Research*. 2020;48(1):1-15. doi:10.1093/nar/gkz1097
38. Ruggiero E, Richter SN. G-quadruplexes and G-quadruplex ligands: targets and tools in antiviral therapy. *Nucleic Acids Res*. Apr 20 2018;46(7):3270-3283. doi:10.1093/nar/gky187
39. Fay MM, Lyons SM, Ivanov P. RNA G-Quadruplexes in Biology: Principles and Molecular Mechanisms. *Journal of molecular biology*. Jul 7 2017;429(14):2127-2147. doi:10.1016/j.jmb.2017.05.017
40. Maizels N. G4-associated human diseases. *EMBO reports*. 2015/08/01 2015;16(8):910-922. doi:10.15252/embr.201540607
41. Ou TM, Lu YJ, Tan JH, Huang ZS, Wong KY, Gu LQ. G-quadruplexes: targets in anticancer drug design. *ChemMedChem*. May 2008;3(5):690-713. doi:10.1002/cmdc.200700300
42. White EW, Tanious F, Ismail MA, et al. Structure-specific recognition of quadruplex DNA by organic cations: influence of shape, substituents and charge. *Biophys Chem*. Mar 2007;126(1-3):140-53. doi:10.1016/j.bpc.2006.06.006
43. Kikin O, D'Antonio L, Bagga PS. QGRS Mapper: a web-based server for predicting G-quadruplexes in nucleotide sequences. *Nucleic Acids Research*. 2006;34(suppl_2):W676-W682. doi:10.1093/nar/gkl253
44. Gonzalez V, Guo K, Hurley L, Sun D. Identification and characterization of nucleolin as a c-myc G-quadruplex-binding protein. *J Biol Chem*. Aug 28 2009;284(35):23622-35. doi:10.1074/jbc.M109.018028
45. Ji D, Juhas M, Tsang CM, Kwok CK, Li Y, Zhang Y. Discovery of G-quadruplex-forming sequences in SARS-CoV-2. *Briefings in Bioinformatics*. 2021;22(2):1150-1160. doi:10.1093/bib/bbaa114

46. Dabral P, Babu J, Zareie A, Verma SC. LANA and hnRNP A1 Regulate the Translation of LANA mRNA through G-Quadruplexes. *J Virol*. Jan 17 2020;94(3)doi:10.1128/JVI.01508-19
47. Artusi S, Ruggiero E, Nadai M, et al. Antiviral Activity of the G-Quadruplex Ligand TMPyP4 against Herpes Simplex Virus-1. *Viruses*. 2021;13(2). doi:10.3390/v13020196
48. Molnár OR, Végh A, Somkuti J, Smeller L. Characterization of a G-quadruplex from hepatitis B virus and its stabilization by binding TMPyP4, BRACO19 and PhenDC3. *Scientific Reports*. 2021/12/01 2021;11(1):23243. doi:10.1038/s41598-021-02689-y
49. Chan DS, Yang H, Kwan MH, et al. Structure-based optimization of FDA-approved drug methylene blue as a c-myc G-quadruplex DNA stabilizer. *Biochimie*. Jun 2011;93(6):1055-64. doi:10.1016/j.biochi.2011.02.013
50. FDA. HIGHLIGHTS OF PRESCRIBING INFORMATION PROVAYBLUETM (methylene blue) injection, for intravenous use Initial U.S. Approval: 2016. FDA2016.
51. do Nascimento TS, Pereira RO, de Mello HL, Costa J. Methemoglobinemia: from diagnosis to treatment. *Rev Bras Anestesiol*. Nov-Dec 2008;58(6):651-64. doi:10.1590/s0034-70942008000600011
52. Nedu M-E, Tertis M, Cristea C, Georgescu AV. Comparative Study Regarding the Properties of Methylene Blue and Proflavine and Their Optimal Concentrations for In Vitro and In Vivo Applications. *Diagnostics*. 2020;10(4). doi:10.3390/diagnostics10040223
53. Multum C. Methylene Blue (injection). Drugs.com. <https://www.drugs.com/mtm/methylene-blue-injection.html>
54. Gendrot M, Andreani J, Duflot I, et al. Methylene blue inhibits the replication of SARS-Cov-2 in vitro. *International Journal of Antimicrobial Agents*. 2020:106202. doi:10.1016/j.ijantimicag.2020.106202
55. Scigliano G, Scigliano GA. Methylene blue in covid-19. *Med Hypotheses*. Jan 2021;146:110455. doi:10.1016/j.mehy.2020.110455
56. Cagno V, Medaglia C, Cerny A, et al. Methylene Blue has a potent antiviral activity against SARS-CoV-2 and H1N1 influenza virus in the absence of UV-activation in vitro. *Scientific Reports*. 2021/07/12 2021;11(1):14295. doi:10.1038/s41598-021-92481-9
57. Schneider Jr JE, Tabatabaie T, Mardt L, et al. Potential Mechanisms of Photodynamic Inactivation of Virus by Methylene Blue_{SEP}^[1]. RNA-Protein Crosslinks and Other Oxidative Lesions in Q β Bacteriophage. <https://doi.org/10.1111/j.1751-1097.1998.tb05209.x>. *Photochemistry and Photobiology*. 1998/03/01 1998;67(3):350-357. doi:<https://doi.org/10.1111/j.1751-1097.1998.tb05209.x>
58. Lau SK, Lee P, Tsang AK, et al. Molecular epidemiology of human coronavirus OC43 reveals evolution of different genotypes over time and recent emergence of a novel genotype due to natural recombination. *J Virol*. Nov 2011;85(21):11325-37. doi:10.1128/JVI.05512-11

59. Jean A, Quach C, Yung A, Semret M. Severity and Outcome Associated With Human Coronavirus OC43 Infections Among Children. *The Pediatric Infectious Disease Journal*. 2013;32(4)
60. Lau SKP, Li KSM, Li X, Tsang KY, Sridhar S, Woo PCY. Fatal Pneumonia Associated With a Novel Genotype of Human Coronavirus OC43. *Front Microbiol*. 2021;12:795449. doi:10.3389/fmicb.2021.795449
61. Jacomy H, Talbot PJ. Vacuolating encephalitis in mice infected by human coronavirus OC43. *Virology*. Oct 10 2003;315(1):20-33. doi:10.1016/s0042-6822(03)00323-4
62. Zhao C, Qin G, Niu J, et al. Targeting RNA G-Quadruplex in SARS-CoV-2: A Promising Therapeutic Target for COVID-19? <https://doi.org/10.1002/anie.202011419>. *Angewandte Chemie International Edition*. 2021/01/04 2021;60(1):432-438. doi:<https://doi.org/10.1002/anie.202011419>
63. Perrone R, Butovskaya E, Daelemans D, Palu G, Pannecouque C, Richter SN. Anti-HIV-1 activity of the G-quadruplex ligand BRACO-19. *J Antimicrob Chemother*. Dec 2014;69(12):3248-58. doi:10.1093/jac/dku280
64. Ravichandran S, Kim YE, Bansal V, et al. Genome-wide analysis of regulatory G-quadruplexes affecting gene expression in human cytomegalovirus. *PLoS Pathog*. Sep 2018;14(9):e1007334. doi:10.1371/journal.ppat.1007334
65. Carvalho J, Lopes-Nunes J, Campello MPC, et al. Human Papillomavirus G-Rich Regions as Potential Antiviral Drug Targets. *Nucleic Acid Ther*. Feb 2021;31(1):68-81. doi:10.1089/nat.2020.0869
66. Wang SR, Min YQ, Wang JQ, et al. A highly conserved G-rich consensus sequence in hepatitis C virus core gene represents a new anti-hepatitis C target. *Sci Adv*. Apr 2016;2(4):e1501535. doi:10.1126/sciadv.1501535
67. Majee P, Pattnaik A, Sahoo BR, et al. Inhibition of Zika virus replication by G-quadruplex-binding ligands. *Molecular Therapy - Nucleic Acids*. 2021/03/05/ 2021;23:691-701. doi:<https://doi.org/10.1016/j.omtn.2020.12.030>
68. Lv L, Zhang L. Characterization of G-Quadruplexes in Enterovirus A71 Genome and Their Interaction with G-Quadruplex Ligands. *Microbiol Spectr*. Jun 29 2022;10(3):e0046022. doi:10.1128/spectrum.00460-22
69. Zhang R, Xiao K, Gu Y, Liu H, Sun X. Whole Genome Identification of Potential G-Quadruplexes and Analysis of the G-Quadruplex Binding Domain for SARS-CoV-2. *Front Genet*. 2020;11:587829. doi:10.3389/fgene.2020.587829
70. Bezzi G, Piga EJ, Binolfi A, Armas P. CNBP Binds and Unfolds In Vitro G-Quadruplexes Formed in the SARS-CoV-2 Positive and Negative Genome Strands. *Int J Mol Sci*. Mar 5 2021;22(5)doi:10.3390/ijms22052614
71. Cui H, Zhang L. G-Quadruplexes Are Present in Human Coronaviruses Including SARS-CoV-2. *Front Microbiol*. 2020;11:567317. doi:10.3389/fmicb.2020.567317
72. Qin G, Zhao C, Liu Y, et al. RNA G-quadruplex formed in SARS-CoV-2 used for COVID-19 treatment in animal models. *Cell Discovery*. 2022/09/06 2022;8(1):86. doi:10.1038/s41421-022-00450-x
73. Groelly FJ, Porru M, Zimmer J, et al. Anti-tumoural activity of the G-quadruplex ligand pyridostatin against BRCA1/2-deficient tumours.

<https://doi.org/10.15252/emmm.202114501>. *EMBO Molecular Medicine*. 2022/03/07 2022;14(3):e14501. doi:<https://doi.org/10.15252/emmm.202114501>

74. Kosiol N, Juranek S, Brossart P, Heine A, Paeschke K. G-quadruplexes: a promising target for cancer therapy. *Molecular Cancer*. 2021/02/25 2021;20(1):40. doi:10.1186/s12943-021-01328-4
75. Asamitsu S, Obata S, Yu Z, Bando T, Sugiyama H. Recent Progress of Targeted G-Quadruplex-Preferred Ligands Toward Cancer Therapy. *Molecules*. Jan 24 2019;24(3)doi:10.3390/molecules24030429
76. Schirmer RH, Coulibaly B, Stich A, et al. Methylene blue as an antimalarial agent. *Redox Rep*. 2003;8(5):272-5. doi:10.1179/135100003225002899
77. Grayling M, Deakin CD. Methylene blue during cardiopulmonary bypass to treat refractory hypotension in septic endocarditis. *J Thorac Cardiovasc Surg*. Feb 2003;125(2):426-7. doi:10.1067/mtc.2003.140
78. Kofidis T, Strüber M, Wilhelmi M, et al. Reversal of severe vasoplegia with single-dose methylene blue after heart transplantation. *J Thorac Cardiovasc Surg*. Oct 2001;122(4):823-4. doi:10.1067/mtc.2001.115153
79. Evora PR, Ribeiro PJ, de Andrade JC. Methylene blue administration in SIRS after cardiac operations. *Ann Thorac Surg*. 1997:1212-3. vol. 4.
80. Bojadzic D, Alcazar O, Buchwald P. Methylene Blue Inhibits the SARS-CoV-2 Spike–ACE2 Protein-Protein Interaction—a Mechanism that can Contribute to its Antiviral Activity Against COVID-19. Brief Research Report. *Frontiers in Pharmacology*. 2021-January-13 2021;11doi:10.3389/fphar.2020.600372
81. Sola I, Almazán F, Zúñiga S, Enjuanes L. Continuous and Discontinuous RNA Synthesis in Coronaviruses. *Annu Rev Virol*. Nov 2015;2(1):265-88. doi:10.1146/annurev-virology-100114-055218
82. van Vliet AL, Smits SL, Rottier PJ, de Groot RJ. Discontinuous and non-discontinuous subgenomic RNA transcription in a nidovirus. *Embo j*. Dec 2 2002;21(23):6571-80. doi:10.1093/emboj/cdf635
83. Dorokhov YL, Ivanov PA, Komarova TV, Skulachev MV, Atabekov JG. An internal ribosome entry site located upstream of the crucifer-infecting tobamovirus coat protein (CP) gene can be used for CP synthesis in vivo. *J Gen Virol*. Sep 2006;87(Pt 9):2693-2697. doi:10.1099/vir.0.82095-0
84. Pasternak AO, Spaan WJM, Snijder EJ. Nidovirus transcription: how to make sense...? *J Gen Virol*. Jun 2006;87(Pt 6):1403-1421. doi:10.1099/vir.0.81611-0
85. Yang Y, Hussain S, Wang H, Ke M, Guo D. Translational control of the subgenomic RNAs of severe acute respiratory syndrome coronavirus. *Virus Genes*. Aug 2009;39(1):10-8. doi:10.1007/s11262-009-0357-y
86. Modrow S, Falke D, Truyen U, Schätzl H. Viruses with Single-Stranded, Positive-Sense RNA Genomes. *Molecular Virology*. © Springer-Verlag Berlin Heidelberg 2013.; 2013:185-349.
87. Kocic G, Hillen HS, Tegunov D, et al. Mechanism of SARS-CoV-2 polymerase stalling by remdesivir. *Nature Communications*. 2021/01/12 2021;12(1):279. doi:10.1038/s41467-020-20542-0
88. Kühn U, Wahle E. Structure and function of poly(A) binding proteins. *Biochim Biophys Acta*. May 25 2004;1678(2-3):67-84. doi:10.1016/j.bbaexp.2004.03.008

89. Kumar GR, Shum L, Glaunsinger BA. Importin alpha-mediated nuclear import of cytoplasmic poly(A) binding protein occurs as a direct consequence of cytoplasmic mRNA depletion. *Mol Cell Biol.* Aug 2011;31(15):3113-25. doi:10.1128/mcb.05402-11
90. Gorgoni B, Gray NK. The roles of cytoplasmic poly(A)-binding proteins in regulating gene expression: a developmental perspective. *Brief Funct Genomic Proteomic.* Aug 2004;3(2):125-41. doi:10.1093/bfgp/3.2.125
91. Burgess HM, Richardson WA, Anderson RC, Salaun C, Graham SV, Gray NK. Nuclear relocalisation of cytoplasmic poly(A)-binding proteins PABP1 and PABP4 in response to UV irradiation reveals mRNA-dependent export of metazoan PABPs. *J Cell Sci.* Oct 1 2011;124(Pt 19):3344-55. doi:10.1242/jcs.087692
92. Mangus DA, Evans MC, Jacobson A. Poly(A)-binding proteins: multifunctional scaffolds for the post-transcriptional control of gene expression. *Genome Biol.* 2003;4(7):223. doi:10.1186/gb-2003-4-7-223
93. Fabian MR, Mathonnet G, Sundermeier T, et al. Mammalian miRNA RISC recruits CAF1 and PABP to affect PABP-dependent deadenylation. *Mol Cell.* Sep 24 2009;35(6):868-80. doi:10.1016/j.molcel.2009.08.004
94. Tsai TL, Lin CH, Lin CN, Lo CY, Wu HY. Interplay between the Poly(A) Tail, Poly(A)-Binding Protein, and Coronavirus Nucleocapsid Protein Regulates Gene Expression of Coronavirus and the Host Cell. *J Virol.* Dec 1 2018;92(23)doi:10.1128/jvi.01162-18
95. Spagnolo JF, Hogue BG. Host protein interactions with the 3' end of bovine coronavirus RNA and the requirement of the poly(A) tail for coronavirus defective genome replication. *J Virol.* Jun 2000;74(11):5053-65. doi:10.1128/jvi.74.11.5053-5065.2000
96. Yang H, Duckett CS, Lindsten T. iPABP, an inducible poly(A)-binding protein detected in activated human T cells. *Mol Cell Biol.* Dec 1995;15(12):6770-6. doi:10.1128/mcb.15.12.6770
97. Oliveira AG, Oliveira LD, Cruz MV, et al. Interaction between poly(A)-binding protein PABPC4 and nuclear receptor corepressor NCoR1 modulates a metabolic stress response. *J Biol Chem.* Jun 2023;299(6):104702. doi:10.1016/j.jbc.2023.104702
98. Pfeffer SR. Unsolved mysteries in membrane traffic. *Annu Rev Biochem.* 2007;76:629-45. doi:10.1146/annurev.biochem.76.061705.130002
99. Pfeffer SR. GTP-binding proteins in intracellular transport. *Trends Cell Biol.* Feb 1992;2(2):41-6. doi:10.1016/0962-8924(92)90161-f
100. Pereira-Leal JB, Seabra MC. The mammalian Rab family of small GTPases: definition of family and subfamily sequence motifs suggests a mechanism for functional specificity in the Ras superfamily. *J Mol Biol.* Aug 25 2000;301(4):1077-87. doi:10.1006/jmbi.2000.4010
101. Mohrmann K, Gerez L, Oorschot V, Klumperman J, van der Sluijs P. Rab4 function in membrane recycling from early endosomes depends on a membrane to cytoplasm cycle. *J Biol Chem.* Aug 30 2002;277(35):32029-35. doi:10.1074/jbc.M203064200
102. van der Sluijs P, Hull M, Webster P, Mâle P, Goud B, Mellman I. The small GTP-binding protein rab4 controls an early sorting event on the endocytic pathway. *Cell.* Sep 4 1992;70(5):729-40. doi:10.1016/0092-8674(92)90307-x

103. Talaber G, Miklossy G, Oaks Z, et al. HRES-1/Rab4 promotes the formation of LC3(+) autophagosomes and the accumulation of mitochondria during autophagy. *PLoS One*. 2014;9(1):e84392. doi:10.1371/journal.pone.0084392
104. Yao P, Zhao H, Mo W, He P. Laminar Shear Stress Promotes Vascular Endothelial Cell Autophagy Through Upregulation with Rab4. *DNA Cell Biol*. Mar 2016;35(3):118-23. doi:10.1089/dna.2015.3041
105. Takeuchi H, Takada A, Kuboniwa M, Amano A. Intracellular periodontal pathogen exploits recycling pathway to exit from infected cells. *Cell Microbiol*. Jul 2016;18(7):928-48. doi:10.1111/cmi.12551
106. Polatoğlu I, Oncu-Oner T, Dalman I, Ozdogan S. COVID-19 in early 2023: Structure, replication mechanism, variants of SARS-CoV-2, diagnostic tests, and vaccine & drug development studies. *MedComm (2020)*. Apr 2023;4(2):e228. doi:10.1002/mco2.228
107. Bettini E, Locci M. SARS-CoV-2 mRNA Vaccines: Immunological Mechanism and Beyond. *Vaccines*. 2021;9(2). doi:10.3390/vaccines9020147
108. Wang F, Kream RM, Stefano GB. An Evidence Based Perspective on mRNA-SARS-CoV-2 Vaccine Development. *Med Sci Monit*. May 5 2020;26:e924700. doi:10.12659/msm.924700
109. Ou X, Liu Y, Lei X, et al. Characterization of spike glycoprotein of SARS-CoV-2 on virus entry and its immune cross-reactivity with SARS-CoV. *Nat Commun*. Mar 27 2020;11(1):1620. doi:10.1038/s41467-020-15562-9
110. Wang Y, Grunewald M, Perlman S. Coronaviruses: An Updated Overview of Their Replication and Pathogenesis. *Methods Mol Biol*. 2020;2203:1-29. doi:10.1007/978-1-0716-0900-2_1
111. Thomson EC, Rosen LE, Shepherd JG, et al. Circulating SARS-CoV-2 spike N439K variants maintain fitness while evading antibody-mediated immunity. *Cell*. Mar 4 2021;184(5):1171-1187.e20. doi:10.1016/j.cell.2021.01.037
112. Liu Y, Liu J, Johnson BA, et al. Delta spike P681R mutation enhances SARS-CoV-2 fitness over Alpha variant. *Cell Rep*. May 17 2022;39(7):110829. doi:10.1016/j.celrep.2022.110829
113. Meng B, Kemp SA, Papa G, et al. Recurrent emergence of SARS-CoV-2 spike deletion H69/V70 and its role in the Alpha variant B.1.1.7. *Cell Rep*. Jun 29 2021;35(13):109292. doi:10.1016/j.celrep.2021.109292
114. Wang R, Hozumi Y, Yin C, Wei GW. Mutations on COVID-19 diagnostic targets. *Genomics*. Nov 2020;112(6):5204-5213. doi:10.1016/j.ygeno.2020.09.028
115. Khan KA, Cheung P. Presence of mismatches between diagnostic PCR assays and coronavirus SARS-CoV-2 genome. *R Soc Open Sci*. Jun 2020;7(6):200636. doi:10.1098/rsos.200636
116. Rahimi A, Mirzazadeh A, Tavakolpour S. Genetics and genomics of SARS-CoV-2: A review of the literature with the special focus on genetic diversity and SARS-CoV-2 genome detection. *Genomics*. Jan 2021;113(1 Pt 2):1221-1232. doi:10.1016/j.ygeno.2020.09.059
117. Samieefar N, Rashedi R, Akhlaghdoust M, Mashhadi M, Darzi P, Rezaei N. Delta Variant: The New Challenge of COVID-19 Pandemic, an Overview of Epidemiological,

- Clinical, and Immune Characteristics. *Acta Biomed.* Mar 14 2022;93(1):e2022179. doi:10.23750/abm.v93i1.12210
118. Biswas SK, Mudi SR. Spike protein D614G and RdRp P323L: the SARS-CoV-2 mutations associated with severity of COVID-19. *Genomics Inform.* Dec 2020;18(4):e44. doi:10.5808/GI.2020.18.4.e44
119. Li P, Xue B, Schnicker NJ, Wong L-YR, Meyerholz DK, Perlman S. Nsp3-N interactions are critical for SARS-CoV-2 fitness and virulence. *Proceedings of the National Academy of Sciences.* 2023/08/01 2023;120(31):e2305674120. doi:10.1073/pnas.2305674120
120. Roxo C, Kotkowiak W, Pasternak A. G-Quadruplex-Forming Aptamers-Characteristics, Applications, and Perspectives. *Molecules.* Oct 21 2019;24(20)doi:10.3390/molecules24203781
121. Rhodes D, Lipps HJ. G-quadruplexes and their regulatory roles in biology. *Nucleic Acids Research.* 2015;43(18):8627-8637. doi:10.1093/nar/gkv862
122. Ruggiero E, Richter SN. Targeting G-quadruplexes to achieve antiviral activity. *Bioorg Med Chem Lett.* Jan 1 2023;79:129085. doi:10.1016/j.bmcl.2022.129085
123. Weinstein J, Scott A, Hunter FE, Jr. THE ACTION OF GRAMICIDIN D ON ISOLATED LIVER MITOCHONDRIA. *J Biol Chem.* Sep 1964;239:3031-7.
124. Wen Y, Li W, Poteet EC, et al. Alternative mitochondrial electron transfer as a novel strategy for neuroprotection. *J Biol Chem.* May 6 2011;286(18):16504-15. doi:10.1074/jbc.M110.208447
125. Riha PD, Bruchey AK, Echevarria DJ, Gonzalez-Lima F. Memory facilitation by methylene blue: dose-dependent effect on behavior and brain oxygen consumption. *Eur J Pharmacol.* Mar 28 2005;511(2-3):151-8. doi:10.1016/j.ejphar.2005.02.001
126. Callaway NL, Riha PD, Bruchey AK, Munshi Z, Gonzalez-Lima F. Methylene blue improves brain oxidative metabolism and memory retention in rats. *Pharmacol Biochem Behav.* Jan 2004;77(1):175-81. doi:10.1016/j.pbb.2003.10.007
127. Atamna H, Nguyen A, Schultz C, et al. Methylene blue delays cellular senescence and enhances key mitochondrial biochemical pathways. *Faseb j.* Mar 2008;22(3):703-12. doi:10.1096/fj.07-9610com
128. Wrubel KM, Riha PD, Maldonado MA, McCollum D, Gonzalez-Lima F. The brain metabolic enhancer methylene blue improves discrimination learning in rats. *Pharmacol Biochem Behav.* Apr 2007;86(4):712-7. doi:10.1016/j.pbb.2007.02.018
129. Lee SK, Mills A. Novel photochemistry of leuco-Methylene Blue. *Chem Commun (Camb).* Sep 21 2003;(18):2366-7. doi:10.1039/b307228b
130. May JM, Qu ZC, Whitesell RR. Generation of oxidant stress in cultured endothelial cells by methylene blue: protective effects of glucose and ascorbic acid. *Biochem Pharmacol.* Sep 1 2003;66(5):777-84. doi:10.1016/s0006-2952(03)00408-8
131. Casares D, Escribá PV, Rosselló CA. Membrane Lipid Composition: Effect on Membrane and Organelle Structure, Function and Compartmentalization and Therapeutic Avenues. *Int J Mol Sci.* May 1 2019;20(9)doi:10.3390/ijms20092167
132. Lozano M, Cid J, Müller TH. Plasma treated with methylene blue and light: clinical efficacy and safety profile. *Transfus Med Rev.* Oct 2013;27(4):235-40. doi:10.1016/j.tmr.2013.08.001

133. Gain C, Song S, Angtuaco T, Satta S, Kelesidis T. The role of oxidative stress in the pathogenesis of infections with coronaviruses. *Front Microbiol.* 2022;13:1111930. doi:10.3389/fmicb.2022.1111930
134. Sun S, Sursal T, Adibnia Y, et al. Mitochondrial DAMPs increase endothelial permeability through neutrophil dependent and independent pathways. *PLoS One.* 2013;8(3):e59989. doi:10.1371/journal.pone.0059989
135. Hu M, Bogoyevitch MA, Jans DA. Subversion of Host Cell Mitochondria by RSV to Favor Virus Production is Dependent on Inhibition of Mitochondrial Complex I and ROS Generation. *Cells.* Nov 11 2019;8(11)doi:10.3390/cells8111417
136. Gabrielli D, Belisle E, Severino D, Kowaltowski AJ, Baptista MS. Binding, aggregation and photochemical properties of methylene blue in mitochondrial suspensions. *Photochem Photobiol.* Mar 2004;79(3):227-32. doi:10.1562/be-03-27.1
137. Atamna H, Kumar R. Protective role of methylene blue in Alzheimer's disease via mitochondria and cytochrome c oxidase. *J Alzheimers Dis.* 2010;20 Suppl 2:S439-52. doi:10.3233/jad-2010-100414
138. Zhang F-T, Nie J, Zhang D-W, Chen J-T, Zhou Y-L, Zhang X-X. Methylene Blue as a G-Quadruplex Binding Probe for Label-Free Homogeneous Electrochemical Biosensing. *Analytical Chemistry.* 2014/10/07 2014;86(19):9489-9495. doi:10.1021/ac502540m
139. Kaur N, Singh R, Dar Z, Bijarnia RK, Dhingra N, Kaur T. Genetic comparison among various coronavirus strains for the identification of potential vaccine targets of SARS-CoV2. *Infect Genet Evol.* Apr 2021;89:104490. doi:10.1016/j.meegid.2020.104490
140. Nag S, Rani S, Mahanty S, et al. Rab4A organizes endosomal domains for sorting cargo to lysosome-related organelles. *J Cell Sci.* Sep 20 2018;131(18)doi:10.1242/jcs.216226
141. Ketter E, Randall G. Virus Impact on Lipids and Membranes. *Annual Review of Virology.* 2019/09/29 2019;6(1):319-340. doi:10.1146/annurev-virology-092818-015748
142. Spearman P. Viral interactions with host cell Rab GTPases. *Small GTPases.* Mar 4 2018;9(1-2):192-201. doi:10.1080/21541248.2017.1346552
143. Jaubert C, Bedrat A, Bartolucci L, et al. RNA synthesis is modulated by G-quadruplex formation in Hepatitis C virus negative RNA strand. *Sci Rep.* May 25 2018;8(1):8120. doi:10.1038/s41598-018-26582-3

CHAPTER 5

5. CONCLUSIONS AND FUTURE DIRECTIONS

5.1 Main Conclusions

Targeting G-quadruplexes has emerged as a successful strategy for controlling viral pathogenicity. Figure 1 shows a schematic of how G4s can regulate viral replication and translation. In Chapter 1, we explored various viruses whose regulation is mediated by integral G4 structures, as well as the advancements in developing G4-stabilizing compounds. For instance, C-exNDIs, which bind to the G4 structure in HIV-1's LTR, achieve a 65% reduction in activity post-genome integration. In comparison, Braco19 is more effective, showing an 80% reduction post-integration and inhibiting 50% of viral activity before integration. C-exNDIs specifically inhibit HIV-1 transcription, while Braco19 not only impedes transcription but also viral replication. This highlights that various G4-stabilizing compounds exhibit differing levels of efficacy and mechanisms in attenuating viruses. Therefore, it's crucial to research and develop derivatives of existing G4-stabilizing compounds to enhance their specificity and binding efficiency, and to minimize their off-target effects.

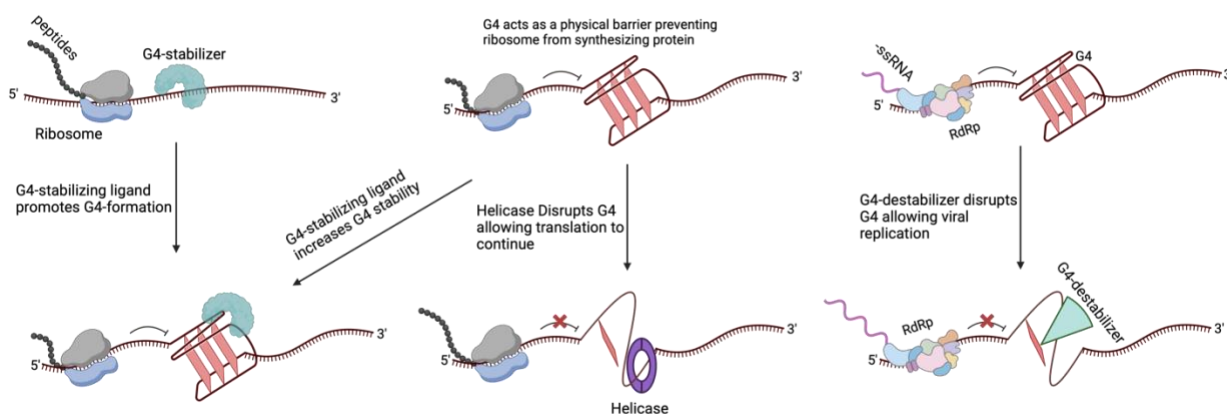


Figure 1: Schematic depicting G4 regulation.

Essential steps for viral maintenance and pathogenicity require protein translation and genome replication. The schematic depicts +ssRNA and G4-stabilizing ligands can promote the formation of G4s in RNA preventing translation from completing (top left to bottom left). If a G4 is already present, a G4-stabilizer can further enhance the stability of the G4 (top middle to bottom left). Specific proteins can act as G4-helicases and disrupt the structure, allow for translation or replication to continue (top middle to bottom middle). Many RNA viruses require RdRp for viral replication, which can be inhibited by G4s. Certain ligands can act as G4 destabilizers causing the G4 structure to weaken and revert to a linear form (top right to bottom right).

Since KSHV's discovery in 1994, every effort to eliminate the infection has been unsuccessful, mainly owing to its complex latency program. The protein, LANA is pivotal in enabling KSHV to avoid host immune detection and sustain latency. EBNA1, a homolog to LANA, in EBV is regulated by NCL. Given this, in Chapter 3, our objective was to explore whether NCL interacts with G4s in LANA mRNA and serves a regulatory function. Using an RNA oligonucleotide sequence corresponding to a G4 in LANA, we effectively pulldown NCL bound to the G4 Oligo. To confirm this interaction, RNA-CLIP was performed, revealing a marked enrichment of NCL binding to a plasmid containing a G4 sequence from LANA. Increasing concentrations of NCL correlated with a decrease in LANA translation, as evidenced by Western blot and luciferase assay results. Notably, stabilizing the G4 structure within LANA mRNA led to diminished antigen presentation. Fluorescent in situ hybridization (FISH) demonstrated a subset of LANA mRNA co-localizing with NCL protein. Upon NCL knockdown, we observed increased NCL localization to the cytoplasm, diminishing its availability in the nucleus for LANA interaction. In KSHV cells with latent infection, this altered NCL distribution, induced by

knockdown, resulted in increased LANA translation. Furthermore, the FISH assay confirmed that this increase in LANA translation predominantly occurs in the cytoplasm. Our results indicate that the interaction between NCL and G4 in LANA mRNA plays a significant regulatory role in LANA translation. This discovery opens new potential strategies for influencing KSHV latency, providing promising avenues for therapeutic developments.

Due to the COVID-19 pandemic, there was a need to develop strategies to prevent the spread and severity of SARS-CoV-2. We initially performed experiments in the less severe coronaviruses OC43, 229E, and NL63. Knowing that viruses can be regulated through their G4s, we searched for FDA-approved drugs with G4-stabilizing properties. This brought us to M-Blue, a dye with low toxicity used to treat methemoglobinemia. We treated cells infected with OC43, 229E, and NL63 with M-Blue and other well-studied G4-stabilizers, TMPyP4, and Braco19. We see that in all instances, remdesivir almost completely inhibited viral replication. M-Blue showed a lesser, but still significant reduction in virus detected, whereas Braco19 showed some reduction, and TMPyP4 essentially no reduction. In the case of SARS-CoV-2, our data indicates that TMPyP4 and Braco19 reduced viral copies by 50-60%, whereas remdesivir and M-Blue nearly eliminated detectable SARS-CoV-2 viruses. Pre-treating cells with M-Blue before infection inhibited viral entry into cells. This suggests that M-Blue can counteract coronaviruses through two distinct mechanisms, demonstrating its potential as a multifaceted antiviral agent.

G-quadruplexes represent a promising target in regulating viruses due to their highly conserved nature. We showed that just like for EBNA1 in EBV, the homolog

LANA in KSHV is regulated through internal viral G4 stabilization by NCL.

Additionally, M-Blue shows significant viral inhibition pre- and post-entry. TMPyP4 and Braco19 have varying efficacies in reducing coronavirus replication. Additionally, SARS-CoV-2 variants maintain a high level of conservation of G4 sequences between them.

This indicates that targeting the right G4 with the appropriate G4-stabilizer could regulate, most, if not all, variants. By focusing on the conserved G4s in viruses, we can maintain control over them despite their high mutation rates. This approach offers a strategic advantage in managing viral mutations and resistance.

5.2 Future Work

Future research should focus on understanding the dynamic between hnRNP A1 and NCL, and how they modulate LANA mRNA. Using an overexpression system for hnRNP A1 and NCL to determine the binding efficiency of both proteins to LANA mRNA. Whichever protein has a greater affinity for LANA mRNA's G4, will have a greater regulatory effect over LANA. This provides insight on how these proteins modulate LANA's function and stability. Furthermore, since LANA is known to regulate itself, we would look at overexpressing LANA and systematically vary concentrations of hnRNP A1. This will reveal the extent to which hnRNP A1 influences LANA's self-regulation.

Additionally, recognizing that the interaction between NCL and LANA mRNA leads to reduced antigen presentation, this interaction could be used as a therapeutic target. Disrupting the interaction between NCL and LANA mRNA would increase antigen presentation. This could enhance the immune system's ability to recognize and

combat infected cells. This strategy could be a significant step toward developing a targeted treatment to cure KSHV.

There is significant homology in the G4s between the SARS-CoV-2 variants. Several G4s in SARS-CoV-2 have high G-scores, such as those in the spike and nucleocapsid. We will synthesize these regions with a high G-score and perform an EMSA assay. We could compare a scrambled variant to samples treated with and without M-Blue. If a G4 forms and is stabilized by M-Blue, there should be a shift that is higher than the scrambled control. This would aid in determining which PQSs M-Blue stabilizes. From here, we can look at how conserved these G4s are between *coronaviruses* and variants.

Transgenic mouse lines have been developed to stably express human ACE2 receptors, providing a valuable tool for studying SARS-CoV-2 infection. Using these models, we propose to evaluate the efficacy of M-Blue in treating SARS-CoV-2-infected mice. This study would involve a comparative analysis of different M-Blue administration methods: intravenous injection, direct pulmonary administration, and inhalation. The primary outcome of this investigation would be the reduction in SARS-CoV-2 viral genomes, as detected in treated mice compared to controls. Additionally, we plan to meticulously document and analyze variations in symptomatology throughout the treatment course. This approach will offer insights into the most effective delivery method for M-Blue and its potential as a therapeutic agent against SARS-CoV-2.

Expanding our research in these areas can give us a more comprehensive understanding of the regulatory role of G4s in KSHV and coronavirus. These findings can lead to more effective therapeutic strategies against this virus.